Dissertation zur Erlangung des Doktorgrades
der Fakultät für Chemie und Pharmazie
der Ludwig-Maximilians-Universität München

The roles of β1 integrin in cartilage development

Aurelia Raducanu
aus
Bukarest, Rumänien

2009

Erklärung

Diese Dissertation wurde im Sinne von § 13 Abs. 3 der Promotionsordnung vom 29. Januar 1998 von Herrn Prof. Dr. Reinhard Fässler betreut.

Ehrenwörtliche Versicherung

Diese Dissertation wurde selbständig, ohne unerlaubte Hilfe erarbeitet.

München, am 23.04.2009

Aurelia Raducanu

Dissertation eingereicht am 23.04.2009

Erster Gutachter: Prof. Dr. Reinhard Fässler

Zweiter Gutachter: PD Dr. Matthias Schieker

Sondergutacher: Dr. Attila Aszódi

Mündliche Prüfung am 29.05. 2009

To my parents

(pentru parintii mei)

1. Table of contents

2. List of Publications

This thesis is based on the following publications, which are referred to in the text by their Roman numerals (I-IV):

I. **Aurelia Raducanu** and Attila Aszodi. β1 integrin-dependent cell shape governs mitotic spindle positioning in growth plate chondrocytes. *Submitted manuscript*

II. **Aurelia Raducanu** and Attila Aszódi* Knock-Out Mice in Osteoarthritis Research *Current Rheumatology Reviews*, 2008, *4,* 183-192

III. **Aurelia Raducanu**, Ernst B. Hunziker, Inga Drosse and Attila Aszódi. β1 integrin-deficiency results in multiple abnormalities of the knee joint. *Submitted manuscript*

IV. Martin Stolz[1]*, Riccardo Gottardi[2], Roberto Raiteri[2], Sylvie Miot[3], Ivan Martin[3], Raphaël Imer[4], Urs Staufer4[5], **Aurelia Raducanu[6]**, Marcel Düggelin[7], Werner Baschong[1,8], A. U. Daniels[9], Niklaus F. Friederich[10], Attila Aszodi[6] and Ueli Aebi[1]. Early detection of aging cartilage and osteoarthritis in mice and patient samples using atomic force microscopy. *Nat Nanotechnol*. 2009 Mar;4(3):186-92.

The following publication was not the focus of my project but I have contributed with tools which I have made during my PhD

V. Kanatsu-Shinohara M[1], Takehashi M[1,5], Takashima S[1], Lee J[1], Morimoto H[1], Chuma S[2], **Raducanu A**[3], Nakatsuji N[2], Fässler R[3], Shinohara T[1,4]. Homing of Mouse Spermatogonial Stem Cells to Germline Niche Depends on β1-Integrin *Cell Stem Cell*. 2008 Nov 6;3(5):533-42.

Reprints were made with permission from the publishers.

3. Abbreviations

AC	articular cartilage
ACTRI	activin receptor type I
ADAM	a disintegrin and metalloproteinase
ADAMTS	a disintegrin and metalloproteinase with trombospondin motifs
AdMIDAS	adjacent to MIDAS
ADP	adenosine diphosphate
AGEs	advanced glycation products
Akt	RAC-alpha serine/threonine-protein kinase
APC	adenomatous polyposis coli
Arp2/3	actin related protein 2/3 complex
BBS4	Bardet-Biedl Syndrome protein 4
BMP	bone morphogenetic protein
BMPR	BMP receptor
BrdU	Bromodeoxyuridine
CaMKII	calmodulin-dependent protein kinase CII
Cbfa1	core-binding factor alpha A
CD	campomelic dysplasia
CD44	cluster designation 44
Cdc42	cell division cycle 42
CE	convergent extension
Cho	chondrodysplasia
CILP	cartilage intermediate layer protein
Cmd	cartilage matrix deficiency
COMP	cartilage oligomeric matrix protein
Cre	cyclization recombinase
DAG	diacylglycerol
DGO	Diego
Dsh/Dvl	Dishevelled
EB1	microtubule plus-end binding protein 1
ECM	extracellular matrix
EGF	epidermal growth factor
ERK	extracellular signal-regulated kinase
FAK	focal adhesion kinase
FGF	fibroblast growth factor
FGFR	fibroblast growth factor receptor
FMI	Flamingo
FN	fibronectin
FNf	Fibronectin fragment
Fzd	Frizzled
GAP	GTP-ase activating protein
GDF	growth and differentiation factor
GDP	guanosine diphosphate
GDI	GDP dissociation inhibitor
GEF	guanine nucleotide exchange factor
GFR	growth factor receptor
Gli	glioma-associated oncogene homolog
GPCRs	G proteins coupled receptors
GSK3β	glycogen synthase kinase 3β
GTP	guanosine triphosphate
ICAMs	intercellular adhesion molecules
IFT	intraflagellar transport
Ift88	intraflagellar transport protein 88
Ig	immunoglobulin
IGF-1	insulin growth factor-1
Ihh	Indian hedgehog
ILK	integrin linked kinase
IPP	ILK-PINCH-Parvin
IP3	inositol triphosphate
IT-AFM	indentation type atomic force microscopy
JAK	Janus kinase
JNK	c-jun N-terminal kinase
kDa	kiloDaltons
Kif3a	kinesin family member 3A
LAP	latency-associated peptide
LEF	lymphoid enhancer-binding factor
LGN	leucine, glycine, asparagine
LRP	lipoprotein receptor-related proteins
LTBP	latent TGFβ binding protein
MAPK	mitogen-activated protein kinase
MEK	MAP kinase-ERK kinase
MFGE8	milk fat globule-EGF factor 8
MIDAS	metal-ion-dependent adhesion site
mInsc	mouse Inscuteable
MLC	myosin light chain
MMP	matrix metalloproteinase
N-CAM	neural cell adhesion molecule
Nck2	noncatalytic region of tyrosine kinase, adaptor protein 2
NRK	normal rat kidney cells
Numa	nuclear/mitotic apparatus protein
OA	osteoarthritis
Par6	partitioning defective 6
Pax1	paired box gene 1
PCP	planar cell polarity
PC1	policystin-1
pFAK	phosphoFAK
PI3-K	phosphatidylinositol 3-kinase
PINCH	Particularly interesting new Cys-His protein

PK	Prickle
PKC	protein kinase C
PKCζ	protein kinase C ζ
PKD	polycystic kidney disease
PLC	phospholipase C
PPR	PTH/PTHrP receptor
Prx1	paired related homeobox 1
PSI	plexin, semaphorins, and integrins
PtdIns	phosphatidylinositol
PtdIns-4,5-P_2	PtdIns4,5-bisphosphate
PTHrP	parathyroid hormone related peptide
Ptc-1	Patched-1
PYK2	pyruvate kinase 2
Rac1	ras-related C3 botulinum toxin substrate 1
Rap1	RAS-related protein-1
Rap-L	Rap1 ligand
Ras	rat sarcoma viral oncogene homolog
RGD	arginine, glycine, aspartate
RhoA	ras homolog gene family, member A
RIAM	Rap1-interacting adaptor molecule
ROS	reactive oxygen species
ROCK	Rho-associated protein kinase
Ror2	receptor tyrosine kinase-like orphan receptor 2
Runx	runt-related transcription factor
Smad	Similar to mothers against decapentaplegic
Smo	Smoothened
Sox	Sry-related high-mobility group box
Src	Rous sarcoma oncogene
Sry	sex determining region Y
STAN	starry night
STAT	signal transducer and activator of transcription
STBM	Strabismus
SyMBS	synergistic metal ion binding site
TCF	T cell-specific transcription factor
TGF-β	transforming growth factor β
TUNEL	Terminal deoxynucleotidyl transferase dUTP nick end labeling
VANG	vanGogh
VCAMs	vascular cell-adhesion molecules
VEGF	vascular endothelial growth factor
WASp	Wiscott-Aldrich Syndrome protein
Wnt	wingless-type MMTV integration site family member

4. Summary

Integrins are heterodimeric cell surface receptors that provide a connection between the actin cytoskeleton and extracellular matrix (ECM). In addition, ECM-bound integrins activate signaling pathways that control various aspects of cell behavior including cell shape, migration, proliferation and differentiation. Genetic deletion of individual integrin subunits has shown that they play a vital role in the development of organisms. In this work, we examined the role of β1 integrin in cartilage function.

In the process of endochondral ossification, long bones of the body are formed by replacement of a previously formed cartilage template. The columnar growth plate cartilage is a highly specialized and organized structure which sustains the elongation of the bone in early life. Lack of β1 integrin on chondrocytes leads to severe chondrodysplasia and perinatal lethality. The mutant chondrocytes in the growth plate are round, display adhesion defects and do not adopt the normal columnar arrangement. Recently β1 integrin was shown to regulate mitotic spindle orientation and the establishment of apical-basal polarity in epithelial cells. This polarity creates asymmetrically distributed cortical cues which dictate the orientation of the mitotic spindle and therefore the cell division plane. The reduced cellularity and loss of the columnar organization of β1 integrin-null chondrocytes led us to hypothesize that the loss of β1 integrin had detrimental effects on cell division and subsequent migratory events in these cells (Paper I). Histological analysis of growth plate chondrocytes in vivo demonstrated that spindle positioning depends on the elongated cell shape and does not requires cortical cues. Late mitotic spindles are aligning parallel to the long axis of the cell and perpendicular to the longitudinal direction of the bone growth, while the cleavage plane is oriented at right angle of the late spindle axis. This cell shape anisotropy is analogous to polarity and is essential for the subsequent migration of the cells to form longitudinal columns. In the absence of β1 integrin the chondrocytes lose their discoid shape (and therefore polarity) leading to arbitrary spindle orientations. This results in a randomized cleavage plane and subsequent inability to form columns. The dependence of cell shape to orient the mitotic spindle was recapitulated in vitro with isolated primary chondrocytes. Taken together, these data indicate that the disorganized columnar structure in the β1 integrin-deficient growth plate is a consequence of the loss of cell anisotropy due to adhesion abnormalities, which leads to mitotic orientation defects. We conclude that β1 integrin is essential for regulating the cell shape, which in turn dictates the division plane in the growth plate chondrocytes.

Next, we studied the role of β1 integrin in the function of adult articular cartilage (AC), by deleting β1 integrin from the limb bud osteochondral progenitors, and therefore from chondrocytes of the joints of the long bones (Paper III). Previous studies deleted β1 integrin from all chondrocytes, which caused the mice to die around birth due to defects in vital skeletal structures; restricting the deletion to the long bones spared the animals and permitted the examination of adult articular cartilage. The limbs of such animals showed characteristics of dwarfism and the columnar organization in the growth plate was lost. Joint defects accompanied by structural changes in the articular cartilage were detected in mutant animals. The shape and proliferation of mutant chondrocytes were altered in knee joint AC. The composition of the ECM surrounding mutant chondrocytes was altered, indicating that the differentiation of mutant chondrocytes did not proceed normally, and the ECM that was deposited was disorganized. Each of these changes is characteristics of ostearthritis, but surprinsigly we were unable to detect accelerated cartilage erosion. As an explanation of this unexpected finding, we noticed normal activity of matrix metalloproteinases and aggrecanases accompanied by normal metabolism of the major cartilage structural proteins, collagen II and aggrecan. Our observations suggest that the loss of β1 integrin on AC chondrocytes may contribute to arthritis but alone is not sufficient for a bona fide arthritis phenotype since cartilage surface erosions are absent in the deficient mice.

The progression of arthritis is characterized by increasing erosion of the AC surface. Diagnosis is possible only after major pathological modifications have occured in the cartilage. To enable the examination of the AC surface in early osteoarthritic events we made significant contributions to the development of a technique to examine the topography and stiffness characteristics of AC using indentation-type atomic force microscopy (IT-AFM) (paper IV). As a proof of principle in this study we used AC from both patients and mice deficient in collagen-IX expression, which serves as a classical model for progressive arthritis. This study demonstrated that nano scaled IT-AFM can resolve individual collagen fibrils and can reliably measure elastic properties in normal and diseased AC. Wild type cartilage displays increased bundling of collagen fibrils and a gradual increase in stiffness with age. The thickness of collagen fibrils was accelerated and increased in the absence of collagen-IX, concomitant with an increase in AC stiffness until six months of age, after which stiffness gradually decreased owing to degeneration of the collagen matrix. Therefore, we could show that IT-AFM is a valid technique to quantitatively compare the physical qualities of AC cartilage, and detect and monitor the progression of arthritis long before other techniques are effective.

5. Introduction

5.1. The integrin family of adhesion receptors

The assembly of cells and extracellular matrix (ECM) molecules into tissues is mediated by adhesion molecules which can either form cell-cell interactions or can anchor cells to the ECM [1]. Integrins are a major class of cell adhesion receptors in metazoan cells, present from sponges to mammals [2, 3]. They are heterodimeric transmembrane proteins which interact either with ECM molecules or with cellular counter-receptors, and they connect to the cytoskeleton via adaptor proteins, thus forming a structural link between the extracellular space and the intracellular milieu [3, 4]. Integrins are dual function receptors, acting both as adhesion and signaling receptors which enable cells to both bind and respond to the extracellular matrix chemically and mechanically. They control cell shape and polarity as well as essential cellular processes such as proliferation and differentiation, survival, apoptosis and cell migration [5].

5.1.1. Integrins and their ligands

Integrins can bind three major classes of ECM ligands: collagens, laminins and molecules which have exposed RGD (arginine, glycine, aspartate) motifs such as fibronectin, vitronectin, tenascin, osteopontin and thrombospondin [6, 7]. Besides interactions with the major ECM ligands, leukocyte-specific integrins establish cell-cell contacts with endothelial cells by interacting with cellular counter-receptors such as intercellular adhesion molecules (ICAMs) and vascular cell-adhesion molecules (VCAMs)[8] (**Fig. 1**). Additional ligands known to interact with integrins are: milk fat globule-EGF factor 8 (MFGE8) and complement factor (iC3b)[9], which are involved in phagocytosis of apoptotic cells and pathogens, respectively; the latency-associated peptide (LAP) of transforming growth factor β (TGF-β) which regulates TGF-β signaling [10], some of the ADAM (a disintegrin and metalloproteinase) family members and MMP-2 (matrix metalloproteinase-2) which participate in ECM remodelling during cell adhesion and migration [11].

18 different α subunits and 8 different β subunits have been described in mammals, that combine to form at least 24 distinct αβ heterodimers with different ligand binding specificities [3] (**Fig.1)**. There is significant overlap in binding, as the same ligand is often recognised by many different integrins, and a given integrin can often recognize more than one ECM molecule [6]. The complexity of the integrin family is further increased by the

presence of splicing isoforms. Different tissues express only a specific isoform and some tissues can switch during development between different isoforms. Although many isoforms have redundant functions some seem to have vital functions for cell physiology. For example the A isoform of β1 integrin (β1A) is expressed in all tissues except muscle and heart which express the β1D isoform. Genetically modified mice that express the β1D isoform exclusively die early during embryonic development whereas substitution of β1D with β1A causes only small abnormalities in the muscles, suggesting that β1D is dispensable for mouse development and cannot compensate for loss of β1A [2].

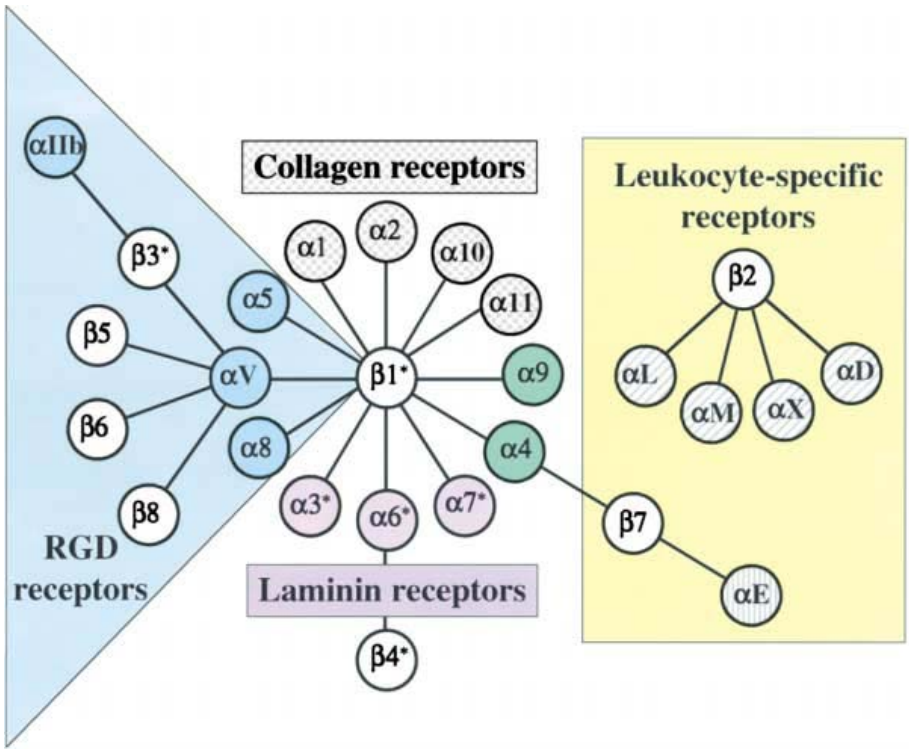

Fig.1 Mammalian family of integrin heterodimers[3]. Based on the binding specificity given by the two subunits of the heterodimer the integrin family can be subdivided into different subfamilies. Some integrins are specific for certain cell types such as the leukocyte-specific integrins, and many cell types express more than one type of integrin [3].

5.1.2. Integrin structure

Integrins are type I transmembrane glycoproteins composed of non-covalently associated α and β subunits. Each subunit consists of a large extracellular domain (80-150 kDa), a single transmembrane alpha helix and, except for the β4 subunit which has an unusually large cytoplasmic domain of 1072 residues, a short cytoplasmic domain of 10-70 amino acids [12]. Electron microscopy and biophysical data revealed a 'head on a stalk' arrangement of the two subunits, whereby their extracellular domains organize into a head sitting on two legs [13, 14]. The crystal structure of the αvβ3 extracellular domains was the first high resolution data to reveal the organization of both subunits [3, 15]. More recently the αIIbβ3 structure has provided even greater resolution and gave some insight into the integrin activation mechanism [14]. The extracellular domain of the α subunit contains an N-terminal β propeller domain followed by an Ig-like (thigh) and two β sandwich domains (calf1 and calf2). Half of the known α subunits (the collagen-binding and leukocytes-specific integrins) contain an I/A domain inserted into the larger β propeller domain and in these integrins this domain participates in ligand binding [3, 12, 16]. The β subunit's extracellular domain is organized in a βI/A domain, which is inserted into an immunoglobulin (Ig)-like "hybrid" domain preceded by an N-terminal 54-residue PSI (plexin, semaphorins, and integrins) domain, four tandem cysteine-rich EGF-like repeats and a β-tail domain (**Fig.2**). The PSI domain is disulfide bonded to the distal I-EGF domain [3, 17].

The β propeller of the α subunit together with the βI/A and the "hybrid" domains of the β subunit comprise the head region. The interface between the propeller and the βI/A domain forms the ligand-binding pocket. Integrin-ligand binding is dependent on divalent cations. The βI/A domain contains three metal binding sites essential for ligand binding: a central Mg^{2+} binding site called MIDAS (metal-ion-dependent adhesion site) and two flanking Ca^{2+} sites one called SyMBS (synergistic metal ion binding site) and the other AdMIDAS (adjacent to MIDAS)[14].

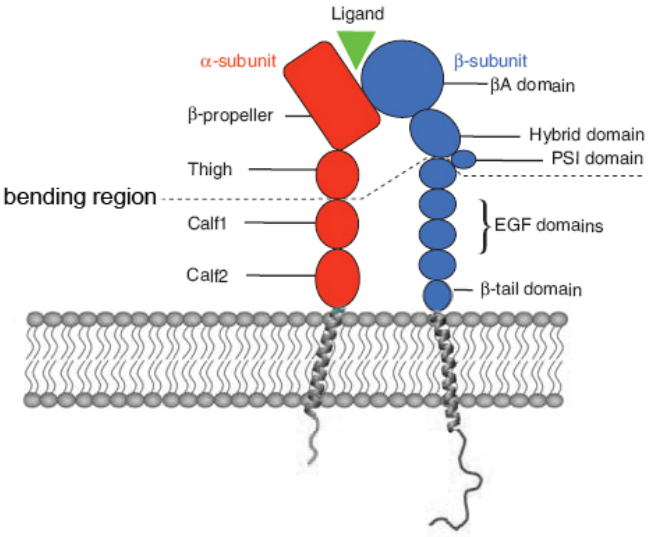

Fig.2 Diagram of integrin heterodimer (adapted from [12] and [18]). The ligand-interacting head is formed of the propeller of the α subunit and the hybrid and βI/A domains of the β subunit. The "switchblade model" of activation postulates that during activation the inactive bent integrins unfold at the bending region (dotted line) to expose the ligand binding site.

5.1.3. Integrin signaling

Integrins are unusual among transmembrane receptors because they can signal across the membrane in both directions. The ECM-binding activity of the integrins can be modulated upon an intracellular signaling event (inside-out signaling) and, upon binding ECM, integrins can transmit signals into the cell (outside-in signaling) [3, 5]

Inside-out signaling. Integrins that are expressed on the cell surface in an inactive conformation, unable to bind to the ECM or cellular counter-receptors, are activated by a series of events referred to as inside-out signaling. Upon induction by intracellular stimuli, activated cytoplasmic ligands such as talin and kindlins interact with the integrin tails to transmit information to the extracellular ligand-binding domain via the transmembrane domain and legs [12, 19]. Inside-out signaling has best been studied in circulating blood cells such as platelets, leukocytes and lymphocytes. Integrin activation in these cells occurs only in certain physiological situations such as thrombus formation, during hemostasis, or extravasation through the blood vessel walls and migration to the site of inflammation [20-22].

Several agonists can activate αIIbβ3 in platelets: immobilized stimuli such as von Willebrand factor and collagen; soluble molecules released locally such as thrombin; and molecules produced by the platelets themselves, ADP and thromboxane A2. These stimuli act either through receptors coupled to heterotrimeric G proteins (GPCRs) or through receptors not directly coupled to G proteins such as the collagen receptor GPVI. Two important enzymes are activated downstream of GPCRs: phosphatidylinositol 3-kinase (PI3-kinase) and phospholipase C (PLC). PI3-kinase products, phosphatidylinositol (PtdIns)-3,4-bisphosphate (PtdIns-3,4-P_2) and PtdIns-3,4,5-P_3, recruit proteins with pleckstrin homology domains to the

cell membrane. PLC cleaves phosphatidylinositol to produce the secondary messengers inositol triphosphate (IP3), which increases cytoplasmic [Ca^{2+}], and diacylglycerol (DAG), which activates protein kinase C and CDGI (a Ca^{2+} and DAG-dependent guanine nucleotide exchange factor (Cal-DAG-GEF) for the ras-like small GTPases Rap1) [20]. Activated Rap1 binds to its effector RIAM which in turn binds to talin [23]. This ternary complex is targeted to the plasma membrane where talin can bind to integrin β2- and β3-tails and together with the actions of kindlins switch these integrins into the high affinity state [21, 24-26].

Additional signaling pathways have been shown to activate integrins in lymphocytes (**Fig.3**). Chemokine-activated GPCRs signal through the same signaling cascades as described for platelets, including activation of PI3K and the small GTPases Rap1 and RhoA. Furthermore, activation of T cell antigen receptor upon antigen binding was proposed to increase integrin activation in a phospholipase C-gamma1- and Rap1-dependent manner [22]. Also, cross-linking of selectins and binding to ICAM-1 in neutrophils leads to integrin activation through a protein kinase C-dependent pathway. [21]

The above pathways ultimately result in the activation of talin, which is proposed to disrupt interactions between the cytoplasmic α and β integrin tails, including a proposed salt bridge between an Asp residue within the β-tail HDRK motif and an Arg residue in the GFFKR motif within the α-tail, by binding to membrane-proximal residues in the β integrin tail [27] (see **Fig. 4** for the position of the putative salt bridge). In addition to talin, the kindlin family of proteins has been recently shown to have a vital role in integrin activation [24, 26, 28]. However, in contrast to talin, nothing is known about how kindlins become activated. Talin and kindlin binding to integrin tails induces a conformational change that is propagated through the transmembrane domains to the

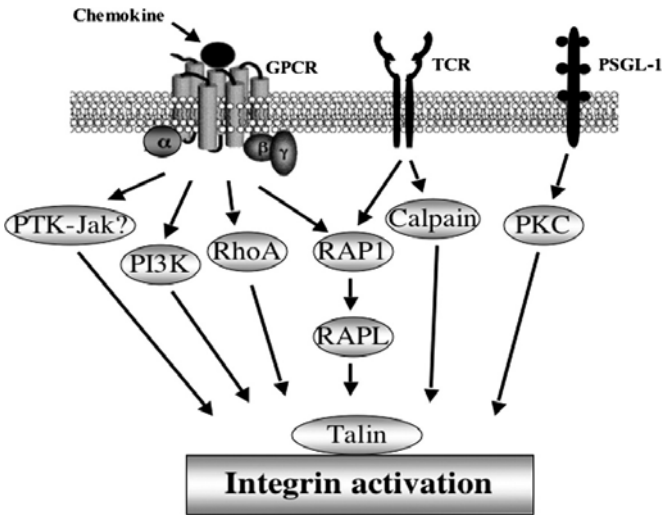

Fig.3 Signaling pathways leading to integrin activation in lymphocytes [22]. Activation of receptors such as GPCRs or TCR leads to talin recruitment to the integrin tails which results in activation of the integrins from within.

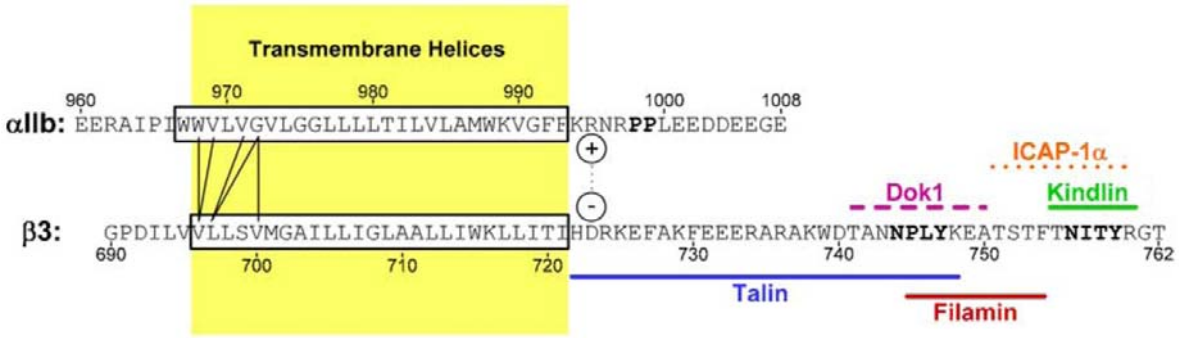

Fig.4 Sequences of the transmembrane and cytoplasmic tails of the αIIb and β3 subunits. The salt bridge forms between the positively charged R (+) and the negatively charged D (-) residues. The binding sites are shown for a few of the proteins known to interact with β integrin tail. [12]

extracellular domains of the integrins. The integrin heterodimer can then switch to an active conformation by unbending the "legs" at the knee or "genu" between the α thigh and calf1 and between the I-EGF domains 1 and 2 of the β leg. Thus the integrin can transit from a low affinity bent conformation to a high affinity extended conformation. Details of the structural changes during integrin activation are still controversial. Two main competing models have emerged from independent studies. First, the switchblade model states that the separation of the cytoplasmic tails and TM domains of the inactive bent integrin causes the knee extension and opening of the ligand binding pocket (**Fig 5A)**. Second, the deadbolt model does not require unbending but, upon a change in the tilt of the transmembrane domains following inside-out signaling, a conformational change occurs within the head domain to reveal the ligand binding site (**Fig. 5B)** [12, 14, 17, 18].

Through still unclear mechanisms, integrins that are in a high affinity state and bound to ligand initiate clustering and the recruitment and activation of other integrin molecules thus strengthening the interaction with ECM[17] and leading to activation of intracellular signaling pathways by the so called outside-in signaling discussed below.

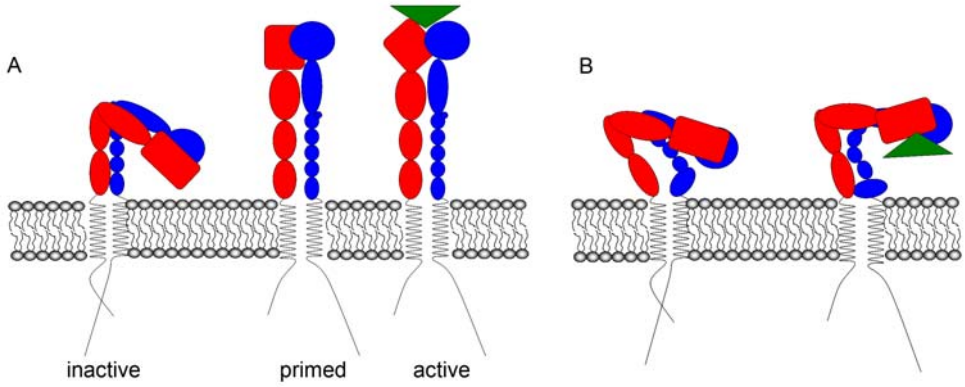

Fig.5 Models of integrin activation. A. In the switchblade model, the inactive heterodimer extends in an inactive primed state which consequently opens the ligand binding site. B. In the deadbolt model, a conformational change of the transmembrane domain is propagated to the extracellular domain to expose the ligand binding site while still in a bent conformation. The two controversial models have been described for αvβ3 and αIIbβ3 integrins. Probably each integrin heterodimer has a unique repertoire of conformational changes. [17 12 14]

Outside-in signaling. The cytoplasmic tails of the integrins are devoid of enzymatic activity; instead they function as docking sites for many adaptor proteins (**Fig. 4**). Following integrin activation a series of molecules are recruited and assembled into a signaling platform on integrin tails, leading to an increase in tyrosine phosphorylation of specific substrates and an increase in the concentration of lipid second messengers such as PtdIns-4,5-P_2 and PtdIns-3,4,5-P_3. Molecules associated with the integrin tails contribute subsequently both to cytoskeletal rearrangements needed during spreading, migration and cell polarity, and to initiation of intracellular signals which ultimately result in gene expression changes that promote cell survival, proliferation and differentiation (**Fig. 6**)[29].

The integrin-actin linkage is established by several molecules in a complex but well controlled network. The integrin-binding molecules talin, α-actinin, and filamin have been described to connect directly to the cytoskeleton by interacting with actin. Both talin and α-actinin can also indirectly regulate the cytoskeleton in a PtdIns-4,5-P_2-dependent manner through an interaction with another actin-binding protein, vinculin. Filamins associate with integrins and are able to link actin filaments in orthogonal networks or parallel bundles. [29, 30]

Other integrin-binding proteins such as integrin linked kinase (ILK), paxillin, FAK and kindlins are linked to the actin cytoskeleton indirectly [29]. ILK associates with integrin tails when it is a part of a tripartite complex containing parvin and PINCH (known as the

ILK-PINCH-parvin or IPP complex) [31]. Parvins link ILK to actin filaments either directly or indirectly through paxillin and vinculin. PINCH, on the other hand, can also modulate actin polymerization through WASp (Wiscott-Aldrich Syndrome protein) via an interaction with the adaptor Nck2 [30].

One of the important downstream effects of integrin activation is the recruitment of the small Rho GTPases and their regulators to the plasma membrane. Many of the mentioned molecules, such as parvin, paxillin, FAK, and filamin act on Rho GTPases. Rho GTPases are major actin regulators which cycle between an active GTP-bound and an inactive GDP-bound conformation. This cycling is regulated by guanine nucleotide exchange factors (GEFs), GTPase-activating proteins (GAPs) and guanine nucleotide-dissociation inhibitors (GDIs) [32]. The three major Rho GTPases involved in integrin-regulated actin remodelling are Cdc42, Rac1 and RhoA. Cdc42 is involved in filopodia formation and Rac1 has been shown to promote lamellipodial protrusion during cell migration [33]. Both act through the activation of the actin nucleator Arp2/3 which initiates de novo actin polymerization or branching of pre-existing actin filaments. RhoA is a major regulator of cell contractility and it has been shown to promote stress fiber formation by activating formins and ROCK kinase which in turn phosphorylates myosin light chain (MLC) thus inducing acto-myosin contraction [29].

Integrin signaling affects multiple signal transduction pathways through the Src-FAK complex which is localized at adhesion sites by binding β integrin cytoplasmic tails and locally produced phosphoinositides [29]. The Src-FAK complex activates the Ras-MEK-MAPK signaling cascade, a major pathway through which integrins can regulate cell cycle, proliferation and gene expression. ERK activation downstream of integrin signaling promotes cell proliferation through activation of cyclin D expression and subsequent cell cycle entry [5]. Survival and differentiation are also regulated by controlling Akt and Gsk3β downstream of PI3K signalling, probably in an IPP-dependent manner. The src-homology adaptor Nck2 has been shown to interact both with growth factor receptors (GFRs) and the IPP complex thereby connecting integrin and GFRs signaling. Thus many of the signaling pathways downstream of integrins are also downstream of GFRs, and a significant amount of crosstalk exists between these two signaling hubs [29].

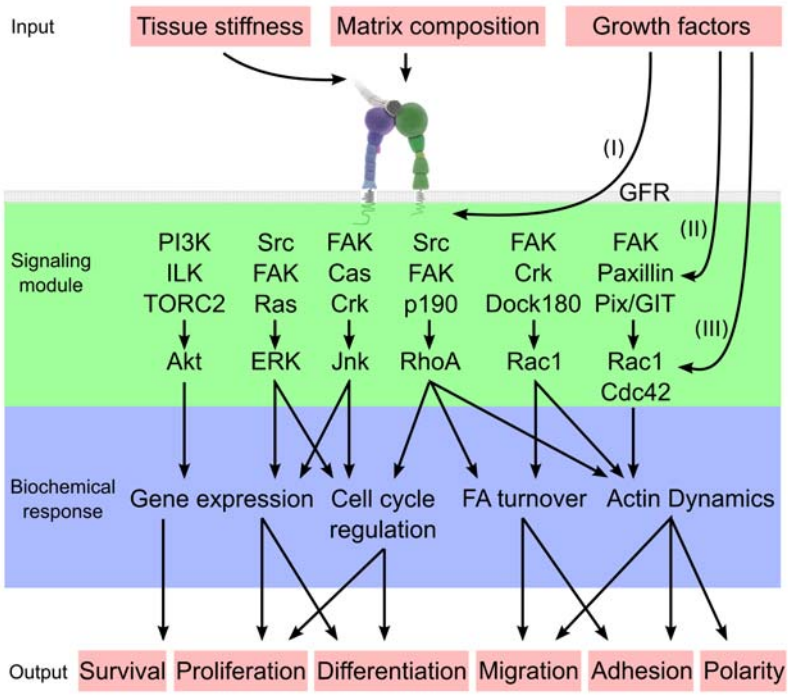

Fig.6 Outside-in signaling[29]. Integrins respond to diverse stimuli and activate a wide variety of intracellular signaling cascades to induce multiple cellular effects in the so called outside-in signaling pathways. Cooperation with other receptors such as GFRs ensures an integrated response to extracellular signals.

5.1.4. Integrins in mouse development

In vivo studies using mouse genetics have significantly increased the understanding of integrin biology. The most important subfamily of integrins is the ubiquitously expressed subfamily of β1 integrins due to its association with more than half of the α subunits. Genetic ablation of β1 integrin leads to the loss of all β1-containing heterodimers (α1β1-α11β1, αvβ1) and results in peri-implantation lethality characterized by an inner cell mass (ICM) failure [34, 35]. α5, α4 and αv integrin knockouts show the next severe phenotypes characterized also by embryonic lethality but at different developmental stages: α5 knockout (ko) embryos die between embryonic day 9.5 (E9.5) and E10 due to extraembryonic and embryonic vascular defects [36]; α4 deletion leads to death between day E11 and E14 as the result of defective choriallantois fusion and abnormal cardiac development [37]; 80% of the αv ko embryos die between E10 and E12 because of a placental defect whereas the remaining 20% die at birth

due to cleft palate and massive hemorrhages [38]. Deletion of α3, α6, α8, β4, or β8 results in perinatal lethality due to various phenotypes. For example the α3 ko mice shows skin blistering, kidney, lung and cerebral cortex defects [39-41]; α8 ko mice have small or absent kidneys as well as inner ear abnormalities [42, 43]. Other integrin ko mice show organ-specific defects but are viable and fertile. For example, deletion of the β7 subunit leads to impaired T cell migration to Peyer's patches and reduced lymphocyte number associated with the gut epithelia [44]. Mice lacking β3 or αIIb have defective blood clot formation due to impaired platelet aggregation [45, 46].

To understand the specific role of essential integrins in specialized organs such as skin, hematopoietic system, bone, cartilage or blood vessels, conditional knock-out strategies are of valuable use since they overcome the problem of early embryonic lethality. The skin-specific ablation of β1 integrin expression results in severe blistering, abnormal basement membrane organization, epidermal proliferation and hair follicle morphogenesis[46, 47]. The use of chimeric mice to study the role of β1 in the hematopoietic system revealed that β1 integrin is required for colonization of hematopoietic organs by the hematopoietic stem cells but it is not essential for their differentiation[48, 49]. More recently the inactivation of β1 integrin specifically in the pericytes of the blood vessel walls results in perinatal lethality due to blood vessel aneurysms and hemorrhages demonstrating a vital role for β1 mediated adhesion in maintaining vessel wall integrity[50]. Deletion of β1 integrin in chondrocytes will be discussed in detail in the chapter 5.2.4.4. All together these in vivo studies show that integrins play important structural as well as signaling roles in development and maintenance of tissue integrity. In the next subchapter, I will summarize our current knowledge about the role of integrins in mitotic spindle positioning and tissue polarity.

5.1.5. β1 Integrin controls orientation of the spindle machinery and cell polarity

The orientation of the mitotic spindle determines the plane of cell division and defines the relative location of daughter cells, which in turn regulates cell fate decisions that are important for tissue morphogenesis. β1 integrin has been recently shown to regulate mitotic spindle orientation both *in vivo* and *in vitro*. In normal skin, basal keratinocytes display apical-basal polarity and cell division is oriented perpendicular (with high percentage) or parallel (with low percentage) to the basement membrane at the time when the epidermis

begins to stratify during embryogenesis. Deletion of β1 integrin from basal keratinocytes leads to the loss of normal apical localization of PKCζ and the polarity complex Par6/LGN/mInsc-Numa-dynactin, which consequently results in random spindle orientation[51]. β1 integrin ablation in the basal cells of the mammary gland epithelium alters the orientation of the cell division axis leading to dislocation of stem-cell progeny into the luminal epithelial compartment [52]. In Drosophila, β1 integrin regulates the proper orientation of the mitotic spindle of follicular cells, thus ensuring that the two daughter cells remain attached to the basement membrane during formation of the ovarian epithelium [53].

In vitro, cell-ECM interactions mediated by integrins determine the shape of the cell in interphase and create cortical cues, which are maintained during mitosis. These cortical cues are used by the dividing cells to establish the cell division axis independent of the cell shape during mitosis [54]. Recently, Toyoshima and Nishida have demonstrated that both in HeLa and normal rat kidney cells (NRK) cells, β1 integrin-mediated adhesion orients the mitotic spindle parallel to the substratum. This process is independent of cell geometry and involves EB1 and myosin X as well as intact astral microtubules [55]. Moreover, changing PtdnIns-3,4,5-P_3 distribution by inhibiting the PI3K pathway, which is downstream of integrin signaling, results in spindle misorientation [56]. Thus, by regulating mitotic spindle orientation, integrin-mediated adhesion establishes the location and fate of the daughter cells also in these two dimensional culture systems.

Many morphogenetic events during embryogenesis depend upon choreographed, polarized cell migration to form specific structures. Convergent extension (CE) represents such a series of polarized cell movements, which result in tissue narrowing along one axis and lengthening along a second, perpendicularly oriented axis. CE is particularly important during gastrulation, neurulation, body axis elongation and organogenesis in both vertebrate and invertebrate embryos. One of the cellular mechanisms of convergent extension is mediolateral intercalation. First, the dispersed cells extend lamellipodial protrusions in random orientations, then lamellipodia become stable and polarized in the mediolateral axis. These polarized protrusions attach to the mediolateral neighbouring cells and exert traction forces, pulling the cells between one another **(Fig.7)** [57]. In *Xenopus* embryos, integrin-ECM interactions modulate cadherin-mediated cell-cell adhesion required for CE. Expression of a dominant negative form of β1 integrin (HAβ1) in gastrulating embryos leads to disruption of cell-intercalation and CE resulting in delayed blastopore closure and shortened antero-posterior axes. This phenotype is most likely due to the impaired modulation of cadherin-mediated cell adhesion during intercalation [58]. When α5β1 integrin binding to fibronectin is

disrupted in *Xenopus*, the mediolateral protrusions become randomized leading to convergent thickening instead of convergent extension [59]. Thus integrin-mediated adhesion and signalling are central players in tissue morphogenesis.

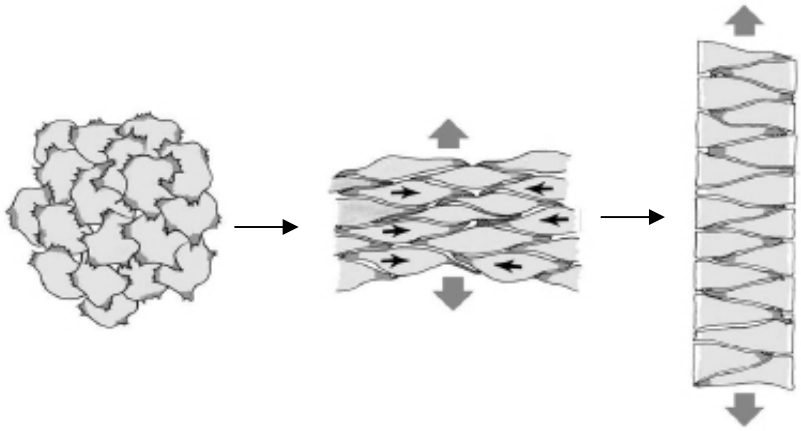

Fig.7 Mediolateral intercalation during convergent extension [60]. The initially non-polarized cells extend medial-lateral polarized protrusions and start migrating in a medial-lateral direction. This series of movements result in narrowing in one direction and elongation in a perpendicular direction.

5.2. Skeletal development

The vertebrate skeleton is formed from more than 250 different elements and plays essential roles in body support and protection, in locomotion, in blood cell production, and in mineral and energy storage [61]. The skeleton is composed of cartilage and bone and its main parts are derived from three different embryonic compartments: the craniofacial skeleton is formed from cranial neural crest cells; the axial skeleton (vertebral column and the rib cage) arises from the paraxial mesoderm; and the apendicular skeleton (limbs) is the product of the lateral plate mesoderm [62]. Cells from these lineages migrate to the locations of presumptive skeletal elements and aggregate to form characteristic mesenchymal condensations that prefigure the future bone [63]. The mesenchymal cells, depending on the function and location of the bone, can undergo two developmental fates: either they differentiate directly into bone producing osteoblasts during the process of intramembranous ossification by which facial and cranial bones are formed; or the progenitors differentiate into chondrocytes that lay down initial cartilaginous templates which are subsequently replaced by bone except in the joint regions. This latter process, called endochondral ossification (or endochondral bone formation) represents the main focus of this chapter [64, 65].

5.2.1. Endochondral ossification

Endochondral ossification (EO) is a complex, multistep process by which more than 95% of the vertebrate skeleton including the vertebrae, ribs, and limbs is formed [66]. The morphogenetic sequence of EO can be divided into five consecutive and partially overlapping stages (**Fig. 8** and **9**):

1. Commitment of mesenchymal cells: When mesenchymal cells migrate to the site of future skeletal elements they become committed to differentiate into chondrocytes. This commitment is caused by the soluble morphogen Sonic hedgehog, which induces nearby cells to express the Pax1 transcription factor. Pax1 initiates a cascade that is dependent on external paracrine factors and internal transcription factors [63, 67].

2. Mesenchymal condensation and chondrogenic differentiation: The previously dispersed, committed mesenchymal progenitors first proliferate then withdraw from the cell cycle and begin to aggregate into tightly packed clusters or nodules followed by

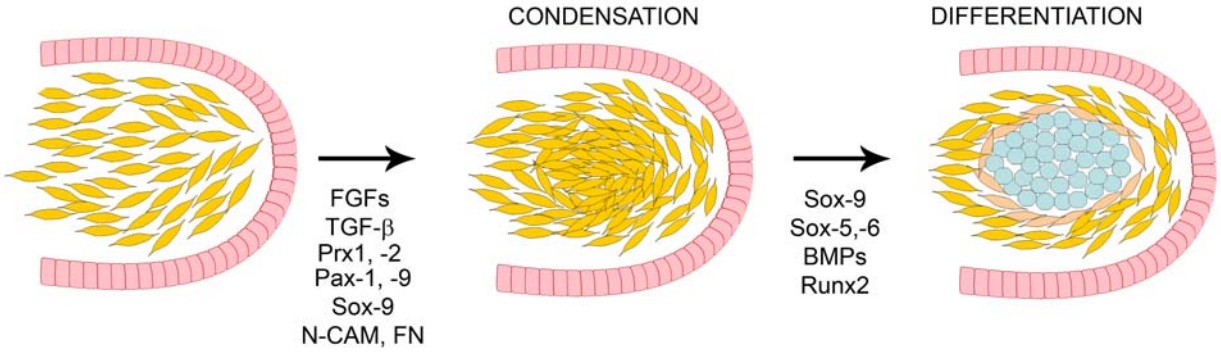

Fig.8 Condensation and differentiation of limb bud mesenchyme into cartilaginous tissue. Mesenchymal cells from lateral plate mesoderm migrate to the site of bone formation. Once there they start to divide and aggregate toward the center without dispersing. Later they differentiate into cartilage (blue). These processes are tightly controlled by transcription factors, morphogens, cell adhesion and ECM molecules. (adapted from [63])

differentiation into chondrocytes (**Fig.8**). At the same time, cells surrounding the condensations elongate and form the perichondrium which prevents further recruitment of mesenchymal cells. The condensation process is a result of complex epithelial-mesenchymal interactions tightly regulated by growth and transcription factors and is recognised by the expression of a characteristic set of cell adhesion and ECM molecules including N-cadherin, N-CAM, fibronectin, and tenascin-c (**Fig. 8**)[63]. When pre-chondrocytes emerge in the centre of skeletal aggregates as a consequence of combinatorial signaling, they switch their expression pattern and start to express early cartilage markers such as collagen II and hyaluronan [68].

3. Chondrocyte proliferation: During the third phase (**Fig. 9**), the chondrocytes rapidly proliferate and deposit the typical cartilaginous matrix containing collagen fibrils, proteoglycans, hyaluronan and non-collagenous glycoproteins. The major proteoglycan component is aggrecan, which is bound to hyaluronan via the link protein, and forms huge aggregates in the matrix. The aggregates swell due to the hydrated nature of the proteoglycans, and are reinforced by the tense collagen network. The cartilage fibrils consist of mainly collagen II and collagen IX and XI as minor components. At the periphery of the cartilage template, cells from the inner layer of the perichondrium constantly differentiate into chondrocytes contributing to the lateral growth of the template. The coordinated cell growth and matrix deposition in both lateral and proximal-distal directions continue to enlarge and

shape the anlage, which is moulded into a central shaft (diaphysis) and club-shaped expansions at the ends (epiphyses) [65].

4. Chondrocyte hypertrophy and mineralization: In the fourth phase, chondrocytes in the central region of the avascular template stop dividing, increase their cell volume and differentiate into hypertrophic chondrocytes that express collagen X and vascular endothelial growth factor (VEGF), an angiogenesis promoting factor which can induce mesodermal mesenchymal cells to differentiate into blood vessels. Subsequently, hypertrophic chondrocytes undergo a terminal step of differentiation. The expression of collagen X is downregulated while the expression of matrix metalloproteinase-13 (MMP13), alkaline phosphatase and osteopontin is upregulated, inducing the mineralization of the cartilage matrix. Finally, the terminally differentiated hypertrophic chondrocytes die by apoptosis. At the time that chondrocyte hypertrophy is first initiated, perichondrial mesenchymal cells flanking the hypertophic core, differentiate into osteoblasts by intramembranous ossification to produce the periosteal bone collar [69].

5. Vascular invasion and ossification: In the fifth phase, the blood vessels from the bone collar invade the hypertrophic core to initiate the formation of the primary ossification center [70]. Vascular invasion delivers chondroclasts that resorb the ECM surrounding the hypertrophic chondrocytes and brings osteoblasts that lay down trabecular bone on the remnants of cartilage matrix [69, 71]. As the bone enlarges, chondrocytes stop proliferating and become hypertrophic at the epiphyses leading to the establishment of secondary ossification centres. At the surface of the epiphyses, the cartilage is not replaced by bone, remains intact and persists as articular cartilage throughout life. In long bones, chondrocytes between the primary and secondary ossification centres form the *growth plate* that ensures the longitudinal elongation of the bone.

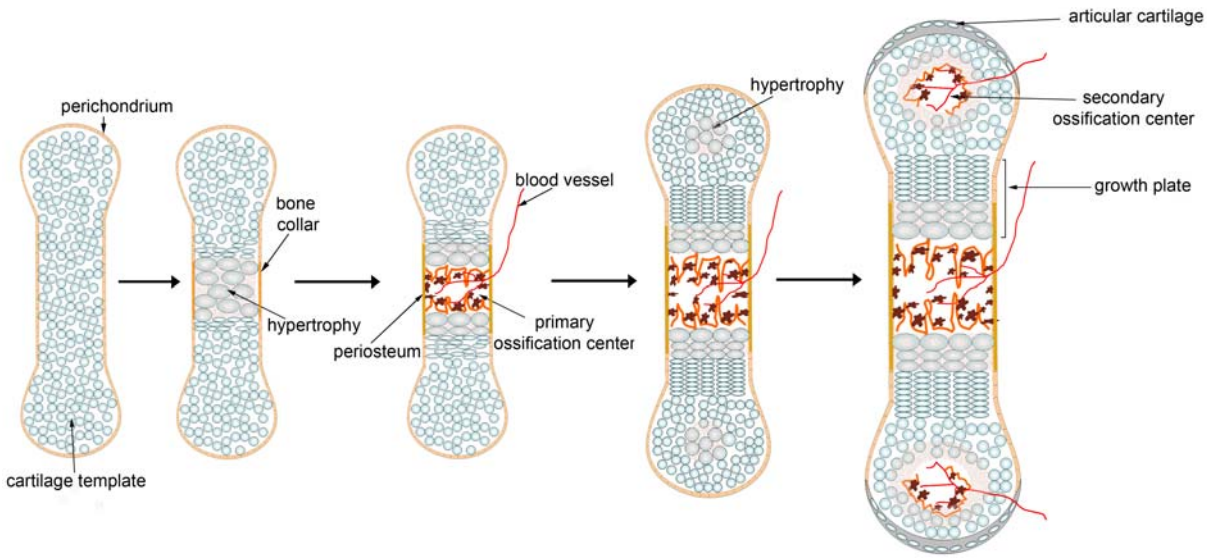

Fig.9 Endochondral ossification. Bone formation occurs during multiple steps when cartilage anlage is replaced by bone. Initially the cells in the center of the anlage undergo hypertrophy which attracts blood vessels. At this step a first ossification center establishes. Later the secondary ossification center recapitulates this process in the epiphysis.

5.2.2. The growth plate – the functional unit of endochondral ossification

Growth plate cartilage is a well-organized and specialized tissue primarily responsible for the proximal-distal elongation of the long bones during endochondral ossification. In human, the growth plate is gradually resolved after the end of puberty, while in other vertebrates (*e.g.* mice) it exists as a senescent plate between the physes throughout the adult life. During the active elongation period, growth plate chondrocytes undergo a temporally tightly controlled differentiation process accompanied by the establishment of cellular polarity that generates the unique spatial structure of the tissue. Chondrocytes in the growth plate are organized into horizontal zones, which reflect their metabolically and transcriptionally distinct stages in the differentiation program, and into vertical columns that in most vertebrates direct the elongation process (**Fig.10**). The narrow *reserve zone* (also known as the *resting zone*) is situated furthest from the ossification front and is composed of small, isotropic chondrocytes that are irregularly dispersed in the matrix. They divide very rarely and are believed to serve as stem cell-like precursors for chondrocytes in the underlying *proliferative zone*. Chondrocytes in the proliferative zone become flattened with their long axis oriented perpendicular to the direction of the longitudinal growth and undergo a clonal

expansion resulting in a characteristic columnar structure with the cells lying on top of one another. Kinetic studies revealed that cells only in the upper half of the zone are mitotically active, whereas chondrocytes in the lower proliferative zone undergo a maturation process. In addition to the rapid proliferation, chondrocytes in the upper zone synthesize the bulk of cartilage matrix mainly composed of collagen II and aggrecan. In the *prehypertophic zone*, chondrocytes begin to increase their size and express specific markers such as Indian hedgehog (Ihh) and parathyroid hormone-related peptide receptor. Most cells in this zone still deposit collagen II and aggrecan together with the hypertrophic marker collagen X. In the *hypertrophic zone*, all cells cease dividing, enlarge and become ovoid in shape. Hypertrophic chondrocytes stop expressing collagen II and deposit collagen X instead. The fates of terminally differentiated chondrocytes are controversial: while generally believed that cells at the cartilage-bone border die by apoptosis/necrosis, another theory suggests that hypertrophic chondrocytes may transdifferentiate into osteoblasts [65, 72-74].

In summary, proximal-distal elongation of the long bone is achieved by the combination of the activity and special arrangement of growth plate chondrocytes. Matrix production, cell proliferation and hypertrophy as well as the columnar alignment are the major factors that ensure growth. Although all these aspects contribute to the efficient elongation of the bone, there are important differences among vertebrates. In birds, chondrocyte proliferation is the major contributing factor for longitudinal elongation, while in mammals proximo-distal elongation mostly depend on the rate of hypertrophic differentiation [75]. Interestingly, in the bullfrog *Rana catesbeiana*, where growth plate columns are not present, bone extension is based on periosteal growth [76].

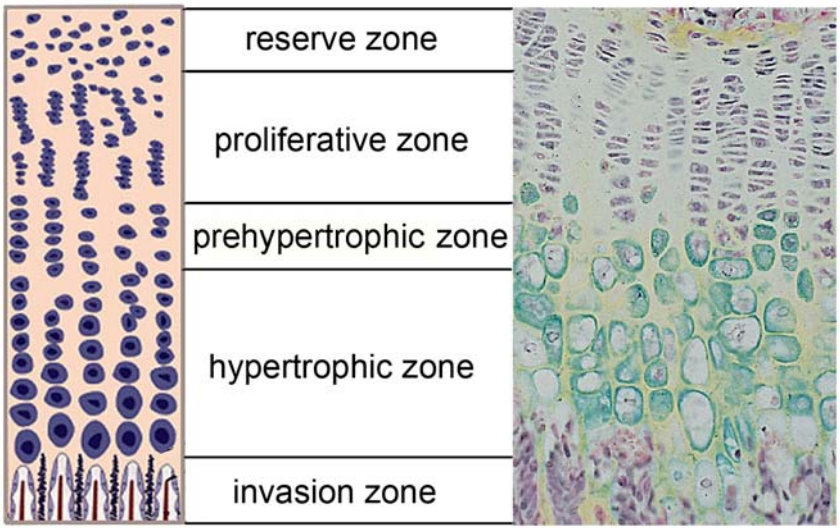

Fig.10 Growth plate architecture. *Left*: schematic diagram of the cellular organization of the growth plate. *Right:* mouse growth plate. The different horizontal zones correspond to different maturation stages of the chondrocytes.

5.2.3. Mechanism of column formation

According to the general view, early chondrocytes (chondroblasts) in the presumptive growth plate region are initially small and round (isotropic) and they elongate medial-laterally after the formation of the hypertrophic core [72, 77]. In contrast, Holmes and Trelstad have reported that the Golgi-nucleus axis of cells in the initial prechondrogenic/cartilaginous aggregates is oriented predominantly toward the proximal-distal axis of the growth suggesting that the polarity and coordinated alignment of a group of cells are established very early during cartilage development [78]. In the 1970s, several hypotheses emerged to explain chondrocyte polarity and orientation in the cartilaginous templates. In the mechanical model [79], chondroblasts situated in the cylinder-like growth plate region extensively secrete matrix which exert pressure on the cells themselves. According to this theory, the expansion of the cylinder is greater in a radial direction than along the long axis, therefore the newly synthesized matrix will flatten the cells at right angles to the long axis. Further explanations for the switch between nonoriented-oriented cellular behaviors include changes in surface properties of the aggregating cells [80], alterations in the diffusible environment of the condensations [81] and the synthesis of local morphogens by limb mesenchymal cells [82].

Once the initial chondrocyte polarity is established, the flattened (anisotropic) chondrocytes in the proliferative zone are arranged into columns oriented parallel to the longitudinal axis of the growing bone. The cells are close together implying their recent division and align their long axis perpendicular to the direction of the bone growth. Each cell is surrounded by a pericellular matrix which may merge with that of a neighboring cell. All of the chondrocytes within a clonal column together with a common surrounding territorial matrix form a chondron, the functional unit of the growth plate. Matrix between chondrons is called interterritorial matrix and histochemically resembles the territorial matrix. However in this region the collagen fibers orient in the direction of growth and organize into septa separating the individual columns.

An attempt to understand the process of column formation was made as early as 1930 by the American anatomist Dodds who observed that the rows are formed by directional divisions of discoid cells [83]. He stated that the long axis and the mitotic figures of the discoid chondrocytes are always arranged perpendicular to the direction of the bone growth. Consequently, the plane of cell division cuts orthogonal to these axes and parallel with the longitudinal orientation of the columns. Thus, following cytokinesis the two daughter cells lie side by side having a semicircular shape. Later, they adopt different wedge-shaped stages

which allow the cells to expand and glide over each other, finally achieving their flattened shape in the same vertical row [83]. Subsequently, AW Ham performed light microscopic studies on rabbit growth plates and identified additional cell division planes; however, diagonally or perpendicularly oriented chondrocyte divisions were much less abundant than the parallel ones described by Dodds [84]. More recently, the laboratory of Jeffrey Baron used transplantation experiments to ectopically place the resting zone perpendicular alongside the proliferative zone in the rabbit growth plate [85]. It was observed that the ectopic resting zone induced a 90° rotation in the orientation of the proliferative zone columns and inhibited hypertrophic differentiation. The authors, therefore, proposed that the resting zone may secrete a growth plate orienting soluble factor and a morphogen that inhibits terminal differentiation. According to their hypothesis, these factors, at least partially, are responsible for the columnar and zonal arrangement of growth plate chondrocytes.

In summary, three levels of structural organization can be observed in the growth plate: (1) flattening of the proliferative chondrocytes (cell anisotropy/polarity); (2) their alignment at a right axis to the proximal-distal direction of the growth (tissue/planar cell polarity); and (3) their columnar stacking along the long axis. Despite the importance of these processes in longitudinal growth, the exact mechanisms responsible for growth plate polarity remain unknown. However, mouse genetics revealed a plethora of intrinsic and extrinsic factors that, in addition to other functions, influence cartilage polarity. In the next chapter, these factors will be discussed in detail.

5.2.4. Regulation of growth plate morphogenesis

5.2.4.1. Transcription and diffusible factors

The Sox transcription factors. Several molecules are central for cartilage development and among them the Sry-related high-mobility group box (Sox) transcription factor Sox9 has essential roles to specify the commitment and differentiation of mesenchymal cells toward the chondrogenic lineage. In 1994, researchers have identified the human genetic disease campomelic dysplasia (CD) as caused by heterozygous mutations in the *SOX9* gene leading to hypoplasia of all endochondral elements [86]. Heterozygous mice, in which a *Sox9* allele was inactivated, die at birth and show a phenotype similar to human CD [87]. During embryogenesis, Sox9 is expressed in chondroprogenitors and chondrocytes, except hypertrophic chondrocytes, largely overlapping with the expression of collagen II (*Col2a1*). It has been shown that Sox9 binds to regulatory elements of *Col2a1*, *Col11a2*, and *Aggrecan*

and together with Sox5 and Sox6, two other members of the Sox family, activate transcription of these genes [88-90]. Inactivation of both *Sox9* alleles in mouse limb-buds prior mesenchymal condensation by using the *Prx1cre* transgene resulted in the complete absence of appendicular skeletal elements due to the lack of mesenchymal aggregations, indicating that *Sox9* is a master gene that controls mesenchyme-chondrocyte transition [91]. When *Sox 9* was ablated after mesenchymal condensation by the *Cola1cre* transgene, *Sox9$^{fl/fl}$-Col2cre* mice developed severe chondrodysplasia characterized by impaired proliferation and maturation of chondrocytes as well as the diminished expression of the Sox9 downstream targets Sox5 and Sox6 [91]. Gain of function mutants, in which Sox9 was overexpressed in chondrocytes (*Col2a1/Sox9* knock in), displayed severe inhibition of cell proliferation resulting from downregulated cyclin D expression mediated via crosstalk between Sox9 and the Wnt canonical pathway (see below) [92]. Thus, genetic approaches have clearly identified Sox 9 as pivotal factor acting in a dose dependent manner at all stages of endochondral bone formation. In addition to its multiple roles in chondrogenesis, Sox9 levels influence polarity of the growth plate. In *Sox9$^{fl/fl}$-Col2cre* mice, small groups of flattened proliferative chondrocytes were found, however they did not organized into orderly columns [91]. In *Col2a1/Sox9* knock in mice, the proliferative chondrocytes were isotropic and lacked an apparent orientation in the growth plate region [92].

The Runx transcription factors. While Sox9 is essential for mesenchymal condensation and chondrogenic differentiation, the Runt domain transcriptional activator Runx2 (previously Cbfa1) determines the commitment of mesenchymal progenitors to the osteoblastic lineage. Mice with targeted inactivation of *Runx2* die around birth and, due to the complete arrest in osteoblast differentiation, are devoid of bone [93, 94]. Mice with heterozygous *Runx2* mutation are viable and develop a phenotype similar to human cleidocranial dysplasia, a skeletal disorder characterized by open fontanelles and short stature [95]. Runx2 is expressed, in addition to the multipotent mesenchymal cells, in prehypertrophic/hypertrophic chondrocytes [96] and plays an important role in chondrocyte maturation. *Runx2$^{-/-}$* mice display arrest in hypertrophic differentiation in the proximal skeletal limb elements (femur, humerus), whereas hypertrophic differentiation is delayed only in the distal elements (*e.g.* tibia, radius) [96 97]. In contrast, *Runx2* overexpression in transgenic mice leads to accelerated hypertrophy of normal growth plate chondrocytes, further demonstrating the essential role of Runx2 in chondrocyte terminal differentiation [98, 99]. It has been shown that Runx2 directly regulates the expression of MMP-13, osteocalcin, osteopontin and osteonectin, which are characteristic markers for chondrocyte hypertrophy and bone formation [93, 100] (reviewd in [72, 101]).

Importantly, Runx2-deficiency in the humerus/femur leads to reduced proliferation and the lack of growth plate polarity since chondrocytes exhibit a rounded shape and do not organize into columns. These defects are extended to the entire limb skeleton in the *Runx2/Runx3* double knockout mice, suggesting the cooperative action of Runx family members on chondrocyte proliferation, maturation and organization [102]. The regulatory roles of Runx2/Runx3 in growth plate chondrocytes are probably mediated, directly or indirectly, via the induction of *Ihh* expression (see below) in prehypertrophic chondrocytes [102, 103].

The Ihh/PTHrP signaling pathway. Indian hedgehog (Ihh) is a secreted peptide from the hedgehog family which co-ordinates chondrocyte proliferation and the onset of hypertrophic differentiation by acting either directly on chondrocytes or in a negative feedback loop together with the parathyroid hormone related peptide (PTHrP) (**Fig. 11**) [101].

During endochondral ossification Ihh is first expressed in the centre of the aggregated cartilage templates, later its expression becomes largely restricted to the transitional zone between proliferative and hypertrophic chondrocytes (prehypertrophic zone). The secreted Ihh acts on both neighboring and distant cells by activating gene transcription via the hedgehog signaling system composed of the transmembrane proteins Patched-1 (Ptc1), Smoothened (Smo) and the downstream target Gli proteins [104]. In the absence of Ihh, Ptc1 keeps Smo in an inactive state which allows the Gli transcription factors to be processed to their repressor form. Upon binding Ihh, Ptc1 loses its repressive role on Smo leading to the processing of Gli1, Gli2 and Gli3 which, depending on the cellular context, act as either transcriptional activators or inhibitors [105]. Cyclin D1 promotes cell cycle progression through the G1/S phase and it has been shown to be expressed at a low level in the cartilage of both Ihh and Smo knockout mice indicating that cyclin D1 expression might be mediated directly by Ihh signaling [106, 107]. Ihh can also directly promote osteoblast differentiation in the perichondrium during endochondral ossification [106] as shown by the lack of bone collar in the long bones of I*hh*$^{-/-}$ mice or in mice in which Smo was conditionally ablated in perichondrial cells [108]. In addition to the direct effects on proliferation and osteoblastgenesis, the major role of Ihh in the developing cartilage is the regulation of the rate of hypertrophic chondrocyte differentiation through the stimulation of PTHrP.

During embryonic development, PTHrP is expressed by perichondrial cells and by chondrocytes at the ends of the growing cartilage (periarticular chondrocytes) [109]. Its main function is to keep the chondrocytes in a proliferative state by diffusing away from the place of synthesis and activating PTH/PTHrP receptor (PPR), which is expressed at a low level on

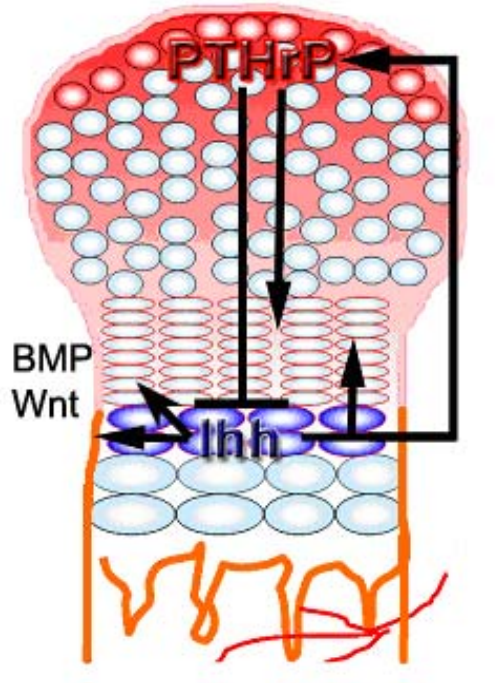

Fig.11 Ihh/PTHrP signaling. Ihh is expressed by the prehypertrophic chondrocytes (blue cells) and upregulates PTHrP expression in the periarticular chondrocytes (red cells). PTHrP diffuses back to the growth plate and stimulates chondrocyte proliferation through interaction with its receptor expressed on the proliferative and prehypertrophic chondrocytes (cells with red contour). Thus PTHrP slows down chondrocyte hypertrophy. In addition, Ihh directly stimulates chondrocyte proliferation in the growth plate (horizontal arrow), osteoblast differentiation in the perichondrium (lateral arrow) and may act independently of PTHrP on chondrocyte hypertrophy mediated by BMP and Wnt signalling (diagonal arrow).

proliferative chondrocytes and at a higher level in prehypertrophic chondrocytes, partially overlapping with Ihh expression. The prehypertrophic and hypertrophic chondrocytes which are far away from the PTHrP source stop proliferating and start secreting Ihh. Ihh signals back and activates PTHrP expression in the periarticular region, which in turn stimulates chondrocyte proliferation and inhibits hypertrophy by delaying their differentiation [110]. Ihh induces PTHrP expression either directly or indirectly through intermediate molecules such as the members of the transforming growth factor-β superfamily (TGFβs) and bone morphogenetic proteins (BMPs)(**Fig.11**) [104].

Several *in vivo* studies have demonstrated the essential role of Ihh/PTHrP crosstalk in coordinating chondrocyte proliferation and hypertrophic differentiation. *Ihh*$^{-/-}$ mice have reduced cartilage elements which are prematurely calcified and do not undergo ossification. These mice die at birth due to an insufficiently developed rib cage which causes respiratory distress. Growth plate chondrocytes do not organize into columns, they have reduced proliferation rate and undergo premature differentiation resulting in an extended hypertrophic zone. These defects are accompanied by the abolished expression of PTHrP in periarticular chondrocytes. Similarly, genetic inactivation of PTHrP or PPR in mouse cartilage leads to reduced chondrocyte proliferation and premature hypertrophic differentiation demonstrating the inhibitory role of the PTHrP/PPR pathway on chondrocyte hypertrophy. Collectively, these results imply that the Ihh/PTHrP negative feedback loop determines where chondrocytes become hypertrophic [107, 109, 111-113]. Interestingly, a more recent study

demonstrated that overexpressing *Ihh* in the cartilage of *PTHrP*$^{-/-}$ embryos accelerates hypertrophic differentiation through BMP and canonical Wnt signaling suggesting that Ihh could signal independently of PTHrP to promote hypertrophy [114]. Furthermore, upregulation of Ihh signaling in PPR-mosaic mice accelerated the differentiation of periarticular chondrocytes to columnar chondrocytes leading to the elongation of the stacks [115]. Hence, Ihh signaling also regulates the columnar cell mass independently of PTHrP.

FGF signaling. Many genetic studies have shown that fibroblast growth factor (FGF) signaling is crucial for chondrocyte proliferation and differentiation during endochondral bone formation (**Fig.12**). Several of the 22 FGF ligands and the 4 FGF receptor (FGFR) tyrosine kinase molecules are expressed during different stages of endochondral ossification. Among them, signaling via FGFR3 is the best studied and understood [116]. In human, activating mutations in the *FGFR3* gene lead to different grades of achondroplasia-like dwarfism phenotypes correlating with the degree of FGFR3 signaling activation [117, 118]. Conversely, deletion of *FGFR3* in mice leads to skeletal overgrowth due to increased chondrocyte proliferation and reduced hypertrophy [119, 120]. Altogether the existing data demonstrates that the main function of FGFR3 signaling is to limit chondrocyte proliferation and differentiation. These effects are mediated either through direct signaling in chondrocytes or indirectly by modulating the Ihh/PTHrP/BMP cascades. FGFR3 inhibits chondrocyte proliferation mainly by activating the Janus kinase-signal transducer and activator of transcription-1 (JAK-STAT1) pathway. This activation results in the nuclear translocation of STAT1 and STAT3, which induces the expression of cell cycle inhibitors such as p21 [121]. Deletion of FGF18 in mice leads to a similar phenotype to that of FGFR3 inactivation, thus identifying FGF18 as one of the important ligands for FGF signaling in chondrocytes [122, 123]. However, other FGFs such as FGF2 and FGF9 have been also reported to be involved in skeletal development. FGF9 is expressed in the apical ectodermal ridge in the limb bud and lack of its expression in mice leads to a shortening of the proximal skeletal elements. FGF9 seems to promote chondrocyte hypertrophy at early stages and to regulate vascular invasion in the growth plate as well as bone formation [124]. Mice lacking FGF2 show only a mild decrease in mineral bone density without any morphological defects in their skeleton. The expression of other FGFs might compensate for its absence [125].

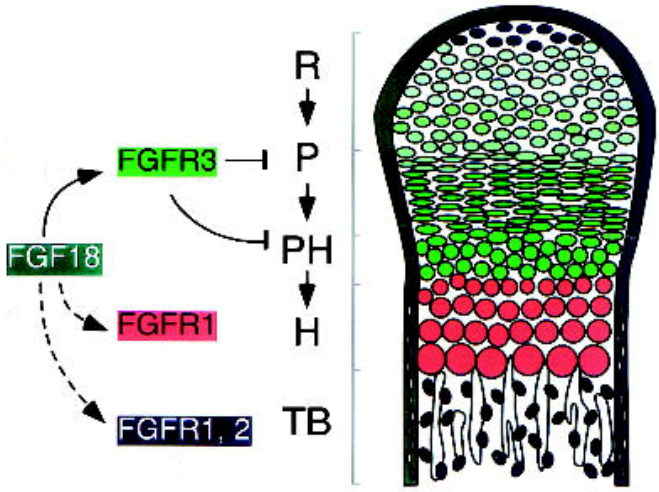

Fig.12 FGFs in cartilage [121]. FGF and FGFRs expression through different zones of cartilage GP (R-reserve, P-proliferative, PH-prehypertrophic H-hypertrophic) FGF18 is one of the most important ligands of the FGF receptors. It is expressed in the perichondrium and may signal to FGFreceptors in both chondrocytes and osteocytes. Activated FGFR3 inhibits chondrocyte proliferation and hypertrophy.

BMPs and TGFβs. Bone morphogenetic proteins (BMPs) together with the transforming growth factors β (TGFβs) form the TGFβ superfamily of secreted signaling molecules. Based on sequence similarities, BMPs are grouped into several classes including the growth and differentiation factor (GDF) subfamily[126].

The role of BMPs in bone development became obvious when they were identified as inducers of ectopic endochondral bone formation at implantation sites under the skin or in muscle [127]. BMPs act through two major types of membrane-bound serine/threonine kinase receptors: the type-I and type-II receptors [128]. After ligand binding, the active receptors form heterotetrameric molecules consisting of two type I and two type II receptors. Type II receptors phosphorylate type I receptors, which transmit the signal by phosphorylating the receptor-regulated Smad (R-Smad) 1, R-Smad5 and R-Smad8 [129, 130]. Three type I receptors are able to transduce the signal: BMP receptor types IA (BMPRIA), IB (BMPRIB) and activin receptor type I (ACTRI). Upon release from the receptors, phosphorylated R-Smads recruit and bind Smad 4 forming a heteromeric complex, which translocates to the nucleus and together with other factors activates target gene expression. For example, in cooperation with Runx2, Smad1 and Smad5 activate type X collagen expression in hypertrophic chondrocytes [131, 132]. The *Ihh* promoter contains several Smad binding elements and its expression seems to be directly controlled by BMPs [133]. Further studies have revealed that

BMPs regulate the appearance and shape of mesenchymal condensations and are involved in skeletal patterning. Many BMPs have overlapping expression patterns, for example, BMP-2, -3, -4 and-5 are expressed in perichondrium, BMP-2 and -6 are expressed in hypertrophic chondrocytes and BMP-7 is expressed both in proliferating chondrocytes and perichondrium. Thus, dissecting the roles of individual BMP molecules in skeletal development is difficult due to functional redundancy. Indeed, loss of function mutations of BMP-5, -6, -7 and GDF-5 produce relatively mild skeletal malformations [126, 134]. To overcome the problem of compensation, Noggin, a secreted antagonist of BMPs that is expressed in early cartilaginous condensations, was manipulated in vertebrate embryos. Both knockout and misexpression experiments revealed that Noggin inhibits cartilage condensation and is required for joint specification through GDF-5 [135, 136]. Further supporting the essential roles of BMPs in cartilage development, mice lacking both BMPRIA and BMPRIB during chondrogenic differentiation display only a few rudimentary skeletal elements, in which chondrocytes never organize into a columnar growth plate [137]. In addition, *Noggin* null mice have skeletal overgrowth and increased chondrocyte proliferation rate [135], whereas *noggin* overexpression leads to reduced chondrocyte proliferation and growth plate size indicating that BMP signaling acts at several steps of endochondral ossification. Additional studies have shown that BMPs likely oppose the effects of FGFs and synergize with the Ihh/PTHrP pathway on chondrocyte proliferation and differentiation [138, 139].

TGFβs are synthesized and assembled into an inactive complex with latency-associated peptide (LAP) and latent TGFβ binding protein (LTBP). This complex is deposited into the ECM and, upon proteolytic cleavage or pH changes TGFβ is released and can bind to its receptors. Similar to BMPs, TGFβs act through heterotetrameric receptors which activate the downstream targets Smads 2 and 3. Active Smads interact with the common Smad4 forming a complex which is translocated to the nucleus to activate gene transcription [140]. TGFβs are expressed in prehypertrophic and hypertrophic chondrocytes, in the perichondrium, in osteoclasts and in osteoblasts but their role in growth plate function is not yet clear [141, 142]. Explant culture experiments demonstrated the importance of TGFβ2 in the perichondrium to mediate Ihh regulation of PTHrP [143], and the expression of a dominant negative type II receptor causes postnatal defects of the growth plate characterized by increased collagen X and Ihh expression in the hypertrophic chondrocytes [144]. However, TGFβ2 knockout mice have a much milder skeletal phenotype than $Ihh^{-/-}$ or $PTHrP^{-/-}$ mice, indicating that TGFβ2 is only moderately involved in the regulation of the Ihh/PTHrP loop *in vivo* [145].

Wnt signaling pathways. Wnt signaling is another fundamental regulatory system used by chondrocytes (**Fig. 13**). The Wnt signaling network comprises the Wnt secreted ligand molecules, specific receptors, antagonists and a large number of intracellular effectors. Three major branches are activated downstream of Wnt receptors at the level of Dishevelled (Dsh/Dvl): the canonical signaling and two non-canonical pathways. The central line of the canonical Wnt cascade is the regulation of the stability of its core component, β-catenin, through a cytoplasmic destruction complex which includes Axin, adenomatous polyposis coli (APC), and glycogen synthase kinase 3β (GSK-3β). In the absence of Wnt signals, β-catenin is captured and N-terminally phosphorylated by the destruction complex, ubiquitinated and targeted to the proteosome. Upon Wnt binding to the receptor complex composed of members of the Frizzled (Fzd) family of seven transmembrane receptors, serpentine receptors and low density lipoprotein receptor-related proteins (LRPs), the activated signaling molecule Dvl inhibits the Axin/APC/GSK-3β complex which is disassembled through the binding of Axin to phosphorylated LRP5/6. Consequently, the free cytoplasmic β-catenin can translocate to the nucleus where it regulates target gene expression through the interaction with the T cell-specific transcription factor/ lymphoid enhancer-binding factor (TCF/LEF) family of transcription factors (reviewed in [146-148]).

The non-canonical pathways are β-catenin independent. Upon activation, the signal can diverge into the Wnt/Ca^{2+} pathway and the planar cell polarity (PCP) pathway. In the Wnt/Ca^{2+} pathway, Wnt binding to Fzd/LRP stimulates intracellular Ca^{2+} release, which leads to the regulation of cell adhesion via the activation of protein kinase C (PKC) and calmodulin-dependent protein kinase C (CaMKII) [149, 150]. In the PCP pathway, Fzd activates the JNK cascade that directs cytoskeletal asymmetry and polarization of cells within a tissue plane. Beside the Fzd receptors and the regulator Dvl, the core molecules of the PCP pathway include Flamingo (FMI, STAN), Strabismus (STBM, VANG), Diego (DGO) and Prickle (PK) which are recruited to the membrane and antagonistically regulate Dvl activity: upon signaling, the Fz-Dvl-DGO complex promotes Dvl activation, whereas the STBM-PK complex limits Dvl activation. Some of the molecules which are activated downstream of Dvl are inturned, fuzzy, Rac1, RhoA, and Rho kinase. In vertebrates, PCP signaling plays important roles in morphogenetic processes such as convergent-extension movements or the alignment of stereocilia bundles in the organ of Corti [151].

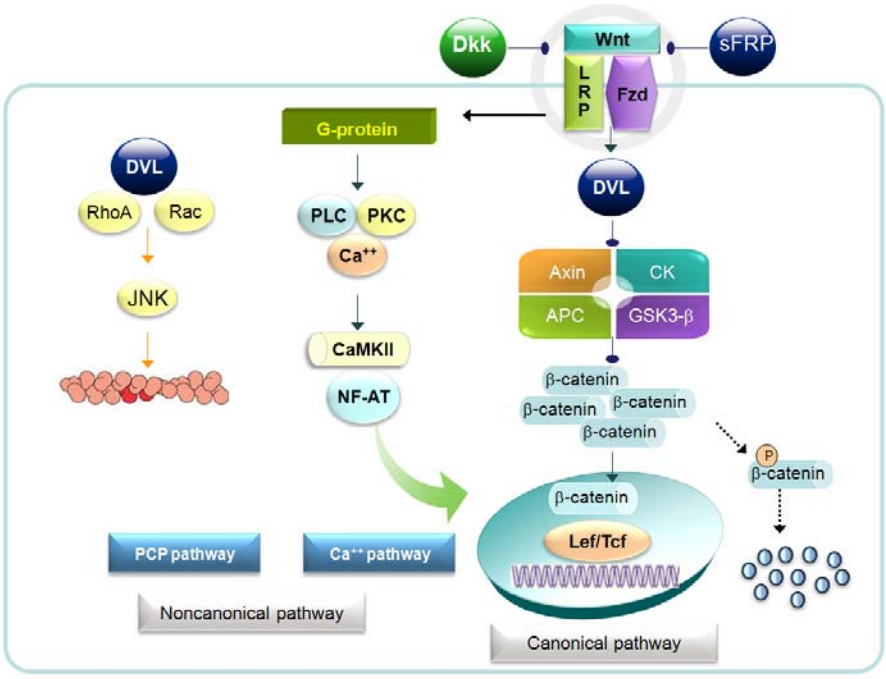

Fig.13 Canonincal and noncanonical Wnt signaling pathways [152]. Wnt ligands binding to their receptors can activate the β-catenin-dependent canonical pathways or the β-catenin-independent non-canonical, PCP or Ca pathways.

Several recent experiments using conditional loss- and gain-of-function mutations of β-catenin in mice explored the important role of canonical Wnt signaling in skeletogenesis. Deletion of β-catenin in skeletal progenitors by *Prx1cre* or *Dermo-cre* results in arrested osteoblast maturation, increased chondrogenesis and ectopic cartilage formation [153-155], while gain-of-function mutations of β-catenin in osteo-chondroprogenitors leads to a block in chondrogenesis [154]. In vitro, β-catenin-deficiency increases the expression of Sox9 and induces precocious chondrogenic differentiation in micromass culture, whereas β-catenin activation mutations reduce Sox9 level and suppress chondrogenesis [154]. These data indicate that the canonical Wnt/ β-catenin pathway negatively regulates chondrocyte differentiation from mesenchymal progenitor cells. Furthermore, mice with stabilized β-catenin in chondrocytes display reduced proliferation and delayed hypertrophic differentiation accompanied by the loss of growth plate polarity. These defects phenocopy the abnormalities of mice overexpressing Sox9 in chondrocytes suggesting direct genetic interaction between the two signaling systems [92]. Furthermore, it has also been shown that β-catenin binds to the C-terminal transactivation domain of Sox9, and this interaction controls the relative levels of both Sox9 and β-catenin, which in turn regulates chondrocyte differentiation and survival [92]. Finally, it has been demonstrated that β-catenin signaling acts downstream from Ihh during

osteoblast differentiation, while β-catenin acts upstream of Ihh to inhibit chondrocyte apoptosis [156].

In contrast to the Wnt/β-catenin pathway, the roles of noncanonical cascades in skeletogenesis are less well defined. Wnt5a is a representative of the noncanonical pathways-activating Wnts and its dysfunction leads to dysregulated convergent extension during vertebrate gastrulation [157]. In the developing limb, Wnt5a inhibits the canonical pathway by promoting β-catenin degradation [158]. It was shown that Ror2, an alternative Wnt receptor, is required for Wnt5a effects on both the noncanonical and canonical signaling pathways [159, 160]. Mice lacking or overexpressing Wnt5a in chondrocytes exhibited defects in chondrocyte proliferation, differentiation and growth plate polarity [161]. Ror2-deficient mice display similar skeletal phenotypes [160, 162] indicating the importance of noncanonical Wnt/frizzled signaling in growth plate morphogenesis. Corroborating evidence has come from a recent study in which the members of the noncanonical Fzd pathway were manipulated in retroviral-infected embryonic chick legs [163]. Disruption of the noncanonical pathway by overexpressing a truncated form of Fzd7, which blocks frizzled signaling, resulted in chondrocyte misorientation in the proliferative zone, whereas the expression of constitutively active CamKII led to chondrocyte rounding.

These data collectively show that canonical/noncanonical Wnt pathways have both positive and negative regulatory effects on cartilage development. However, further studies are required to fully understand the roles of Wnt signaling network during skeletogenesis [150, 152].

5.2.4.2. The primary cilium and endochondral bone formation

Cilia (or flagella) are specialized organelles that project from the surface of most eukaryotic cells. They originate from the plasma membrane-associated basal body during interphase and are made of microtubule-based axoneme surrounded by a bilayer lipid membrane. Axoneme are generated through the process of intraflagellar transport (IFT), a bidirectional transport system mediating the movements of large protein complexes (IFT particles). The anterograde transport directs structural components from the cell body to the axoneme driven by kinesin-2 motors, whereas the retrograde transport returns proteins from the cilium driven by a dynein motor. Cilia can be classified as “motile” characterized by an axoneme consisting of nine doublets of microtubules arranged around a central microtubule pair (9+2), or as "non-motile” or primary cilia, which lack the central microtubule pair (9+0). Primary cilia function as cellular antennae that sense a broad range of chemical and

mechanical signals important for smell, sight and mechanoreception. Defects in their normal structure and function are associated with congenital human syndromes with multiple defects in kidney, retina and skeleton. The mechanical function of the cilium was studied mostly in kidney cells. It has been shown that cilia on renal cells play a role in transmitting mechanical signals by sensing fluid shear stress and responding with changes in the concentration of cytosolic Ca^{2+}. Defective Ca^{2}+ channel proteins policystin-1 and -2, which are localized in the cilium membrane fail to transmit essential signals for normal renal cell polarity, growth and differentiation, and mutations in either genes (*PC1* or *PC2*) cause polycystic kidney disease [164, 165].

The chondrocyte has an immotile cilium, which was proposed to bend in response to mechanical forces transmitted through the cartilage ECM [166]. Confocal microscopy studies suggest that cilia on columnar chondrocytes originate from the center of the cell between Golgi and nucleus [166]. Mathematical studies have attempted to describe a certain pattern in cilium orientation in different types of cartilage [167], however strictly polarized cilia alignment was not verified experimentally.

The importance of primary cilia in transmitting chemical signals was revealed relatively recently in mice lacking components of IFT. The defects all converged onto abnormal hedgehog signaling, suggesting that cilia coordinate Hh functions in mammals [168, 169]. Indeed, several components of Hh signaling including the Smo/Ptc1 complex and Gli proteins are localized to the cilia [170]. In the absence of Shh or Ihh, Smo is localized on intracellular vesicles and its function is repressed by Ptc1. At the same time, transcriptional repressor forms of Gli proteins move from the cilium into the nucleus and silence Hh transcription. In the presence of Hh proteins, Ptc1 leaves the cilia allowing the accumulation of active Smo in the cilium, which in turn activates gene transcription through the transcriptional activator forms of Gli proteins [171].

The strong connection between cilia function and Ihh signaling during endochondral bone formation is reflected in the skeletal phenotype of mice with mutations in IFT components. Mice with a conditional ablation of *Ift88* (intraflagellar transport protein 88/Tg737/polaris), a core component of IFT particles, or *Kif3a* (a subunit of heterotrimeric kinesin 2 motors involved in anterograde transport) show several abnormalities during endochondral ossification depending on the time of deletion. When *IFT88* or *Kif3a* were deleted in the osteo-chondroprogenitors of early limb bud, mice had short bones associated with accelerated hypertrophic differentiation, delay of vascular invasion and the lack of bone collar [172]. In addition, Ptc1 and Gli expression was reduced both in the perichondrium and in

the chondrocytes indicating disrupted Ihh signaling. When deletion of *Ift88* and *Kif3a* was restricted to chondrocytes by using the chondrocyte-specific *Col2a1cre* transgenic line, the embryonic development of long bones was surprisingly normal but starting from postnatal day 7, the mutant growth plates showed signs of degeneration. By postnatal days 10, the columnar organization of the proliferative zone was severely altered characterized by chondrocyte rounding and column misorientation, which was accompanied by altered pFAK localization and an abnormal actin cytoskeleton. The observed defects were apparently independent of Ihh signaling suggesting an additional function of the cilia in maintaining the columnar organization after birth [173]. Cilia were proposed to interact with the ECM through β1 integrins, which have been localized to the cilia in chondrocytes [174]. These findings corroborated in vitro studies showing defects in adhesion and spreading of renal epithelial cells lacking ciliary proteins, raising the possibility of a link between primary cilia and integrin mediated adhesion [166].

Besides the role in hedgehog signaling, several studies have attributed a role for cilia in the planar cell polarity pathway. Two proteins which are known to be essential for ciliogenesis, inversin and Bardet-Biedl Syndrome protein 4 (BBS4) were implicated in PCP signaling [175, 176]. Worth noting, the inactivation of two PCP effectors encoded by the *Inturned* and *Fuzzy* genes leads to defective ciliogenesis in the amphibian *Xenopus laevis*. As a consequence, the mutant embryos exhibited a phenotype which reflects a failure of hedgehog signaling due to lack of primary cilia. Importantly, the PCP-dependent convergent extension movements of cells of the Meckel's cartilage were disrupted resulting in the loss of columnar structures. This observation was consistent with the phenotype caused by the dominant-negative PCP-specific mutants dishevelled and Frizzled 8 [177]. It seems that both Inturned and Fuzzy control the assembly of an apical actin network that is essential for normal orientation of ciliary microtubules. However, the exact mechanisms involved in PCP/ciliogenesis crosstalk are not completely understood.

5.2.4.3. The impact of ECM proteins on cartilage development

Cartilage is characterized by an elaborated and complex ECM, which is secreted by a relatively low number of chondrocytes. The ECM contains collagens, proteoglycans, and non-collagenous glycoproteins that are organized into specific marcromolecular assemblies providing the tissue with its specific mechanical properties such as mechanical strength and elasticity. Furthermore, the cartilage ECM gives a physical framework for chondrocytes and

serves as storage source of growth factors and morphogens. Several lines of evidence suggest that collagen fibrils and proteoglycan aggregates contribute essentially to the establishment and maintenance of normal growth plate structure. The homotrimeric collagen II accounts for about 95% of the total collagen content in hyaline cartilage. Mutations in the *COL2A1* gene encoding collagen II leads to various hereditary skeletal disorders in human with severity ranging from moderate to lethal. Mice lacking collagen II die at birth and develop a cartilaginous skeleton without significant endochondral bone formation [178]. Although, the chondrocytes deposit collagen I instead of collagen II, the collagen fibrils are sparse and not organized into a network [178]. Interestingly, *Col2a1*-null proliferative zone chondrocytes are flattened and oriented properly in early (E13-E14) cartilage templates (A. Aszodi unpublished information). At later stages, however, the chondrocytes become disoriented and never organize into columns [178]. Similarly, the naturally occurring *cho*/*cho* mice, harbouring a premature stop codon at the N-terminal region of the α1(XI) chain of collagen XI, die at birth due to breathing difficulties and display a reduced number of abnormally thick fibrils in the cartilage matrix leading to a severely disorganized growth plate with no columns [179]. Mice with a targeted inactivation of the *Col9a1* gene encoding the α1 chain of collagen IX are viable but develop degenerative changes of the articular cartilage [180]. Although growth plate abnormalities were not reported in the original publication, recent studies indicate age-dependent disorganization of the proliferative zone [181 182]; (A. Aszodi unpublished). While the initial elongation and alignment of chondrocytes is normal in *Col9a1*$^{-/-}$ embryos, newborn mice exhibit rounded and misoriented cells that become normalized again in 8-weeks old animals. Taken together, these mice imply that the collagen network is not required for the establishment of early growth plate polarity, but they are necessary for its stabilization and for columnar alignment of chondrocytes.

The lack of functional aggrecan in the spontaneous mutant *cmd/cmd* mouse strain leads to perinatal lethality owing to cleft palate and severe impairment of endochondral bone formation characterized by compression of the cartilage ECM, disorganization of the growth plate and alterations in the expression pattern of cartilage specific genes [183, 184]. The binding of aggrecan to hyaluronan is stabilized by the link protein, a glycoprotein showing structural similarities to the G1 domain of aggrecan. Link protein knockout mice display similar but milder chondrodysplasia than *cmd* mice. Newborn mutants have abnormal growth plate with a proliferative zone lacking columnar structures and intermingled prehypertrophic and hypertrophic zones [185]. Perlecan is a heparan-sulfate proteoglycan which is present in the growth plate as well as in the articular cartilage. Perlecan null mice die at two stages: at E

10.5-12.5 due to basement membrane defects and perinatally due to respiratory failure caused by severe chondrodysplasia. The growth plate of the mutants is disorganized associated with impaired chondrocyte proliferation, differentiation and endochondral bone formation [186, 187].

5.2.4.4. Integrin expression and function during endochondral ossification

The ECM receptors on chondrocytes include integrins, syndecans and hyaluronan receptor, CD44. The integrins expressed on growth plate or articular cartilage chondrocytes are the collagen receptors α1β1, α2β1 and α10β1; the RGD receptors α5β1, αvβ3 and αvβ5; and the laminin receptor α6β1. The roles of integrins in cartilage development were first studied in culture systems. In high density micromass culture, which recapitulates several steps of chondrogenesis, β1 integrin blocking antibodies were shown to prevent the formation of cartilaginous nodules implying that integrins may be important for the transition from mesenchymal cells to chondrocytes [188]. In chicken sternal organ culture, blocking β1 integrin resulted in reduced growth, increased apoptosis and abnormal organization of the actin cytoskeleton [189].

A major breakthrough in understanding the roles of β1 integrin during skeletogenesis came from a genetic study of mice in which β1 integrin was deleted in chondrocytes using the *Col2a1cre* transgene [190]. β1 integrin-deficient mice develop severe chondrodysplasia leading to perinatal lethality of most mutant animals. The major phenotypes of the $\beta^{1fl/fl}$-*Col2a1cre* mice can be summarized as follows:

1) *Destroyed growth plate polarity.* The columnar arrangement of proliferative chondrocytes was completely missing in the mutants accompanied by cell rounding. The defects in chondrocyte shape and rotational movements are probably the consequence of loss of adhesion to collagen II, to laminin and, partially, to fibronectin.

2) *Abnormal actin cytoskeleton.* The role of β1 integrin in actin network remodelling was demonstrated by the inability of mutant chondrocytes to spread and form proper stress fibers when cultured in vitro. In addition, β1-deficient chondrocytes in vivo displayed a punctuated cortical actin network, while control cells had an even cortical actin distribution.

3) *Cytokinesis defect*. Mutant cartilage contained increased number of chondrocytes in the G2/M phase of the cell cycle which were frequently binucleated indicating a defect in cytokinesis. During cell division, both adhesion-generated pulling forces and actomyosin ring constriction at the cleavage furrow are required to separate the two daughter cells. Thus

reduced adhesion and the abnormal actin network observed in the β1-null cells might account for defective cytokinesis of chondrocytes. Interestingly, a very recent study suggests that Rab21-mediated trafficking of integrins to and from the cleavage furrow is necessary for normal cell division providing adhesive and signaling cues during telophase [191].

4) *Reduced chondrocyte proliferation and increased apoptosis*. BrdU incorporation assay and cyclin D expression analysis demonstrated progressive proliferation defects, whereas TUNEL assay showed a slightly increased apoptotic rate in the mutant cartilage. A significant portion of β1-null chondrocytes exhibited impaired G1/S transition probably caused by increased Fgfr3 expression, which in turn increased the nuclear translocation of Stat1/Stat5 and elevated the expression levels of cell cycle inhibitors p16 and p21.

5) *Abnormal collagen matrix assembly.* Electron microscopy of mutant limb cartilage specimens showed a reduced density of collagen fibrils in the proliferative and hypertrophic zones compared with that of controls. Moreover, collagen fibrils assembled in bundles of variable diameter, implying that β1 integrins control collagen fibrillogenesis.

6) *Cartilage differentiation*: β1-deficient growth plates have decreased hypertrophic but increased prehypertrophic zones as shown by Collagen X, Ihh and PTHrP localization. The underlaying mechanisms of the differentiation defect are not completely understood but β1-matrix interactions may directly control hypertrophic differentiation or the disorganized matrix network could affect diffusion of soluble morphogens important for this process.

Collectively, these findings clearly demonstrate that β1 integrin-mediated adhesion plays crucial roles in cartilage morphology and function regulating chondrocyte proliferation, survival, differentiation, cytokinesis and ECM assembly. The importance of integrins in endochondral bone formation was further demonstrated by two additional genetic studies. Mice deficient in the major collagen-binding integrin α10β1 are viable but develop progressive growth retardation [192]. α10-null mice exhibit defects in chondrocyte/growth plate polarity, cell proliferation and survival as well as in collagen fibril distribution resembling the abnormalities of the $\beta^{1fl/fl}$-*Col2a1cre* mice, however, the defects are milder suggesting a partial redundancy among the various β1 integrin heterodimers expressed on chondrocytes. Integrin-linked kinase (ILK) is associated with the cytoplasmic domain of β1/β3 integrins. Cartilage-specific deletion of ILK also results in "β1 null-like" abnormalities suggesting that integrin signaling through ILK may contribute to the skeletal phenotype of $\beta^{1fl/fl}$-*Col2a1cre* mice [193].

5.3. The articular cartilage

Diarthroidal joints ensure load transmission within skeletal structures and coordinate their movement. Diarthroidal joints unite different types of tissues to exert their specific functions: the opposing bones are covered with articular cartilage and are separated by a joint cavity enclosed in a capsule linking the skeletal elements. The capsule is lined by a synovial membrane (synovium) that secretes synovial fluid which lubricates and provides nutrition to the joint's components. Most capsules are strengthened by tendons and ligaments which can be arranged around the capsule or can be found inside the joint like the cruciate ligaments of the knee joint [194].

Below, a brief overview of the normal and diseased articular cartilage will be presented. More detailed information can be found in our recent review presented as Paper II.

5.3.1. Morphology of the normal articular cartilage

Articular cartilage (AC) is a specialized, type of hyaline cartilage, which covers the ends of the long bones and persists for the entire life of the organism [195]. It functions as a load bearing tissue and can resist shearing forces and friction [196]. AC is characterized by a high degree of anisotropy and is divided into four zones with distinct organization of the matrix and cells: the superficial (tangential), intermediate (transitional), deep (radial) and calcified zone (**Fig. 15**). *The superficial zone* is the thin, outermost layer of cartilage facing the joint cavity. It contains densely packed collagen fibrils arranged parallel to the surface and a layer of flat cells, which elongate in the same direction as the fibrils. The chondrocytes of this zone synthesize less aggrecan but more small proteoglycans such as biglycan and decorin. The *intermediate zone* contains individual spherical cells and a relatively disorganized collagen network. This zone stains intensively with cationic dyes due to its high chondroitin sulphate concentration. In the *deep zone* the chondrocytes tend to organize into chondrons oriented perpendicular to the surface resembling the columns of the growth plate. The extracellular matrix is rich in proteoglycans and the collagen fibrils form radial bundles which extend into the calcified zone. The *calcified zone* is a physical and mechanical barrier between cartilage and subchondral bone and its main function is to anchor the cartilage to the bone. It consists of mineralized matrix containing collagen X and hypertrophic chondrocytes and is separated

from the noncalcified upper zones by a tidemark, which represents the mineralization front [194, 196, 197].

The specific biomechanical function of the articular cartilage is confined to the structure and organization of the matrix molecules produced by a sparse population of cells. The structural scaffold, which confers strength and resilience, is composed of a fibrillar network of collagens, mainly collagens II and XI and the associated collagens IX and VI [198]. The collagen network entraps proteoglycans (*e.g.* aggrecan) rich in polyanionic glycosaminoglycan chains, which creates an osmotic pressure that draws water into the tissue and expands the collagen network [199]. Several noncollagenous proteins such as fibronectin, cartilage oligomeric matrix protein protein (COMP), decorin, biglycan, matrilins, fibromodulin, cartilage intermediate layer protein (CILP), chondroadherin and others are required for the proper assembly of this complex network (**Fig.15**). The correct balance between tensile strength and osmotic pressure conferred by the collagen and proteoglycans, respectively, are essential for AC physiology. Therefore the continuous and tightly controlled metabolism of the matrix is the main task of the chondrocytes, which can respond to direct biomechanical perturbations by secreting various matrix remodelling and signaling molecules [200].

Proteolysis of the ECM is a normal feature of cartilage remodelling and several enzymes are implicated in this process including metalloproteinases (MMPs) and aggrecanases. In cartilage, MMP-13 is the major collagenase, which is able to degrade the native collagen triple helix, whereas MMP-2 and -9 (gelatinases) further degrade the predigested collagen fragments. MMP-3 (or stromelysin) together with ADAMTS (a disintegrin and metalloproteinase with trombospondin motifs) -4 and -5 are the major aggrecan degrading enzymes in AC. An imbalance in the anabolic and catabolic activities of the cartilage leads to various pathological conditions, including osteoarthritis [201].

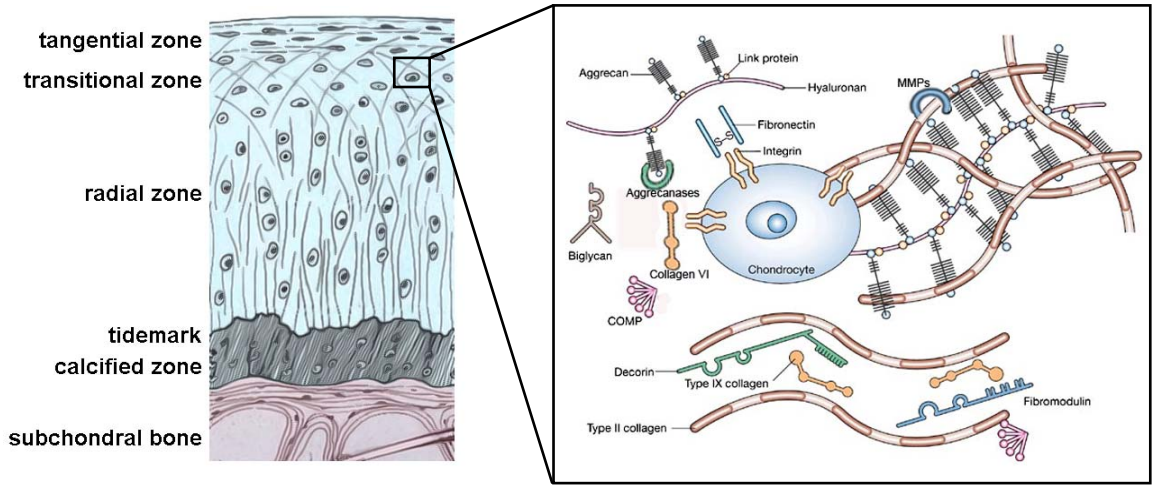

Fig.15. Articular cartilage organization and the principal components of the ECM [202]. AC is composed of chondrocytes and ECM organized into distinct morphological and functional zones. Three classes of proteins exist in AC ECM: collagens (mostly type II collagen); proteoglycans (primarily aggrecan); and other noncollagenous proteins (including link protein, fibronectin, cartilage oligomeric matrix protein) and the smaller proteoglycans (biglycan, decorin and fibromodulin)

5.3.2. Osteoarthritic articular cartilage

Osteoarthritis (OA) is a common, age-associated disease that causes significant functional impairment, pain, inflammation, stiffness and loss of mobility in the elderly. It is characterized by degeneration of AC, which in more advanced cases is accompanied by limited intra-articular inflammation with synovitis (inflammation of the synovial membrane) and in the worst cases by cartilage erosion and exposure of subchondral bone [203, 204] (**Fig. 16**). There are several factors involved in OA aetiology: aging, genetic factors, obesity, gender and biomechanical stress [203, 204]. These factors alone or in combination can initiate the disease through the activation of stress induced pathways, cytoskeletal changes and, in case of aging, production of reactive oxygen species (ROS) and accumulation of advanced glycation products (AGEs) [204]. Although the articular cartilage is thought to be the central tissue for the initiation and the progression of OA, the other elements of the joints (synovial membrane, ligaments and tendons, and subchondral bone) contribute equally to the disease process [205].

The first, morphological indication of pathological changes is the appearance of small lesions in the superficial zone of AC associated with increased denaturation and loss of type II collagen fibrils. As a consequence of the damaged collagen network, the entrapped proteoglycans such as aggrecan, decorin and biglycan are depleted from the matrix, ultimately

leading to biomechanical and functional impairment of the AC. However, the exact order in which an ECM component (collagen network or proteoglycans) is degraded is still controversial. The initial damage is causeing an increase in MMP activity, which amplifies further ECM degradation. The chondrocytes sense AC destruction through their numerous ECM receptors and attempt to repair the lesion by increasing their anabolic and catabolic activities. The change in their metabolic status is accompanied by a change in the repertoire of gene expression: growth factors such as insulin growth factor-1 (IGF-1), proinflammatory cytokines (interleukin-1, -6, tumor necrosis factor-α), and nitric oxide synthase are upregulated in osteoarthritic cartilage. Furthermore, ECM molecules atypical for AC such as collagen I and III are synthesized by the chondrocytes during the progression of OA. In addition, ECM degradation products (fibronectin and collagen fragments) further stimulate the chondrocytes to produce MMPs through cell surface receptor signalling (see below). Despite the increase in anabolic activity, the metabolic balance favours catabolism and the attempt by chondrocytes to repair the cartilage is unsuccessful, leading to further cartilage damage [204, 206-208]. In the calcified zone, a series of additional pathological changes occur: tidemark duplication and the presence of fibrous cartilage that often advances into the non-calcified regions. The changes described above cause the softening of the cartilage and wearing and tearing produce deeper lesions in the cartilage and eventually complete AC erosion [209]. Although OA is not an inflammatory disease, the synovium often becomes inflamed as a result of cartilage breakdown. Synovitis is usually confined to areas close to the cartilage and can further accelerate cartilage damage in OA by producing proinflammatory cytokines capable of inducing MMPs expression [204].

As the cartilage breaks down, changes occur in the underlying bone, which thickens to form bony outgrowths, or osteophytes, that usually appear at margins of the joint. It is still controversial if these structures are beneficial or harmful: they may help to stabilize the joint or they may cause more pain and damage to the innervated neighbouring tissues (synovium, joint capsule, ligaments and meniscus). Osteophytes are formed through a process which recapitulates endochondral ossification under the control of TGFβ and bFGF signaling. In advanced stages of OA, necrosis of the bone occurs which lead to presences of the cysts in subarticular bone [204, 209].

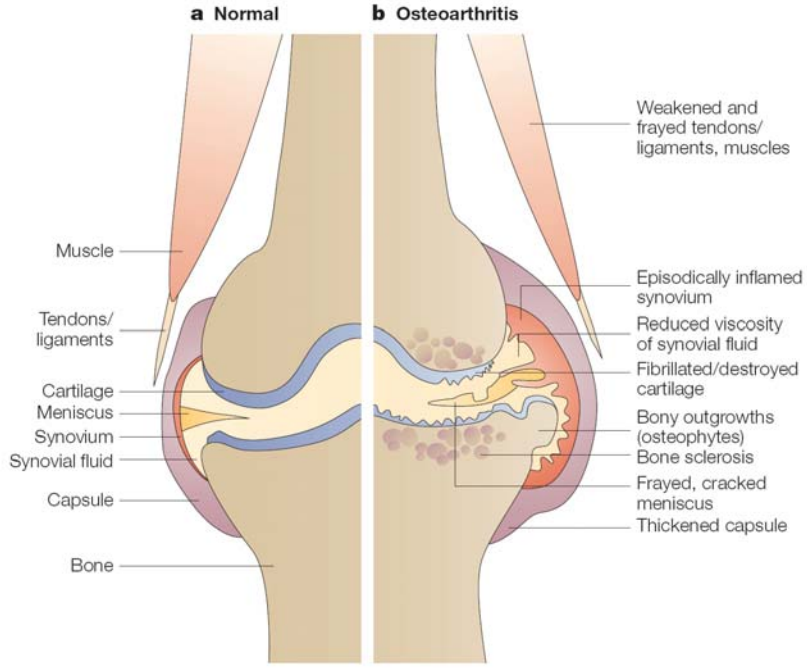

Fig.16. Normal and osteoarthritic cartilage [209]. Fibrillated cartilage, bony outgrowth, subchondral sclerosis as well as synovial inflammation are common features of osteoarthritis.

5.3.3. The role of β1 integrin in articular cartilage functions

Integrins are the major ECM receptors on AC chondrocytes that are believed to act both as signal transducers and as mechanoreceptors responding to physical forces exerted through the matrix. Despite their anticipated importance, our knowledge about the actual roles of integrin-mediated adhesion and signaling in AC physiology is limited. To date, only a few studies have attempted to address this important question. The collagen binding α1β1 integrin is expressed at a low level on chondrocytes of the normal AC but its expression is up-regulated during OA suggesting that α1β1 may be involved in repair processes. Indeed, mice lacking the α1 subunit display early onset osteoarthritis characterized by increased MMP-2 and -3 expression, proteoglycan loss, synovial hyperplasia and reduced cartilage cellularity [210].

Numerous reports have shown that fibronectin (FN) and collagen fragments are released in arthritic cartilage as a result of increased catabolic activity and these fragments can further mediate joint destruction. Treatment of cultured synovial fibroblasts with the central, cell-binding 120kDa FN fragment or with blocking antibodies to α5β1 integrin was shown to

stimulate expression of MMP-1 and MMP-3[211]. Similarly, when the 120 kDa FN fragment or activating antibodies against α5β1 or α2β1 were added to primary human chondrocytes, the expression of MMP-13 was upregulated. Mechanistically, the activation of α5β1 integrin induces PKC-delta, which in turn phosphorylates the non-receptor tyrosine kinase PYK2 [212], resulting in increased MAP kinase signaling and increased phosphorylation of c-jun and nuclear factor-κb inhibitor [213]. Moreover, treatment with antisense oligonucleotides to α5 reduced the ability of bovine chondrocytes to degrade proteoglycans in response to 120kDa cell-binding, 29kDa heparin binding or 50kDa gelatine binding FN-fragments [214]. Beside degradation fragments, collagen itself is able to induce MMPs expression upon integrin binding. In the chondrogenic cell line MC615, type I collagen stimulates expression of MMP13 via the activation of ERK and JNK MAP kinases. In the presence of blocking antibodies against the α1 or β1 subunit the induction of MMP13 expression is inhibited [215].

Taken together, the upregulation of MMPs expression in response to matrix products suggests an amplifying effect of integrin-mediated interactions in OA progression. However, the contradictory results from in vivo and in vitro experiments call for more detailed analysis of integrin signaling during OA.

5.4. Atomic force microscopy (AFM)

The first atomic force microscope (AFM) was developed in 1986 by Binnig. AFM is an unconventional microscope because it does not use any lenses to create an image. Instead, a sharp stylus at the end of a long cantilever detects the contours of an object as the tip scans over the sample. Cantilever deflection is monitored by a fine laser beam that is reflected at distal end of the cantilever and whose motion is registered by a position-sensitive photo-diode (**Fig.17**). In high resolution imaging, the force between the tip and the sample is kept constant and as small as possible to minimise sample deformation. Thus the AFM senses the sample surface height as a function of position producing a quantitative 3D map of the surface from the mm to the nm scale.

Indentation-type (IT) AFM it is used to measure the mechanical properties of a sample, for example its compressive stiffness. When AFM is operated in the force mode, the specimen is pushed against the tip by the position transducer while monitoring the deflection of the cantilever. Depending on the stiffness of the specimen, the indentation of the tip into the sample is more or less deep for a given Z-displacement of the position transducer. In this way, the stiffness (or dynamic elastic modulus) of the sample can be calculated from a "displacement-deflection" curve. The steeper the "displacement-deflection" curve the stiffer the sample [216].

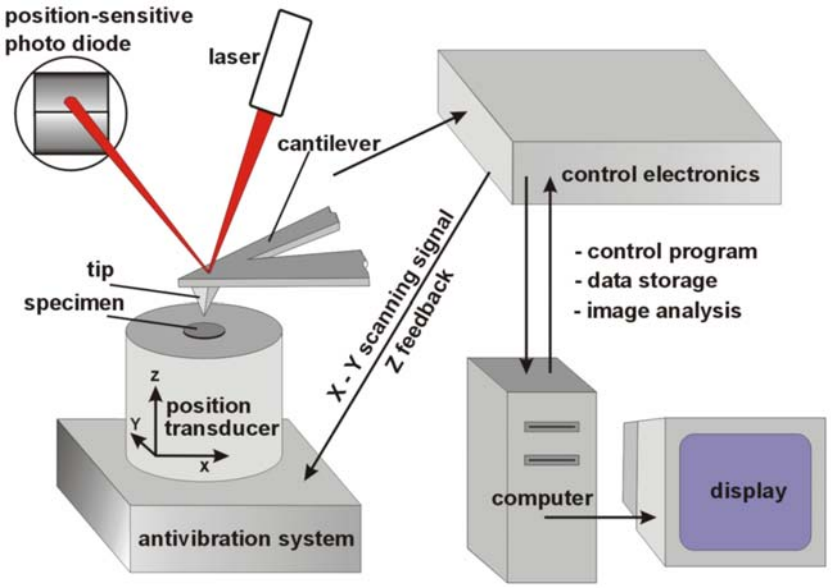

Fig.17. Principle of atomic force microscopy (courtesy of Dr. Martin Stolz)

IT-AFM was recently proven to be a valuable tool in evaluating biomechanical properties of the cartilage. Normal and enzymatically digested porcine cartilage stiffness was measured at both the micrometer and nanometer scale. The micrometer scale measurements gave information about elastic modulus of cartilage as a multi-compound biomaterial and individual chondrocytes embedded in a compact ECM can be observed. At the nanometer scale, AFM operated in the scanning mode were able to resolve individual collagen fibrils and the supramolecular organization of cartilage was visualized. In the force mode, the compressive stiffness measurements showed a 100 to 500 fold lower elastic modulus compared to that of the micrometer scale. Moreover, the enzymatically digested cartilage, which mimics osteoarthtritic cartilage, exhibited significant stiffening detectable only at the nanometer scale [217]. Thus IT-AFM, can principally be used to measure biomechanical properties of normal and damaged articular cartilage as well as to detect early molecular changes at the cartilage surface associated with cartilage pathologies.

6. Aim of thesis

Recently, β1 integrins emerged as essential regulators of mitotic spindle orientation in polarized epithelial cells. In basal keratinocytes, integrins are involved in the establishment of apical-basal polarity and in proper orientation of the division plane. Similarly, in mammary gland epithelium as well as in Drosophila follicular cells integrins are required for proper orientation of the mitotic spindle and consequently the proper location of the daughter cells. In metaphase, cultured cells orient their spindle parallel to a surface coated with β1 integrin ligands, and along the cell's long axis which is established in interphase. However, in mesenchymal cells such as chondrocytes the role of β1 integrin in proper orientation of the division plane was not previously addressed. Mice lacking β1 integrin in cartilage have a disorganized growth plate lacking columns and chondrocytes display adhesion, spreading and cytokinesis defects. These data led to the hypothesis that β1 integrin might be involved in mitotic spindle orientation and column formation during growth plate development. In the first paper, we addressed the role of β1 integrin in mitotic spindle orientation using both genetically modified mice, which lack β1 integrin on chondrocytes, as well as wild type and β1-deficient chondrocytes cultured on various ECM substrates.

Next, we were interested in the role of β1 integrin-mediated cell-matrix interactions in the functions of adult knee joints. Several studies have attempted to clarify the contribution of integrins to articular cartilage morphogenesis and function but the present information is still contradictory. In vivo, genetic ablation of the α1 subunit in mice causes age-dependent osteoarthritis with early signs of proteoglycan depletion and increased cartilage degradation accompanied by MMP-2 and MMP-3 expression. Fibronectin and collagen fragments, present in synovial fluid and cartilage of osteoarthritic patients, have been previously suggested to be β1 integrin-dependent stimulators of catabolic activities in chondrocytes. To assess the role of integrins in knee joint formation, function and articular cartilage metabolism we analyzed the phenotype of mice which lack β1 integrins in the limbs.

Furthermore, we participated in a study aiming to develop a tool for detecting early physical changes in cartilage pathologies. Osteoarthritis is a degenerative joint disease found mostly in older people. It is characterized by the destruction of articular cartilage starting from small injuries at the joint surface followed by progressive cartilage erosion and bone damage. Currently, diagnostic methods such as radiography, MRI and macroscopic examination detect pathological changes at a more advanced stage of the disease, when strategies to prevent further damage are no longer applicable. IT-AFM was previously

employed for determining mechanical properties of biomaterials such as pig cartilage and gave good results in resolving fine structural details of the cartilage macromolecular structure. Therefore, for this study we used nano-scale IT-AFM to detect early osteoarthritic changes in normal and diseased samples from both humans and genetically modified mice, which were previously described to develop age-dependent OA.

7 Brief summaries of the publications

7.1 PAPER I: β1 integrin-dependent cell shape governs mitotic spindle positioning in growth plate chondrocytes

Growth plate cartilage is a specialized and polarized structure, which is responsible for growth of the long bones during endochondral ossification. It is organized in morphologically distinct zones, which reflect the differentiation stages of the chondrocytes. In the proliferative zones the chondrocytes are flattened and arrange into stacks. The long axes of the cells are oriented perpendicular to the longitudinal axis of the bone. The mechanism of column formation was investigated initially by Dodds who proposed that when the flattened cells divide the spindle is oriented perpendicular to the proximo-distal (P-D) axis of the bone and along the long axis of the cell. Upon division, the two daughter cells initially lie side by side and then migrate and rotate on top of one other. In mice with β1 integrin deficient chondrocytes, the columnar structure is lost due to cell rounding and impaired intercalation movements caused by diminished chondrocytes anchorage to the ECM. Cell division orientation is a well known mechanism implicated in tissue morphogenesis. Recently, integrins have been described to play a major role in epithelial tissue polarity by determining the mitotic spindle orientation and thus the spatial localization of the daughter cells.

To understand the role of β1 integrin in growth plate morphogenesis, we mated mice carrying β1 floxed alleles with mice expressing a Cre recombinase under the control of either the *Prx1* or *Col2a1* promoters. First, we analyzed the early morphogenetic process of the wild type growth plate starting from initial stages of cartilage formation. We observed that chondrocyte shape anisotropy and tissue polarity is established very early during development. Thus, from E12 the cells become progressively flatter and by E14 short stacks containing 2-3 discoid cells are already present in the presumptive growth plate. Spindle alignments and division axes were examined in these mice in vivo by fluorescence confocal microscopy. At E12, early metaphase spindles were randomly oriented, whereas late ana- and telophase spindles showed a tendency to orient along the long axis of the cell and perpendicular to the P-D axis of the bone. The tendency toward perpendicular orientation of the late spindle increases with developmental stage and consequently with the degree of flattening. By late stages of development the metaphase spindles also tend to align parallel to the long axis of the cells suggesting that the orientation of elongated chondrocytes determine spindle orientation independent of guiding cortical cues. In contrast, β1 integrin-null chondrocytes are round and both late and early spindles are misaligned, leading to random

cleavage planes. Prx1cre-mediated deletion of β1 integrin leads to mosaicism in the *β1$^{fl/f}$-lPrx1cre* mice and the growth plates of these mice contain both β1 positive and negative cells. The rare positive cells are flat, oriented and can form columns demonstrating that β1 controls shape and polarity in a cell autonomous manner. In vitro studies have shown that in Hela cells that are rounding up during mitosis, β1 integrin controls metaphase spindle orientation parallel to the substratum independently of the cellular geometry. To test if this is the case in more adhesive cell types, we used wild type and β1-deficient chondrocytes and cultured them on collagen, fibronectin or vitronectin. Wild type chondrocytes were able to spread on FN and VN and consequently oriented their spindle parallel to the substrate. On collagen, the cells were round and they showed a random orientation of the spindle. Similarly, mutant chondrocytes spread on vitronectin via αvβ3 and oriented their spindle parallel to the culture dish. In contrast, mutant chondrocytes were round on fibronectin and collagen and the spindles were randomly aligned. Altogether, our data suggest that geometrical constrains established and maintained by β1-mediated adhesion provides a default guiding cue for the orientation of the spindle and division apparatus in chondrocytes both in vivo and in vitro.

7.2 PAPER II: Knock-Out Mice in Osteoarthritis Research

Various animal models have been used to study the complex etiology and pathological features characteristic for osteoarthritis. Of these, genetically modified mice have proved to be one of the most powerful tools to dissect the mechanisms involved in OA. Conditional targeting additionally increased the number of strains available for OA studies. In this paper, we reviewed the mouse strains with naturally occurring mutations as well as transgenic and knockout mice which have contributed to our understanding of OA pathology. Important data came from mice deficient in proteolytic enzymes and their inhibitors, which demonstrated that a proper balance must exist between matrix synthesis and degradation, contradicting the solely destructive role previously attributed to MMPs. ECM composition and assembly as well as the proper interaction of ECM proteins with cellular receptors are essential for normal cartilage function as demonstrated by numerous OA mouse models with ablation in genes coding for various matrix molecules or cell surface receptors. Mice which lack or overexpress signaling molecules like cytokines and growth factors develop more severe or accelerated AC destruction in surgically induced OA models demonstrating that important cellular processes are regulated through numerous signaling molecules and alterations in their functions can have harmful effects on the joints.

In conclusion, genetically modified mice are very useful for studying the in vivo

molecular pathology of OA and definitely their number will continue to grow in the future.

7.3 PAPER III: β1 integrin-deficiency results in multiple abnormalities of the knee joint

The aim of this work was to examine the long term consequences of β1 integrin deletion in chondrocytes of limb skeleton. A previous study demonstrated that ablation of β1 integrin in all cartilaginous skeletal elements results in the death of the animals at birth, precluding any possibility to study post-natal events such as the maintenance of articular cartilage with age. Therefore, we deleted the β1 integrin gene using the cre recombinase under the control of the *Prx1* promoter, which is expressed in early limb bud mesenchyme. These animals were viable at birth and developed skeletal abnormalities restricted to the limbs, as expected. Histological analysis of knee joints revealed that from 1 month old mutant mice the secondary ossification centers were delayed and the articular cartilage architecture was highly disorganized. The superficial zone of AC was expanded and lacked flattened cells, while characteristic column-like structure in the radial zone was missing implicating that β1 integrins are pivotal for structural anisotropy of the AC. The level of disorganization increased at later stages: mutant cartilage was thicker and displayed higher calcified/noncalcified ratio when compared to the control. Ultrastructural studies revealed an abnormal collagen fibril organization and extended pericellular matrix (PM) compartment associated with impaired expression of the PM marker collagen VI suggesting a role of β1 integrins in matrix assembly. Articular chondrocytes, in contrast to growth plate chondrocytes, arrest their differentiation program before hypertrophy. We found that β1-deficient AC chondrocytes deposit the hypertrophic marker type X collagen close to the articular surface implying an abnormally activated terminal differentiation. The ECM abnormalities were accompanied by decreased proliferation and increased binucleation rates of mutant chondrocytes leading to hypocellularity of the AC. In addition, the actin cytoskeleton of chondrocytes was disrupted in aged mutants at the weight bearing areas of the AC. Despite these features, most of them characteristic for diseased AC, the cartilage of mutant animals did not show accelerated or more severe erosions compared with control mice indicating that the lack of β1 integrin does not affect the progression of osteoarthritic cartilage destruction. Corroborating this observation, the catabolic activity of cartilage judged by the expression of MMPs, aggrecanases and their degradation products were similar in both genotype groups. MAPK signaling is often activated in OA but we could not detect any significant changes in the mutant cartilage. In addition, when we stimulated femoral head explants with the central, cell-

binding fragment of FN, which is known to activate MAPKs, we did not find differences in Erk, p38 and JNK phosphorylation between wild type and mutant chondrocytes. These findings clearly demonstrate that MAPK activation is efficiently compensated by signaling through either β3/β5 integrins or growth factor receptors in β1 integrin-deficient chondrocytes. Next, we examined the synovial tissue development. Starting at E16, multiple abnormalities were present in the mutant synovium and by 7 months of age fibrosis, invasion of the synovial tissue in the joint space accompanied by chondrogenic differentiation were obvious.

All together, our data demonstrate that the lack of β1 in the joints leads to severe structural defects in both AC and synovium reminiscent of OA but does not result in premature erosion of AC surface.

7.4 PAPER IV: Early detection of aging cartilage and osteoarthritis in mice and patient samples using atomic force microscopy

Osteoarthritis is a degenerative joint disease which starts with early perturbation of the cartilage ECM supramolecular assembly. Such subtle defects are not detectable by conventional diagnosis methods and a more sensitive tool is required for early detection in order to halt or reverse the progression of the disease. Previously IT-AFM was used to image native surface of porcine articular cartilage and to measure its compressive properties. The fine structural details of the cartilage and significant elasticity changes in enzymatically digested cartilage could be resolved only with nanometer-sized tips. Therefore in this study we compared the biomechanical properties of the cartilage from wild type and collagen IX deficient mice as well as from patients at both nanometer and micrometer scales. First, to validate the method, we measured the age-dependent changes in the normal cartilage from the femoral heads of mice. Using nanometer-sized tips we could detect a progressive thickening of collagen fibrils which was not detected by scanning electron microscopy (SEM). Similarly, only at the nanometer scale could we measure increased cartilage stiffness with age. Next, we used collagen IX-deficient mice to test if nanometer scaled IT-AFM can monitor pathological changes in a well-established mouse model for OA. As early as 1 month of age, cartilage fibril thickening and increased nanostiffness were observed by IT-AFM, in contrast to SEM or normal histology techniques which could not detect these changes, suggesting that pathological changes may occur very early during disease progression. Next, we measured the changes at 3, 6, and 12 months of age and we noticed an accelerated increase in collagen

thickening in the mutant mice when compared to the wild type. In addition both 3 months and 6 months old mutant mice displayed an increased nanostiffness but similar microstiffness. Surprisingly, the 12 months old knock out mice manifested a decrease in stiffness at both nano- and micrometer scale suggesting that collagen meshwork is dramatically destroyed resulting in softening of the cartilage. These changes where confirmed also by SEM and histology. To test the applicability of IT-AFM in clinical practice we analyzed samples from osteoarthritic patients of different ages. All the samples were evaluated for OA changes using the Outerbridge scoring system. Analysis revealed increased softening of the cartilage with increasing OA scores at a given age only at the nanometer scale. Furthermore we could detect age-dependent increased nanostiffness in the cartilage from normal patients which are different from OA changes.

In conclusion, nanoscale IT-AFM can be used to detect subtle topographical and biomechanical alterations in the cartilage ECM which occur very early in OA.

8. References

1. Alberts, B. Molecular biology of the cell (Garland Science, New York, 2002).
2. van der Flier, A. & Sonnenberg, A. Function and interactions of integrins. Cell Tissue Res 305, 285-98 (2001).
3. Hynes, R.O. Integrins: bidirectional, allosteric signaling machines. Cell 110, 673-87 (2002).
4. Bokel, C. & Brown, N.H. Integrins in development: moving on, responding to, and sticking to the extracellular matrix. Dev Cell 3, 311-21 (2002).
5. Giancotti, F.G. & Ruoslahti, E. Integrin signaling. Science 285, 1028-32 (1999).
6. Humphries, J.D., Byron, A. & Humphries, M.J. Integrin ligands at a glance. J Cell Sci 119, 3901-3 (2006).
7. Legate, K.R. & Fassler, R. Mechanisms that regulate adaptor binding to beta-integrin cytoplasmic tails. J Cell Sci 122, 187-98 (2009).
8. Ley, K., Laudanna, C., Cybulsky, M.I. & Nourshargh, S. Getting to the site of inflammation: the leukocyte adhesion cascade updated. Nat Rev Immunol 7, 678-89 (2007).
9. Dupuy, A.G. & Caron, E. Integrin-dependent phagocytosis: spreading from microadhesion to new concepts. J Cell Sci 121, 1773-83 (2008).
10. Sheppard, D. Integrin-mediated activation of latent transforming growth factor beta. Cancer Metastasis Rev 24, 395-402 (2005).
11. White, J.M. ADAMs: modulators of cell-cell and cell-matrix interactions. Curr Opin Cell Biol 15, 598-606 (2003).
12. Wegener, K.L. & Campbell, I.D. Transmembrane and cytoplasmic domains in integrin activation and protein-protein interactions (review). Mol Membr Biol 25, 376-87 (2008).
13. Xiong, J.P. et al. Crystal structure of the extracellular segment of integrin alpha Vbeta3. Science 294, 339-45 (2001).
14. Zhu, J. et al. Structure of a complete integrin ectodomain in a physiologic resting state and activation and deactivation by applied forces. Mol Cell 32, 849-61 (2008).
15. Xiong, J.P. et al. Crystal structure of the extracellular segment of integrin alpha Vbeta3 in complex with an Arg-Gly-Asp ligand. Science 296, 151-5 (2002).
16. Springer, T.A., Zhu, J. & Xiao, T. Structural basis for distinctive recognition of fibrinogen gammaC peptide by the platelet integrin alphaIIbbeta3. J Cell Biol 182, 791-800 (2008).
17. Arnaout, M.A., Mahalingam, B. & Xiong, J.P. Integrin structure, allostery, and bidirectional signaling. Annu Rev Cell Dev Biol 21, 381-410 (2005).
18. Askari, J.A., Buckley, P.A., Mould, A.P. & Humphries, M.J. Linking integrin conformation to function. J Cell Sci 122, 165-70 (2009).
19. Calderwood, D.A. Integrin activation. J Cell Sci 117, 657-66 (2004).
20. Coller, B.S. & Shattil, S.J. The GPIIb/IIIa (integrin alphaIIbbeta3) odyssey: a technology-driven saga of a receptor with twists, turns, and even a bend. Blood 112, 3011-25 (2008).
21. Alon, R. & Ley, K. Cells on the run: shear-regulated integrin activation in leukocyte rolling and arrest on endothelial cells. Curr Opin Cell Biol 20, 525-32 (2008).
22. Constantin, G. Chemokine signaling and integrin activation in lymphocyte migration into the inflamed brain. J Neuroimmunol 198, 20-6 (2008).
23. Lee, H.S., Lim, C.J., Puzon-McLaughlin, W., Shattil, S.J. & Ginsberg, M.H. RIAM activates integrins by linking talin to ras GTPase membrane-targeting sequences. J Biol Chem 284, 5119-27 (2009).

24. Montanez, E. et al. Kindlin-2 controls bidirectional signaling of integrins. Genes Dev 22, 1325-30 (2008).
25. Moser, M. et al. Kindlin-3 is required for beta2 integrin-mediated leukocyte adhesion to endothelial cells. Nat Med 15, 300-5 (2009).
26. Moser, M., Nieswandt, B., Ussar, S., Pozgajova, M. & Fassler, R. Kindlin-3 is essential for integrin activation and platelet aggregation. Nat Med 14, 325-30 (2008).
27. Wegener, K.L. et al. Structural basis of integrin activation by talin. Cell 128, 171-82 (2007).
28. Ma, Y.Q., Qin, J., Wu, C. & Plow, E.F. Kindlin-2 (Mig-2): a co-activator of beta3 integrins. J Cell Biol 181, 439-46 (2008).
29. Legate, K.R., Wickstrom, S.A. & Fassler, R. Genetic and cell biological analysis of integrin outside-in signaling. Genes Dev 23, 397-418 (2009).
30. Brakebusch, C. & Fassler, R. The integrin-actin connection, an eternal love affair. Embo J 22, 2324-33 (2003).
31. Legate, K.R., Montanez, E., Kudlacek, O. & Fassler, R. ILK, PINCH and parvin: the tIPP of integrin signalling. Nat Rev Mol Cell Biol 7, 20-31 (2006).
32. Hall, A. Rho GTPases and the actin cytoskeleton. Science 279, 509-14 (1998).
33. Etienne-Manneville, S. & Hall, A. Rho GTPases in cell biology. Nature 420, 629-35 (2002).
34. Fassler, R. et al. Lack of beta 1 integrin gene in embryonic stem cells affects morphology, adhesion, and migration but not integration into the inner cell mass of blastocysts. J Cell Biol 128, 979-88 (1995).
35. Stephens, L.E. et al. Deletion of beta 1 integrins in mice results in inner cell mass failure and peri-implantation lethality. Genes Dev 9, 1883-95 (1995).
36. Yang, J.T., Rayburn, H. & Hynes, R.O. Embryonic mesodermal defects in alpha 5 integrin-deficient mice. Development 119, 1093-105 (1993).
37. Yang, J.T., Rayburn, H. & Hynes, R.O. Cell adhesion events mediated by alpha 4 integrins are essential in placental and cardiac development. Development 121, 549-60 (1995).
38. Bader, B.L., Rayburn, H., Crowley, D. & Hynes, R.O. Extensive vasculogenesis, angiogenesis, and organogenesis precede lethality in mice lacking all alpha v integrins. Cell 95, 507-19 (1998).
39. Kreidberg, J.A. et al. Alpha 3 beta 1 integrin has a crucial role in kidney and lung organogenesis. Development 122, 3537-47 (1996).
40. DiPersio, C.M., Hodivala-Dilke, K.M., Jaenisch, R., Kreidberg, J.A. & Hynes, R.O. alpha3beta1 Integrin is required for normal development of the epidermal basement membrane. J Cell Biol 137, 729-42 (1997).
41. Anton, E.S., Kreidberg, J.A. & Rakic, P. Distinct functions of alpha3 and alpha(v) integrin receptors in neuronal migration and laminar organization of the cerebral cortex. Neuron 22, 277-89 (1999).
42. Muller, U. et al. Integrin alpha8beta1 is critically important for epithelial-mesenchymal interactions during kidney morphogenesis. Cell 88, 603-13 (1997).
43. Littlewood Evans, A. & Muller, U. Stereocilia defects in the sensory hair cells of the inner ear in mice deficient in integrin alpha8beta1. Nat Genet 24, 424-8 (2000).
44. Wagner, N. et al. Critical role for beta7 integrins in formation of the gut-associated lymphoid tissue. Nature 382, 366-70 (1996).
45. Hodivala-Dilke, K.M. et al. Beta3-integrin-deficient mice are a model for Glanzmann thrombasthenia showing placental defects and reduced survival. J Clin Invest 103, 229-38 (1999).

46. Tronik-Le Roux, D. et al. Thrombasthenic mice generated by replacement of the integrin alpha(IIb) gene: demonstration that transcriptional activation of this megakaryocytic locus precedes lineage commitment. Blood 96, 1399-408 (2000).
47. Brakebusch, C. et al. Skin and hair follicle integrity is crucially dependent on beta 1 integrin expression on keratinocytes. Embo J 19, 3990-4003 (2000).
48. Hirsch, E., Iglesias, A., Potocnik, A.J., Hartmann, U. & Fassler, R. Impaired migration but not differentiation of haematopoietic stem cells in the absence of beta1 integrins. Nature 380, 171-5 (1996).
49. Potocnik, A.J., Brakebusch, C. & Fassler, R. Fetal and adult hematopoietic stem cells require beta1 integrin function for colonizing fetal liver, spleen, and bone marrow. Immunity 12, 653-63 (2000).
50. Abraham, S., Kogata, N., Fassler, R. & Adams, R.H. Integrin beta1 subunit controls mural cell adhesion, spreading, and blood vessel wall stability. Circ Res 102, 562-70 (2008).
51. Lechler, T. & Fuchs, E. Asymmetric cell divisions promote stratification and differentiation of mammalian skin. Nature 437, 275-80 (2005).
52. Taddei, I. et al. Beta1 integrin deletion from the basal compartment of the mammary epithelium affects stem cells. Nat Cell Biol 10, 716-22 (2008).
53. Fernandez-Minan, A., Martin-Bermudo, M.D. & Gonzalez-Reyes, A. Integrin signaling regulates spindle orientation in Drosophila to preserve the follicular-epithelium monolayer. Curr Biol 17, 683-8 (2007).
54. Thery, M. et al. The extracellular matrix guides the orientation of the cell division axis. Nat Cell Biol 7, 947-53 (2005).
55. Toyoshima, F. & Nishida, E. Integrin-mediated adhesion orients the spindle parallel to the substratum in an EB1- and myosin X-dependent manner. Embo J 26, 1487-98 (2007).
56. Toyoshima, F., Matsumura, S., Morimoto, H., Mitsushima, M. & Nishida, E. PtdIns(3,4,5)P3 regulates spindle orientation in adherent cells. Dev Cell 13, 796-811 (2007).
57. Wallingford, J.B., Fraser, S.E. & Harland, R.M. Convergent extension: the molecular control of polarized cell movement during embryonic development. Dev Cell 2, 695-706 (2002).
58. Marsden, M. & DeSimone, D.W. Integrin-ECM interactions regulate cadherin-dependent cell adhesion and are required for convergent extension in Xenopus. Curr Biol 13, 1182-91 (2003).
59. Davidson, L.A., Marsden, M., Keller, R. & Desimone, D.W. Integrin alpha5beta1 and fibronectin regulate polarized cell protrusions required for Xenopus convergence and extension. Curr Biol 16, 833-44 (2006).
60. Keller, R. et al. Mechanisms of convergence and extension by cell intercalation. Philos Trans R Soc Lond B Biol Sci 355, 897-922 (2000).
61. Steele, D.G. & Bramblett, C.A. The anatomy and biology of the human skeleton (Texas A&M University Press, College Station, 1988).
62. Olsen, B.R., Reginato, A.M. & Wang, W. Bone development. Annu Rev Cell Dev Biol 16, 191-220 (2000).
63. Hall, B.K. & Miyake, T. All for one and one for all: condensations and the initiation of skeletal development. Bioessays 22, 138-47 (2000).
64. Horton, W.A. Skeletal development: insights from targeting the mouse genome. Lancet 362, 560-9 (2003).
65. Aszodi, A., Bateman, J.F., Gustafsson, E., Boot-Handford, R. & Fassler, R. Mammalian skeletogenesis and extracellular matrix: what can we learn from knockout mice? Cell Struct Funct 25, 73-84 (2000).

66. de Crombrugghe, B., Lefebvre, V. & Nakashima, K. Regulatory mechanisms in the pathways of cartilage and bone formation. Curr Opin Cell Biol 13, 721-7 (2001).
67. Gilbert, S.F. Developmental biology (Sinauer Associates, Inc. Publishers, Sunderland, Mass., 2006).
68. Lefebvre, V. & de Crombrugghe, B. Toward understanding SOX9 function in chondrocyte differentiation. Matrix Biol 16, 529-40 (1998).
69. Karsenty, G. & Wagner, E.F. Reaching a genetic and molecular understanding of skeletal development. Dev Cell 2, 389-406 (2002).
70. Haigh, J.J., Gerber, H.P., Ferrara, N. & Wagner, E.F. Conditional inactivation of VEGF-A in areas of collagen2a1 expression results in embryonic lethality in the heterozygous state. Development 127, 1445-53 (2000).
71. Yin, M., Gentili, C., Koyama, E., Zasloff, M. & Pacifici, M. Antiangiogenic treatment delays chondrocyte maturation and bone formation during limb skeletogenesis. J Bone Miner Res 17, 56-65 (2002).
72. Kronenberg, H.M. Developmental regulation of the growth plate. Nature 423, 332-6 (2003).
73. van der Eerden, B.C., Karperien, M. & Wit, J.M. Systemic and local regulation of the growth plate. Endocr Rev 24, 782-801 (2003).
74. Ortega, N., Behonick, D.J. & Werb, Z. Matrix remodeling during endochondral ossification. Trends Cell Biol 14, 86-93 (2004).
75. Hunziker, E.B. Mechanism of longitudinal bone growth and its regulation by growth plate chondrocytes. Microsc Res Tech 28, 505-19 (1994).
76. Felisbino, S.L. & Carvalho, H.F. The epiphyseal cartilage and growth of long bones in Rana catesbeiana. Tissue Cell 31, 301-7 (1999).
77. Lefebvre, V. & Smits, P. Transcriptional control of chondrocyte fate and differentiation. Birth Defects Res C Embryo Today 75, 200-12 (2005).
78. Holmes, L.B. & Trelstad, R.L. Cell polarity in precartilage mouse limb mesenchyme cells. Dev Biol 78, 511-20 (1980).
79. Gould, R.P., Selwood, L., Day, A. & Wolpert, L. The mechanism of cellular orientation during early cartilage formation in the chick limb and regenerating amphibian limb. Exp Cell Res 83, 287-96 (1974).
80. Hewitt, A.T. & Elmer, W.A. Reactivity of normal and brachypod mouse limb mesenchymal cells with con A. Nature 264, 177-8 (1976).
81. Caplan, A.I. & Koutroupas, S. The control of muscle and cartilage development in the chick limb: the role of differential vascularization. J Embryol Exp Morphol 29, 571-83 (1973).
82. Holmes, L.B. & Trelstad, R.L. Identification of rapidly labeled, small molecular weight hydroxyproline-containing peptides in developing mouse limbs in vitro and in vivo. Dev Biol 72, 41-9 (1979).
83. Dodds, G.S. in Anatomical Records 385-399 (1930).
84. Ham, A.W. in Anatomical Records 125-133 (1931).
85. Abad, V. et al. The role of the resting zone in growth plate chondrogenesis. Endocrinology 143, 1851-7 (2002).
86. Foster, J.W. et al. Campomelic dysplasia and autosomal sex reversal caused by mutations in an SRY-related gene. Nature 372, 525-30 (1994).
87. Bi, W. et al. Haploinsufficiency of Sox9 results in defective cartilage primordia and premature skeletal mineralization. Proc Natl Acad Sci U S A 98, 6698-703 (2001).
88. Lefebvre, V., Huang, W., Harley, V.R., Goodfellow, P.N. & de Crombrugghe, B. SOX9 is a potent activator of the chondrocyte-specific enhancer of the pro alpha1(II) collagen gene. Mol Cell Biol 17, 2336-46 (1997).

89. Bridgewater, L.C., Lefebvre, V. & de Crombrugghe, B. Chondrocyte-specific enhancer elements in the Col11a2 gene resemble the Col2a1 tissue-specific enhancer. J Biol Chem 273, 14998-5006 (1998).
90. Xie, W.F., Zhang, X., Sakano, S., Lefebvre, V. & Sandell, L.J. Trans-activation of the mouse cartilage-derived retinoic acid-sensitive protein gene by Sox9. J Bone Miner Res 14, 757-63 (1999).
91. Akiyama, H., Chaboissier, M.C., Martin, J.F., Schedl, A. & de Crombrugghe, B. The transcription factor Sox9 has essential roles in successive steps of the chondrocyte differentiation pathway and is required for expression of Sox5 and Sox6. Genes Dev 16, 2813-28 (2002).
92. Akiyama, H. et al. Interactions between Sox9 and beta-catenin control chondrocyte differentiation. Genes Dev 18, 1072-87 (2004).
93. Ducy, P., Zhang, R., Geoffroy, V., Ridall, A.L. & Karsenty, G. Osf2/Cbfa1: a transcriptional activator of osteoblast differentiation. Cell 89, 747-54 (1997).
94. Otto, F. et al. Cbfa1, a candidate gene for cleidocranial dysplasia syndrome, is essential for osteoblast differentiation and bone development. Cell 89, 765-71 (1997).
95. Mundlos, S., Huang, L.F., Selby, P. & Olsen, B.R. Cleidocranial dysplasia in mice. Ann N Y Acad Sci 785, 301-2 (1996).
96. Kim, I.S., Otto, F., Zabel, B. & Mundlos, S. Regulation of chondrocyte differentiation by Cbfa1. Mech Dev 80, 159-70 (1999).
97. Inada, M. et al. Maturational disturbance of chondrocytes in Cbfa1-deficient mice. Dev Dyn 214, 279-90 (1999).
98. Takeda, S., Bonnamy, J.P., Owen, M.J., Ducy, P. & Karsenty, G. Continuous expression of Cbfa1 in nonhypertrophic chondrocytes uncovers its ability to induce hypertrophic chondrocyte differentiation and partially rescues Cbfa1-deficient mice. Genes Dev 15, 467-81 (2001).
99. Ueta, C. et al. Skeletal malformations caused by overexpression of Cbfa1 or its dominant negative form in chondrocytes. J Cell Biol 153, 87-100 (2001).
100. Jimenez, M.J. et al. Collagenase 3 is a target of Cbfa1, a transcription factor of the runt gene family involved in bone formation. Mol Cell Biol 19, 4431-42 (1999).
101. Colnot, C. Cellular and molecular interactions regulating skeletogenesis. J Cell Biochem 95, 688-97 (2005).
102. Yoshida, C.A. et al. Runx2 and Runx3 are essential for chondrocyte maturation, and Runx2 regulates limb growth through induction of Indian hedgehog. Genes Dev 18, 952-63 (2004).
103. Komori, T. Regulation of skeletal development by the Runx family of transcription factors. J Cell Biochem 95, 445-53 (2005).
104. Lai, L.P. & Mitchell, J. Indian hedgehog: its roles and regulation in endochondral bone development. J Cell Biochem 96, 1163-73 (2005).
105. Ingham, P.W. & McMahon, A.P. Hedgehog signaling in animal development: paradigms and principles. Genes Dev 15, 3059-87 (2001).
106. St-Jacques, B., Hammerschmidt, M. & McMahon, A.P. Indian hedgehog signaling regulates proliferation and differentiation of chondrocytes and is essential for bone formation. Genes Dev 13, 2072-86 (1999).
107. Long, F., Zhang, X.M., Karp, S., Yang, Y. & McMahon, A.P. Genetic manipulation of hedgehog signaling in the endochondral skeleton reveals a direct role in the regulation of chondrocyte proliferation. Development 128, 5099-108 (2001).
108. Long, F. et al. Ihh signaling is directly required for the osteoblast lineage in the endochondral skeleton. Development 131, 1309-18 (2004).

109. Lee, K., Deeds, J.D. & Segre, G.V. Expression of parathyroid hormone-related peptide and its receptor messenger ribonucleic acids during fetal development of rats. Endocrinology 136, 453-63 (1995).
110. Kronenberg, H.M. PTHrP and skeletal development. Ann N Y Acad Sci 1068, 1-13 (2006).
111. Karaplis, A.C. et al. Lethal skeletal dysplasia from targeted disruption of the parathyroid hormone-related peptide gene. Genes Dev 8, 277-89 (1994).
112. Vortkamp, A. et al. Regulation of rate of cartilage differentiation by Indian hedgehog and PTH-related protein. Science 273, 613-22 (1996).
113. Lanske, B. et al. PTH/PTHrP receptor in early development and Indian hedgehog-regulated bone growth. Science 273, 663-6 (1996).
114. Mak, K.K., Kronenberg, H.M., Chuang, P.T., Mackem, S. & Yang, Y. Indian hedgehog signals independently of PTHrP to promote chondrocyte hypertrophy. Development 135, 1947-56 (2008).
115. Kobayashi, T. et al. PTHrP and Indian hedgehog control differentiation of growth plate chondrocytes at multiple steps. Development 129, 2977-86 (2002).
116. Naski, M.C. & Ornitz, D.M. FGF signaling in skeletal development. Front Biosci 3, d781-94 (1998).
117. Rousseau, F. et al. Mutations of the fibroblast growth factor receptor-3 gene in achondroplasia. Horm Res 45, 108-10 (1996).
118. Shiang, R. et al. Mutations in the transmembrane domain of FGFR3 cause the most common genetic form of dwarfism, achondroplasia. Cell 78, 335-42 (1994).
119. Colvin, J.S., Bohne, B.A., Harding, G.W., McEwen, D.G. & Ornitz, D.M. Skeletal overgrowth and deafness in mice lacking fibroblast growth factor receptor 3. Nat Genet 12, 390-7 (1996).
120. Deng, C., Wynshaw-Boris, A., Zhou, F., Kuo, A. & Leder, P. Fibroblast growth factor receptor 3 is a negative regulator of bone growth. Cell 84, 911-21 (1996).
121. Ornitz, D.M. & Marie, P.J. FGF signaling pathways in endochondral and intramembranous bone development and human genetic disease. Genes Dev 16, 1446-65 (2002).
122. Liu, Z., Xu, J., Colvin, J.S. & Ornitz, D.M. Coordination of chondrogenesis and osteogenesis by fibroblast growth factor 18. Genes Dev 16, 859-69 (2002).
123. Ohbayashi, N. et al. FGF18 is required for normal cell proliferation and differentiation during osteogenesis and chondrogenesis. Genes Dev 16, 870-9 (2002).
124. Hung, I.H., Yu, K., Lavine, K.J. & Ornitz, D.M. FGF9 regulates early hypertrophic chondrocyte differentiation and skeletal vascularization in the developing stylopod. Dev Biol 307, 300-13 (2007).
125. Itoh, N. & Ornitz, D.M. Functional evolutionary history of the mouse Fgf gene family. Dev Dyn 237, 18-27 (2008).
126. Tsumaki, N. & Yoshikawa, H. The role of bone morphogenetic proteins in endochondral bone formation. Cytokine Growth Factor Rev 16, 279-85 (2005).
127. Wozney, J.M. Bone morphogenetic proteins. Prog Growth Factor Res 1, 267-80 (1989).
128. Moustakas, A., Pardali, K., Gaal, A. & Heldin, C.H. Mechanisms of TGF-beta signaling in regulation of cell growth and differentiation. Immunol Lett 82, 85-91 (2002).
129. Hoodless, P.A. et al. MADR1, a MAD-related protein that functions in BMP2 signaling pathways. Cell 85, 489-500 (1996).
130. Nishimura, R. et al. Smad5 and DPC4 are key molecules in mediating BMP-2-induced osteoblastic differentiation of the pluripotent mesenchymal precursor cell line C2C12. J Biol Chem 273, 1872-9 (1998).

131. Chikazu, D. et al. Bone morphogenetic protein 2 induces cyclo-oxygenase 2 in osteoblasts via a Cbfal binding site: role in effects of bone morphogenetic protein 2 in vitro and in vivo. J Bone Miner Res 17, 1430-40 (2002).
132. Leboy, P. et al. Smad-Runx interactions during chondrocyte maturation. J Bone Joint Surg Am 83-A Suppl 1, S15-22 (2001).
133. Seki, K. & Hata, A. Indian hedgehog gene is a target of the bone morphogenetic protein signaling pathway. J Biol Chem 279, 18544-9 (2004).
134. Yoon, B.S. & Lyons, K.M. Multiple functions of BMPs in chondrogenesis. J Cell Biochem 93, 93-103 (2004).
135. Brunet, L.J., McMahon, J.A., McMahon, A.P. & Harland, R.M. Noggin, cartilage morphogenesis, and joint formation in the mammalian skeleton. Science 280, 1455-7 (1998).
136. Pizette, S. & Niswander, L. BMPs are required at two steps of limb chondrogenesis: formation of prechondrogenic condensations and their differentiation into chondrocytes. Dev Biol 219, 237-49 (2000).
137. Yoon, B.S. et al. Bmpr1a and Bmpr1b have overlapping functions and are essential for chondrogenesis in vivo. Proc Natl Acad Sci U S A 102, 5062-7 (2005).
138. Minina, E., Kreschel, C., Naski, M.C., Ornitz, D.M. & Vortkamp, A. Interaction of FGF, Ihh/Pthlh, and BMP signaling integrates chondrocyte proliferation and hypertrophic differentiation. Dev Cell 3, 439-49 (2002).
139. Yoon, B.S. et al. BMPs regulate multiple aspects of growth-plate chondrogenesis through opposing actions on FGF pathways. Development 133, 4667-78 (2006).
140. Grimaud, E., Heymann, D. & Redini, F. Recent advances in TGF-beta effects on chondrocyte metabolism. Potential therapeutic roles of TGF-beta in cartilage disorders. Cytokine Growth Factor Rev 13, 241-57 (2002).
141. Thorp, B.H., Anderson, I. & Jakowlew, S.B. Transforming growth factor-beta 1, -beta 2 and -beta 3 in cartilage and bone cells during endochondral ossification in the chick. Development 114, 907-11 (1992).
142. Minina, E., Schneider, S., Rosowski, M., Lauster, R. & Vortkamp, A. Expression of Fgf and Tgfbeta signaling related genes during embryonic endochondral ossification. Gene Expr Patterns 6, 102-9 (2005).
143. Alvarez, J. et al. TGFbeta2 mediates the effects of hedgehog on hypertrophic differentiation and PTHrP expression. Development 129, 1913-24 (2002).
144. Serra, R. et al. Expression of a truncated, kinase-defective TGF-beta type II receptor in mouse skeletal tissue promotes terminal chondrocyte differentiation and osteoarthritis. J Cell Biol 139, 541-52 (1997).
145. Sanford, L.P. et al. TGFbeta2 knockout mice have multiple developmental defects that are non-overlapping with other TGFbeta knockout phenotypes. Development 124, 2659-70 (1997).
146. Clevers, H. Wnt/beta-catenin signaling in development and disease. Cell 127, 469-80 (2006).
147. Krishnan, V., Bryant, H.U. & Macdougald, O.A. Regulation of bone mass by Wnt signaling. J Clin Invest 116, 1202-9 (2006).
148. Johnson, M.L. & Kamel, M.A. The Wnt signaling pathway and bone metabolism. Curr Opin Rheumatol 19, 376-82 (2007).
149. Veeman, M.T., Axelrod, J.D. & Moon, R.T. A second canon. Functions and mechanisms of beta-catenin-independent Wnt signaling. Dev Cell 5, 367-77 (2003).
150. Yates, K.E., Shortkroff, S. & Reish, R.G. Wnt influence on chondrocyte differentiation and cartilage function. DNA Cell Biol 24, 446-57 (2005).
151. Seifert, J.R. & Mlodzik, M. Frizzled/PCP signalling: a conserved mechanism regulating cell polarity and directed motility. Nat Rev Genet 8, 126-38 (2007).

152. Chun, J.S., Oh, H., Yang, S. & Park, M. Wnt signaling in cartilage development and degeneration. BMB Rep 41, 485-94 (2008).
153. Day, T.F., Guo, X., Garrett-Beal, L. & Yang, Y. Wnt/beta-catenin signaling in mesenchymal progenitors controls osteoblast and chondrocyte differentiation during vertebrate skeletogenesis. Dev Cell 8, 739-50 (2005).
154. Hill, T.P., Spater, D., Taketo, M.M., Birchmeier, W. & Hartmann, C. Canonical Wnt/beta-catenin signaling prevents osteoblasts from differentiating into chondrocytes. Dev Cell 8, 727-38 (2005).
155. Hu, H. et al. Sequential roles of Hedgehog and Wnt signaling in osteoblast development. Development 132, 49-60 (2005).
156. Mak, K.K., Chen, M.H., Day, T.F., Chuang, P.T. & Yang, Y. Wnt/beta-catenin signaling interacts differentially with Ihh signaling in controlling endochondral bone and synovial joint formation. Development 133, 3695-707 (2006).
157. Kilian, B. et al. The role of Ppt/Wnt5 in regulating cell shape and movement during zebrafish gastrulation. Mech Dev 120, 467-76 (2003).
158. Topol, L. et al. Wnt-5a inhibits the canonical Wnt pathway by promoting GSK-3-independent beta-catenin degradation. J Cell Biol 162, 899-908 (2003).
159. Mikels, A.J. & Nusse, R. Purified Wnt5a protein activates or inhibits beta-catenin-TCF signaling depending on receptor context. PLoS Biol 4, e115 (2006).
160. Oishi, I. et al. The receptor tyrosine kinase Ror2 is involved in non-canonical Wnt5a/JNK signalling pathway. Genes Cells 8, 645-54 (2003).
161. Yang, Y., Topol, L., Lee, H. & Wu, J. Wnt5a and Wnt5b exhibit distinct activities in coordinating chondrocyte proliferation and differentiation. Development 130, 1003-15 (2003).
162. DeChiara, T.M. et al. Ror2, encoding a receptor-like tyrosine kinase, is required for cartilage and growth plate development. Nat Genet 24, 271-4 (2000).
163. Li, Y. & Dudley, A.T. Noncanonical frizzled signaling regulates cell polarity of growth plate chondrocytes. Development 136, 1083-92 (2009).
164. Singla, V. & Reiter, J.F. The primary cilium as the cell's antenna: signaling at a sensory organelle. Science 313, 629-33 (2006).
165. Veland, I.R., Awan, A., Pedersen, L.B., Yoder, B.K. & Christensen, S.T. Primary cilia and signaling pathways in mammalian development, health and disease. Nephron Physiol 111, p39-53 (2009).
166. Serra, R. Role of intraflagellar transport and primary cilia in skeletal development. Anat Rec (Hoboken) 291, 1049-61 (2008).
167. Ascenzi, M.G., Lenox, M. & Farnum, C. Analysis of the orientation of primary cilia in growth plate cartilage: a mathematical method based on multiphoton microscopical images. J Struct Biol 158, 293-306 (2007).
168. Huangfu, D. et al. Hedgehog signalling in the mouse requires intraflagellar transport proteins. Nature 426, 83-7 (2003).
169. Huangfu, D. & Anderson, K.V. Cilia and Hedgehog responsiveness in the mouse. Proc Natl Acad Sci U S A 102, 11325-30 (2005).
170. Haycraft, C.J. et al. Gli2 and Gli3 localize to cilia and require the intraflagellar transport protein polaris for processing and function. PLoS Genet 1, e53 (2005).
171. Rohatgi, R., Milenkovic, L. & Scott, M.P. Patched1 regulates hedgehog signaling at the primary cilium. Science 317, 372-6 (2007).
172. Haycraft, C.J. et al. Intraflagellar transport is essential for endochondral bone formation. Development 134, 307-16 (2007).
173. Song, B., Haycraft, C.J., Seo, H.S., Yoder, B.K. & Serra, R. Development of the post-natal growth plate requires intraflagellar transport proteins. Dev Biol 305, 202-16 (2007).

174. McGlashan, S.R., Jensen, C.G. & Poole, C.A. Localization of extracellular matrix receptors on the chondrocyte primary cilium. J Histochem Cytochem 54, 1005-14 (2006).
175. Watanabe, D. et al. The left-right determinant Inversin is a component of node monocilia and other 9+0 cilia. Development 130, 1725-34 (2003).
176. Ross, A.J. et al. Disruption of Bardet-Biedl syndrome ciliary proteins perturbs planar cell polarity in vertebrates. Nat Genet 37, 1135-40 (2005).
177. Park, T.J., Haigo, S.L. & Wallingford, J.B. Ciliogenesis defects in embryos lacking inturned or fuzzy function are associated with failure of planar cell polarity and Hedgehog signaling. Nat Genet 38, 303-11 (2006).
178. Aszodi, A., Chan, D., Hunziker, E., Bateman, J.F. & Fassler, R. Collagen II is essential for the removal of the notochord and the formation of intervertebral discs. J Cell Biol 143, 1399-412 (1998).
179. Li, Y. et al. A fibrillar collagen gene, Col11a1, is essential for skeletal morphogenesis. Cell 80, 423-30 (1995).
180. Fassler, R. et al. Mice lacking alpha 1 (IX) collagen develop noninflammatory degenerative joint disease. Proc Natl Acad Sci U S A 91, 5070-4 (1994).
181. Dreier, R., Opolka, A., Grifka, J., Bruckner, P. & Grassel, S. Collagen IX-deficiency seriously compromises growth cartilage development in mice. Matrix Biol 27, 319-29 (2008).
182. Blumbach, K., Niehoff, A., Paulsson, M. & Zaucke, F. Ablation of collagen IX and COMP disrupts epiphyseal cartilage architecture. Matrix Biol 27, 306-18 (2008).
183. Wai, A.W. et al. Disrupted expression of matrix genes in the growth plate of the mouse cartilage matrix deficiency (cmd) mutant. Dev Genet 22, 349-58 (1998).
184. Watanabe, H. et al. Mouse cartilage matrix deficiency (cmd) caused by a 7 bp deletion in the aggrecan gene. Nat Genet 7, 154-7 (1994).
185. Czipri, M. et al. Genetic rescue of chondrodysplasia and the perinatal lethal effect of cartilage link protein deficiency. J Biol Chem 278, 39214-23 (2003).
186. Arikawa-Hirasawa, E., Watanabe, H., Takami, H., Hassell, J.R. & Yamada, Y. Perlecan is essential for cartilage and cephalic development. Nat Genet 23, 354-8 (1999).
187. Costell, M. et al. Perlecan maintains the integrity of cartilage and some basement membranes. J Cell Biol 147, 1109-22 (1999).
188. Shakibaei, M. Inhibition of chondrogenesis by integrin antibody in vitro. Exp Cell Res 240, 95-106 (1998).
189. Hirsch, M.S., Lunsford, L.E., Trinkaus-Randall, V. & Svoboda, K.K. Chondrocyte survival and differentiation in situ are integrin mediated. Dev Dyn 210, 249-63 (1997).
190. Aszodi, A., Hunziker, E.B., Brakebusch, C. & Fassler, R. Beta1 integrins regulate chondrocyte rotation, G1 progression, and cytokinesis. Genes Dev 17, 2465-79 (2003).
191. Pellinen, T. et al. Integrin trafficking regulated by Rab21 is necessary for cytokinesis. Dev Cell 15, 371-85 (2008).
192. Bengtsson, T. et al. Loss of alpha10beta1 integrin expression leads to moderate dysfunction of growth plate chondrocytes. J Cell Sci 118, 929-36 (2005).
193. Grashoff, C., Aszodi, A., Sakai, T., Hunziker, E.B. & Fassler, R. Integrin-linked kinase regulates chondrocyte shape and proliferation. EMBO Rep 4, 432-8 (2003).
194. Hunziker, E. Articular cartilage and osteoarthritis (ed. Kuettner, K.E.) (Raven Press, New York, 1992).
195. Bruckner, P. Dynamics of bone and cartilage metabolism (eds. Seibel, M.J., Robins, S.P. & Bilezikian, J.P.) (Academic Press, San Diego, 2006).

196. Martel-Pelletier, J., Boileau, C., Pelletier, J.P. & Roughley, P.J. Cartilage in normal and osteoarthritis conditions. Best Pract Res Clin Rheumatol 22, 351-84 (2008).
197. Poole, A.C. Articular cartilage and osteoarthritis (ed. Kuettner, K.E.) (Raven Press, New York, 1992).
198. Olsen, B. Articular cartilage and osteoarthritis (ed. Kuettner, K.E.) (Raven Press, New York, 1992).
199. von der Mark, K. Dynamics of bone and cartilage metabolism (eds. Seibel, M.J., Robins, S.P. & Bilezikian, J.P.) (Academic Press, San Diego, 2006).
200. HeinegardDick , L.P., Saxne Tore Dynamics of bone and cartilage metabolism (eds. Seibel, M.J., Robins, S.P. & Bilezikian, J.P.) (Academic Press, San Diego, 2006).
201. Clark Ian M , M.G. Dynamics of bone and cartilage metabolism (eds. Seibel, M.J., Robins, S.P. & Bilezikian, J.P.) (Academic Press, San Diego, 2006).
202. Chen, F.H., Rousche, K.T. & Tuan, R.S. Technology Insight: adult stem cells in cartilage regeneration and tissue engineering. Nat Clin Pract Rheumatol 2, 373-82 (2006).
203. Ge, Z. et al. Osteoarthritis and therapy. Arthritis Rheum 55, 493-500 (2006).
204. Goldring, M.B. & Goldring, S.R. Osteoarthritis. J Cell Physiol 213, 626-34 (2007).
205. Aspden, R.M. Osteoarthritis: a problem of growth not decay? Rheumatology (Oxford) 47, 1452-60 (2008).
206. Poole, A.R. An introduction to the pathophysiology of osteoarthritis. Front Biosci 4, D662-70 (1999).
207. Sandell, L.J. & Aigner, T. Articular cartilage and changes in arthritis. An introduction: cell biology of osteoarthritis. Arthritis Res 3, 107-13 (2001).
208. Fukui, N., Purple, C.R. & Sandell, L.J. Cell biology of osteoarthritis: the chondrocyte's response to injury. Curr Rheumatol Rep 3, 496-505 (2001).
209. Wieland, H.A., Michaelis, M., Kirschbaum, B.J. & Rudolphi, K.A. Osteoarthritis - an untreatable disease? Nat Rev Drug Discov 4, 331-44 (2005).
210. Zemmyo, M., Meharra, E.J., Kuhn, K., Creighton-Achermann, L. & Lotz, M. Accelerated, aging-dependent development of osteoarthritis in alpha1 integrin-deficient mice. Arthritis Rheum 48, 2873-80 (2003).
211. Werb, Z., Tremble, P.M., Behrendtsen, O., Crowley, E. & Damsky, C.H. Signal transduction through the fibronectin receptor induces collagenase and stromelysin gene expression. J Cell Biol 109, 877-89 (1989).
212. Loeser, R.F., Forsyth, C.B., Samarel, A.M. & Im, H.J. Fibronectin fragment activation of proline-rich tyrosine kinase PYK2 mediates integrin signals regulating collagenase-3 expression by human chondrocytes through a protein kinase C-dependent pathway. J Biol Chem 278, 24577-85 (2003).
213. Forsyth, C.B., Pulai, J. & Loeser, R.F. Fibronectin fragments and blocking antibodies to alpha2beta1 and alpha5beta1 integrins stimulate mitogen-activated protein kinase signaling and increase collagenase 3 (matrix metalloproteinase 13) production by human articular chondrocytes. Arthritis Rheum 46, 2368-76 (2002).
214. Homandberg, G.A., Costa, V., Ummadi, V. & Pichika, R. Antisense oligonucleotides to the integrin receptor subunit alpha(5) decrease fibronectin fragment mediated cartilage chondrolysis. Osteoarthritis Cartilage 10, 381-93 (2002).
215. Ronziere, M.C. et al. Integrin alpha1beta1 mediates collagen induction of MMP-13 expression in MC615 chondrocytes. Biochim Biophys Acta 1746, 55-64 (2005).
216. Stolz, M., R. Imer, U. Staufer, and U. Aebi Development of an Arthroscopic Atomic Force Microscope Bioworld 2-5 (2003).
217. Stolz, M. et al. Dynamic elastic modulus of porcine articular cartilage determined at two different levels of tissue organization by indentation-type atomic force microscopy. Biophys J 86, 3269-83 (2004).

9. Acknowledgements

This work would not have been possible without the support and contribution of many people whom I would like to acknowledge:

My direct supervisor Dr. Attila Aszodi who has been during these years a great teacher to me. Despite the ups and downs that we have been through, his continuous support and patience made this thesis possible. Thanks for accepting and tolerating me as I am!

Prof.Dr. Reinhard Fässler for giving me the opportunity to work in his lab and for accepting to be the first referee of my thesis. My sincere gratitude for his support, encouragement and the great working conditions that he offered me during these years.

PD Dr. Matthias Schieker, who agreed to be the second referee of my thesis and Prof. Dr. Martin Biel, Prof. Dr. Karl-Peter Hopfner, Prof. Dr. Angelika Vollmar and Prof. Dr. Christian Wahl-Schott, the members of my thesis committee for taking the time to review my work.

Dr.Martin Stolz, Prof. Dr. Ernst Hunziker and Dr. Inga Drosse for nice collaborations and constructive discussions.

Dr. Walter Göhring for making things work smoothly in the lab!

The animal caretakers from the Rb facility for the often underappreciated but extremely valuable work.

Zsuzsa Farkas and Mischa Reiter for their precious hands in helping me with good quality sections and stainings and for their moral support during these years.

All people from the Department of Molecular Medicine for the friendly and warm atmosphere. I would like to thank especially Tim Lämmerman, Eloi Miralles-Montanez and Korana Radovanac for maintaining my sanity.

“Grasutzelor” my lovely friends from Romania for being there, somewhere….

Finally I would like to thank my parents Ileana and Alexandru, and my sister Georgeta (Gibica) for their love, care and for believing in me. Many thanks and all my love to my greatest source of strength, my husband Kyle, for his affection and his help at home and at work and for offering me a kaleidoscope!

10. Curriculum vitae

Aurelia Raducanu

Address

Kruckenburgstr. 3, 81375 Munich, Germany

Date and Place of Birth

07.03.1977, Bucharest, Romania

Marital status

married

Education and Scientific Experience

03/2004 – present	**Max Planck Institute of Biochemistry Munich, Germany** Ph.D. student in the group of Dr. Attila Aszodi in the Department of Molecular Medicine headed by Prof.Dr. Reinhard Fässler
03/ 2002 – 03/2004:	**Institute of Biochemistry of the Romanian Academy, Bucharest**, **Romania** Research assistant in the "Ligand – Receptor Interactions" Group
10/2001 – 02/2003	**University of Bucharest , Faculty of Biology, Dept. of Biochemistry** Master studies in Biochemistry and Molecular biology Master thesis in the "Ligand-Receptor interactions" group at the Institute of Biochemistry, Bucharest. Title: "*Antiviral activity of lactoferrin against bovine viral diarrhea virus"*
10/1997- 06/2001	**University of Bucharest , Faculty of Biology, Dept. of Biochemistry** Undergraduate studies
09/1991-07/1995	**Theoretic High School "Matei Basarab", Bucharest, Romania** Class of chemistry-biology. Baccalaureate
09/1983-07/1991	**General School Number. 55, Bucharest, Romania** Primary school

11. Supplements

In the following, papers I to V are reprinted.

PAPER I

β1 integrin-dependent cell shape governs mitotic spindle positioning in growth plate chondrocytes

Aurelia Raducanu[1] and Attila Aszodi[1*]

[1]Department of Molecular Medicine, Max Planck Institute of Biochemistry, Am Klopferspitz 18, D-82152 Martinsried, Germany

Running title: cell shape regulates spindle orientation

Key words: integrin, cartilage, mitotic spindle, cell shape

[*]corresponding author: aszodi@biochem.mpg.de

Tel:+49 89 8578 2466; Fax: +49 89 8578 2422

Characters with spaces: 29 979

Abstract

Recently, members of the β1 integrin family of cell-adhesion receptors have emerged as important orienting factors of the mitotic apparatus in epithelial tissues. In contrast, the role of β1 integrins for spindle positioning in mesenchymal tissues such as the columnar, cartilaginous growth plate in the long bones is unknown. Here we show by mouse genetics that β1 integrin function is pivotal for flattening and mediolateral orientation of proliferative chondrocytes in the growth plate, which in turn dictates spindle alignment along the long axis of the cell. The rounded, nonoriented β1-null chondrocytes display random spindle and division axes and fail to intercalate into columns. We further demonstrate that in vitro, integrin-dependent adhesion defines relative spindle orientation to the substratum by modulating chondrocyte geometry. Based on the above findings, we propose that cell shape anisotropy maintained by β1 integrins provides a default guiding cue for spindle and division positioning in chondrocytes.

INTRODUCTION

Endochondral bone formation (Kronenberg, 2003) is the primary mechanism of skeletogenesis which begins with the aggregation and chondrogenic differentiation of mesenchymal precursors at the sites of future skeletal elements. During development, the cartilaginous templates of long bones display club-shaped expansions at the ends (epiphyses) separated by a middle shaft. While the epiphysis contains rounded cells dispersed in extracellular matrix (ECM), midshaft-resident chondrocytes form a polarized structure called the growth plate (GP) (Fig. 1A). At birth, GP chondrocytes arrange into longitudinal columns and distinct zones reflecting the various stages of differentiation. In the proliferation zone (PZ), cells exhibit high mitotic activity, are flattened and oriented along the mediolateral (ML) axis of the GP. As stated by Dodds (Dodds, 1930), mitotic figures in the elongated chondrocytes lie perpendicular to the proximal-distal (PD) direction of growth, while cell divisions occur parallel to the columns (Fig. 1B). This observation is in agreement with Hertwig´s laws postulating that 1) the axis of the spindle takes “the direction of the greatest protoplasmic masses” and 2) “the plane of division always cuts the axis of the spindle perpendicularly” (Hertwig, 1912). In Dodds' model, following cytokinesis the semi-circular daughter cells adopt a wedge-shape and glide around each other until they reach the same vertical plane and become discoid again. Later, chondrocytes withdraw from the cell cycle and become hypertrophic. Thus, longitudinal bone growth is achieved by proliferation, matrix production and hypertrophy of GP chondrocytes. Surprisingly, the mechanisms responsible for the geometrical anisotropy and columnar arrangement of proliferative chondrocytes are poorly understood, although the roles of ECM mechanics (Gould et al., 1974), secreted

morphogens (Abad et al., 2002) and noncanonical frizzled signaling (Li and Dudley, 2009) have been suggested.

The heterodimeric (αβ) integrins are the major class of adhesion molecules that control various aspects of cell behavior including shape, migration, proliferation and survival (Lo, 2006). We previously reported that *β1$^{fl/fl}$-Col2a1cre* mice, in which the β1 integrin gene was ablated in chondrocytes, develop severe chondrodysplasia and lack GP columns at birth due to cell rounding and impaired cell motility in the PZ (Aszodi et al., 2003). Mice lacking the collagen-binding integrin α10β1 or integrin-linked kinase in cartilage display similar but milder GP abnormalities (Bengtsson et al., 2005), (Grashoff et al., 2003). Although these findings clearly demonstrate the crucial importance of chondrocyte-ECM interactions in GP organization, the role of β1 integrins for spindle orientation in chondrocytes was not addressed.

Growing evidence suggests that integrin functions are critical for spindle alignment and daughter cell positioning both in vivo and in vitro (Streuli, 2009). In the skin, β1 integrins are involved in the establishment of apical polarity of basal keratinocytes which in turn determines whether the spindle orients parallel or perpendicular to the basement membrane (Lechler and Fuchs, 2005). In mammary epithelium, ablation of β1 integrin randomizes the division plane in basal cells resulting in the mislocation of stem cell progeny to the luminal compartment (Taddei et al., 2008). In *Drosophila* ovary, signaling via βPS integrins is required for the correct spindle orientation in follicular epithelial cells (Fernandez-Minan et al., 2007). Furthermore, in vitro studies demonstrated that β1 integrins regulate the angle between the mitotic spindle and the substrate plane in cultured, non-polarized adherent cells (Toyoshima and Nishida, 2007). HeLa cells plated on fibronectin or

collagen orient their metaphase spindle parallel to the substratum, whereas spindle axes are misoriented when β1 integrin function is compromised.

To assess whether mitotic spindle positioning is affected by β1 integrins in the GP we used conditional knock-out mouse strains. Here we show that β1 integrins are necessary for establishing GP polarity and for correct orientation of the mitotic spindle in chondrocytes both in vivo and in vitro by maintaining their geometrical anisotropy.

RESULTS

Chondrocyte shape change and column formation in the growth plate

To gain detailed insight into GP morphogenesis, we characterized the cellular changes that occur in the PZ during the development of the mouse tibia (Fig. 1C). At the aggregation phase (embryonic day 11, E11), mesenchymal cells show no obvious orientation relative to the PD axis. Morphometric analysis of tissue cryosections revealed that pre-chondrocytes are polygonal and display a shape index (SI) of 1.43±0.30. Upon chondrogenic differentiation at E12, presumptive GP chondrocytes exhibit moderate flattening (SI=1.93±0.45) and their long axes tend to align perpendicular to the PD direction. Thus, chondrocyte shape anisotropy and spatial tissue polarity are established very early in cartilage development. At E13, proliferative chondrocytes further flatten (SI=3.41±0.60) along the ML axis and largely organize into parallel lines. At E14, PZ chondrocytes are slightly more flattened (SI=3.58±0.72) and show the first signs of column formation, composed of short stacks of 2-3 discoid chondrocytes. At newborn stage, the SI increases to 4.91±1.41

indicating the extreme flattening of PZ chondrocytes. In contrast, epiphyseal chondrocytes are rounded or ovoid in shape (SI=1.42±0.25).

Spindle position depends on the orientation and shape of chondrocytes

To monitor spindle alignments and division axes in proliferative chondrocytes, we imaged tibial GPs of normal mice. Spindle orientations during metaphase (early spindle) and during anaphase-telophase (late spindle) were determined by measuring the angle (α°), from 0° (parallel) to 90° (perpendicular) between the PD axis and the spindle axis in the *xy* plane. At E12, early spindles were randomly oriented, whereas 57% of the late spindles aligned within 30° of perpendicular to the PD axis. In contrast, only 15% of the late spindles were within 30° of a parallel orientation (Fig. 2A,B). Early spindles were still randomly aligned at E13, but now perpendicularly aligned (60°-90°) late spindles accounted for more than 81% of all mitotic figures (Fig. 2D). Consequently, midbodies and cleavage furrows were mostly positioned parallel to the PD axis, although diagonal orientations were occasionally observed (Fig. 2C). Increasingly stringent perpendicular late spindle orientation was observed between E12 and E13, with 15% and 48% of late spindles within 10° of perpendicular, respectively (Fig. 2B,D). From E14, perpendicular alignment of late spindle became the default orientation. At E18, early spindles displayed a bias towards perpendicular orientation with 75% of the spindle angles falling between 60°-90°, whereas all late spindles were oriented within 20° of perpendicular to the PD axis (Fig. 2E,F). Importantly, while 93% of late spindles aligned completely perpendicular (80°-90°), only 27.5% of metaphase spindles showed stringently perpendicular orientation (Fig. 2F). Next, we examined the relationship between

spindle orientation in mitotic cells and long axis orientation of interphase cells relative to the PD axis (Fig. 2G). The angles of the long axis during interphase and the spindle angles in anaphase/telophase correlated well at all stages (E12, E13 and E18) suggesting that the orientation of the elongated chondrocytes within the GP determines late spindle orientation and, therefore, the cleavage plane. However, such a correlation was not observed between early spindle and interphase long axis angles at E12 and E13, and only a partial correlation was found at E18.

The above findings led us to modify and extend Dodds´ model (Fig. 2H). Following aggregation, differentiated chondrocytes elongate and align their long axis either perpendicular or, to a lesser extent, diagonal to the PD axis of growth. Between E13-E14, late spindles align parallel to the long axis of the cells according to Hertwig´s rule. After cytokinesis, daughter cells of perpendicularly-oriented chondrocytes either remain in the same row as the mother cell, contributing to the lateral expansion of the cartilaginous template, or undergo a rotational movement of 90° to initiate a two-cell stack. Column initiation can also be achieved by the division and subsequent rotation of diagonally-oriented chondrocytes. At later stages, chondrocytes are more flattened and aligned more strictly perpendicular to the PD axis. Following cytokinesis, the daughter cells intercalate to expand the columns, mature and become hypertrophic to accomplish the longitudinal elongation of the tissue. Importantly, Hertwig´s rule can strictly be applied only for late mitotic figures of E12-NB proliferative chondrocytes implying that misoriented metaphase spindles adjust their orientation to ensure chromosomal segregation along the long axis of the flattened cell during anaphase/telophase. Furthermore, this observation argues against the existence of cortical cues in GP chondrocytes that could specifically guide spindle orientation at the time of mitotic entry.

β1 integrins control mitotic spindle positioning in the growth plate

Our model suggests that chondrocyte geometry and orientation are important determinants of spindle and cell division positioning in the GP which may depend on integrin-mediated cell adhesion. By immunostaining wild type tibial sections, we observed even deposition of the β1 integrin subunit on the surface of interphase, mitotic and intercalating proliferative GP chondrocytes (Fig. 3A). To determine the impact of β1 integrins on chondrocyte spindle orientation, we imaged the cartilage from *β1$^{fl/fl}$-Col2a1cre* mice (Aszodi et al., 2003). Because deletion of β1 integrin occurs at around E12, a significant amount of β1 integrin was still visible on proliferative chondrocytes at E13 that was apparently sufficient for their normal ML elongation (Fig. 3B, upper insert). At E14, when little if any, β1 integrin is detected, the cells rounded and lost their orientation (Fig. 3B, lower insert). This rapid change between E13 and E14 implies that β1 integrins are vitally important to maintain chondrocyte shape and tissue polarity in the proliferative zone of the GP. At E18, cells of the epiphysis and the PZ were morphologically indistinguishable (Figure 3C) (SI_{epi}=1.27±0.14 and SI_{PZ}=1.37±0.20). Moreover, mutant chondrocytes in the PZ displayed random orientation of both early and late spindles (Fig. 3D,E), similar to what we observed in mutant and wild type epiphyses (Fig. 3F and not shown). These data indicate that rounded chondrocyte geometry is accompanied by the randomized orientation of the mitotic apparatus.

To further examine the role of β1 integrins in GP polarity, we generated *β1$^{fl/fl}$-Prx1cre* mice to achieve deletion of the β1 integrin gene in early limb-bud mesenchymal cells. In the hind-limb, the *Prx1cre*-driven deletion is complete in most, but not all mesenchymal progenitors of skeletal lineages at E10.5 leading to mosaic expression of β1 integrin during cartilage development. At E13, β1 integrin-positive

chondrocytes were flattened and aligned at a right angle to the PD axis, whereas β1-negative chondrocytes were rounded (Fig. 3G, upper insert). At E14, β1-positive chondrocytes intercalated, forming the first 2-cell columns (Figure 3G, lower insert) that by E18 had expanded to 6-10 cells (Fig. 3H). β1 integrin-expressing cells in the largely β1-deficient GP properly oriented their long axis and aligned the late spindle perpendicular to the PD axis (Fig. 3H and not shown). In contrast, *β1$^{fl/fl}$-Prx1cre* PZ chondrocytes had misoriented spindles comparable to *β1$^{fl/fl}$-Col2a1cre* chondrocytes (not shown). These findings therefore demonstrate that β1 integrins regulate chondrocyte polarity and arrangement in a cell autonomous manner.

In summary (Fig. 3I), β1-deficiency in the GP leads to chondrocyte rounding, randomizes spindle and cleavage plane orientation, and blocks gliding movements necessary for column initiation and elongation.

β1 integrins regulate spindle orientation relative to the substrate plane in vitro

To determine the role of β1 integrins for spindle orientation in vitro, primary chondrocytes isolated from wild type and *β1$^{fl/fl}$-Col2a1cre* embryos were plated on various substrates and imaged in metaphase. On collagen II (Fig. 4A), wild type (wt) and mutant (mt) chondrocytes failed to spread and remained round (SI_{wt}=1.02±0.2 and SI_{mt}=1.57±0.2). Control chondrocytes attached to the collagen II-coated surface via β1 integrins, while *β1$^{fl/fl}$-Col2a1cre* chondrocytes deposited a focal fibronectin matrix beneath them and attached to it via β3 integrins (not shown). Surprisingly, both control and β1-deficient chondrocytes displayed average spindle angles of 29.81°±4.13° and 20.92°±3.26°, respectively, and showed no preference to orient their metaphase spindle parallel with the substratum (α°= 0° to 10°, Fig. 4A). In

contrast, control and mutant chondrocytes spread and flattened well on vitronectin via β3 integrins (SI_{wt}=4.11±0.23 and SI_{mt}=4.20±0.22). In most cases the spindle was aligned parallel to the adhesion plane (Fig. 4B) leading to low average spindle angles ($\alpha°_{wt}$=6.36°±1.22° and $\alpha°_{mt}$=5.19°±1.33°). On fibronectin, mutant cells which lack the major fibronectin receptor α5β1 integrin, spread significantly less and are more rounded than control chondrocytes (Fig. 4C). Wild type chondrocytes had a high shape index (SI=3.26±0.21), low spindle angle (α°=7.25°±1.40°) and about 80% of the spindles were oriented parallel to the substratum, whereas for mutant cells the same parameters were 1.73±0.13, 22.66°±3.49° and about 37% (Fig. 4C). To manipulate their shape in culture by crowding, wild type cells were plated at high density on fibronectin and the shape indexes and spindle orientations were compared to those of sparse culture (Fig. 4D). We observed a significant decrease in the shape index ($3.26±0.21_{sparse}$ and $2.19±0.07_{dense}$, p<0.0001 by t-test) and increase in the average spindle angle ($7.25°±1.40°_{sparse}$ and $11.98°±1.41°_{dense}$, p<0.05). Importantly, only 40% of the wild type metaphase cells oriented their spindle parallel to the surface in dense culture. Collectively, our results suggest that geometric constraints are the primary determinants of the angle between the spindle axis and the substrate plane in cultured chondrocytes; and integrin-mediated anchorage has a pivotal role on ligand-selective cellular geometry. Thus, integrins govern spindle alignment via cell shape regulation both in vivo and in vitro.

DISCUSSION

Our findings demonstrate that β1 integrin-based adhesion is essential for several key steps of GP morphogenesis. First, β1 integrins are critically required for the

establishment of chondrocyte polarity and orientation in the GP upon chondrogenic differentiation. The primary mechanism triggering chondrocyte elongation and ML orientation is speculative, and may involve mechanical or secreted signals (Gould et al., 1974); (Abad et al., 2002). In the forming GP, integrins may act as mechanoreceptors or co-receptors for morphogen pathways and orchestrate the cellular commands for shape change by providing a physical platform for matrix engagement and by organizing the cytoskeleton. It has been recently demonstrated that noncanonical frizzled (Fzd) signaling controls chondrocyte orientation in chicken GP without significant impact on cell anisotropy (Li and Dudley, 2009). Therefore, it seems unlikely that the noncanonical Fzd pathway modulates the expression and/or localization of β1 integrins on the cell surface, although a role in polarized matrix deposition cannot be excluded.

Second, β1 integrin-based anchorage to the ECM is needed for proliferative chondrocytes to adopt their elongated shape. β1-null mouse basal keratinocytes also change their shape, but become elongated rather than rounded (Raghavan et al., 2000). In contrast, depletion of the β1 equivalent βPS integrin does not significantly change the cuboidal shape of follicle cells in *Drosophila* ovary epithelium (Fernandez-Minan et al., 2007). Since collagen II is by far the most abundant adhesive ligand in cartilage, it is possible that the loss of β1 integrins in such a “β1-specific matrix” creates a quasi suspension-like environment leading to chondrocyte rounding. Indeed, chondrocytes lacking the major collagen receptor α10β1 integrin also show a tendency to become round (Bengtsson et al., 2005).

Third, β1 integrins control the direction of cytokinesis by maintaining chondrocyte shape anisotropy that guides late spindle orientation and chromosome segregation along the long axis of the cell. Basal keratinocytes round up when they

enter mitosis and align their spindles relative to the basement membrane depending on intrinsic polarity cues, cell-cell and β1 integrin-mediated cell-ECM interactions (Lechler and Fuchs, 2005). In contrast, chondrocytes are completely surrounded by the ECM, do not round up in metaphase and do not show obvious cortical polarity. Taking into account the extreme flattening of proliferative chondrocytes, we propose that GP cartilage represents a rather unique tissue in which the cells achieve symmetrical and oriented cell division by using solely geometric constraints inherent to the elongated shape. This concept is further supported by our in vitro analysis demonstrating that the metaphase spindle aligns parallel to the substratum in flat chondrocytes, whereas the spindle is misoriented in rounded cells. In HeLa cells, which exhibit mitotic rounding, depletion of β1-integrin impairs parallel spindle alignment by inhibiting the activation of PI3K (Toyoshima et al., 2007). We show here that spindle orientation in chondrocytes relies on cell spreading and not on the expression of β1 integrin *per se*. Thus, cell type-specific differences could generate distinct mechanisms for spindle alignments in two-dimensional culture systems.

Finally, β1 integrins are necessary for ML intercalation of proliferative chondrocytes to produce vertical columns (Aszodi et al., 2003). This process is similar to convergence extension movements of the dorsal mesoderm in *Xenopus* that also require β1 integrin-ECM interactions (Marsden and DeSimone, 2003); (Davidson et al., 2006). However, while in *Xenopus* the primary driving mechanism of motility is the traction generated by cell-cell contacts, in cartilage chondrocyte rotation may only depend on matrix adhesion-induced traction forces.

In summary, β1 integrins provide adhesive cues for chondrocyte geometry and orientation, which in turn orients the mitotic spindle and determines the division axis,

and for chondrocyte intercalation to shape the three-dimensional structure of the GP during endochondral bone formation.

METHODS

Mice

The *β1$^{fl/fl}$-Col2a1cre* strain was described previously (Aszodi et al., 2003). *β1$^{fl/fl}$-Prx1cre* mice were generated by crossing mice carrying the floxed β1 alleles with transgenic mice expressing the Cre-recombinase under the control of the Prx1 enhancer (Logan et al., 2002).

Tissue samples and immunostaining

Hindlimbs were fixed in 4% paraformaldehyde (PFA) in phosphate buffered saline (PBS, pH 7.4) at room temperature overnight. Fixed samples were immersed into 30% sucrose/PBS for 24h, frozen in OCT and cut longitudinally (50 μm) using a cryostat. Sections were treated with hyaluronidase (2mg/ml in PBS, 2h, 37°C), blocked in 2% BSA, 0.5% Triton X-100 in PBS, and incubated with the following primary antibodies: anti-α tubulin (Chemicon MAB1864), anti-pericentrin (Covance PRB-432) and anti-β1 integrin (Chemicon MAB 1997). Primary antibodies were visualized by the appropriate fluorescently labelled secondary antibodies. Actin was stained with phalloidin Alexa 488 (Invitrogen) and the DNA was stained with DAPI (Sigma). Tissues were also embedded into paraffin or plastic resin for standard immunohistochemistry and histology, respectively.

Primary chondrocytes and immunocytochemistry

Rib chondrocytes from E18 mice were isolated and cultured for 36 hours on substrate-coated chamber slides as described (Aszodi et al., 2003). For spindle analysis, cells were prefixed in 0.5% glutaraldehyde/0.2% TritonX-100 in modified

Hank's balanced salt solution (137mM NaCl; 5mM KCl; 1.1mM Na_2HPO_4; 0.4mM KH_2PO_4; 2mM $MgCl_2$; 2mM EGTA; 5mM PIPES; 5.5mM glucose; 4mM $NaHCO_3$; 0.11% MES ; pH 6.5) for 1 min, postfixed in 1% glutaraldehyde for 10 min and were sequentially stained with anti-α-tubulin and anti-pericentrin antibodies, with fluorescently-labelled secondary antibodies, with phalloidin (1h each) and DAPI.

Image analyses

Confocal stacks were built from images acquired every 0.5 microns by confocal microscopy (DMIRE2; Leica) with a 63x 1.4 oil objective. From the acquired stacks of tissue sections, the long and the short axes of chondrocytes, corresponding to the major and minor axes of an ellipse, were measured using the Leica Confocal Software (version 2.5) as well as the angle between the spindle axis and the proximodistal axis of the cartilage using MetaMorph 6.0. Cell orientation was determined by measuring the angle between the long axis of the cell and the proximodistal axis of the growth. For in vitro data, the angle values were obtained using inverse trigonometric function: $\alpha° = \tan^{-1} Z/l$ (Z is the vertical distance between the centrosomes; l is the projection of the linear distance between the centrosomes, measured using Leica Confocal Software (modified from (Toyoshima and Nishida, 2007)). Shape indexes were calculated as follows: the ratio of the long and short axes of the cell (in vivo) or the ratio of the length and height of the cell (in vitro).

Acknowledgements

We thank Dr. K. Legate for careful reading of the manuscript and Zs Farkas for technical assistance. This work was supported by the Max Planck Society.

References

Abad, V., Meyers, J.L., Weise, M., Gafni, R.I., Barnes, K.M., Nilsson, O., Bacher, J.D. and Baron, J. (2002) The role of the resting zone in growth plate chondrogenesis. *Endocrinology*, **143**, 1851-1857.

Aszodi, A., Hunziker, E.B., Brakebusch, C. and Fassler, R. (2003) Beta1 integrins regulate chondrocyte rotation, G1 progression, and cytokinesis. *Genes Dev*, **17**, 2465-2479.

Bengtsson, T., Aszodi, A., Nicolae, C., Hunziker, E.B., Lundgren-Akerlund, E. and Fassler, R. (2005) Loss of alpha10beta1 integrin expression leads to moderate dysfunction of growth plate chondrocytes. *J Cell Sci*, **118**, 929-936.

Davidson, L.A., Marsden, M., Keller, R. and Desimone, D.W. (2006) Integrin alpha5beta1 and fibronectin regulate polarized cell protrusions required for Xenopus convergence and extension. *Curr Biol*, **16**, 833-844.

Dodds, G.S. (1930) Row formation and other types of arrangement of cartilage cells in endochondral ossification. Vol. 46, pp. 385-399.

Fernandez-Minan, A., Martin-Bermudo, M.D. and Gonzalez-Reyes, A. (2007) Integrin signaling regulates spindle orientation in Drosophila to preserve the follicular-epithelium monolayer. *Curr Biol*, **17**, 683-688.

Gould, R.P., Selwood, L., Day, A. and Wolpert, L. (1974) The mechanism of cellular orientation during early cartilage formation in the chick limb and regenerating amphibian limb. *Exp Cell Res*, **83**, 287-296.

Grashoff, C., Aszodi, A., Sakai, T., Hunziker, E.B. and Fassler, R. (2003) Integrin-linked kinase regulates chondrocyte shape and proliferation. *EMBO Rep*, **4**, 432-438.

Hertwig, O. (1912) *Text-book of the Embryology of man and mammals*. George Allen & co., LTD. Ruskin House, London.

Kronenberg, H.M. (2003) Developmental regulation of the growth plate. *Nature*, **423**, 332-336.

Lechler, T. and Fuchs, E. (2005) Asymmetric cell divisions promote stratification and differentiation of mammalian skin. *Nature*, **437**, 275-280.

Li, Y. and Dudley, A.T. (2009) Noncanonical frizzled signaling regulates cell polarity of growth plate chondrocytes. *Development*.

Lo, S.H. (2006) Focal adhesions: what's new inside. *Dev Biol*, **294**, 280-291.

Logan, M., Martin, J.F., Nagy, A., Lobe, C., Olson, E.N. and Tabin, C.J. (2002) Expression of Cre Recombinase in the developing mouse limb bud driven by a Prxl enhancer. *Genesis*, **33**, 77-80.

Marsden, M. and DeSimone, D.W. (2003) Integrin-ECM interactions regulate cadherin-dependent cell adhesion and are required for convergent extension in Xenopus. *Curr Biol*, **13**, 1182-1191.

Raghavan, S., Bauer, C., Mundschau, G., Li, Q. and Fuchs, E. (2000) Conditional ablation of beta1 integrin in skin. Severe defects in epidermal proliferation, basement membrane formation, and hair follicle invagination. *J Cell Biol*, **150**, 1149-1160.

Streuli, C.H. (2009) Integrins and cell-fate determination. *J Cell Sci*, **122**, 171-177.

Taddei, I., Deugnier, M.A., Faraldo, M.M., Petit, V., Bouvard, D., Medina, D., Fassler, R., Thiery, J.P. and Glukhova, M.A. (2008) Beta1 integrin deletion from the basal compartment of the mammary epithelium affects stem cells. *Nat Cell Biol*, **10**, 716-722.

Toyoshima, F., Matsumura, S., Morimoto, H., Mitsushima, M. and Nishida, E. (2007) PtdIns(3,4,5)P3 regulates spindle orientation in adherent cells. *Dev Cell*, **13**, 796-811.

Toyoshima, F. and Nishida, E. (2007) Integrin-mediated adhesion orients the spindle parallel to the substratum in an EB1- and myosin X-dependent manner. *Embo J*, **26**, 1487-1498.

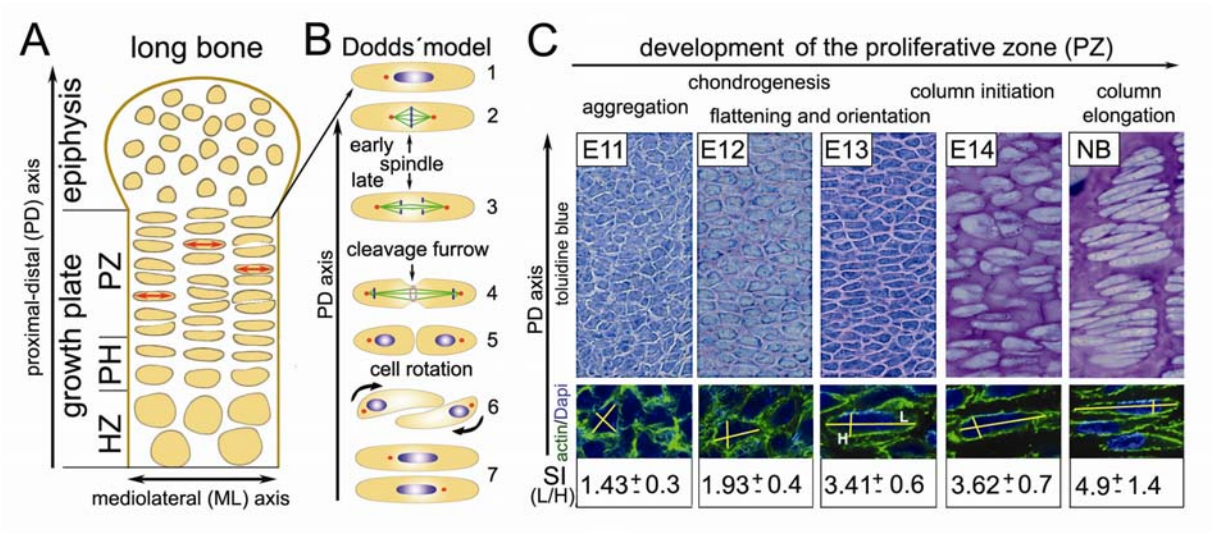

Figure 1. Cell shape and orientation in the normal growth plate.

(A) Schematic structure of a long bone at birth. Cells in the proliferative zone are organized into vertical columns and their long cell axes (red arrows) orient perpendicular to the proximal-distal direction of the bone. (B) Drawings showing the sequential steps of column formation (after (Dodds, 1930)). (C) Morphogenesis of the proliferative zone. Toluidine blue histochemistry showing the gradual flattening, orientation and columnar organization of the proliferative cells. Shape indexes (SI) were calculated from the ratio of the long (L) and short (S) axes (yellow lines) of the cells after double staining tissue cyrosections with actin and DAPI.

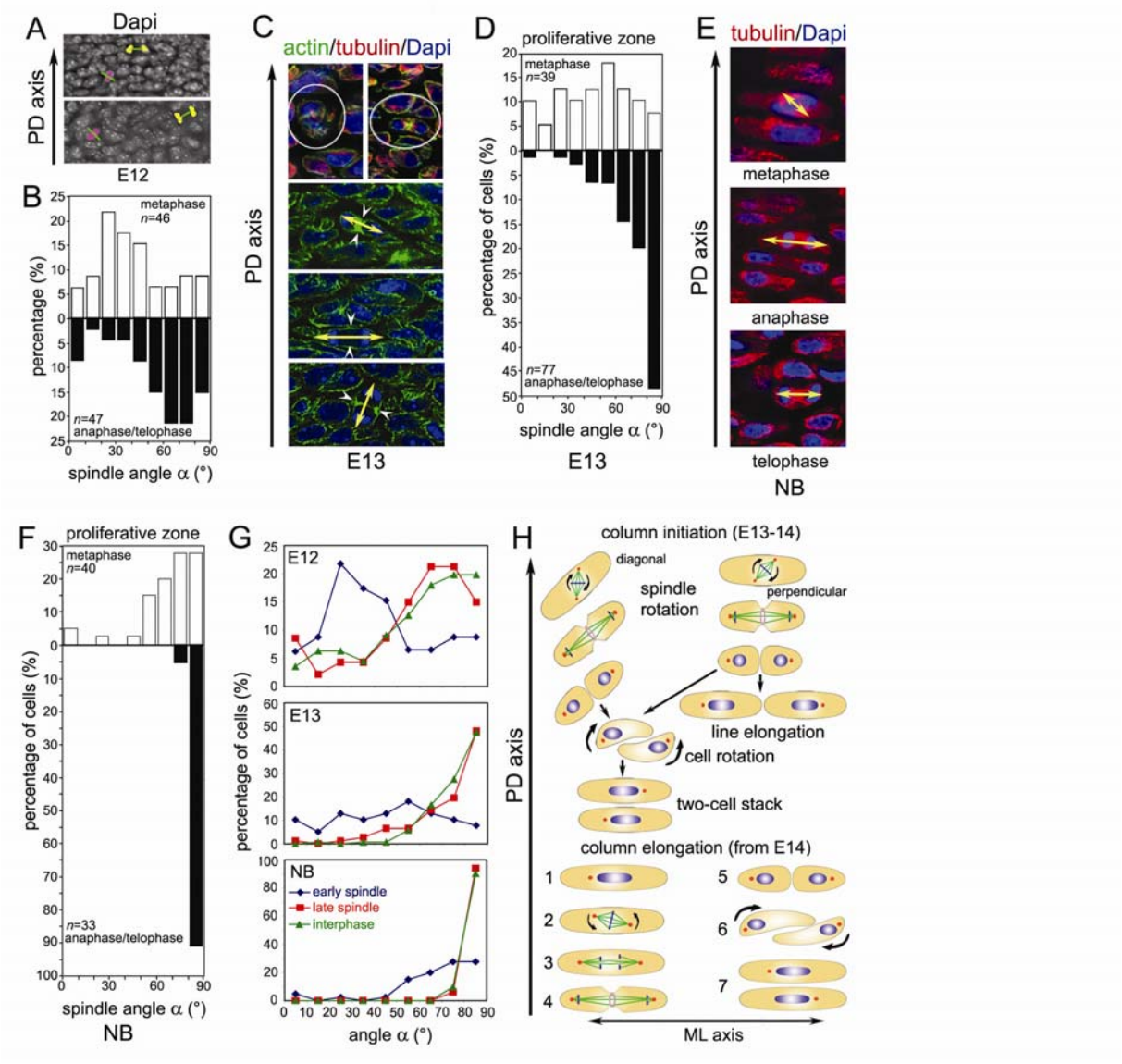

Figure 2. Mitotic spindle orientation during morphogenesis of the proliferative zone.

(A) Images of tibia at E12 showing the orientation of the mitosis (metaphase, purple; anaphase/telophase, yellow) relative to the PD axis. (B) Quantification of early and late spindle orientation at E12. (C) Immunofluorescence staining demonstrating the orientation of midbodies (circles), telophase spindles (yellow arrows) and cleavage furrows (arrowheads) at E13. (D) Quantification of spindle orientation at E13. (E) Images showing the spindle axis (arrows) and (F) quantitative analysis of spindle alignment at the newborn stage. (G) Plot diagrams of mitotic spindle and cell elongation orientation with respect the PD axis. (H) The modified Dodd´s model.

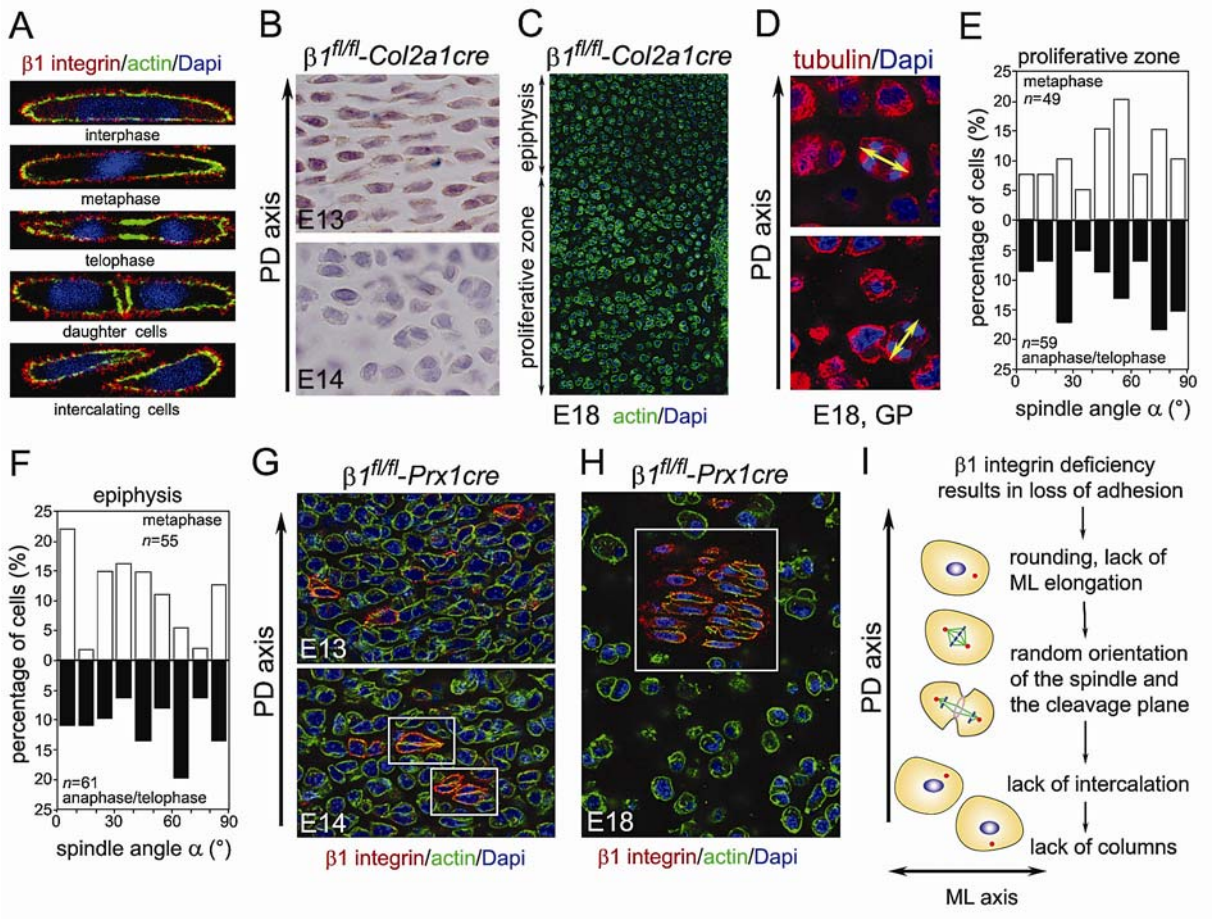

Figure 3. β1 integrins regulate chondrocyte shape and spindle orientation in the growth plate.

(A) Immunostaining of β1 integrin expression on the surface of interphase, mitotic and intercalating proliferative chondrocytes. (B) Depletion of β1 integrin results in rapid shape change and loss of chondrocyte orientation in the GP of *β1$^{fl/fl}$-Col2a1cre* mice. (C) At E18, *β1$^{fl/fl}$-Col2a1cre* epiphyseal and GP chondrocytes are indistinguishable by shape and orient both early and late mitotic spindles randomly (D, E, F). (G and H) In the mosaic growth plate of *β1$^{fl/fl}$-Prx1cre* mice, β1 integrin positive cells elongate perpendicular to the PD axis at E13 (G, upper), initiate chondrocyte stacks (G, lower) at E14 and form columns at E18 (H). (I) Cartoon, summarizing he consequence of β1 integrin deficiency on spindle orientation and GP morphogenesis.

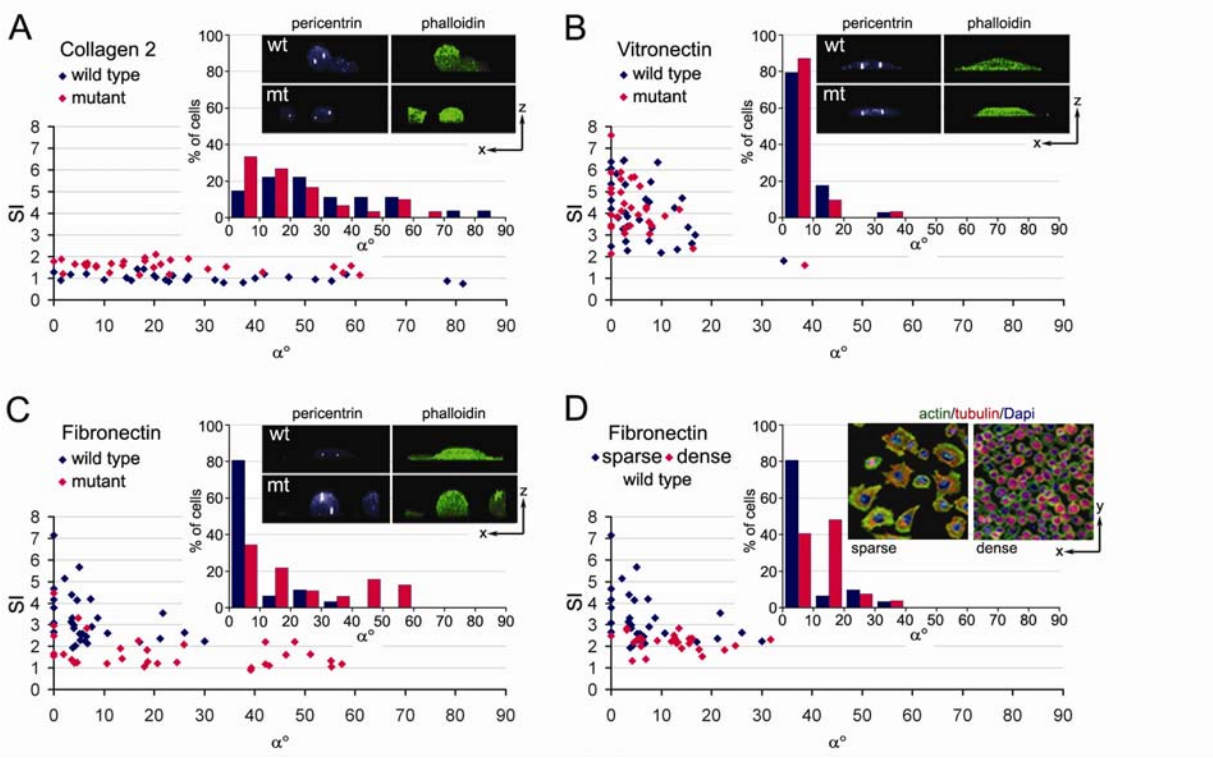

Figure 4. The angle between the spindle axis and the substrate plane is regulated by the shape of cultured chondrocytes.

(A-D) Wild type (wt) and *β1*$^{fl/fl}$*-Col2a1cre* (mutant, mt) primary chondrocytes were cultured on various adhesive surfaces and metaphase spindle angles (α°) were plotted as a function of the shape index (SI, bottom graphs). Middle graphs demonstrate the distribution of metaphase spindle orientation. Right upper inserts on A-C are representative pictures showing the position of centrosomes (pericentrin staining) and the shape of the chondrocytes (phalloidin staining). The right upper insert on D shows the spreading of control chondrocytes on fibronectin in sparse and dense culture.

PAPER II

Knock-Out Mice in Osteoarthritis Research

Aurelia Raducanu and Attila Aszódi*

Department of Molecular Medicine, Max Planck Institute for Biochemistry, Martinsried, Germany

Abstract: Osteoarthritis (OA) is the most common degenerative disorder of the joints with an etiology involving genetic and environmental factors. Although various animal models have been used to elucidate the pathogenesis of OA, in the past decade gene targeting in mice has become one of the most powerful tools to dissect the molecular mechanisms of the disease. The generation of knockout mice has enormously accelerated the identification of the key genetic players in articular cartilage homeostasis and made a significant contribution to further our understanding of OA pathology. In this review, we will outline the phenotypes of the currently available mouse strains, carrying either engineered or spontaneous gene mutations, which provide insight into the processes of articular cartilage destruction. The analysis of these mice reveals a complex interaction among cytokines, proteases, transcription factors, extracellular matrix, cell surface and signaling molecules during the initiation and progression of OA and, in some cases, suggests new therapeutic interventions for the disease.

Keywords: Osteoarthritis, gene targeting, mouse models, extracellular matrix, signaling, proteolysis, cytokines, growth factors.

INTRODUCTION

Osteoarthritis (OA) is a non-systemic degenerative joint disease affecting millions of people world-wide and is the prevalent cause of disability over 65. Although OA is characterized by the gradual deterioration of the articular cartilage, both destructive and repair processes are activated at certain phases of the disease, suggesting a highly dynamic interplay among catabolic and anabolic molecular cascades. Osteoarthritis is generally accepted as a complex disorder influenced by both environmental and genetic factors [1]. To assess the contribution of genetic factors and to explore the pathogenesis of OA, murine models of human skeletal disorders are important tools. These models include mouse strains carrying spontaneous mutations and induced mutant strains generated by classical transgenesis (transgenic mice) or by gene targeting (knockout mice). Since the publication of OA-like changes in transgenic and knockout mice with mutations in the collagen IX gene in the mid 1990s [2, 3], gene ablation experiments have yielded more than 40 knockout mouse strains which have significantly advanced our knowledge of normal and pathobiology of the articular cartilage. Genetically modified mice not only provide a deeper insight into molecular mechanisms controlling joint development and OA pathogenesis, but also identify potential target molecules for therapeutic interventions against OA. In this review, we summarize the currently available knockout and the most relevant transgenic and spontaneous mouse models for OA research.

MATRIX TURNOVER AND ECM DEGRADING ENZYMES

Articular cartilage (AC) is composed of a structurally well organized, interactive set of extracellular matrix (ECM) molecules produced by chondrocytes. The two major structural components of the cartilage ECM are the type II collagen fibrils and the proteoglycan (PG) aggrecan. It is generally accepted that in OA the normal turnover of ECM molecules is disturbed, and the imbalance between anabolic and catabolic processes favors proteolytic degradation of aggrecan (aggrecanolysis) and collagens (collagenolysis), which eventually leads to articular cartilage destruction.

Several families of proteinases and proteinase inhibitors have been implicated in the initiation and progression of OA. Matrix metalloproteinases (MMPs) are a family of more than 20 zinc- and calcium-dependent proteinases that play crucial roles in various developmental, repair and pathological processes facilitating the turnover and breakdown of most ECM molecules [4-6]. A second family of MMP-related proteinases is composed of the membrane-anchored ADAMs (a disintegrin and metalloproteinases) and the secreted ADAMTSs (ADAM with thrombospondin motifs). Concerning the cartilage, ADAMTS proteins are particularly important because many of them are able to degrade aggrecan (aggrecanases) [7]. The activities of both MMPs and ADAMTSs are tightly regulated at multiple levels including inhibition by tissue inhibitors of metalloproteinases (TIMPs) [8]. Recent expression profiling revealed that most *MMP*, *ADAMTS* and *TIMP* genes are expressed in both normal and osteoarthritic human joints demonstrating the potential importance of these three protein families in OA [9, 10]. Finally, cysteine proteinases such as cathepsins B, L and K and their inhibitor (cystatin C) represent other important molecules that might be involved in AC destruction [11].

Aggrecanolysis

Proteoglycan depletion is among the first detectable alterations in osteoarthritic cartilage, usually preceding collagen degradation. Aggrecan consists of two N-terminal globular domains (G1 and G2), separated by an interglobular domain (IGD); regions substituted with keratan sulfate (KS) and chondroitin sulfate (CS) glycosaminoglycan (GAG) side chains; and a C-terminal globular domain (G3). Multiple cleavage sites for MMPs and aggrecanases have been identified in aggrecan *in vitro* and the corresponding degradation

*Address correspondence to this author at the Department of Molecular Medicine, Max Planck Institute for Biochemistry, Am Klopferspitz 18, D-82152 Martinsried, Germany; Tel: +49-89-8578-2466; Fax: +49-89-8578-2077; E-mail: aszodi@biochem.mpg.de

1573-3971/08 $55.00+.00

fragments can be detected in human OA synovial fluid and/or cartilage [12]. Two important cleavage sites associated with articular cartilage destruction are located in the IGD: all MMPs expressed in cartilage cleave predominantly between Asn^{341}-Phe^{342} generating the G1-$IPEN^{341}$ neoepitope; whereas ADAMTS aggrecanases cleave at Glu^{373}-Ala^{374} generating the G1-$TEGE^{373}$ fragment. Since aggrecanase but not MMP inhibitors are able to suppress aggrecan loss from human OA cartilage explants [13], most studies have focused on the identification of the key aggrecanase responsible for destructive aggrecanolysis.

ADAMTS-4 and ADAMTS-5, two aggrecanases possessing high aggrecanolytic activity, are expressed in normal and OA cartilage and their contribution to cartilage pathology was recently dissected in genetically modified mice [14-16]. Surprisingly, neither ADAMTS-4 nor ADAMTS-5 knockout mice exhibit obvious abnormalities indicating that these aggrecanases are dispensable for skeletal development. In unchallenged mutants, the level of G1-$TEGE^{373}$ fragment in cartilage was reduced suggesting that both proteases contribute to physiological aggrecanolysis in mice. However, inflammatory stimulation of aggrecan breakdown in IL-α-treated articular cartilage explants was blocked in ADAMTS-5 knockouts but not in ADAMTS-4 mutant mice. Similarly, only ADAMTS-5 mutant mice were protected from aggrecan loss and articular cartilage erosion in inflammatory or surgically induced *in vivo* models of arthritis. Thus, ADAMTS-5 is the sole enzyme responsible for IGD cleavage and for the initiation of early aggrecan breakdown, however, a recent study showed that some aggrecanolysis still occurs at the CS-rich region in the ADAMTS-5 knockout mice [17]. Furthermore, cartilage explants from ADAMTS-4/ADAMTS-5 double mutant mice release intact or G1 domain-containing aggrecan molecules upon retinoic acid stimulation demonstrating that aggrecan loss is not necessarily coupled to its proteolytic processing [18]. Nevertheless, blocking IGD cleavage by aggrecanase inhibitors might be a useful therapeutic strategy to reduce or even reverse cartilage destruction. Consistent with this assumption, the so-called "Jaffa" mice, in which the aggrecan core protein is rendered resistant to aggrecanase-mediated cleavage, are partially protected against aggrecan loss and cartilage damage progression in surgically and inflammatory-induced experimental models of arthritis [19].

Explant culture experiments revealed that MMPs account for only a small percentage of total aggrecan catabolism in porcine cartilage implying that MMPs are rather involved in basal turnover of aggrecan in the pericellular microenvironment of chondrocytes than in destructive aggrecanolysis [20]. In line with the *in vitro* data, the so-called "Chloe" mice with a mutation resistant to MMP-driven cleavage of aggrecan IGD show normal skeletal development [21] and have no protection against cartilage deterioration in induced models of arthritis [19]. Among the MMPs capable of degrading aggrecan, MMP3 was studied in knockout mice in detail. MMP3 can degrade, in addition to aggrecan, various cartilage ECM components; and is able to activate procollagenases and progelatinases [4]. The incidence of spontaneous OA was recently compared between *Mmp3*-null and wild type mice [22]. While mild OA-like changes were similar in knockout and control 1-year-old mice, the exposure of G1-$IPEN^{341}$ and the deterioration of the AC were significantly less prominent in MMP3-deficient mice at 2 years of age. In inflammatory arthritis models, *Mmp3*-null mice showed normal PG depletion, but did not expose type II collagen-cleavage neoepitopes [23, 24]. Since the findings were accompanied by a lack of significant cartilage destruction, the major function of MMP3 in these arthritis models seems to be the initiation of collagenase-mediated cartilage breakdown by activating procollagenases. In contrast, in a surgically-induced knee joint instability model *Mmp3*-null mice exhibited accelerated OA changes with increased G1-$IPEN^{341}$ and collagenase-cleavage neoepitope staining around the lesion sites [25]. These data imply that MMP3 could be replaced by functionally related MMPs to accelerate OA in some arthritis models, and that MMP3-regulated matrix turnover is important to maintain normal cartilage homeostasis.

Collagenolysis

The cleavage of the triple helical domain of type II collagen fibrils by collagenases occurs in both normal and arthritic cartilage. All three collagenases (MMP1, MMP8 and MMP13) cleave at the Gly^{906}-Leu^{907} site of each α-chain resulting in the generation of characteristic three-quarter and one-quarter collagen fragments. At the cleavage site, neoepitopes are exposed which can be detected by specific antibodies (C2C or C1,2C) either in the cartilage itself or in body fluids. In addition to collagenases, MMP2 and the membrane-bound MMP14 (MT1-MMP) also cleave native fibrillar collagens. In OA cartilage excessive collagen fragmentation is believed to increase the expression of proteolytic enzymes leading to further degradation of matrix proteins and subsequent cartilage resorption [26, 27].

A transgenic mouse line overexpressing constitutively active human MMP13 in postnatal joint cartilage exhibits deteriorated AC at 5 months of age accompanied by increased C1,2C immunostaining in the pericellular matrix [28]. Loss of Safranin O staining in the AC was also observed demonstrating that the disintegrated collagen network cannot retain proteoglycans in the tissue. In addition, MMP13 transgenic mice exhibit strong collagen X expression above the tidemark in the non-calcified upper and middle zones suggesting that MMP13 overexpression is linked to the reactivation of the normally suppressed differentiation program of AC chondrocytes. Interestingly, mice heterozygous for Runx2, a runt-related transcription factor which may activate both MMP13 and collagen X transcription, show decreased AC degradation along with reduced MMP13 and collagen X expression in a surgically induced OA model [29]. Whether MMP13 is a valuable target for OA treatment is still a question, since articular cartilage was not studied in *Mmp13*-null mice [30].

The emerging view that MMPs are not simply destructive but rather constructive enzymes of the cellular microenvironment [5, 6] is further illustrated by the phenotype of the *Mmp2*$^{-/-}$ and *Mmp14*$^{-/-}$ mice. MMP2-deficiency leads to multiple defects including disrupted long bone and craniofacial development [31]. Arthritic changes of the tibia and femur are visible at 3 months of age and are accompanied by the invasion of fibrous tissue and inflammatory cells into the joints. Ablation of the *Mmp14* gene results in a similar skeletal phenotype and severe, generalized soft tissue fibroses

leading to lethality at 1-3 months of age [32]. Although the pathomechanism of arthritis in *Mmp14*$^{-/-}$ mice was not addressed specifically, it has been suggested that inappropriate remodeling caused by impaired pericellular collagenolysis at the AC-soft tissue interfaces induces AC destruction. On the other hand, MMP14 is a critical activator of other proteases and the conversion of pro-MMP2 to active MMP2 was strongly reduced in *Mmp14*-null mice [33]. This raises the possibility that the common skeletal pathology observed in the two mutant strains are ascribed, at least partially, to diminished MMP2 function.

Timp3 and Cathepsin K in Articular Cartilage

The balance between MMPs and their endogenous inhibitors TIMPs are critical to prevent excessive ECM degradation in connective tissues. Among the four TIMPs, TIMP3 is uniquely sequestered in the matrix and effectively inhibits, in addition to MMPs, several members of the ADAM and ADAMTS families predicting its role in cartilage homeostasis [8]. Indeed, *Timp3*$^{-/-}$ mice exhibit mild, age-dependent AC degradation characterized by reduced Safranin O staining [34]. Consistent with the inhibitory potential of TIMP3, knockout mice show elevated levels of both aggrecan and type II collagen cleavage products in the AC. Interestingly, the exposure of the G1-IPEN^{341} is more prominent than the exposure of G1-TEGE^{373} implying that TIMP3 modulates proteoglycan turnover primarily *via* the inhibition of MMPs and not aggrecanases.

In addition to the pivotal role of MMPs in cartilage destruction accumulating evidence has suggested that cathepsin K, a lysosomal cysteine proteinase that is able to degrade both aggrecan and fibrillar collagens, is also involved in degenerative cartilage diseases. In normal mice which develop mild OA spontaneously at 9 months of age, cathepsin K is upregulated in close vicinity of the cartilage lesions [35]. Transgenic mice overexpressing cathepsin K under its endogenous promoter display progressive synovitis accompanied by severe destruction of the articular cartilage and subchondral bone [36]. In cathepsin-K-deficient mice (*Ctsk*$^{-/-}$), which develop osteopetrosis due to impaired bone resorption, joints were not investigated [37]. Worth noting, however, is that in the null mice a compensation mechanism is activated resulting in the transcriptional upregulation of several MMPs (including MMP13) and the elevation of collagens I and II degradation products [38, 39].

CYTOKINES AND GROWTH FACTOR SIGNALING

The permanent communication of chondrocytes with their environment is essentially mediated by soluble growth factors and cytokines. They interact with specific cell surface receptors and control gene expression in order to maintain a balanced ratio between the anabolic and catabolic activities of chondrocytes. To understand the role of cytokine/growth factor-mediated signaling in cartilage biology and OA pathology several models of genetically modified mice have been established.

Cytokines and Cartilage Homeostasis

Although OA is not defined as a classical inflammatory arthropathy, there is strong evidence for the involvement of catabolic inflammatory cytokines in the evolution of the disease [40]. IL-1 cytokines are probably the most well studied pro-inflammatory cytokines that play important roles in OA [41, 42]. Upon binding to type I IL-1 receptor on chondrocytes, IL-1 activates NF-κB and mitogen-activated protein kinase (MAPK) signaling pathways and stimulates the expression of inducible nitric oxide synthase (iNOS), various cytokines and chemokines, and matrix degrading enzymes such as MMPs and aggecanases. Knockout mice lacking either IL-1β, ICE (IL-1β-converting enzyme) or iNOS develop accelerated OA [25] after knee surgery. This unexpected observation suggests that the primary role of IL-1β is to maintain a balanced metabolism in the AC and IL-1-deficiency might up-regulate the expression of other catabolic enzymes in the knockout mice.

IL-6 is a multifunctional cytokine that mediates joint inflammation, but it also induces the expression of proteinase inhibitors in chondrocytes [43, 44] implicating IL-6 as a protective factor against cartilage destruction. This assumption was supported in a study with IL-6-deficient mice. Aging *IL-6*$^{-/-}$ male mice exhibit severe cartilage erosion, subchondral sclerosis, reduced PG synthesis and bone mineral density with higher incidence than *IL-6*$^{-/-}$ females or wild type mice [45]. In the STR/ort mouse strain, which develop spontaneous OA-like changes more severely in males than in females, young females display increased expression of IL-6 and the chondroprotective IL-4 and TGF-β [46]. It was hypothetized that in *IL-6*$^{-/-}$ females the upregulation of IL-4/TGF-β may compensate for the loss of IL-6, ameliorating OA pathology [45].

Growth Factors

It is generally accepted that growth factors including the members of the transforming growth factor (TGF)-β superfamily, insulin-like growth factor (IGF)-I and fibroblasts growth factors (FGFs) play pivotal roles in AC biology owing to their ability to modulate chondrocyte differentiation, proliferation and metabolism [42, 47, 48]. IGF-I modulates cartilage homeostasis by promoting PG synthesis and chondrocyte survival, and by opposing the catabolic effects of IL-1 and TNF-α. IGF-I is produced primarily by growth hormone (GH) stimulation and transgenic mice over-expressing bovine GH develop arthritic joints exhibiting AC lesions and osteophyte formation [49, 50]. The tissue degradation correlated with a high TNF-α level, and decreased proliferation and increased apoptosis of the chondrocytes [50].

Numerous *in vitro* studies have shown that mammalian TGF-β isoforms potently induce chondrocyte PG and collagen II biosynthesis and, at the same time, suppress the expression of IL-1-regulated genes [51, 52]. Although many findings imply that TGF-β could be used for treatment of OA, repeated injection of TGF-β into mouse knee joints resulted in osteophyte formation and cartilage lesions suggesting a role for excessive TGF-β in OA development [53]. Transgenic mice expressing a dominant negative form of the human TGF-β type II receptor (*TGFβRII*^{DN}) develop progressive joint degeneration characterized by PG depletion, synovial hyperplasia, ectopic hypertrophy and osteophyte formation [54]. Targeted disruption of exon 8 of the *Smad3* (*Smad3*$^{ex8/ex8}$) gene encoding a receptor-activated SMAD which transduces TGF-β signals into the nucleus, leads to a similar phenotype as seen in *TGFβRII*^{DN} transgenics [55]. A recent microarray analysis of *Smad3*$^{ex8/ex8}$ articular chondro-

cytes indicated the enhanced expression of MMPs as well as alterations in the expression of genes responsible for protein synthesis, cellular respiration and growth factor signaling, implying that Smad3-deficiency interferes with several cellular mechanisms which might contribute to the development of OA [56]. LTBP (latent TGF-β binding protein)-3 is a structural component of the ECM which modulates TGF-β availability [57]. Mice lacking LTBP-3 have impaired membranous ossification and develop progressive osteosclerosis and OA associated with ectopic hypertrophic chondrocyte differentiation in the superficial zone of the AC [58]. Collectively, these mouse models demonstrate that TGF-β/Smad-3 signaling is necessary to repress articular chondrocyte differentiation and to maintain normal articular cartilage function.

Bone morphogenetic proteins (BMPs), members of the TGF-β superfamily, are critically involved in the control of multiple aspects of embryogenesis including bone and cartilage formation [47, 59]. The physiological role of BMP signaling in the maintenance of AC was recently addressed by conditional targeting of the gene encoding BMP receptor 1a (BMPR1A) [60]. Since *Bmpr1a*$^{-/-}$ mice die during early embryogenesis, the floxed *Bmpr1a* allele was deleted by expressing Cre recombinase under the control of the joint-specific *Gdf-5* (growth differentiation factor-5) regulatory regions. Young *Gdf5-Cre/Bmpr1a*$^{fl/fl}$ mice showed defective joint development in the ankle, whereas most other joints of the body developed normally. This initially mild phenotype, however, was followed by severe OA-like changes in adult digit and knee joints characterized by PG loss and progressive destruction of the AC. Interestingly, the expression of the *Agn* and *Col2a1* genes was also reduced by the mutant articular chondrocytes but, in contrast to mice with defective TGF-β signaling, the articular cartilage showed no signs of hypertrophic differentiation. These findings reveal that BMPR1A function is required for 1) the formation of specific joints and 2) for the maintenance of adult articular cartilage by stimulating the expression of key ECM molecules. BMP and TGF-β signaling pathways therefore play partially distinct roles in OA pathogenesis.

While the importance of FGF/FGF receptor signaling in limb patterning and skeletal development is well appreciated [61], the role of FGFs in AC was only recently addressed using mice lacking FGF receptor 3 (FGFR-3). *Fgfr-3*$^{-/-}$ mice develop skeletal overgrowth [62], osteopenia [63] and early-onset osteoarthritis [64]. The OA phenotype is characterized by enhanced expression of MMP13 and increased exposure of MMPs-generated aggrecan and collagen II cleavage products accompanied by PG loss and alteration of the biomechanical properties of the articular cartilage. In addition, collagen X is expressed above the tidemark in the mutant AC suggesting that FGFR-3 is not only a critical regulator of AC metabolism but it is also required to suppress terminal differentiation of articular chondrocytes.

Mitogen-inducible gene 6 (Mig-6) is an immediate early response gene that can be activated by growth factors [65]. *Mig-6*$^{-/-}$ mice develop severe joint defects and most mice die around 6 month of age due to tempomandibular (TM) joint ankylosis [66]. The phenotype includes early-onset degradation of the AC, synovial hyperplasia, subchondral cyst and osteophyte formation. It was suggested that following mechanical stress Mig-6 suppresses the stimulatory effects of growth factors on the proliferation and differentiation of mesenchymal progenitors required for joint renewal. Consequently, the ablation of *Mig-6* leads to overproliferation of these cells causing bony outgrowths and joint deformities.

MATRIX INTEGRITY AND SIGNALING

The composition and structural organization of the matrix varies throughout the articular cartilage to fulfill specific mechanical demands [67]. In addition to the structural role, the matrix provides an instructive environment from which extracellular information is transduced to chondrocytes *via* cell surface receptors. The heterodimeric (αβ) integrins are the major class of adhesion molecules that mediate chondrocyte-ECM interactions. Articular cartilage chondrocytes primarily express β1-subunit-containing integrins including receptors for fibrillar collagens (α1β1, α2β1 and α10β1) and fibronectin (α5β1). It has been suggested that ECM degradation products of the AC stimulate MMP13 synthesis through integrin-mediated activation of Erk, p38 and JNK, members of the MAPK family [68, 69]. Type II collagen fibrils also bind to and activate the tyrosine kinase receptor discoidin domain receptor 2 (DDR2), which in turn induces MMP13 expression in human OA cartilage [70, 71].

The Fibrillar Collagen Network and Collagen Receptors

Collagen fibrils of the cartilage are heterotypic consisting of the abundant type II and the quantitatively minor type IX and XI collagens. Mutations in these collagens lead to a range of heritable disorders primarily affecting the cartilaginous skeleton [72]. In general, the consequence of mutations in the genes encoding collagen IX (*COL9A1*, *COL9A2* and *COL9A3*) are the mildest leading to multiple epiphyseal chondrodysplasia (MED), a heterogenous group of skeletal dysplasias characterized by moderately short stature and early onset osteoarthritis. Some collagen II (*COL2A1*) and collagen XI (*COL11A1* and *COL11A2*) mutations result in Stickler syndrome, a phenotypically and genetically variable disorder associated with ocular defects and OA of the hip and knee joints [73].

Mice with collagen II deficiency in the cartilage matrix as a consequence of engineered (*Col2a1*$^{-/-}$) or spontaneous mutations (*dmm/dmm*; disproportionate micromelia) and transgenic mice expressing high levels of a deleted version of the murine *Col2a1* gene (Del1$^{+/+}$) exhibit severe dwarfism and die at birth from respiratory failure [74]. In contrast, heterozygous animals survive and develop variable degrees of OA. In the Del1$^{+/-}$ mice, OA-like lesions appear at 3 months of age that gradually progress in older mice [75]. Severe AC damage develops slightly slower in *dmm*/+ mice [76]. Whereas Del1$^{+/-}$ and *dmm*/+ mice show early-onset OA, *Col2a1*$^{+/-}$ develop a milder phenotype characterized by a higher prevalence of OA in aged mice in association with a softened articular cartilage [77, 78]. In the Del1$^{+/-}$ mice the onset of cartilage destruction coincides with the upregulation of cathepsin K in chondrocytes, suggesting the involvement of this cysteine protease in the development of OA [35].

The heterotrimeric (α1α2α3) collagen IX and collagen XI molecules are associated with the fibrillar surface or buried in the core of the fibers, respectively. Homozygous *cho/cho* (*chondrodysplasia*) mice harboring a *Col11a1* gene with a naturally mutated premature stop codon develop lethal

chondrodysplasia [79], whereas *cho/+* mice show a normal skeleton at birth but exhibit age-dependent OA-like changes of the knee and TM joints [80-82]. Homozygous transgenic mice expressing a truncated version of the α1(IX) chain or *Col9a1*$^{-/-}$ mice lacking the triple-helical collagen IX molecules survive and develop early-onset OA [2, 3, 82, 83]. A possible molecular mechanism underlying the OA-like phenotype of the *Col9a1*$^{-/-}$ and *cho/+* mice was proposed in a series of recent publications [80-84]. As the result of the structural disorganization of the collagen network, mechanical stress first elevates pericellular PG synthesis and chondrocyte proliferation leading to the formation of cell clusters in the mutant AC by 3 months of age. This repair step is followed by the overproduction of MMP13, PG depletion and collagen degradation by 6 months of age, and severe cartilage erosion over the age of 9-12 months. The key event in the progression of OA is the increasing contacts between type II collagen fibrils and the chondrocyte surface receptor DDR2. The enhanced activation of DDR2 up-regulates the expression of MMP13 as well as the expression of DDR2 itself in the articular cartilage. *In vitro* experiments with mouse chondrocytes revealed that the interaction between native type II collagen and the collagen binding discoidin domain of DDR2 is a prerequisite for the ERK/p38-mediated induction of MMP13 expression. *In vivo*, the MMP13-mediated degradation of the collagen fibrils and fibronectin may further stimulate MMP13 production *via* activation of the integrin receptors α2β1 and α5β1, respectively, resulting in the progressive destruction of the articular cartilage [84].

Chondrocyte integrins act as mechanoreceptors and transduce signals from the pericellular matrix into intracellular pathways regulating cartilage homeostasis [85]. Despite the numerous integrin knockouts described in the literature, the *in vivo* role of integrins in OA pathogenesis is largely unknown. Most mutant lines lacking a particular integrin subunit develop a normal skeleton without reported AC abnormalities [86], whereas the cartilage-specific deletion of the β1 subunit-containing integrins results in severe chondrodysplasia and high mortality rate at birth [87]. To date only α1 integrin-deficiency has been linked to pathological abnormalities of the knee articular cartilage [88]. α1-null mice show precocious PG loss, synovial hyperplasia and cartilage erosion associated with increased MMP2 and MMP3 expression. The mutant AC is also characterized by hypocellularity and increased cell death. Interestingly, a similar, accelerated development of knee OA was observed in mice lacking the membrane-anchored ADAM15 [89]. ADAM15 possesses multiple pericellular functions including the modulation of outside-in signaling of integrins. Altogether, these data implicate collagen-binding integrins as critically involved in the regulation of AC remodeling and chondrocyte survival in response to ECM stimuli.

Proteoglycans

Aggrecan is the most abundant proteoglycan of the articular cartilage and association of aggrecan gene (*AGC1*) polymorphism with various forms of OA has been demonstrated [90, 91]. More recently, a frameshift mutation in exon 12 of *AGC1* was identified in patients with autosomal dominant spondyloepiphyseal dysplasia type Kiberley (SEDK) characterized by mild short stature and early onset OA [92]. In the *cmd* (*cartilage matrix deficiency*) mice, a spontaneous mutation leads to a premature stop codon in exon 6 and to the absence of mature aggrecan in the matrix [93]. Homozygous mutants exhibit severe chondrodysplasia and die at birth due to respiratory failure. Heterozygous mice (*cmd/+*) survive and develop mild dwarfism and age-dependent spinal abnormalities [94]. In contrast to SEDK, no OA-like changes were reported in these mice [95]. A possible explanation for this discrepancy is that the SEDK *AGC1* mutation predicts the formation of a relatively large truncated protein, which may be retained in the endoplasmatic reticulum (ER), impairing chondrocyte function in the articular cartilage.

The small leucine-rich proteoglycans (SLRPs) play pivotal roles in connective tissues interacting with various matrix macromolecules and growth factors, thereby modulating both ECM organization and cellular metabolism [96]. Mice lacking SLRPs exhibit a broad range of phenotypes primarily affecting collagen fibrillogenesis in tissues rich in type I collagen such as skin, bone, tendon and cornea [96]. Several SLRPs are expressed in the articular cartilage including biglycan, fibromodulin and lumican. Mice double deficient in biglycan/fibromodulin [97] or lumican/fibromodulin [98] develop premature knee OA characterized by severe erosion of the articular cartilage at 3-6 months of age. The corresponding single knockout mice, except lumican-null, also exhibit OA which is milder and occurs later than in the double mutants [97-99]. The cause of OA pathology in these mice is unclear but it could be secondary to structural and functional defects in tendons and/or ligaments. Biglycan/fibromodulin double knockout mice also develop TM joint OA with significantly later onset and slower progression than knee OA [100]. Biglycan/fibromodulin double knockout mice also develop TM joint OA with significantly later onset and slower progression than knee OA [100]. The overt TM joint OA is preceded by reduced chondrocyte proliferation suggesting that misregulated cell growth could be an important factor in this type of OA. Knockout mouse models demonstrate that SLRPs are involved in the control of cell growth in various tissues via the modulation of TGFb/BMP availability [101], therefore it is possible that biglycan and/or fibromodulin deficiency impairs chondrocyte proliferation by disturbing growth factor signaling.

Perlecan (HSPG2) is a large secreted proteoglycan abundant in basement membranes (BMs) and cartilage. The levels of perlecan protein and mRNA were found to be increased in late stage OA samples from human knee joints which might suggest that perlecan is involved in repair processes activated around the defect areas [102]. The importance of perlecan in skeletogenesis is illustrated by the severe chondrodysplasia developed in human and mice lacking functional perlecan. Patients with dyssegmental dysplasia of the Silverman-Handmaker type (DDSH) and perlecan-null (*Hspg2*$^{-/-}$) mice are characterized by defective endochondral bone formation and embryonic/perinatal lethality [103]. In contrast, mutations reducing the level of perlecan lead to the non-lethal, autosomal-recessive Schartz-Jampel syndrome (SJS) characterized by osteochondrodysplasia and myotonia [104]. Recently a mouse model of SJS with altered *Hspg2* transcription and reduced perlecan matrix deposition was generated [105]. The hypomorphic mutants (C1532Yneo) mimic typical SJS and exhibit rough surface and clefts on the humeral head resembling OA.

Table 1. Gene Modified Mouse Models Relevant in Osteoarthritis Research

Protein/Gene	Model	Articular Cartilage Phenotype	Ref.
Proteolytic Enzymes and Related Molecules			
ADAM15	KO	Accelerated knee OA; modulation of integrin signaling?	[89]
ADAMTS-1	KO	Normal susceptibility to experimentally induced arthritis	[119]
ADAMTS-4	KO	Normal susceptibility to experimentally induced arthritis	[14-16]
ADAMTS-5	KO	Protection from experimental arthritis; major aggrecanase in OA	[14, 16]
ADAMTS-4/-5	KO	Similar to ADAMTS-5 KO, AC releases intact aggrecan	[18, 120]
Cathepsin K	TR	Joint destruction associated with sever bone defects	[36]
Cathepsin K	KO	Osteopetrosis, OA was not investigated	[37]
MMP2	KO	Age-dependent AC destruction, bone defects	[31]
MMP3	KO	Decreased susceptibility to spontaneous OA and inflammatory arthritis	[22-24]
		Increased susceptibility to surgically-induced OA	[25]
MMP9	KO	Spontaneous OA-like changes in young mice	[22]
MMP13	TR	Accelerated OA, ectopic collagen X expression	[28]
MMP14	KO	Skeletal defects including AC destruction, impaired MMP2 activation	[32, 33]
Runx2 (+/-)	KO	Amelioration of surgically induced OA, reduced MMP-13 expression	[29]
TIMP3	KO	Mild OA, increased cleavage of aggrecan and collagen II	[34]
ECM Molecules and Receptors			
α1 integrin	KO	Accelerated OA, increased MMP2 and MMP3 expression	[88]
Aggrecan (*Cmd*/+)	KO	No reported OA-like changes	[95]
Aggrecan "Jaffa"	KI	Resistant to aggrecanase-mediated IGD cleavage	[19]
		Partially protected from experimental arthritis	
Aggrecan "Chloe"	KI	Resistant to MMP-mediated IGD cleavage	[21]
		Normal susceptibility to experimentally induced arthritis	[19]
Biglycan	KO	OA-like changes, ectopic tendon ossification	[97]
Fibromodulin	KO	Age-dependent OA-like changes, ectopic tendon ossification	[99]
Biglycan/Fibromodulin	dKO	Early onset OA, ectopic tendon ossification, accelerated TMJ OA	[97, 100]
Lumican	KO	OA was not reported	[98]
Lumican/Fibromodulin	dKO	Early onset OA, ectopic tendon ossification	[98]
Collagen II, α1 (+/-)	KO	Higher prevalence of OA in aging mice, softer AC	[77, 78]
Collagen II, α1 (*dmm*/+)	NO	Early-onset OA, AC thinning, increased cell density, reduced matrix	[76]
Collagen II, α1 (Del/+)	TR	Early-onset OA, up-regulation of cathepsin K	[75]
Collagen IX, α1	KO	Early onset OA, up-regulation of DDR2 and MMP13 expression	[3, 82, 83]
Collagen IX, α1	TR	Early onset OA	[2]
Collagen XI, α1 (*cho*/+)	NO	Early onset OA, up-regulation of DDR2 and MMP13 expression	[80-82]
Collagen XI, α2	KO	Mild abnormalities of the AC, no obvious OA	[121]
Proteoglycan 4	KO	Surface changes followed by AC deterioration	[108]
Matrilin-3	KO	No obvious OA in one study; high OA prevalence at 12 months in	[113]
	KO	another study	[118]
Matrilin-1/Matrilin-3	dKO	Similar incidence of OA in controls and double mutants at 14 months	[117]
Perlecan	KO	OA-like changes on the femoral head	[105]
Cytokines and Growth Factors			
Growth hormone	TR	OA-like changes of the AC, osteophyte formation	[49, 50]
BMPR1A	cKO	Progressive AC degradation	[60]
Fgfr3	KO	Premature OA, increased MMP13 expression	[64]
IL-1β	KO	Acceleration of surgically induced OA	[25]
IL-6	KO	Age-dependent OA and subchondral sclerosis in males	[45]
ICE	KO	Acceleration of surgically induced OA	[25]
Ltbp-3	KO	Progressive AC degradation, abnormal chondrocyte hypertrophy	[58]
Mig-6	KO	Early-onset OA, osteophyte formation	[66]
iNOS	KO	Acceleration of surgically induced OA	[25]
Smad3	KO	Progressive OA, osteophyte formation, increased Col10 expression	[55]
TGFβRII	TR	Progressive OA, osteophyte formation, increased Col10 expression	[54]

Note: KO, knock-out; dKO, double knock-out; cKO, conditional knock-out; KI, knock-in; NO, naturally occurring; TG, transgenic.

Proteoglycan 4 (PRG4) is highly abundant in the synovial fluid and on the surface of AC, and is secreted by both superficial chondrocytes and synoviocytes. Mutations in *PRG4* lead to CACP syndrome characterized by precocious joint failure demonstrating the essential role of PRG4 in maintaining joint integrity [106]. PRG4 levels decrease at early OA stages in surgically induced degenerative AC animal models [107] implicating PRG4 in OA pathology. Mice

lacking proteoglycan 4 (*Prg4*$^{-/-}$) show age-dependent synovial hyperplasia, irregular AC surface with protein deposits, loss of the flattened layer of superficial zone chondrocytes and subsequent AC deterioration [108]. In addition, the mice exhibit abnormal calcification of tendons in the ankle joint. Collectively, these data suggest a protective role for proteoglycan 4 on AC and provide a novel therapeutic target for treatment of OA.

Glycoproteins Modulating ECM Structure and Function

In hyaline cartilage the collagen-aggrecan networks are interconnected *via* molecular associates containing SLRPs and non-collagenous glycoproteins such as cartilage oligomeric matrix protein (COMP) and the members of the matrilin family [109]. COMP is abundant in both the developing growth plate and the articular cartilage, and mutations in the COMP gene results in MED and pseudoachondrodysplasia [110]. Matrilins, especially matrilin-1 and -3, are highly expressed during cartilage development and matrilin-3 mutations are linked to various skeletal disorders including a distinct group of MED [109]. COMP, matrilin-1 and matrilin-3 levels are upregulated in articular cartilage and/or the synovial fluid during joint diseases; they therefore may serve as markers for disturbed cartilage metabolism. Mice lacking these proteins do not develop chondrodysplasia implying a dominant negative pathomechanism behind the human disorders [111-113]. Similarly, no signs of OA were observed in COMP- and matrilin-1-deficient mice [111, 112]. The role of matrilin-3 in articular cartilage function is more controversial. In humans, the association of matrilin-3 polymorphisms with hand osteoarthritis but not with knee osteoarthritis was demonstrated [114-116]. Matrilin-3-deficient single and double knockout mice (*Matn3*$^{-/-}$ and *Matn1*$^{-/-}$*/Matn3*$^{-/-}$) generated in our laboratory showed no evidence for higher incidence of OA-like changes in the knee joints compared with control mice up to 14 months of age [113, 117]. In contrast, a higher prevalence of severe knee OA at one year of age was reported in a second matrilin-3-deficient mouse line suggesting that matrilin-3 may protect articular cartilage from degradation [118]. The discrepancy between these works might be explained by background or gender specific differences of the investigated mice and call for further, more detailed studies.

CONCLUSION

During the last decade, the number of genetically modified mice with OA-like changes has dramatically expanded. These mouse models are particularly effective to elucidate the molecular basis of articular cartilage homeostasis under both normal and pathological conditions. The analysis of the phenotypic consequences of gene modifications in transgenic, knockout and knock-in mice has yielded a wealth of information about the complex functional interactions among cytokines, growth factors and ECM structural proteins of the joints and has provided valuable insight to the pathogenesis of cartilage degeneration in osteoarthritis. The genetic mouse models not only help to dissect signal transduction pathways that regulate the catabolic/anabolic balance in AC, they are also useful in identifying OA-candidate genes and to validate potential target molecules to treat or prevent OA. There is no doubt that gene targeting in mice will continue to be an important tool of OA research in the future.

ACKNOWLEDGEMENTS

We thank Dr. Kyle Legate for critical reading the manuscript. A.R. and A.A. are supported by the Deutsche Forschungsgemeinschaft and the Max Planck Society.

REFERENCES

[1] Buckwalter JA, Martin JA. Osteoarthritis. Adv Drug Deliv Rev 2006; 58: 150-67.

[2] Nakata K, Ono K, Miyazaki J, *et al*. Osteoarthritis associated with mild chondrodysplasia in transgenic mice expressing alpha 1(IX) collagen chains with a central deletion. Proc Natl Acad Sci USA 1993; 90: 2870-4.

[3] Fassler R, Schnegelsberg PN, Dausman J, *et al*. Mice lacking alpha 1 (IX) collagen develop noninflammatory degenerative joint disease. Proc Natl Acad Sci USA 1994; 91: 5070-4.

[4] Murphy G, Knauper V, Atkinson S, *et al*. Matrix metalloproteinases in arthritic disease. Arthritis Res 2002; 4 Suppl 3: S39-49.

[5] Mott JD, Werb Z. Regulation of matrix biology by matrix metalloproteinases. Curr Opin Cell Biol 2004; 16: 558-64.

[6] Page-McCaw A, Ewald AJ, Werb Z. Matrix metalloproteinases and the regulation of tissue remodelling. Nat Rev Mol Cell Biol 2007; 8: 221-33.

[7] Jones GC, Riley GP. ADAMTS proteinases: a multi-domain, multifunctional family with roles in extracellular matrix turnover and arthritis. Arthritis Res Ther 2005; 7: 160-9.

[8] Baker AH, Edwards DR, Murphy G. Metalloproteinase inhibitors: biological actions and therapeutic opportunities. J Cell Sci 2002; 115: 3719-27.

[9] Kevorkian L, Young DA, Darrah C, *et al*. Expression profiling of metalloproteinases and their inhibitors in cartilage. Arthritis Rheum 2004; 50: 131-41.

[10] Davidson RK, Waters JG, Kevorkian L, *et al*. Expression profiling of metalloproteinases and their inhibitors in synovium and cartilage. Arthritis Res Ther 2006; 8: R124.

[11] Yasuda Y, Kaleta J, Bromme D. The role of cathepsins in osteoporosis and arthritis: rationale for the design of new therapeutics. Adv Drug Deliv Rev 2005; 57: 973-93.

[12] Struglics A, Larsson S, Pratta MA, *et al*. Human osteoarthritis synovial fluid and joint cartilage contain both aggrecanase- and matrix metalloproteinase-generated aggrecan fragments. Osteoarthritis Cartilage 2006; 14: 101-13.

[13] Malfait AM, Liu RQ, Ijiri K, Komiya S, Tortorella MD. Inhibition of ADAM-TS4 and ADAM-TS5 prevents aggrecan degradation in osteoarthritic cartilage. J Biol Chem 2002; 277: 22201-8.

[14] Glasson SS, Askew R, Sheppard B, *et al*. Deletion of active ADAMTS5 prevents cartilage degradation in a murine model of osteoarthritis. Nature 2005; 434: 644-8.

[15] Glasson SS, Askew R, Sheppard B, *et al*. Characterization of and osteoarthritis susceptibility in ADAMTS-4-knockout mice. Arthritis Rheum 2004; 50: 2547-58.

[16] Stanton H, Rogerson FM, East CJ, *et al*. ADAMTS5 is the major aggrecanase in mouse cartilage *in vivo* and *in vitro*. Nature 2005; 434: 648-52.

[17] East CJ, Stanton H, Golub SB, Rogerson FM, Fosang AJ. ADAMTS-5 deficiency does not block aggrecanolysis at preferred cleavage sites in the the chondroitin sulfate-rich region of aggrecan. J Biol Chem 2007; 282(12): 8632-40. Epub 2007 Jan 25.

[18] Ilic MZ, East CJ, Rogerson FM, Fosang AJ, Handley CJ. Distinguishing aggrecan loss from aggrecan proteolysis in ADAMTS-4 and ADAMTS-5 single and double deficient mice. J Biol Chem 2007; 282: 37420-8.

[19] Little CB, Meeker CT, Golub SB, *et al*. Blocking aggrecanase cleavage in the aggrecan interglobular domain abrogates cartilage erosion and promotes cartilage repair. J Clin Invest 2007; 117: 1627-36.

[20] Fosang AJ, Last K, Stanton H, *et al*. Generation and novel distribution of matrix metalloproteinase-derived aggrecan fragments in porcine cartilage explants. J Biol Chem 2000; 275: 33027-37.

[21] Little CB, Meeker CT, Hembry RM, *et al*. Matrix metalloproteinases are not essential for aggrecan turnover during normal skeletal growth and development. Mol Cell Biol 2005; 25: 3388-99.

[22] Blom AB, van Lent PL, Libregts S, *et al*. Crucial role of macrophages in matrix metalloproteinase-mediated cartilage destruction

during experimental osteoarthritis: involvement of matrix metalloproteinase 3. Arthritis Rheum 2007; 56: 147-57.

[23] van Meurs J, van Lent P, Holthuysen A, *et al*. Active matrix metalloproteinases are present in cartilage during immune complex-mediated arthritis: a pivotal role for stromelysin-1 in cartilage destruction. J Immunol 1999; 163: 5633-9.

[24] van Meurs J, van Lent P, Stoop R, *et al*. Cleavage of aggrecan at the Asn341-Phe342 site coincides with the initiation of collagen damage in murine antigen-induced arthritis: a pivotal role for stromelysin 1 in matrix metalloproteinase activity. Arthritis Rheum 1999; 42: 2074-84.

[25] Clements KM, Price JS, Chambers MG, *et al*. Gene deletion of either interleukin-1beta, interleukin-1beta-converting enzyme, inducible nitric oxide synthase, or stromelysin 1 accelerates the development of knee osteoarthritis in mice after surgical transection of the medial collateral ligament and partial medial meniscectomy. Arthritis Rheum 2003; 48: 3452-63.

[26] Fichter M, Korner U, Schomburg J, *et al*. Collagen degradation products modulate matrix metalloproteinase expression in cultured articular chondrocytes. J Orthop Res 2006; 24: 63-70.

[27] Yasuda T, Tchetina E, Ohsawa K, *et al*. Peptides of type II collagen can induce the cleavage of type II collagen and aggrecan in articular cartilage. Matrix Biol 2006; 25: 419-29.

[28] Neuhold LA, Killar L, Zhao W, *et al*. Postnatal expression in hyaline cartilage of constitutively active human collagenase-3 (MMP-13) induces osteoarthritis in mice. J Clin Invest 2001; 107: 35-44.

[29] Kamekura S, Kawasaki Y, Hoshi K, *et al*. Contribution of runt-related transcription factor 2 to the pathogenesis of osteoarthritis in mice after induction of knee joint instability. Arthritis Rheum 2006; 54: 2462-70.

[30] Stickens D, Behonick DJ, Ortega N, *et al*. Altered endochondral bone development in matrix metalloproteinase 13-deficient mice. Development 2004; 131: 5883-95.

[31] Mosig RA, Dowling O, DiFeo A, *et al*. Loss of MMP-2 disrupts skeletal and craniofacial development and results in decreased bone mineralization, joint erosion and defects in osteoblast and osteoclast growth. Hum Mol Genet 2007; 16: 1113-23.

[32] Holmbeck K, Bianco P, Caterina J, *et al*. MT1-MMP-deficient mice develop dwarfism, osteopenia, arthritis, and connective tissue disease due to inadequate collagen turnover. Cell 1999; 99: 81-92.

[33] Zhou Z, Apte SS, Soininen R, *et al*. Impaired endochondral ossification and angiogenesis in mice deficient in membrane-type matrix metalloproteinase I. Proc Natl Acad Sci USA 2000; 97: 4052-7.

[34] Sahebjam S, Khokha R, Mort JS. Increased collagen and aggrecan degradation with age in the joints of Timp3(-/-) mice. Arthritis Rheum 2007; 56: 905-9.

[35] Morko JP, Soderstrom M, Saamanen AM, Salminen HJ, Vuorio EI. Up regulation of cathepsin K expression in articular chondrocytes in a transgenic mouse model for osteoarthritis. Ann Rheum Dis 2004; 63: 649-55.

[36] Morko J, Kiviranta R, Joronen K, *et al*. Spontaneous development of synovitis and cartilage degeneration in transgenic mice overexpressing cathepsin K. Arthritis Rheum 2005; 52: 3713-7.

[37] Saftig P, Hunziker E, Wehmeyer O, *et al*. Impaired osteoclastic bone resorption leads to osteopetrosis in cathepsin-K-deficient mice. Proc Natl Acad Sci USA 1998; 95: 13453-8.

[38] Kiviranta R, Morko J, Alatalo SL, *et al*. Impaired bone resorption in cathepsin K-deficient mice is partially compensated for by enhanced osteoclastogenesis and increased expression of other proteases *via* an increased RANKL/OPG ratio. Bone 2005; 36: 159-72.

[39] Sondergaard BC, Henriksen K, Wulf H, *et al*. Relative contribution of matrix metalloprotease and cysteine protease activities to cytokine-stimulated articular cartilage degradation. Osteoarthritis Cartilage 2006; 14: 738-48.

[40] Goldring SR, Goldring MB. The role of cytokines in cartilage matrix degeneration in osteoarthritis. Clin Orthop Relat Res 2004; S27-36.

[41] Goldring MB. Update on the biology of the chondrocyte and new approaches to treating cartilage diseases. Best Pract Res Clin Rheumatol 2006; 20: 1003-25.

[42] Aigner T, Soeder S, Haag J. IL-1beta and BMPs--interactive players of cartilage matrix degradation and regeneration. Eur Cell Mater 2006; 12: 49-56.

[43] Fukui N, Zhu Y, Maloney WJ, Clohisy J, Sandell LJ. Stimulation of BMP-2 expression by pro-inflammatory cytokines IL-1 and TNF-alpha in normal and osteoarthritic chondrocytes. J Bone Joint Surg Am 2003; (85-A Suppl 3): 59-66.

[44] Fischer DC, Siebertz B, van de Leur E, *et al*. Induction of alpha1-antitrypsin synthesis in human articular chondrocytes by interleukin-6-type cytokines: evidence for a local acute-phase response in the joint. Arthritis Rheum 1999; 42: 1936-45.

[45] De Hooge AS, van de Loo FA, Bennink MB, *et al*. Male IL-6 gene knock out mice developed more advanced osteoarthritis upon aging. Osteoarthritis Cartilage 2005; 13: 66-73.

[46] Mahr S, Menard J, Krenn V, Muller B. Sexual dimorphism in the osteoarthritis of STR/ort mice may be linked to articular cytokines. Ann Rheum Dis 2003; 62: 1234-7.

[47] Goldring MB, Tsuchimochi K, Ijiri K. The control of chondrogenesis. J Cell Biochem 2006; 97: 33-44.

[48] Blaney Davidson EN, van der Kraan PM, van den Berg WB. TGF-beta and osteoarthritis. Osteoarthritis Cartilage 2007; 15: 597-604.

[49] Ogueta S, Olazabal I, Santos I, Delgado-Baeza E, Garcia-Ruiz JP. Transgenic mice expressing bovine GH develop arthritic disorder and self-antibodies. J Endocrinol 2000; 165: 321-8.

[50] Fernandez-Criado C, Martos-Rodriguez A, Santos-Alvarez I, Garcia-Ruiz JP, Delgado-Baeza E. The fate of chondrocyte in osteoarthritic cartilage of transgenic mice expressing bovine GH. Osteoarthritis Cartilage 2004; 12: 543-51.

[51] Redini F, Galera P, Mauviel A, Loyau G, Pujol JP. Transforming growth factor beta stimulates collagen and glycosaminoglycan biosynthesis in cultured rabbit articular chondrocytes. FEBS Lett 1988; 234: 172-6.

[52] Takahashi N, Rieneck K, van der Kraan PM, *et al*. Elucidation of IL-1/TGF-beta interactions in mouse chondrocyte cell line by genome-wide gene expression. Osteoarthritis Cartilage 2005; 13: 426-38.

[53] Van Beuningen HM, Glansbeek HL, van der Kraan PM, van den Berg WB. Osteoarthritis-like changes in the murine knee joint resulting from intra-articular transforming growth factor-beta injections. Osteoarthritis Cartilage 2000; 8: 25-33.

[54] Serra R, Johnson M, Filvaroff EH, *et al*. Expression of a truncated, kinase-defective TGF-beta type II receptor in mouse skeletal tissue promotes terminal chondrocyte differentiation and osteoarthritis. J Cell Biol 1997; 139: 541-52.

[55] Yang X, Chen L, Xu X, *et al*. TGF-beta/Smad3 signals repress chondrocyte hypertrophic differentiation and are required for maintaining articular cartilage. J Cell Biol 2001; 153: 35-46.

[56] Wang H, Zhang J, Sun Q, Yang X. Altered gene expression in articular chondrocytes of Smad3ex8/ex8 mice, revealed by gene profiling using microarrays. J Genet Genomics 2007; 34: 698-708.

[57] Todorovic V, Jurukovski V, Chen Y, *et al*. Latent TGF-beta binding proteins. Int J Biochem Cell Biol 2005; 37: 38-41.

[58] Dabovic B, Chen Y, Colarossi C, *et al*. Bone abnormalities in latent TGF-[beta] binding protein (Ltbp)-3-null mice indicate a role for Ltbp-3 in modulating TGF-[beta] bioavailability. J Cell Biol 2002; 156: 227-32.

[59] Kishigami S, Mishina Y. BMP signaling and early embryonic patterning. Cytokine Growth Factor Rev 2005; 16: 265-78.

[60] Rountree RB, Schoor M, Chen H, *et al*. BMP receptor signaling is required for postnatal maintenance of articular cartilage. PLoS Biol 2004; 2: e355.

[61] Ornitz DM, Marie PJ. FGF signaling pathways in endochondral and intramembranous bone development and human genetic disease. Genes Dev 2002; 16: 1446-65.

[62] Colvin JS, Bohne BA, Harding GW, McEwen DG, Ornitz DM. Skeletal overgrowth and deafness in mice lacking fibroblast growth factor receptor 3. Nat Genet 1996; 12: 390-7.

[63] Valverde-Franco G, Liu H, Davidson D, *et al*. Defective bone mineralization and osteopenia in young adult FGFR3-/- mice. Hum Mol Genet 2004; 13: 271-84.

[64] Valverde-Franco G, Binette JS, Li W, *et al*. Defects in articular cartilage metabolism and early arthritis in fibroblast growth factor receptor 3 deficient mice. Hum Mol Genet 2006; 15: 1783-92.

[65] Zhang YW, Vande Woude GF. Mig-6, signal transduction, stress response and cancer. Cell Cycle 2007; 6: 507-13.

[66] Zhang YW, Su Y, Lanning N, *et al*. Targeted disruption of Mig-6 in the mouse genome leads to early onset degenerative joint disease. Proc Natl Acad Sci USA 2005; 102: 11740-5.

[67] Poole AR, Kojima T, Yasuda T, *et al*. Composition and structure of articular cartilage: a template for tissue repair. Clin Orthop Relat Res 2001; (391 Suppl): S26-33.

[68] Forsyth CB, Pulai J, Loeser RF. Fibronectin fragments and blocking antibodies to alpha2beta1 and alpha5beta1 integrins stimulate mitogen-activated protein kinase signaling and increase collagenase 3 (matrix metalloproteinase 13) production by human articular chondrocytes. Arthritis Rheum 2002; 46: 2368-76.

[69] Loeser RF, Forsyth CB, Samarel AM, Im HJ. Fibronectin fragment activation of proline-rich tyrosine kinase PYK2 mediates integrin signals regulating collagenase-3 expression by human chondrocytes through a protein kinase C-dependent pathway. J Biol Chem 2003; 278: 24577-85.

[70] Xu L, Peng H, Glasson S, *et al*. Increased expression of the collagen receptor discoidin domain receptor 2 in articular cartilage as a key event in the pathogenesis of osteoarthritis. Arthritis Rheum 2007; 56: 2663-73.

[71] Sunk IG, Bobacz K, Hofstaetter JG, *et al*. Increased expression of discoidin domain receptor 2 is linked to the degree of cartilage damage in human knee joints: a potential role in osteoarthritis pathogenesis. Arthritis Rheum 2007; 56: 3685-92.

[72] Reginato AM, Olsen BR. The role of structural genes in the pathogenesis of osteoarthritic disorders. Arthritis Res 2002; 4: 337-45.

[73] Snead MP, Yates JR. Clinical and Molecular genetics of Stickler syndrome. J Med Genet 1999; 36: 353-9.

[74] Aszodi A, Pfeifer A, Wendel M, Hiripi L, Fassler R. Mouse models for extracellular matrix diseases. J Mol Med 1998; 76: 238-52.

[75] Saamanen AK, Salminen HJ, Dean PB, *et al*. Osteoarthritis-like lesions in transgenic mice harboring a small deletion mutation in type II collagen gene. Osteoarthritis Cartilage 2000; 8: 248-57.

[76] Bomsta BD, Bridgewater LC, Seegmiller RE. Premature osteoarthritis in the Disproportionate micromelia (Dmm) mouse. Osteoarthritis Cartilage 2006; 14: 477-85.

[77] Lapvetelainen T, Hyttinen M, Lindblom J, *et al*. More knee joint osteoarthritis (OA) in mice after inactivation of one allele of type II procollagen gene but less OA after lifelong voluntary wheel running exercise. Osteoarthritis Cartilage 2001; 9: 152-60.

[78] Hyttinen MM, Toyras J, Lapvetelainen T, *et al*. Inactivation of one allele of the type II collagen gene alters the collagen network in murine articular cartilage and makes cartilage softer. Ann Rheum Dis 2001; 60: 262-8.

[79] Li Y, Lacerda DA, Warman ML, *et al*. A fibrillar collagen gene, Col11a1, is essential for skeletal morphogenesis. Cell 1995; 80: 423-30.

[80] Xu L, Flahiff CM, Waldman BA, *et al*. Osteoarthritis-like changes and decreased mechanical function of articular cartilage in the joints of mice with the chondrodysplasia gene (cho). Arthritis Rheum 2003; 48: 2509-18.

[81] Xu L, Peng H, Wu D, *et al*. Activation of the discoidin domain receptor 2 induces expression of matrix metalloproteinase 13 associated with osteoarthritis in mice. J Biol Chem 2005; 280: 548-55.

[82] Lam NP, Li Y, Waldman AB, *et al*. Age-dependent increase of discoidin domain receptor 2 and matrix metalloproteinase 13 expression in temporomandibular joint cartilage of type IX and type XI collagen-deficient mice. Arch Oral Biol 2007; 52: 579-84.

[83] Hu K, Xu L, Cao L, *et al*. Pathogenesis of osteoarthritis-like changes in the joints of mice deficient in type IX collagen. Arthritis Rheum 2006; 54: 2891-900.

[84] Li Y, Xu L, Olsen BR. Lessons from genetic forms of osteoarthritis for the pathogenesis of the disease. Osteoarthritis Cartilage 2007; 15: 1101-5.

[85] Loeser RF. Integrins and cell signaling in chondrocytes. Biorheology 2002; 39: 119-24.

[86] Bouvard D, Brakebusch C, Gustafsson E, *et al*. Functional consequences of integrin gene mutations in mice. Circ Res 2001; 89: 211-23.

[87] Aszodi A, Hunziker EB, Brakebusch C, Fassler R. Beta1 integrins regulate chondrocyte rotation, G1 progression, and cytokinesis. Genes Dev 2003; 17: 2465-79.

[88] Zemmyo M, Meharra EJ, Kuhn K, Creighton-Achermann L, Lotz M. Accelerated, aging-dependent development of osteoarthritis in alpha1 integrin-deficient mice. Arthritis Rheum 2003; 48: 2873-80.

[89] Bohm BB, Aigner T, Roy B, *et al*. Homeostatic effects of the metalloproteinase disintegrin ADAM15 in degenerative cartilage remodeling. Arthritis Rheum 2005; 52: 1100-9.

[90] Horton WE, Jr., Lethbridge-Cejku M, Hochberg MC, *et al*. An association between an aggrecan polymorphic allele and bilateral hand osteoarthritis in elderly white men: data from the Baltimore Longitudinal Study of Aging (BLSA). Osteoarthritis Cartilage 1998; 6: 245-51.

[91] Kirk KM, Doege KJ, Hecht J, Bellamy N, Martin NG. Osteoarthritis of the hands, hips and knees in an Australian twin sample-evidence of association with the aggrecan VNTR polymorphism. Twin Res 2003; 6: 62-6.

[92] Gleghorn L, Ramesar R, Beighton P, Wallis G. A mutation in the variable repeat region of the aggrecan gene (AGC1) causes a form of spondyloepiphyseal dysplasia associated with severe, premature osteoarthritis. Am J Hum Genet 2005; 77: 484-90.

[93] Watanabe H, Kimata K, Line S, *et al*. Mouse cartilage matrix deficiency (cmd) caused by a 7 bp deletion in the aggrecan gene. Nat Genet 1994; 7: 154-7.

[94] Watanabe H, Nakata K, Kimata K, Nakanishi I, Yamada Y. Dwarfism and age-associated spinal degeneration of heterozygote cmd mice defective in aggrecan. Proc Natl Acad Sci USA 1997; 94: 6943-7.

[95] Watanabe H, Yamada Y. Chondrodysplasia of gene knockout mice for aggrecan and link protein. Glycoconj J 2002; 19: 269-73.

[96] Ameye L, Young MF. Mice deficient in small leucine-rich proteoglycans: novel *in vivo* models for osteoporosis, osteoarthritis, Ehlers-Danlos syndrome, muscular dystrophy, and corneal diseases. Glycobiology 2002; 12: 107R-16R.

[97] Ameye L, Aria D, Jepsen K, *et al*. Abnormal collagen fibrils in tendons of biglycan/fibromodulin-deficient mice lead to gait impairment, ectopic ossification, and osteoarthritis. FASEB J 2002; 16: 673-80.

[98] Jepsen KJ, Wu F, Peragallo JH, *et al*. A syndrome of joint laxity and impaired tendon integrity in lumican- and fibromodulin-deficient mice. J Biol Chem 2002; 277: 35532-40.

[99] Gill MR, Oldberg A, Reinholt FP. Fibromodulin-null murine knee joints display increased incidences of osteoarthritis and alterations in tissue biochemistry. Osteoarthritis Cartilage 2002; 10: 751-7.

[100] Wadhwa S, Embree MC, Kilts T, Young MF, Ameye LG. Accelerated osteoarthritis in the temporomandibular joint of biglycan/fibromodulin double-deficient mice. Osteoarthritis Cartilage 2005; 13: 817-27.

[101] Aszodi A, Legate KR, NakchbandiI, Fassler R. What mouse mutants teach us about extracellular matrix function. Annu Rev Cell Dev Biol 2006; 22: 591-621.

[102] Tesche F, Miosge N. Perlecan in late stages of osteoarthritis of the human knee joint. Osteoarthritis Cartilage 2004; 12: 852-62.

[103] Costell M, Gustafsson E, Aszodi A, *et al*. Perlecan maintains the integrity of cartilage and some basement membranes. J Cell Biol 1999; 147: 1109-22.

[104] Nicole S, Davoine CS, Topaloglu H, *et al*. Perlecan, the major proteoglycan of basement membranes, is altered in patients with Schwartz-Jampel syndrome (chondrodystrophic myotonia). Nat Genet 2000; 26: 480-3.

[105] Rodgers KD, Sasaki T, Aszodi A, Jacenko O. Reduced perlecan in mice results in chondrodysplasia resembling Schwartz-Jampel syndrome. Hum Mol Genet 2007; 16: 515-28.

[106] Marcelino J, Carpten JD, Suwairi WM, *et al*. CACP, encoding a secreted proteoglycan, is mutated in camptodactyly-arthropathy-coxa vara-pericarditis syndrome. Nat Genet 1999; 23: 319-22.

[107] Elsaid KA, Jay GD, Warman ML, Rhee DK, Chichester CO. Association of articular cartilage degradation and loss of boundary-lubricating ability of synovial fluid following injury and inflammatory arthritis. Arthritis Rheum 2005; 52: 1746-55.

[108] Rhee DK, Marcelino J, Baker M, *et al*. The secreted glycoprotein lubricin protects cartilage surfaces and inhibits synovial cell overgrowth. J Clin Invest 2005; 115: 622-31.

[109] Wagener R, Ehlen HW, Ko YP, *et al*. The matrilins-adaptor proteins in the extracellular matrix. FEBS Lett 2005; 579: 3323-9.

[110] Briggs MD, Chapman KL. Pseudoachondroplasia and multiple epiphyseal dysplasia: mutation review, molecular interactions, and genotype to phenotype correlations. Hum Mutat 2002; 19: 465-78.

[111] Svensson L, Aszodi A, Heinegard D, *et al*. Cartilage oligomeric matrix protein-deficient mice have normal skeletal development. Mol Cell Biol 2002; 22: 4366-71.

[112] Aszodi A, Bateman JF, Hirsch E, *et al*. Normal skeletal development of mice lacking matrilin 1: redundant function of matrilins in cartilage? Mol Cell Biol 1999; 19: 7841-5.

[113] Ko Y, Kobbe B, Nicolae C, *et al*. Matrilin-3 is dispensable for mouse skeletal growth and development. Mol Cell Biol 2004; 24: 1691-9.

[114] Stefansson SE, Jonsson H, Ingvarsson T, *et al*. Genomewide scan for hand osteoarthritis: a novel mutation in matrilin-3. Am J Hum Genet 2003; 72: 1448-59.

[115] Min JL, Meulenbelt I, Riyazi N, *et al*. Association of matrilin-3 polymorphisms with spinal disc degeneration and osteoarthritis of the first carpometacarpal joint of the hand. Ann Rheum Dis 2006; 65: 1060-6.

[116] Pullig O, Tagariello A, Schweizer A, *et al*. MATN3 (matrilin-3) sequence variation (pT303M) is a risk factor for osteoarthritis of the CMC1 joint of the hand, but not for knee osteoarthritis. Ann Rheum Dis 2007; 66: 279-80.

[117] Nicolae C, Ko YP, Miosge N, *et al*. Abnormal collagen fibrils in cartilage of matrilin-1/matrilin-3-deficient mice. J Biol Chem 2007; 282: 22163-75.

[118] van der Weyden L, Wei L, Luo J, *et al*. Functional knockout of the matrilin-3 gene causes premature chondrocyte maturation to hypertrophy and increases bone mineral density and osteoarthritis. Am J Pathol 2006; 169: 515-27.

[119] Little CB, Mittaz L, Belluoccio D, *et al*. ADAMTS-1-knockout mice do not exhibit abnormalities in aggrecan turnover in vitro and *in vivo*. Arthritis Rheum 2005; 52: 1461-72.

[120] Majumdar MK, Askew R, Schelling S, *et al*. Double-knockout of ADAMTS-4 and ADAMTS-5 in mice results in physiologically normal animals and prevents the progression of osteoarthritis. Arthritis Rheum 2007; 56: 3670-4.

[121] Li SW, Takanosu M, Arita M, *et al*. Targeted disruption of Col11a2 produces a mild cartilage phenotype in transgenic mice: comparison with the human disorder otospondylomegaepiphyseal dysplasia (OSMED). Dev Dyn 2001; 222: 141-52.

Received: February 5, 2008 Revised: February 7, 2008 Accepted: February 15, 2008

PAPER III

β1 integrin-deficiency results in multiple abnormalities of the knee joint

Aurelia Raducanu[1], Ernst B. Hunziker[2], Inga Drosse[3] and Attila Aszódi[1]

From the [1]Max Planck Institute for Biochemistry, Department of Molecular Medicine, 82152 Martinsried, Germany; the [2]Center of Regenerative Medicine for Skeletal Tissues, Department of Clinical Research, University of Bern, 3010 Bern, Switzerland; and the [3]Experimental Surgery and Regenerative Medicine, Department of Surgery, University of Munich (LMU), 80336 Munich, Germany

Running head: β1 integrin-deficiency causes complex joint pathology

Address correspondence to: Attila Aszodi, Ph.D. Department of Molecular Medicine, Max Planck Institute of Biochemistry, Am Klopferspitz 18, 82152 Martinsried, Germany. Tel:49-89-8578-2466; Fax: 49-89-8578-2422; E-mail:aszodi@biochem.mpg.de

The lack of β1 integrins on chondrocytes leads to severe chondrodysplasia associated with high mortality rate around birth. To assess the impact of β1 integrin-mediated cell-matrix interactions on the function of adult knee joints, we conditionally deleted the *β1 integrin* gene in early limb mesenchyme using the *Prx1-cre* transgene. Mutant mice developed short-limbed dwarfism and had joint defects owing to β1 integrin-deficiency in articular regions. The articular cartilage (AC) was structurally disorganized accompanied by accelerated terminal differentiation, altered shape and disrupted actin cytoskeleton of the chondrocytes. Defects in chondrocyte proliferation, cytokinesis and survival resulted in hypocellularity. However, no significant differences in cartilage erosion, in the expression of matrix-degrading proteases or in the exposure of aggrecan and collagen II cleavage neoepitopes were observed between control and mutant AC. We found no evidence for disturbed activation of MAP kinases (ERK1/2, p38 and JNK) in vivo. Furthermore, fibronectin fragment-stimulated ERK activation and MMP-13 expression were indistinguishable in control and mutant femoral head explants. The mutant synovium was hyperplastic and frequently underwent chondrogenic differentiation. β1-null synoviocytes showed increased proliferation and phospho-focal adhesion kinase expression. Taken together, deletion of β1 integrins in knee joints results in multiple abnormalities reminiscent of osteoarthritis, however, it does not accelerate AC destruction, perturb cartilage metabolism or influence intracellular MAP kinase signaling pathways.

Chondrocytes of the articular cartilage (AC) secrete a unique set of extracellular matrix (ECM) molecules that assemble into interactive associates composed of collagens, proteoglycans (PGs) and non-collagenous glycoproteins (1). The fibrillar collagen meshwork supplies cartilage with its tensile strength, while the hydrated glycosaminoglycan (GAG) chains of PGs (mainly aggrecan) generate an osmotic swelling pressure that resists compressive forces. In diarthrodial joints, the molecular composition and the physical properties of the cartilage are principal determinants for the shock absorbing function of articular surfaces upon mechanical loading. During the development of osteoarthritis (OA), an imbalance between anabolic and catabolic processes increases the proteolysis of PGs and collagens (2, 3), which eventually leads to the mechanical weakening of the AC and culminates in its progressive destruction. Physiological and pathological remodeling of the AC ECM is primarily attributed to the activities of matrix metalloproteinases (MMPs) and ADAMTS (a disintegrin and metalloproteinase with thrombospondin-like repeat) proteases (4, 5), and is controlled by the communication between the cells and their environment.

An increasing amount of evidence suggests that interactions between chondrocytes and the ECM through the integrin family of heterodimeric (αβ) transmembrane receptors play a central role in cartilage function (6). Integrins connect the pericellular matrix to cytoskeletal and intracellular signaling complexes and modulate

various cellular functions including survival, proliferation, differentiation as well as matrix assembly and metabolism (7, 8). Chondrocytes express several integrin receptors for cartilage matrix ligands such as α1β1, α2β1 and α10β1 (for collagen II), α5β1, αvβ3 and αvβ5 (for fibronectin) and α6β1 (for laminin) (6, 9). We have previously demonstrated that *β1*$^{fl/fl}$*-Col2a1cre*$^{+}$ mice, in which the floxed *β1 integrin* gene (*β1*$^{fl/fl}$) was deleted using the chondrocyte-specific *Col2a1cre* transgene, display severe chondrodysplasia and a high mortality rate at birth (10). Homozygous mutant mice exhibit multiple growth plate abnormalities during endochondral bone formation characterized by defects in chondrocyte adhesion, shape, proliferation, cytokinesis and actin organization. In addition, the cartilage matrix shows a sparse, distorted collagen network. Similar, but milder abnormalities were found in mice lacking the collagen-binding integrin α10β1 or integrin-linked kinase in cartilage (11, 12).

Although these works have identified β1 integrins as essential regulators of growth plate development, the role of integrins in joint morphogenesis, adult joint function and pathology is incompletely understood. In embryonic mouse limb culture system, administration of β1 and α5 blocking antibodies or RGD peptides induced ectopic joint formation between proliferating and hypertrophic chondrocytes of the growth plate suggesting that α5β1 integrin controls the decision between cartilage differentiation and joint formation during development (13). In adult joints, increased immunostaining of β1 integrin was reported in osteoarthritic monkey cartilage compared to normal cartilage (14) and in human OA samples at minimally damaged locations compared to areas with more severe lesions (15). In another study, the neo-expression of α2, α4 and β2 integrins were observed in osteoarthritic human femoral head cartilage (16). In vitro experiments have suggested that signaling through the fibronectin (FN) receptor α5β1 integrin is pivotal to prevent cell death of normal and osteoarthritic human articular chondrocytes (17). FN fragments (FN-fs) present in synovial fluid and cartilage of OA patients have been implicated in cartilage breakdown (18-21). Human AC chondrocytes treated with the central, 110-120 kDa cell-binding FN-f but not with intact FN were shown to increase MMP-13 synthesis through the stimulation of α5β1 integrin and the subsequent activation of the proline-rich tyrosine kinase-2 and mitogen activated protein kinases (MAPKs) ERK-1/2, JNK and p38 (22, 23). Similarly, an adhesion-blocking antibody against α2β1 integrin induced the phosphorylation of MAPKs in human AC chondrocytes (22). Treatment of cultured rabbit synovial fibroblasts with central FN-fs or activating antibodies against α5β1 integrin elevated MMP-1 and MMP-3 expression (24). While these experiments suggest that blocking integrin signaling through α2β1/α5β1 in respond to degradation fragments may attenuate OA, mice lacking α1β1 integrin are prone to osteoarthritis (25). Knee joints of α1-null mice display precocious PG loss, cartilage erosion associated with increased MMP-2 and MMP-3 expression, and synovial hyperplasia.

To further explore the role of β1 integrins in joint biology, here we report the deletion of the floxed *β1 integrin* gene in embryonic limb-bud mesenchymal cells using the *Prx1cre* transgene (26). *β1*$^{fl/fl}$*-Prx1cre*$^{+}$ mice were born alive with short limbs owing to the lack of β1 integrin heterodimers on chondrocytes. We found that β1 integrin-deficiency in knee joints leads to multiple abnormalities of the AC and the synovium but it is not associated with accelerated AC destruction, perturbed AC metabolism and MAPK signaling. Our data suggest that β1 integrins are required for the proper structural organization of the AC by anchoring chondrocytes to the ECM but signaling through β1 integrins is less important for normal cartilage homeostasis.

EXPERIMENTAL PROCEDURES

Mice and radiography- Conditional β1 integrin mutant mice (*β1*$^{fl/fl}$*-Prx1cre*$^{+}$) were generated by intercrossing homozygous floxed (fl) *β1 integrin* females (27) with males double heterozygous for the *β1 integrin* (*β1*$^{fl/+}$) and *Prx1cre* transgenic alleles (26). *β1*$^{fl/+}$*-Prx1cre*$^{+}$ and *β1*$^{fl/+}$*-Prx1cre*$^{-}$ mice were phenotypically indistinguishable, therefore both genotypes were used as controls. For X-ray analysis, 16-month-old mice were euthanized and radiographs were taken with a sealed X-ray cabinet (Faxitron, model 43855A) at 35 kV, 2 mA and 2 seconds of exposure time.

Histology, OA grading and X-gal staining- Control and *β1*$^{fl/fl}$*-Prx1cre*$^{+}$ mice were euthanized and knee joints were harvested at various time points. For histology, samples were fixed in 4% paraformaldehyde (PFA) in phosphate buffered saline (PBS, pH 7.4), decalcified in 10% EDTA-

PBS and processed for paraffin embedding. Approximately 300 consecutive, 6-µm-thick sagittal sections were collected from each specimen, and every 10th section was stained with Hematoxylin-Eosin (HE) for general histology or Safranin O-Fast green (SO) to monitor PG depletion. To asses osteoarthritis-like changes of the articular cartilage, we used a scoring system as follows: I. Cartilage erosion (0-5): 0-smooth cartilage surface; 1-surface irregularities; 2-cleft to transition zone; 3-cleft to radial zone; 4-cleft to calcified zone; 5-exposure of subchondral bone. II. Cellularity (0-3): 0-normal; 1-hypercellularity; 2-clustering; 3-hypocellularity. III. Tidemark integrity (0-1): 0-normal; 1-loss of tidemark. IV. GAG content in the pericellular matrix (PM) (0 to 2): 0-normal SO staining intensity; 1-focally increased intensity; 2-increased intensity throughout the cartilage. V. GAG content in the interterritorial matrix (ITM) (0 to 3): 0-normal SO staining intensity; 1-reduced staining; 2-focal patchy loss of staining; 3-50% of cartilage without staining. VI. Osteophyte formation (0-2): 0-none; 1-formation of cartilage; 2-formation of bone. Total scale (0-16) and OA severity: 0-1, normal; 2-5 mild OA; 6-11 moderate OA; 12-16, severe OA.

Picrosirius red and X-gal staining were performed as described elsewhere (28, 29).

Ultrastructural analysis-Knee joints including the subchondral bone were isolated and the tibial and femoral sides were separated under a stereomicroscope. Specimens were fixed in 2% glutaraldehyde in 0.1 M sodium cacodylate buffer (pH 7.4) for 3 days and processed for electron microscopy as previously described (30).

Analysis of the actin cytoskeleton- Tibiae were freshly dissected and ~80 µm thick sagittal sections were obtained using a vibratome (Microm). Sections were then fixed in 4% PFA/PBS for 2 hours at room temperature, permeabilized with 0.1%Triton X-100 and stained with phalloidin Alexa488 (Invitrogen) to visualize the actin cytoskeleton and with DAPI (Sigma) to visualize the nucleus.

Cell proliferation and apoptosis- To assess chondrocyte proliferation, PCNA (proliferating cell nuclear antigen) immunostaining was performed on tissue sections. To determine the labeling index, the percentage of immunoreactive nuclei per 100 cells, the numbers of brown-colored nuclei were counted. To detect apoptotic cells, TUNEL assay was used as described in (10).

RT-PCR- To examine the mRNA levels of matrix degrading enzymes, tibiae were harvested from 4-month-old control and $\beta1^{fl/fl}$-*Col2a1cre*$^{+}$ mice. Vibratome sections (100 µm) were cut and the articular cartilages were dissected using a sharp blade and a stereomicroscope. Cartilage pieces were pooled and total RNA was isolated using the RNeasy Lipid Tissue Mini Kit (Qiagen). The cDNA was synthesized using the SuperScript III RNaseH^{-} Reverse Transcriptase (Invitrogene). For semiquantitative RT-PCR the following primers were used: $Mmp2_{forward}$: 5′-GACAAGTGGTCC-GCGTAAAG and $Mmp2_{reverse}$: 5′-CATCTGCAT-TGCCACCCATG; $Mmp3_{forward}$: 5′-CCTACTTCT-TTGTAGAGGAC and $Mmp3_{reverse}$: 5′- GTCAA-ATTCCAACTGCGAAG; $Mmp8_{forward}$: 5′-GTAA-ACTGTAGAGTCGATGC and $Mmp8_{reverse}$: 5′-CATAGGGTGCGTGCAAGGAC; $Mmp9_{forward}$: 5′-CGAGTGGACGCGACCGTAG-TTGG and $Mmp9_{reverse}$: 5′-CAGGCTTAGAGCCACGACCA-TACAG; $Mmp13_{forward}$: 5′-GTGTGGAGTTATG-ATGATGT and $Mmp13_{reverse}$: 5′-TGCGATTAC-TCCAGATACTG; $Gapdh_{forward}$: 5′- TCGTGGAT-CTGACGTGCCGCCTG and $Gapdh_{reverse}$: 5′-ACCCTGTTGCTGTAGCCGTAT.

Immunohistochemistry (IHC) and ELISA assays-Knee joints were fixed in 4% PFA/PBS, decalcified and processed either for paraffin or cryo embedding. To enhance antibody penetration, both paraffin and cryo-sections were treated with bovine testicular hyaluronidase (2 mg/ml in PBS) at 37°C for 30 min. When needed, antigen retrieval was performed by incubating the sections either in 0.1M citrate buffer (pH 6.0) at 95°C for 20 min or in 6M guanidine hydrochloride for 15 min at room temperature. Primary antibodies against the following antigens were used: β1 integrin (Chemicon MAB1997); aggrecan (Chemicon AB1031); G1-TEGE (Acris SP5418P); G1-PEN and ADAMTS-5 (gifts from Amanda Fosang); MMP-1 (Calbiochem IM35L); MMP-2 (Chemicon AB19167); MMP-3 (Oncogene Research Products IM70); MMP-9 (Chemicon AB19016); MMP-13 (Chemicon AB8120); C1,2C (IBEX #50-1035); phospho-p38 (#4631), phospho-ERK1/ERK2 (#4376), and phospho–JNK (#9251) (all obtained from Cell Signaling) and phospho-FAK (pY397, Invitrogen #44624G). Immunostaining was performed using the appropriate Vectastain ABC Elite kit (Vector

Laboratories) and 3,3´-diaminobenzidine (Sigma) as chromogenic substrate.

Commercial ELISA assay kits were used to detect the levels of collagen II degradation products either in urine samples (CTX-II, which measures C-telopeptides fragments; Nordic Bioscience 2CAL4000) or in serum samples (C2C, which measures the carboxyl-terminal ¾ fragment collagen II cleavage neoepitope; IBEX 60-1001-001). The CPII ELISA kit (IBEX 60-1003-001) was used to measure the serum level of collagen II C-propeptide, which correlates with collagen II biosynthesis.

Cartilage explant culture- Femoral heads were harvested from 4-week-old control and mutant mice and cultured in 300 µl serum-free DMEM supplemented with streptomycin-penicillin in 48-well plate for 4 days. Treated cartilages received 1µM fibronectin fragment (40.1 kDa FNIII7-10RGD) from the beginning of the culture. At the end of the culture period the femoral heads were fixed in 4% PFA/PBS and cryo-embedded. Sections from treated and untreated as well as from day 0 samples were immunostained for phospho-ERK1/ERK2 and MMP-13.

Statistical analysis- Non-parametric Mann-Whitney U test was used to compare the median of total OA and cartilage erosion scores. All other data were expressed as the mean ± SD and significance was assessed using either Student´s *t* test or Mann-Whitney test.

RESULTS

Generation of the $\beta1^{fl/fl}$-Prx1cre^{+} mice. To assess the function of β1 integrins in joint biology, we deleted the floxed *β1 integrin* gene in embryonic limb-bud mesenchyme by using the *Prx1cre* transgenic line (26). Since the ablation of the $\beta1^{fl}$ allele activates a promoter-less *LacZ* gene (10), we performed X-gal staining to demonstrate β-galactosidase (β-gal) activity and monitor the deletion of the gene. Forelimb sections of $\beta1^{fl/fl}$-*Prx1cre*$^{+}$ mice at E 18.5 showed β-gal activity in tissues of mesenchymal origin including cartilage, periosteum/perichondrium, ligaments, tendons, synovium and vessels (Fig.1, *A-D*). While β-gal negative chondrocytes were occasionally observed in the growth plate, the developing AC contained only β-gal positive chondrocytes indicating very high deletion efficiency of *β1 integrin* in this region (Fig. 1*B*).

$\beta1^{fl/fl}$-*Prx1cre*$^{+}$ mice recapitulate the embryonic skeletal phenotype of $\beta1^{fl/fl}$-*Col2a1cre*$^{+}$ mice (not shown) and survive after birth. Immunostaining of control knee joints at 1 month showed abundant expression of β1 integrin on AC chondrocytes, while little if any expression was detected in $\beta1^{fl/fl}$-*Prx1cre*$^{+}$ AC (Fig. 1*E*). Similarly, β1 integrin was largely absent in the synovium (Fig. 1*F*), meniscus, patella and joint ligaments (not shown). Adult mutant mice exhibited shortened long bones and abnormal gait which were associated with reduced flexibility of the knee joints from 7 months. X-ray analysis of the hind-limb at 16 months (Fig. 1*G*) demonstrated misaligned bones, irregular joint surfaces, joint space narrowing and the appearance of radio-dense plaques in the vasculature of $\beta1^{fl/fl}$-*Prx1cre*$^{+}$ mice. The mutant mice were able to walk at all stages, however, their mobility was apparently reduced from 8 months of age compared to control littermates. The frequency of vascular calcification increases with age and is associated with high mortality rate between 8-12 months of age.

Histopathological changes of the articular cartilage. At birth, the forming AC in control and mutant tibiae was unstratified with rounded chondrocytes exhibiting a random, isotropic distribution pattern (Fig. 2*A*). At 1 month, control tibia showed advanced ossification of the epiphysis, while in mutants the secondary ossification centre was narrowed and entirely composed of chondrocytes (Fig. 2*B*). Control AC displayed structural anisotropy characterized by the appearance of flattened chondrocytes in the superficial layer and formation of columns in deeper regions. In contrast, the mutant AC was still isotropic lacking flat cells and column-like structures and showed a broad, acellular surface area facing the joint cavity (Fig. 2*C*). After 1 month of age, endochondral ossification was also evident in the mutant epiphyses and the AC exhibited several abnormalities including thickening (Fig. 2*G*), disorganized cell arrangement with frequent clustering, flattening of the tibial plateau and formation of less subchondral bone (Fig. 2*D*). In 1- and 4-month-old control and mutant mice the AC surface was largely intact with slightly increased roughening in mutants (Fig. 2*C* and not shown). At later stages, we found typical signs of cartilage erosion in both experimental groups (Fig. 2*D*). In general, SO staining indicated comparable levels of negatively charged PGs in control and mutant AC (Fig. 2, *E*

and *F*). At 1 month, the tidemark separating the uncalcified and calcified AC was only detectable in controls (Fig. 2*E*). At later stages the tidemark appeared in the mutants, however, it was irregular and often discontinuous (Fig. 2*F*). Typically, extended pericellular matrix (PM) staining was observed in the calcified zone of mutants. Furthermore, the length of the uncalcified zones with strong SO staining in the interterritorial matrix (ITM) is decreased, while the length of the calcified zone with less intense staining in the ITM is increased in mutants (Fig. 2, *E*, *F* and *H*).

Quantification of the OA-like histopathological changes of the knee joint revealed that the total score (the sum of sub-scores, see Experimental Procedures) is increased in each age group (4, 7 and 12 months) of mutants compared to controls (Fig. 3*A*). Separate evaluation of cartilage erosion, however, did not reveal significant differences in AC destruction between control and mutant mice (Fig. 3*B*). Whereas the median score was slightly higher in mutants at 4 and 7 months, it moderately decreased at 12 months compared with controls.

Ultrastructural and cytoskeletal abnormalities of the mutant articular cartilage. Electron microscopy at 4 months revealed abnormalities throughout the mutant AC (Fig. 4*A*). Compared with controls, mutant mice displayed an enlarged superficial zone with extra layers of disorganized collagen fibrils and rounded chondrocytes. In all AC zones the PM compartment was expanded, most prominently in the lower radial and the calcified zones, the chondrocytes were frequently binucleated and extended long microvilli into the matrix. In the ITM compartment the fibrillar network was less organized with a high variation of fibril density (not shown), whereas in the PM thick collagen bundles occasionally appeared near the chondrocyte surface (Fig. 4*A*).

To test the impact of β1 integrin-deficiency on the actin cytoskeleton of AC chondrocytes, we analysed phalloidin-stained tissue sections by confocal microscopy. At 4 months, the actin network was only mildly affected in mutants (not shown), however, by 11 months marked abnormalities of the cytoskeleton were observed in chondrocytes located at the weight-bearing regions of the tibial plateau (Fig. 4*B*). Whereas control chondrocytes in the uncalcified zones exhibited a strong and even cortical actin staining, mutant chondrocytes showed a faint and punctuated actin distribution indicating a disrupted actin cytoskeleton in the absence of β1 integrins.

Chondrocyte proliferation and survival. Quantification of AC cellularity in the tibial plateau revealed that $\beta 1^{fl/fl}$-*Prx1cre*$^{+}$ mice have reduced chondrocyte density (Fig. 5*A*). 1 month old samples showed only a moderate reduction, whereas at later stages the mutants showed significantly fewer chondrocytes per unit area compared with controls. To study the underlying mechanism of hypocellularity, chondrocyte proliferation and death were investigated. Using PCNA immunostaining, we observed a normal proliferation rate at day 4, however, at 2 weeks the fraction of PCNA-positive cells was reduced by about 25% in mutants (Fig. 5*B*). At 1 and 4 months of age, the PCNA index was very low and comparable in mutant and control samples. A closer view at 2 weeks revealed that in controls most PCNA-positive cells were located throughout the AC including the most superficial layer, whereas in mutants PCNA-labelled chondrocytes were more prominent in deeper zones and were frequently binucleated (Fig. 5*C*). Because abnormal cytokinesis could also contribute to the reduced cell density, the binucleation rate of tibial plateau chondrocytes was quantified (Fig. 5*D*). The percentage of binucleated chondrocytes increased with age from 0.89% (1 month) to 1.62% (4 months) and to 2.19% (10 months) in control, whereas in mutant the binucleation rate was 5% at 1 month and it increased to 7.66% and 10.57% by the age of 4 and 10 months, respectively. Assessing cell death by TUNEL assay, we observed no difference in the apoptotic rates at 4 and 12 months, however, the percentage of TUNEL-positive chondrocytes was significantly higher at 7 months in the mutants (Fig. 5*F*).

The expression of collagen X and collagen VI is altered in the mutant AC. IHC showed that most ECM molecules including aggrecan and collagen type II were normally expressed and deposited in the mutant tibial plateau cartilage (not shown). In contrast, collagen X, which is produced by hypertrophic chondrocytes and present in the calcified zone of the AC, displayed an abnormal staining pattern (Fig. 6*A*). In controls, collagen X was detectable below the tidemark at a distance of 6-7 cell layers from the surface, while in $\beta 1^{fl/fl}$-*Prx1cre*$^{+}$ AC collagen X appeared at a distance of 2-3 cell layers, consistent with the reduced depth of the uncalcified cartilage. Occasionally, mutant

cells in the uncalcified zone displayed strong collagen X deposition suggesting premature differentiation of *β1$^{fl/fl}$-Prx1cre^{+}* chondrocytes. Furthermore, collagen VI was detectable in the PM of all control cells in the uncalcifed zones but it was apparently missing at certain locations around mutant chondrocytes (Fig. 6*B*).

The lack of β1 integrin on chondrocytes does not lead to detectable changes in articular cartilage metabolism. To assess the expression of matrix degrading enzymes, first the mRNA levels of *Mmp2, Mmp8; Mmp9 and Mmp13* were examined by semiquantitative RT-PCR at four months of age. In three independent experiments, we found comparable levels of MMP mRNAs in control and *β1$^{fl/fl}$-Prx1cre^{+}* mice (Fig. 7*A*). Next, we performed immunostaining for MMP-1, MMP-2, MMP-3, MMP-9, MMP-13, ADAMTS-4 and ADAMTS-5. In general, the expression of MMPs was low or undetectable in the AC, and no significant differences were observed between mutant and control samples at 4, 7 and 12 months of age (Fig. 7*B* and not shown). ADAMTS-5 and ADAMTS-4 were evident around chondrocytes in the non-mineralized AC and their expression was indistinguishable between control and *β1$^{fl/fl}$-Prx1cre^{+}* mice (Figure 7*B* and not shown). To further examine matrix catabolism, collagen and aggrecan degradation products were investigated on tissue sections by IHC (Fig. 7*C*). The aggrecan neoepitope G1-IPEN^{341} (generated by MMPs) was predominantly detectable in the calcified zone, whereas the G1-TEGE^{373} (generated by aggrecanases) was abundant in the pericellular matrix of chondrocytes in the uncalcified zones. We noticed no changes in the amount of degraded aggrecan in *β1$^{fl/fl}$-Prx1cre^{+}* mice compared to controls at 7 and 12 months. Similarly, there was no detectable difference in type II collagen degradation *in situ* judged by the C1,2C polyclonal antibody which recognizes the Col2-3/4C$_{short}$ neoepitope upon cleavage by collagenases such as MMP13 (Fig. 7*C*). Finally, body fluid samples were investigated by ELISA assays to detect type II collagen degradation (C2C and CTX-II) or synthesis (CPII) products. Again, no statistically significant differences were found between mutant and control samples (Fig. 7, *D-F*).

β1 integrin null chondrocytes display normal activation of MAP kinases. Signaling pathways via MAPKs are activated by extracellular stimuli and may play important role in joint destruction by regulating the expression of proinflammatory cytokines and MMPs (31). To check the activity of "classical" MAPKs in β1-deficient AC chondrocytes, we performed IHC using antibodies that specifically recognize the phosphorylated forms of ERK-1/2, p38 and JNK. At 1 month of age, numerous femoral head AC chondrocytes stained positive and we observed no obvious differences in activation of MAPKs between controls and mutants (Fig. 8*A*). Next, femoral head articular cartilage was removed from control and mutant mice, cultured in serum free medium with or without the central, cell binding fragment of fibronectin (FnIII7-10). After 4 days in culture, the explants were investigated for ERK phosphorylation and MMP-13 expression by IHC (Fig. 8*B*). In untreated samples, no ERK activation and MMP-13 deposition were observed in the articular cartilage. In contrast, both control and mutant articular cartilage that received Fn-f exhibited comparable ERK phosphorylation and MMP-13 expression. This data indicates that FnIII7-10 fragments could stimulate MMP-13 expression via MAP kinase activation in the absence of the major Fn binding integrin α5β1. Finally, we analyzed the activation of the focal adhesion kinase (FAK), a central player of integrin signaling pathways, by using an antibody that recognizes the auto-phosphorylated Tyr397 residue. In agreement with previous results on growth plate chondrocytes (10), mutant AC chondrocytes at 2 weeks of age showed moderately decreased immunostaining compared to controls (not shown).

Histopathological changes of the synovial tissue. Mid-sagittal sections through the developing knee joint at embryonic day 16 showed poorly differentiated synovium, collateral and cruciate ligaments in *β1$^{fl/fl}$-Prx1cre^{+}* mice compared with controls (Fig. 9*A*). In newborns, the control synovium was compact and the joint ligaments were well-developed, whereas in mutants the synovial tissue had a loose-appearance, the cruciate ligament was disorganized and the collateral ligament was thinned (not shown). At 2 weeks, the control synovium was composed of a narrow lining layer and a large adipose compartment. The mutant synovium showed fibrosis with extensive collagen deposits, revealed by strong birefringence under polarization microscopy (Fig. 9, *B* and *C*). At 1 month, SO-stained sections through the nonarticular area of the control joints showed non-cartilaginous surfaces of the tibia and the femur

interconnected by the cruciate ligaments, whereas the intercondylar surface of the mutant tibia was still cartilaginous (Fig. 9*D*). In mutant, the fibrotic synovial tissue invaded the joint space and began to undergo chondrogenic differentiation revealed by PG deposits and by 7 months of age, the joint cavity was frequently filled with chondrophytes (Fig. 9, *D* and *E*). IHC at 2 weeks demonstrated increased numbers of PCNA-positive cells in the mutant synovium (Fig. 9*F*). In contrast to cartilage, increased phosphorylation of FAK was observed in the $\beta1^{fl/fl}$-*Prx1cre*$^{+}$ synovial tissue (Fig. 9*G*).

DISCUSSION

Previous in vivo studies in mice revealed that the loss of β1 integrins on chondrocytes results in severe growth plate defects and perinatal lethality (10), whereas ablation of the α1β1 integrin leads to accelerated knee OA (25). Here we report the generation of $\beta1^{fl/fl}$-*Prx1cre*$^{+}$ mice and demonstrate that targeting β1 integrin in limb skeletal precursor cells leads to a complex knee joint phenotype characterized by multiple AC and synovial abnormalities but is not accompanied by altered cartilage metabolism.

Histology of the knee joints revealed increased AC depth and a reduced ratio of uncalcified/calcified cartilage thicknesses in mutant mice compared to controls. This phenomenon might be the consequence of abnormal secondary ossification and subchondral bone formation. Since the articular cartilage and the underlying subchondral bone together provide the joint with its normal biomechanical properties, it is possible that the increased thickness of the calcified zone in mutant mice is due to a physiological compensation of the reduced subchondral bone mass to adopt mechanical loading. Supporting this hypothesis, it was recently reported that C57Bl/6 mice with a thin subchondral plate exhibit a higher calcified/uncalcified ratio in the AC than C3H/HEJ mice, which have a thick subchondral plate (32). At the molecular level, the increased calcified thickness of the $\beta1^{fl/fl}$-*Prx1cre*$^{+}$ AC was also apparent from the expression of collagen X, a hypertrophic chondrocyte marker which is normally deposited below the tidemark (1). Several previous studies have indicated an inductive role of β1 integrins in hypertrophic differentiation. Signaling via α1β1 and α5β1 integrins was required for hypertrophy of cultured AC chondrocytes induced by transglutaminases (33, 34), β1 integrin-blocking antibody impaired chondrocyte hypertrophy and collagen X deposition in sternal organ culture (35) and miss-expression of α5β1 integrin in embryonic chick legs resulted in joint fusion and initiation of the hypertrophic differentiation program (13). Finally, we have demonstrated that hypertrophic differentiation is delayed in $\beta1^{fl/fl}$-*Col2cre*$^{+}$ growth plate and epiphyseal cartilages (10). Here we show that collagen X demarcates a broader calcified zone in $\beta1^{fl/fl}$-*Prx1cre*$^{+}$ knee joints and appears in cells above the tidemark, suggesting that β1 integrin signaling may actually prevent terminal differentiation of AC chondrocytes. This implies that integrins have a complex role in chondrocyte hypertrophy, which obviously depends on the tissue context.

$\beta1^{fl/fl}$-*Prx1cre*$^{+}$ AC displays several abnormalities, which are reminiscent of those found previously in the growth plate of the $\beta1^{fl/fl}$-*Col2a1cre* mice (10). In the normal growth plate, chondrocytes are flattened in the proliferative zone where they arrange into distinct vertical columns (36), whereas in the normal AC, flat chondrocytes are apparent in the superficial zone and column-like, vertical alignment of chondrocytes can be observed in the radial and calcified zones of the condyles (37). The growth plate of $\beta1^{fl/fl}$-*Col2a1cre* mice has rounded proliferative chondrocytes that are unable to form vertical columns due to a migratory block following cytokinesis (10). Similarly, $\beta1^{fl/fl}$-*Prx1cre*$^{+}$ chondrocytes were rounded in the superficial zone and were not aligned into columns in deeper regions resulting in a more isotropic cell distribution compared to the normal, structural anisotropy seen in the control AC. The inability of β1 integrin-deficient chondrocytes to form organized structures in cartilage can be explained, by the impaired adhesion and by the disruption of the F-actin and the normal matrix architecture. It has been shown that administration of anti-β1 integrin blocking antibody to chicken sternum organ culture disrupts the cortical actin network and reduces chondrocyte-matrix interactions revealed by fewer collagen fibrils and filopodia-like cell projections in the PM (35). Interestingly, our electron microscopic analysis of $\beta1^{fl/fl}$-*Prx1cre*$^{+}$ AC revealed an enlarged PM compartment with unusually thick collagen fibrils closely associated with the plasma membrane and

with large number of long microvilli. The normal PM consists of proteins that bind to β1 integrins such as collagens II, VI and fibronectin (1, 6). The observation that β1 integrin-deficiency result in abnormalities of the collagen II network and deposition of collagen VI suggest that β1 integrins are pivotal organizers of the collagenous architecture of the matrix. Defects in pericellular collagen assembly could directly affect the size of the compartment leading to its expansion as observed around *β1*$^{fl/fl}$*-Prx1cre*$^{+}$ chondrocytes. The elongation of the cell processes are probably due to the altered pericellular environment as suggested in a recent study demonstrating multiple, elongated microvilli in human OA femoral head cartilage (38).

Finally, both growth plate and AC β1-null chondrocytes exhibit proliferation defect, frequent binucleation and increased apoptosis. As the current view suggests that AC growth is primarily achieved by apposition from the surface (39), the depletion of proliferative chondrocytes in this region could be the primary cause of reduced cellularity seen in the *β1*$^{fl/fl}$*-Prx1cre*$^{+}$ mice. Binucleation, caused by cytokinesis failure, cell fusion or amitosis, is relatively common in auricular and articular chondrocytes (40). Since β1 integrins are localized in the cleavage furrow (10) and adhesion-mediated pulling forces are required to separate daughter cells (41), it is likely that the high binucleation rate in β1-integrin-null chondrocytes is due to impaired cytokinesis. *β1*$^{fl/fl}$*-Prx1cre*$^{+}$ AC also displays slightly elevated numbers of apoptotic chondrocytes at 7 months of age. The lack of massive cell death in the mutant AC suggests that other integrins (*e.g* αvβ3) or non-integrin surface receptors may also support cell survival and partially prevent chondrocyte apoptosis in the absence of β1 integrins.

Despite the AC abnormalities, histology and histochemistry did not indicate increased proteoglygan depletion and cartilage erosion in the mutant AC compared to control mice. These results were corroborated with the normal expression of MMP and ADAMTS proteases and their degradation products implying that β1 integrins are apparently dispensable for overall cartilage metabolism in vivo. Mice lacking the major, chondrocyte-specific collagen binding integrin α10β1 have no obvious AC abnormalities (11) further supporting the view that β1 integrins are less important for cartilage homeostasis. However, these observations are in contrast with the phenotype of the α1β1 integrin–deficient mice that display precocious PG loss and severe cartilage lesions associated with elevated levels of MMP-2 and MMP-3 (25). In normal joints, α1 integrin expression is low, whereas in OA cartilage α1 is significantly up-regulated (14) suggesting that this particular integrin heterodimer might be required for cartilage matrix remodeling at the damaged regions. Our finding, however, clearly show that the loss of all β1 heterodimers on chondrocytes does not phenocopy the AC abnormalities of the α1-null mice. Could this contradiction be accounted to the abnormal gait and reduced mobility of *β1*$^{fl/fl}$*-Prx1cre*$^{+}$ mice? The fact that we did not notice significantly reduced mobility of mutant mice until 8 months of age, whereas α1 knockout mice develop severe AC degeneration as early as 4 months, argues against the possibility that reduced joint usage would prevent physical activity-induced cartilage damage in *β1*$^{fl/fl}$*-Prx1cre*$^{+}$ mice. Alternatively, the lack of β1 integrin heterodimers may attenuate AC destruction. Several studies indicate that integrins are involved in the regulation of MMPs expression in response to matrix degradation fragments in AC chondrocytes. First, the 110-140 kDa cell-binding and the 29 kDa, amino-terminal heparin-binding FN-fs are both capable of interacting with α5β1 integrin, and upregulate MMP-3 and/or MMP-13 via activation of the ERK1/2, p38 and JNK MAPKs (18, 20). Second, engagement of α2β1 or α5β1 integrins by adhesion-blocking antibodies on human AC chondrocytes increases ERK1/2, p38 and JNK phosphorylation and blocking antibody to α5β1 stimulates gelatinase production (22). These studies implicate β1 integrins, particularly α2β1 and α5β1, as active participants in matrix degradation and their absence may lower MMPs expression. However, the phosphorylation of MAPKs was apparently indistinguishable between *β1*$^{fl/fl}$*-Prx1cre*$^{+}$ and control ACs indicating that β1 integrins are either not required for MAPKs activation *per se* or their lack can be efficiently compensated via signaling through β3/β5 integrins or growth factor receptors. More surprisingly, we found that FnIII7-10 fragments in explant culture were able to activate ERK and upregulate MMP-13 expression in both control and β1 integrin-deficient femoral heads. Since not only α5β1 but also αvβ3 and αvβ5 integrins are

capable to bind FnIII7-10 (42), it is likely that Fn-fs-induced cartilage degradation is a complex process involving signaling through several integrin heterodimers.

Synovial changes including hyperplasia and inflammation are often characteristics of OA joints and, via production of various cytokines and proteinases, synovitis likely contributes to cartilage destruction (43). *$\beta1^{fl/fl}$-Prx1cre^{+}* mice display synovial fibrosis accompanied by frequent chondrification but the mutant synovial tissue shows no clear sign of inflammatory infiltrates, suggesting that the observed alterations are unlikely to be linked to immunological processes. Recent findings indicate that synovial-lining cells in OA patients display enhanced activation of FAK (44) that may lead to increased cell proliferation and/or migration. Indeed, and in contrast to chondrocytes, we detected upregulation of phospho-FAK expression in mutant synovial tissue. Since FAK is tyrosine phosphorylated in response to αvβ3 integrin ligation in osteoclasts (45), it is tempting to speculate that β1-deficient synovial fibroblasts may over-use αvβ3-mediated signaling pathways resulting in altered FAK activation. However, the precise mechanism how altered cell-matrix interactions and integrin signaling contribute to the synovial pathology of *$\beta1^{fl/fl}$-Prx1cre^{+}* mice remains to be elucidated.

Taken together, our study indicates that β1 integins are pivotal for joint development regulating structural organization, differentiation and growth of the AC and the synovium. The lack of β1 integrins in the AC, however, has no obvious impact on cartilage homeostasis, excluding β1-integrin signaling as a good candidate for intervention in degenerative cartilage diseases. Owing to the complex phenotype of *$\beta1^{fl/fl}$-Prx1cre^{+}* joints, however, the generation of a transgenic line with AC-specific deletion is required to precisely define the role of β1 integrin-mediated chondrocyte-ECM interactions in AC destruction.

REFERENCES

1. Poole, A.R., Kojima, T., Yasuda, T., Mwale, F., Kobayashi, M., and Laverty, S. (2001) *Clin. Orthop. Relat. Res.* **391,** S26-33
2. Caterson, B., Flannery, C.R., Hughes, C.E., and Little, C.B. (2000) *Matrix Biol.* **19,** 333-344
3. Poole, A.R., Nelson, F., Dahlberg, L., Tchetina, E., Kobayashi, M., Yasuda, T., Laverty, S., Squires, G., Kojima, T., Wu, W., and Billinghurst, R.C. (2003) *Biochem. Soc. Symp.* **70,** 115-123
4. Jones, G.C., and Riley, G.P. (2005) *Arthritis Res. Ther.* **7,**160-169
5. Murphy, G., Knauper, V., Atkinson, S., Butler, G., English, W., Hutton, M., Stracke, J., and Clark, I. (2004) *Arthritis Res.* **4,** S39-49
6. Knudson, W., and Loeser, R.F. (2002), *Cell Mol. Life Sci.* **59,**36-44
7. Brakebusch, C., Bouvard, D., Stanchi, F., Sakai, T., and Fassler, R. (2002) *J. Clin. Invest*. **109,** 999-1006
8. Hynes, R.O. (2002) *Cell* **110,** 673-687
9. Loeser, R.F. (2000) *Biorheology* **37,** 109-116
10. Aszodi, A., Hunziker, E.B., Brakebusch, C., and Fassler, R. (2003) *Genes Dev.* **17,** 2465-2479
11. Bengtsson, T., Aszodi, A., Nicolae, C., Hunziker, E.B., Lundgren-Akerlund, E., and Fässler, R. (2005) *J. Cell. Sci.* **118,** 929-936
12. Grashoff, C., Aszódi, A., Sakai, T., Hunziker, E.B., and Fässler, R. (2003) *EMBO Rep.* **4,** 432-438
13. Garciadiego-Cazares, D., Rosales, C., Katoh, M., and Chimal-Monroy, J. (2004) *Development* **131,** 4735-4742
14. Loeser, R.F., Carlson, C.S., and McGee, M.P. (1995) *Exp. Cell Res.* **217,** 248-257
15. Lapadula, G., Iannone, F., Zuccaro, C., Grattagliano, V., Covelli, M., Patella, V., Lo Bianco, G., and Pipitone, V. (1998) *Clin Rheumatol* **17,** 99-104
16. Ostergaard, K., Salter, D.M., Petersen, J., Bendtzen, K., Hvolris, J., and Andersen, C.B. (1998) *Ann. Rheum. Dis.* **57,** 303-308
17. Pulai, J.I., Del Carlo, M, Jr., and Loeser, R.F. (2002) *Arthritis Rheum*. **46,** 1528-1535
18. Ding, L., Guo, D., and Homandberg, G.A. (2008) *Osteoarthritis Cartilage* **16,** 1253-1262

19. Homandberg, G.A., Meyers, R., and Xie, D.L. (1992) *J. Biol. Chem.* **267,** 3597-3604
20. Stanton, H., Ung, L., and Fosang, A.J. (2002) *Biochem. J.* **364,** 181-190
21. Xie, D.L., Hui, F., Meyers, R., and Homandberg, G.A. (1994) *Arch. Biochem. Biophys.* **311,** 205-212
22. Forsyth, C.B., Pulai, J., Loeser, R.F. (2002) *Arthritis Rheum.* **46,** 2368-2376
23. Loeser, R.F., Forsyth, C.B., Samarel, A.M., and Im, H.J. (2003) *J. Biol. Chem.* **278,** 24577-24585
24. Werb. Z., Tremble, P.M., Behrendtsen, O., Crowley, E., and Damsky, C.H. (1989) *J. Cell. Biol*. **109,** 877-889
25. Zemmyo, M., Meharra, E.J., Kuhn, K., Creighton-Achermann. L., and Lotz, M. (2003) *Arthritis Rheum*. **48,** 2873-2880
26. Logan, M., Martin, J.F., Nagy, A., Lobe, C., Olson, E.N., and Tabin, C.J. (2002) *Genesis* **33,** 77-80
27. Potocnik, A.J., Brakebusch, C., and Fassler, R. (2000) *Immunity* **12,** 653-663
28. Modis, L. (1991) *Organization of the extracellular matrix: a polarization microscopic approach.* CRC Press, Boca Raton, Florida
29. Sakai, K., Hiripi, L., Glumoff, V., Brandau, O., Eerola, R., Vuorio, E., Bosze, Z., Fassler, R., and Aszodi, A. (2001) *Matrix Biol.* **19,** 761-767
30. Aszodi, A., Chan, D., Hunziker, E., Bateman, J.F., and Fassler, R. (1998) *J. Cell. Biol.* **143,** 1399-1412
31. Loeser, R.F., Erickson, E.A., and Long, D.L. (2008) *Curr. Opin. Rheumatol.* **20,** 581-586
32. Botter, S.M., van Osch, G.J., Waarsing, J.H., van der Linden, J.C., Verhaar, J.A., Pols, H.A., van Leeuwen, J.P., Weinans, H. (2008) *Osteoarthritis Cartilage* **16,** 506-514
33. Johnson, K.A., Rose, D.M., Terkeltaub, R.A. (2008*) J. Cell. Sci.* **121,** 2256-2264
34. Tanaka, K., Yokosaki, Y., Higashikawa, F., Saito, Y., Eboshida, A., and Ochi, M. (2007) *Matrix Biol.* **26,** 409-418
35. Hirsch, M.S., Lunsford, L.E., Trinkaus-Randall, V., and Svoboda, K.K. (1997) *Dev. Dyn.* **210,** 249-263
36. Erlebacher, A., Filvaroff, E.H., Gitelman, S.E., and Derynck, R. (1995) *Cell* **80,** 371-378
37. Hunziker, E. (1992) *Articular cartilage and osteoarthritis.* Edited by Kuettner KE. Raven, Press, New York
38. Holloway, I., Kayser, M., Lee, D.A., Bader, D.L., Bentley, G., and Knight, M.M. (2004) *Osteoarthritis Cartilage* **12,** 17-24
39. Dowthwaite, G.P., Bishop, J.C., Redman, S.N., Khan, I.M., Rooney, P., Evans, D.J., Haughton, L., Bayram, Z., Boyer, S., Thomson, B., Wolfe, M.S, and Archer, C.W. (2004) *J. Cell. Sci.* **117,** 889-897
40. Lipman, J.M., Hicks, B.J., and Sokoloff, L. (1984) *Experientia* **40,** 553-554
41. Böttcher, R.T., Wiesner, S., Braun, A., Wimmer, R., Berna, A., Elad, N., Medalia, O., Pfeifer, A., Aszódi, A., Costell, M., and Fässler, R. (2009) *EMBO J.* doi:10.1038/emboj.2009.58
42. Leiss, M., Beckmann, K., Girós, A., Costell, M., and Fässler, R. (2008) *Curr. Opin. Cell. Biol.* **20,** 502-507
43. Goldring, M.B., and Goldring, S.R. (2007) J. Cell. Physiol. **213,** 626-634
44. Shahrara, S., Castro-Rueda, H.P., Haines, G.K., and Koch, A.E. (2007) *Arthritis Res. Ther.* **9,** R112
45. Chen, H.C., and Guan, J.L. (1994) *Proc. Natl. Acad. Sci .U S A* **91,** 10148-10152

FOOTNOTES

The authors thank Zsuzsanna Farkas, Jannine Wagner and Hildegard Reiter for the excellent technical assistance. This study was supported by the Max Planck Society to AR and AA and the Swiss National Science Foundation to EBH.

The abbreviations used are: AC, articular cartilage; ECM, extracellular matrix; PG, proteoglycan; GAG, glycosaminoglycan; OA, osteoarthritis; MMP, matrix metalloproteinase; ADAMTS, a disintegrin and metalloproteinase with thrombospondin-like repeat; FN, fibronectin; FN-f, fibronectin fragment; MAPK, mitogen activated protein kinase, ERK, extracellular signal regulated kinase; JNK, c-Jun N-terminal kinase; HE, hematoxylin and eosin; SO, safranin orange; PM, pericellular matrix; ITM, interterritorial matrix; PCNA, proliferating cell nuclear antigen; TUNEL, terminal deoxynucleotidyl transferase mediated dUTP nick end labeling; IHC, immunohistochemistry; PFA, paraformaldehyde; PBS, phosphate buffered saline; FAK, focal adhesion kinase.

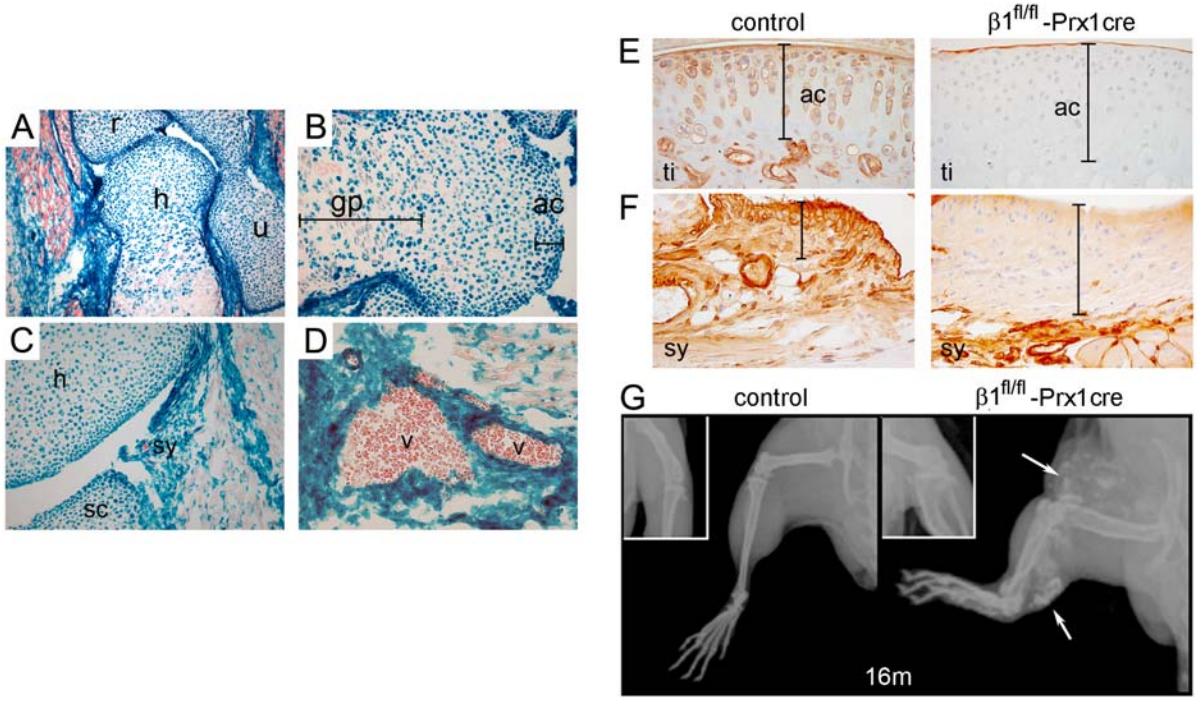

Figure 1. Deletion of the *β1 integrin* gene in mice using the *Prx1-cre* transgenic line. *A,* X-gal staining of a forelimb section from $\beta 1^{fl/fl}$-*Prx1cre*$^{+}$ E18.5 embryo shows cre activity in cartilaginous and bony tissues of the elbow and in muscle fibroblasts (h, humerus; r, radius; u, ulna). *B,* Distal epiphysis of the humerus exhibits cre activity in all chondrocytes (blue) of the presumptive articular cartilage (ac), while in the growth plate (gp) some chondrocytes (red) are negative. *C* and *D*, X-gal staining demonstrates cre activity in the forming synovium (sy, *C*) and in the vessels (v, *D*). *E* and *F*, β1 integrin immunostaining at 1 month of age demonstrates the absence of β1 integrin on articular cartilage chondrocytes of mutant tibia (ti, *E*) and on synoviocytes of the synovium (sy, *F*). The bars on *F* indicate the intimal/subintimal layers of the synovium. *G,* X-ray of the hindlimb at 16 months indicates short bones, joint space narrowing and blood vessel calcification (arrows) in mutants.

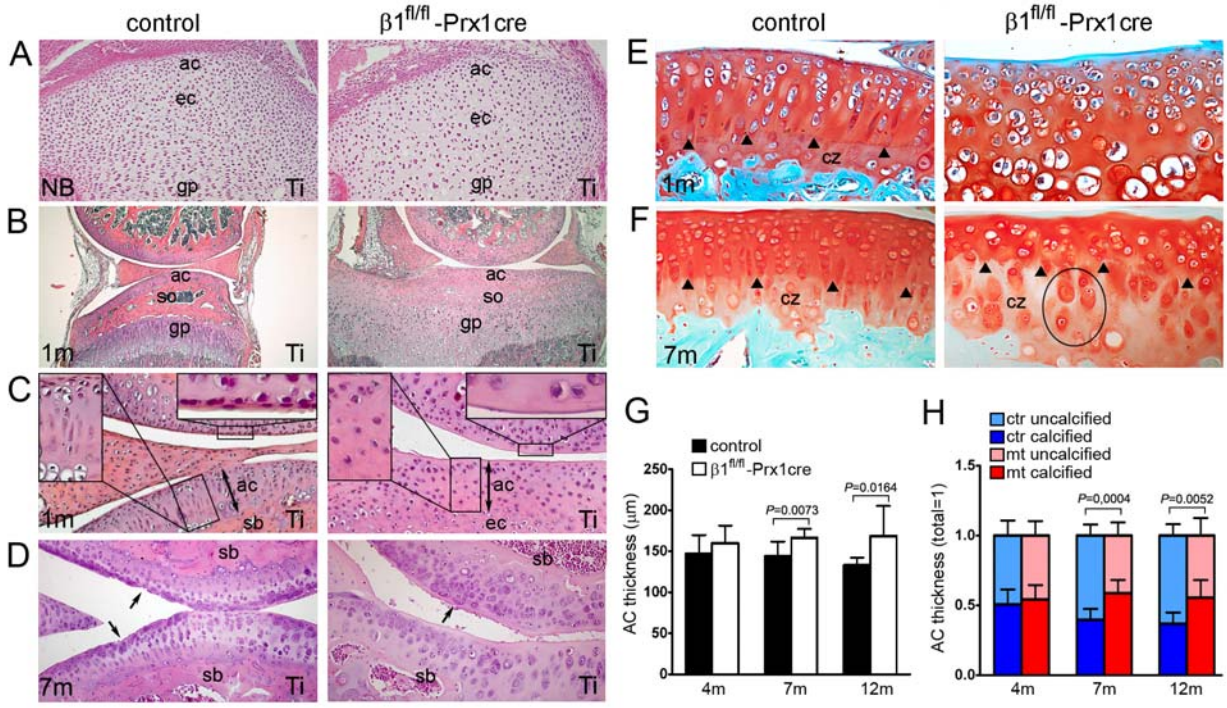

Figure 2. Comparison of the articular cartilage from the knee joints of control and *β1$^{fl/fl}$-Prx1cre^{+}* mice. *A-D*, Photomicrographs of hematoxylin-eosin-stained sections (Ti, tibia). *A,* In newborn (NB), both control and mutant articular cartilage (ac) chondrocytes are rounded and exhibit isotropic distribution pattern (ec, epiphyseal cartilage; gp, growth plate). *B,* At 1 month (1m), *β1$^{fl/fl}$-Prx1cre^{+}* joints show a delay in the formation of the secondary ossification centre (so) and display flat tibial surface. *C,* Closer view from (*B*) indicates fewer chondrocytes, a broad, cell-free superficial layer (upper-right inset) and the lack of column-like structures (upper-left inset) in mutant AC. Subchondral bone (sb) does not form in the mutant tibia at this age. *D,* Micrographs demonstrate surface irregularities (arrows) of control and mutant articular cartilage at 7 months of age. Chondrocyte columns are missing and less subchondral bone forms in mutants. *E* and *F*, Photomicrographs of Safranin orange-Fast green-stained sections through the medial tibial plateau. At 1 month (*E*), chondrocyte clustering, structural disorganization and the lack of tidemark are characteristic for the mutant articular cartilage. In control, the tidemark (arrowheads) separates the calcified zone (cz) from the upper uncalcified region. At 7 months (*F*), the mutant articular cartilage is thicker with expanded calcified and reduced uncalcified zones. Note the enlarged pericellular matrix staining around mutant chondrocytes (ellipses) in the calcified zone. *G,* Quantification of the articular cartilage (AC) thickness. *H*, Quantification of the ratio of uncalcified and calcified zones. The total AC thicknesses were set as 1.

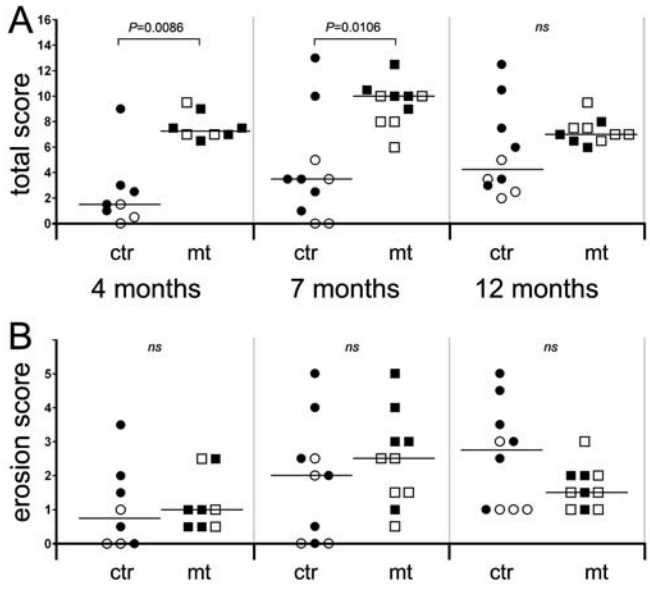

Figure 3. Quantification of the histopathological changes of the knee. *A,* Total score indicates increased severity of joint histopathology in mutants at 4 and 7 months of age. By 12 months, the difference between controls and mutants are not significant (ns). Open symbols denote female mice and filled symbols denote male mice. *B,* Quantification of cartilage erosion reveals no significant difference in articular cartilage destruction between controls and mutants.

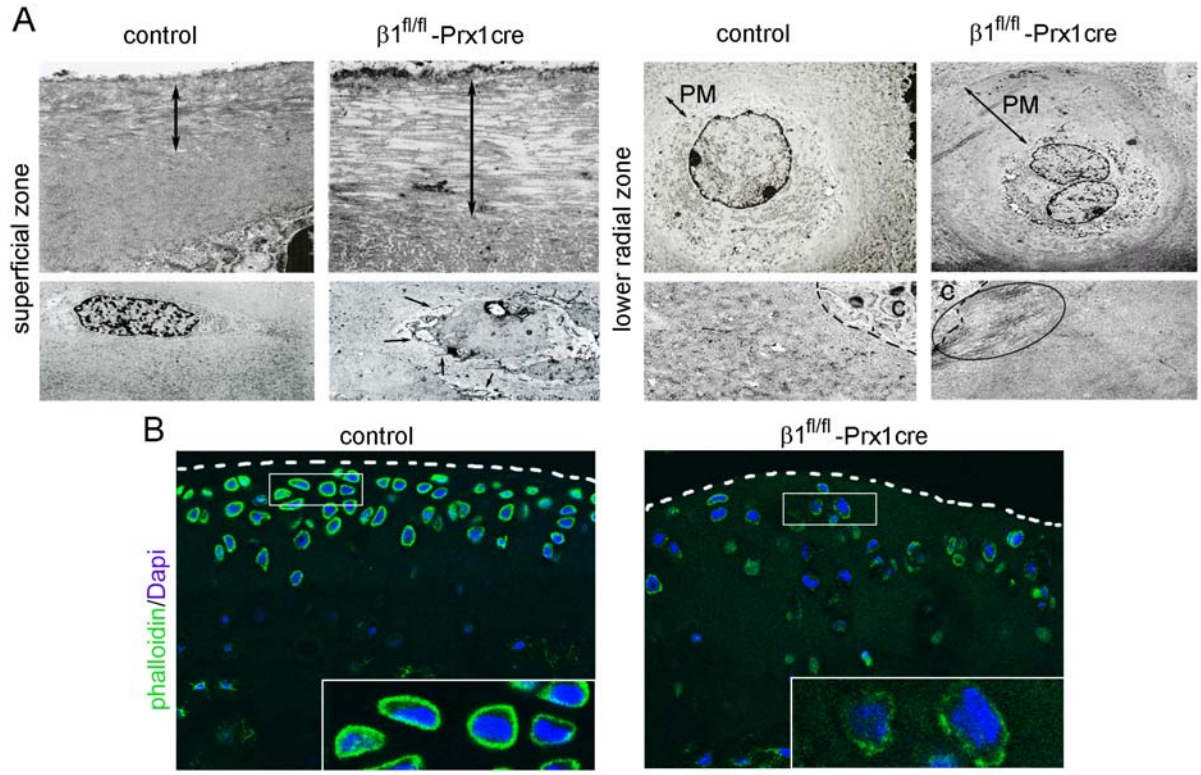

Figure 4. Electron and confocal microscopy of articular cartilage from control and *β1$^{fl/fl}$-Prx1cre^{+}* mice. *A,* Representative electron micrographs of the cartilage surface (superficial zone) reveal additional disorganized layers of collagen fibrils (double arrow) in the mutant sample. The superficial chondrocytes are more rounded and extend long microvilli into the matrix (arrows). In the lower radial zone, the mutant cartilage displays frequent binucleation, an enlarged pericellular matrix compartment (PM) and large collagen bundles near the chondrocyte surface (ellipse). *B,* Confocal micrographs of sections stained for phalloidin (to visualize actin, green) and DAPI (to visualize nuclei, blue) from tibial plateau of 11-month-old mice demonstrate a reduced and irregular cortical actin network in *β1$^{fl/fl}$-Prx1cre^{+}* chondrocytes. The dashed lines demarcate the surface of the articular cartilage. The insets show magnified images of control and mutant chondrocytes.

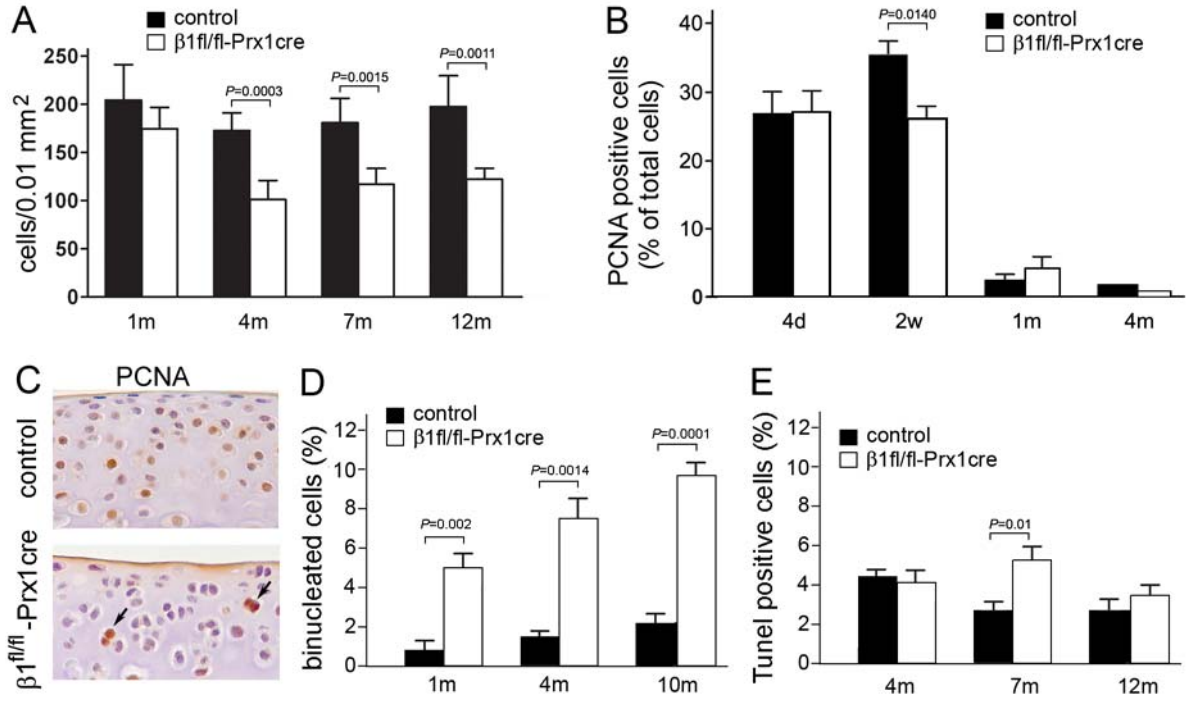

Figure 5. Chondrocyte cellularity, proliferation and survival in control and *β1$^{fl/fl}$-Prx1cre^{+}* articular cartilage. *A,* Quantification of cell density at the tibial plateau demonstrates fewer chondrocytes per unit area in mutant than in control. *B,* Percentage of PCNA-positive cells. Note the moderatly reduced proliferation rate in mutant at 2 weeks of age. *C,* PCNA immunostaining reveals the depletion of proliferative chondrocytes close to the articular surface compared with controls. Arrows indicate binucleated, PCNA-positive mutant chondrocytes in deeper regions of the articular cartilage. *D,* Diagram showing the percentage of binucleated chondrocytes in control and mutant articular cartilage. *E,* Percentage of apoptotic chondrocytes throughout the uncalcified articular cartilage.

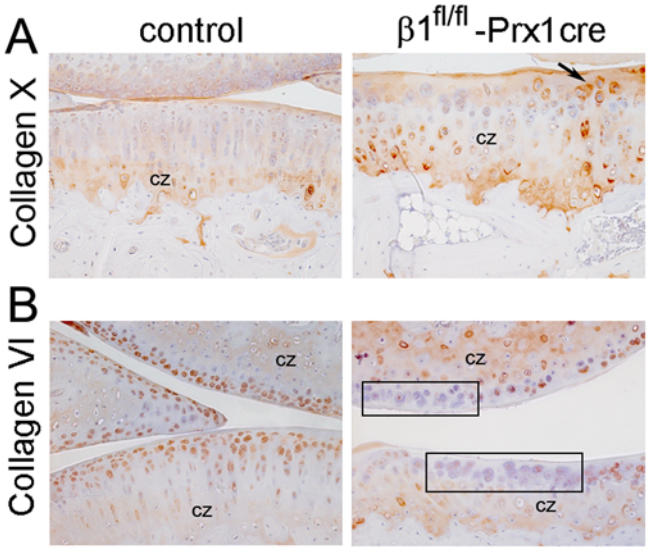

Figure 6. Abnormal deposition of collagens X and VI in the mutant articular cartilage. *A,* At 7 months, collagen X, a marker of the calcified zone (cz), appears closer to the cell surface in mutant compared with control. The arrow indicates mutant cells in the uncalcified zone depositing collagen X into the matrix. *B,* Collagen VI is abundant in the pericellular matrix of control chondrocytes in the uncalcified zone. However, areas (boxes) with mutant chondrocytes in the uncalcified zone are devoid of immunoreactivity.

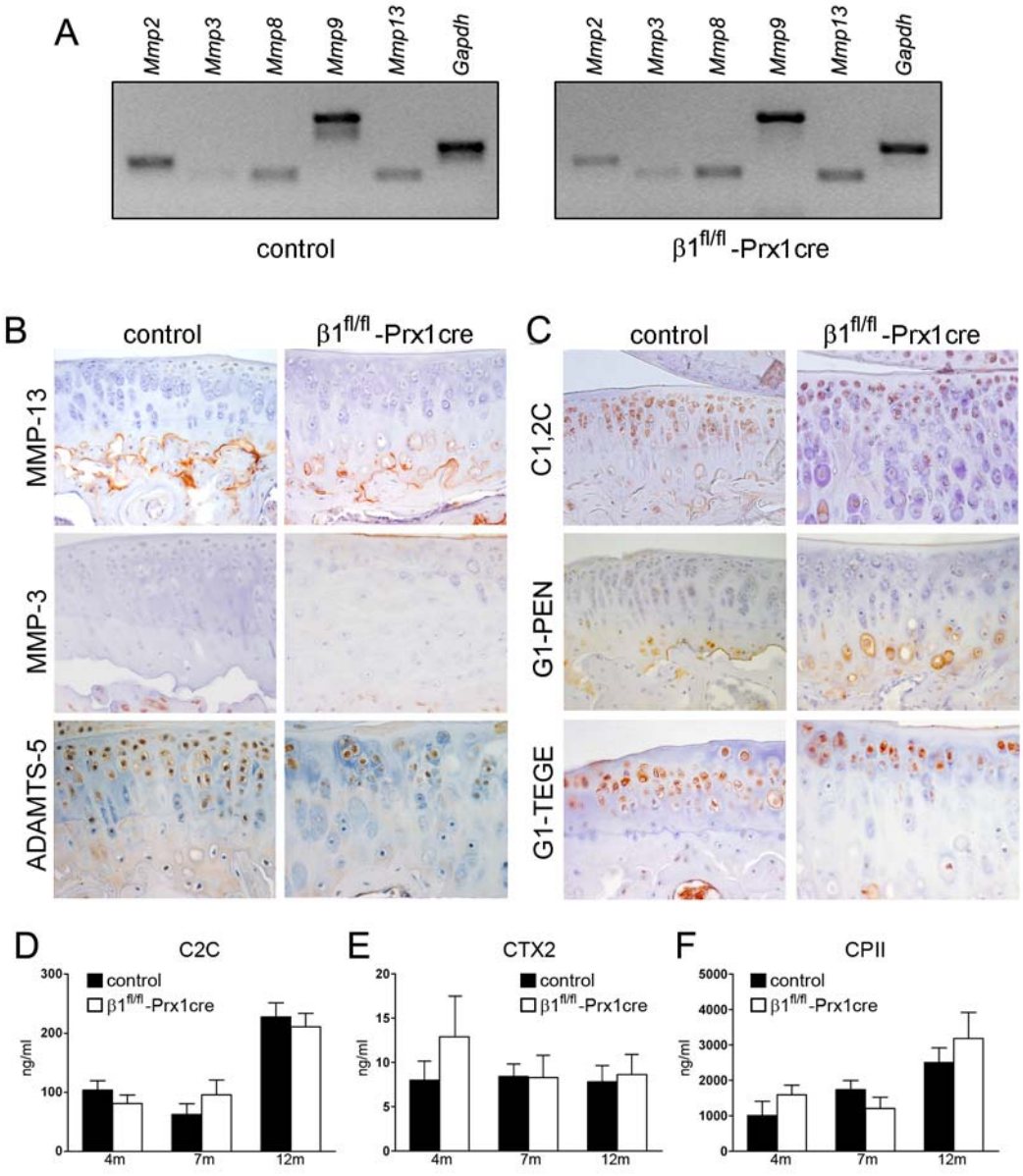

Figure 7. Characterization of articular cartilage metabolism. *A,* Representative RT-PCR analysis at 4 months of age indicates that the levels of MMP mRNAs are comparable in control and mutant articular cartilage samples. *B,* Immunohistochemistry at 7 months reveals no changes in the deposition of MMP-13, MMP-3 and ADAMTS-5 in mutants compared with controls. *C,* Immunohistochemistry at 7 months demonstrates that the degradation neoepitopes for collagen II (C1,2C) and aggrecan (G1-IPEN^{341} and G1-TEGE^{373}) are exposed similarly in mutant and control. *D-F***,** At 7 months, comparable levels of collagen degradation (C2C, CTX-II) and synthesis (CPII) products were found in body fluids of control and *β1$^{fl/fl}$-Prx1cre^{+}* mice.

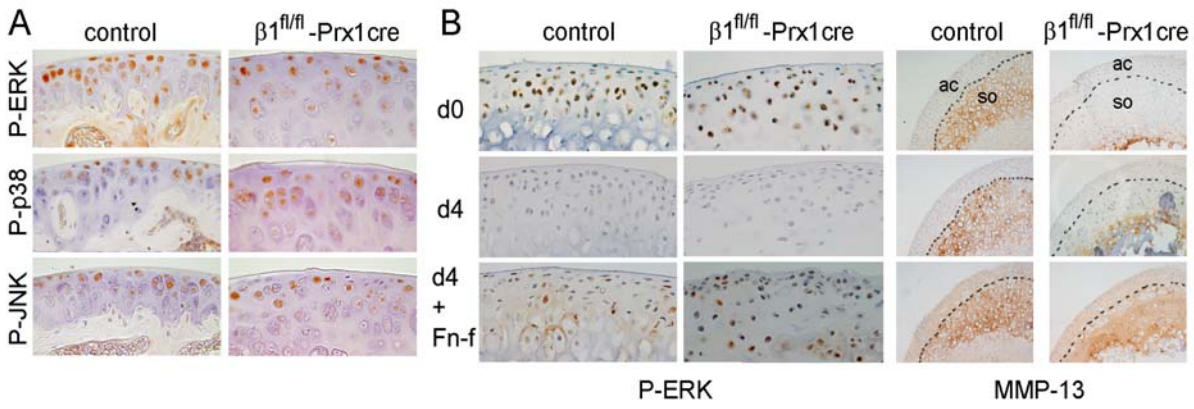

Figure 8. Normal activation of MAP kinases in the mutant articular cartilage . *A*, Immunostaining for phospho-ERK1/2 (P-ERK), phospho-p38 (P-p38) and phospho-JNK (P-JNK) shows no detectable difference in the activation of MAP kinases in control and mutant femoral head chondrocytes at 1 month of age. *B,* Fn-f stimulation of ERK activation and MMP-13 expression in femoral head explant culture. At day 0 (d0), ERK is phosphorylated in many control and mutant chondrocytes. MMP-13 staining is visible only in the centre of secondary ossification (so) but not in the articular cartilage (ac) of control samples. Due to the delay of terminal hypertrophic chondrocyte differentiation, mutant explants show only restricted MMP-13 deposition in the area of secondary ossification. At day 4 (d4), both control and $\beta 1^{fl/fl}$-*Prx1cre*$^{+}$ samples treated with Fn-f show ERK reactivation and MMP-13 expression in the articular cartilage.

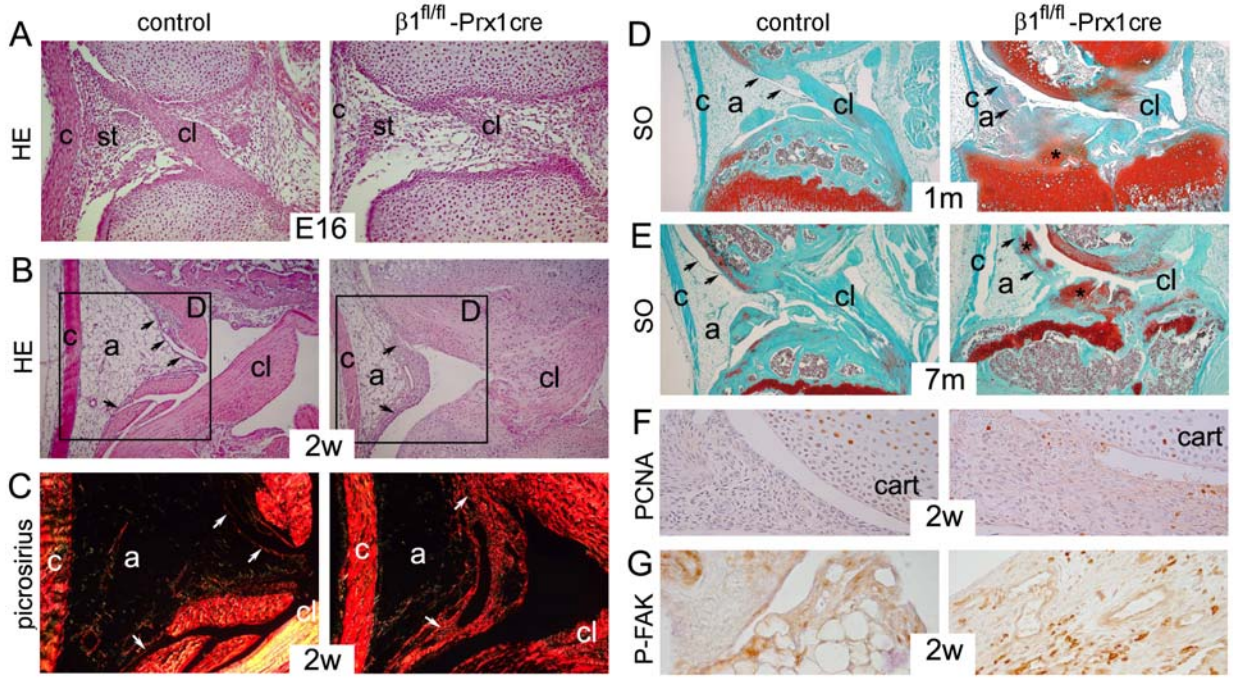

Figure 9. Synovial abnormalities in *β1$^{fl/fl}$-Prx1cre^{+}* mice. *A* and *B*, Photomicrographs of hematoxylin-eosin-stained (HE) mid-sagittal sections of the knee joints. *A,* Looser appearance of the developing synovial tissue (st) and the delayed formation of the cruciate ligament (cl) were observed in 16-day-old mutant embryo (E16). Also note the thinner collateral ligament (c) in mutant. *B,* At 2 weeks (2w), the control synovium consists of a thin lining layer (arrows) and a large adipose (a) tissue. In mutant, the lining is hyperplastic with large vessels and the amount of adipose tissue is reduced. *C,* Picrosirius staining followed by polarization microscopy of the boxed areas in (*B*) reveals fibrosis of the mutant synovium as shown by the strongly birefringent collagen deposits (white arrows). *D* and *E*, Photomicrographs of Safranin orange-Fast green (SO)-stained sections. *D*, At 1 month, the intercondylar tibial surface is cartilaginous in the mutant and covered by the synovial tissue showing sign of chondrification (asterisk). *E*, By 7 months, extensive chondrification (asterisks) is observed in the joint space and in the synovial lining (arrows) of mutant. *F,* Increased numbers of PCNA-positive synovial cells are visible in the mutant. *G*, Increased phosphorylation of FAK was evident in fibroblast-like cells of the mutant synovium.

PAPER IV

nature nanotechnology

ARTICLES

PUBLISHED ONLINE: 1 FEBRUARY 2009 | DOI: 10.1038/NNANO.2008.410

Early detection of aging cartilage and osteoarthritis in mice and patient samples using atomic force microscopy

Martin Stolz[1]*, Riccardo Gottardi[2], Roberto Raiteri[2], Sylvie Miot[3], Ivan Martin[3], Raphaël Imer[4], Urs Staufer[4,5], Aurelia Raducanu[6], Marcel Düggelin[7], Werner Baschong[1,8], A. U. Daniels[9], Niklaus F. Friederich[10], Attila Aszodi[6] and Ueli Aebi[1]

The pathological changes in osteoarthritis—a degenerative joint disease prevalent among older people—start at the molecular scale and spread to the higher levels of the architecture of articular cartilage to cause progressive and irreversible structural and functional damage. At present, there are no treatments to cure or attenuate the degradation of cartilage. Early detection and the ability to monitor the progression of osteoarthritis are therefore important for developing effective therapies. Here, we show that indentation-type atomic force microscopy can monitor age-related morphological and biomechanical changes in the hips of normal and osteoarthritic mice. Early damage in the cartilage of osteoarthritic patients undergoing hip or knee replacements could similarly be detected using this method. Changes due to aging and osteoarthritis are clearly depicted at the nanometre scale well before morphological changes can be observed using current diagnostic methods. Indentation-type atomic force microscopy may potentially be developed into a minimally invasive arthroscopic tool to diagnose the early onset of osteoarthritis *in situ*.

Articular cartilage is a highly specialized load-bearing tissue that provides low-friction, wear-resistant diarthrodial joint surfaces. The physiological functions of articular cartilage depend on the precise interplay of the molecules that compose its extracellular matrix. Proteoglycans embedded in a meshwork of heterotypic types II/IX/XI collagen fibrils are the two principal supramolecular matrix components that are responsible for the unique biomechanical properties of articular cartilage. The meshwork of collagen fibrils provides tensile strength to the tissue. Aggrecan, the major proteoglycan in cartilage, has a high density of fixed negative charges owing to its anionic glycosaminoglycan side chains. This in turn draws water into the tissue and generates an osmotic swelling pressure that is counteracted by the tense collagen meshwork. Thus, collagens and proteoglycans create a hydrated tissue that resists compressive loads. Age-related changes in the composition and/or structure of the proteoglycans and collagens affect the mechanical quality of the articular cartilage and may lead to osteoarthritic degradation. Although the aetiology of osteoarthritis is largely unknown, its onset is characterized by the imbalance between catabolic and anabolic processes, favouring matrix degradation. This degradation process starts with proteoglycan depletion followed by degradation of collagen II, which, in turn, causes mechanical failure and ultimately complete erosion of the articular cartilage. Hence, any method to diagnose the onset of osteoarthritis must detect the early changes in the articular cartilage's proteoglycan gel before significant changes in its collagen matrix occur[1,2].

Diagnosis of osteoarthritis generally relies on radiography or arthroscopic evaluation of the joint surface, which only detect macroscopic damage to the articular cartilage. Magnetic resonance imaging (MRI) has been proposed as a promising non-invasive method for early detection of osteoarthritis[3–5]. Unfortunately, the underlying physical effect is too weak to detect changes at molecular resolution[6]. In addition, the different orientations of collagen fibrils in distinct cartilage zones, as well as the heterogeneous distribution of the chondrocytes within the articular cartilage exclude MRI from providing bulk precision measurements that could be compared to a normal reference[7]. Osteoarthritis-specific biomarkers in body fluids would allow assessment of the disease[8,9], but their levels can significantly vary owing to physical activity or food consumption, so the interpretation of results often leads to incorrect conclusions. Invasive millimetre-scale methods assess mechanical properties *in situ* using ultrasound and micro-mechanical devices, but they lack the sensitivity and resolution to detect changes of stiffness at the early stage of osteoarthritis[10]. Similarly, a lack of sensitive tools also limits our understanding of the pathogenesis of the disease.

We have previously compared the capability of indentation-type atomic force microscopy (IT-AFM) to image the surface of porcine articular cartilage and measure its compressive stiffness at the micrometre and nanometre scales[11]. We found that only nanometre-sized tips resolved the fine structural details such as individual collagen fibrils, in both imaging and indentation mode. Importantly, enzymatic digestion of cartilage proteoglycans had little effect on the microstiffness, but yielded clear stiffening at the

[1]M.E. Müller Institute for Structural Biology, Biozentrum University of Basel, Switzerland, [2]Department of Biophysical and Electronic Engineering, University of Genoa, Italy, [3]Departments of Surgery and of Biomedicine, University Hospital Basel, Switzerland, [4]Institute of Microtechnology, University of Neuchâtel, Switzerland, [5]Micro and Nano Engineering Lab, TU Delft, Netherland, [6]Max Planck Institute of Biochemistry, Martinsried, Germany, [7]Center for Microscopy, University of Basel, Switzerland, [8]Department of Oral Surgery, Oral Radiology and Oral Medicine, University of Basel, Switzerland, [9]Laboratory for Orthopaedic Biomechanics, University of Basel Faculty of Medicine, Basel, Switzerland, [10]Department of Orthopaedic Surgery and Traumatology, Kantonsspital Bruderholz/Basel, Switzerland; *e-mail: martin.stolz@unibas.ch

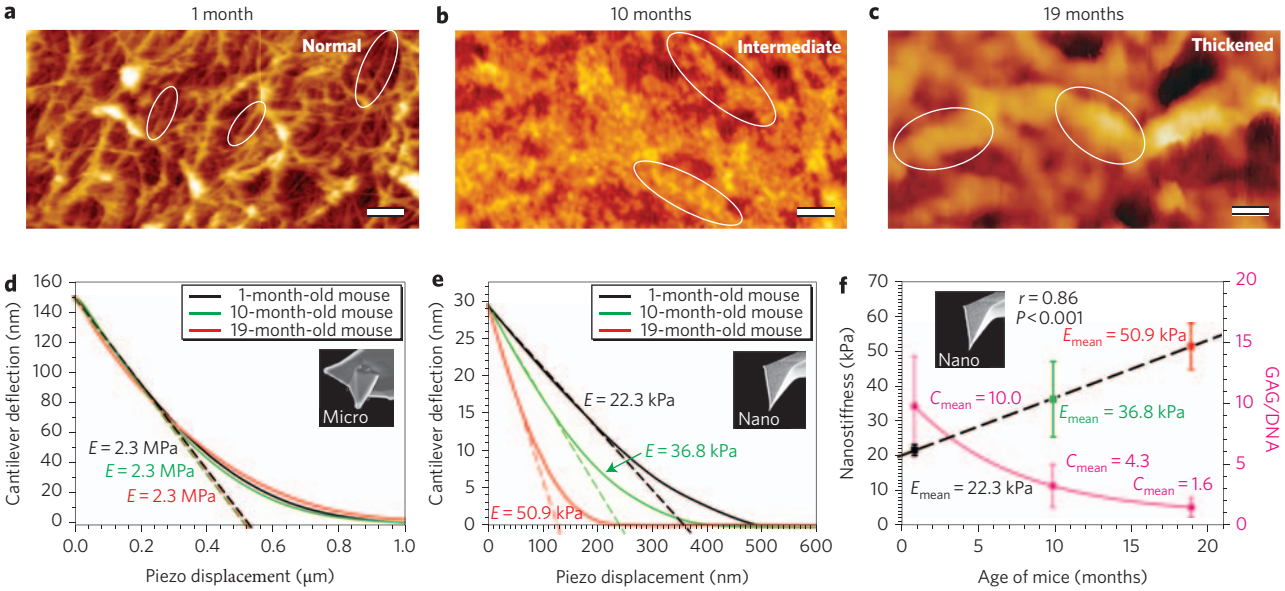

Figure 1 | Surface imaging and indentation tests for articular cartilage of normal mice at various ages. a–c, AFM surface topography of articular cartilage imaged in buffer solution (scale bars, 1 μm). Nanometre-sized AFM tips resolved the individual collagen fibrils. Collagen fibrils of older mice appear thicker (circles). Micrometre (**d**) and nanometre (**e**,**f**) scale AFM indentation tests of articular cartilage from aging C57BL/6 mice ($n = 15$ per group). **d**,**e**, Average unloading curves for the different mice ages; for a qualitative comparison of the different curves the linear fit of the upper 50% of the curve was also plotted. Microstiffness values (**d**) were not affected by age: $E_{micro} = 2.3 \pm 0.4$ MPa (1 month), $E_{micro} = 2.3 \pm 0.4$ MPa (10 months) and $E_{micro} = 2.3 \pm 0.4$ MPa (19 months). **f**, Nanostiffness increases on average from $E_{nano} = 22.3 \pm 1.5$ kPa (1 month; black), to $E_{nano} = 36.8 \pm 10.7$ kPa (10 months; green), to $E_{nano} = 50.9 \pm 4.7$ kPa (19 months; red). The linear fit (dashed line) shows increased nanostiffness with age. The pink curve reveals the concomitant loss of glycosaminoglycans measured by biochemical analysis. A positive correlation ($r = 0.86$) between nanostiffness and age of mice was detected ($P < 0.001$).

nanometre scale. Based on these observations we hypothesized that nanoscale IT-AFM may be used to monitor subtle structural and mechanical changes of articular cartilage that occur during aging and at the onset of osteoarthritis[11].

Articular cartilage of normal mice changes with age

For validation of the IT-AFM method in a biologically relevant model system, in this study we first recorded age-dependent morphological and biomechanical alterations of the articular cartilage surface in the femoral heads of C57BL/6 mice at 1, 10 and 19 months of age. In all experimental groups the articular cartilage surface was apparently smooth and intact on histological sections (see Supplementary Information, Fig. S1). Scanning electron microscopy (SEM) following enzymatic digestion of proteoglycans (see Methods) revealed an indistinguishable collagen fibril meshwork to a depth of ~0.25 μm with fibril diameters of $d_{1\ month} = 30.5 \pm 3.6$ nm, $d_{10\ months} = 31.5 \pm 4.8$ nm and $d_{19\ months} = 30.1 \pm 3.8$ nm in all age groups. In contrast, AFM imaging of the native articular cartilage surface in near-physiological buffer revealed an age-dependent thickening of the collagen fibrils (Fig. 1a–c), sometimes with grain-like structures decorating the fibrils (Fig. 1b). The apparent diameter of the fibrils increased from $d_{1\ month} = 52 \pm 5$ nm, to $d_{10\ months} = 170 \pm 64$ nm, to $d_{19\ months} = 812 \pm 172$ nm ($n = 15$ fibrils each). This phenomenon may be caused by the deposition of short proteoglycan fragments onto the collagen fibrils, and/or by fibril bundling as a consequence of the reduced interfibrillar glycosaminoglycan content. Because SEM revealed neither thickened nor bundled collagen fibrils, it is conceivable that the exhaustive enzymatic treatment during SEM sample preparation removed the proteoglycans from the bundled collagen fibrils, thereby allowing their dissociation. Taken together, AFM imaging by nanometre-sized tips of normal mouse articular cartilage demonstrates an age-dependent thickening of the collagen fibrils, which most likely represents a physiological rather than a pathological process.

Next, we measured the stiffness (dynamic elastic modulus, E) of aging articular cartilage by IT-AFM at both the micrometre and nanometre scales. Whereas the microstiffness did not change with age and remained at 2.3 ± 0.4 MPa (Fig. 1d), the corresponding nanostiffness was two orders of magnitude lower compared to the microstiffness (Fig. 1e,f). Most importantly, the nanostiffness increased with age from $E_{nano} = 22.3 \pm 1.5$ kPa (at 1 month), to $E_{nano} = 36.8 \pm 10.7$ kPa (at 10 months), to $E_{nano} = 50.9 \pm 4.7$ kPa (at 19 months) (Fig. 1f). To examine whether the observed age-dependent stiffening of the mouse articular cartilage correlates with its glycosaminoglycan content, the glycosaminoglycan/DNA ratio of the samples was determined after mechanical testing. We found that the glycosaminoglycan/DNA ratio decreased with age from $C_{1\ month} = 10.0 \pm 4.1$ ($n = 24$), to $C_{10\ month} = 4.3 \pm 3.6$ ($n = 13$), to $C_{19\ month} = 1.6 \pm 0.6$ ($n = 29$) (Fig. 1f). Taken together, our data document an age-dependent increase of the articular cartilage's nanostiffness with a concomitant decrease in its glycosaminoglycan/DNA ratio.

Monitoring osteoarthritis and aging in knockout mice

Mice deficient in type IX collagen ($Col9a1^{-/-}$) develop osteoarthritis-like changes in their knee joints that begin with chondrocyte clustering at 3 months, followed by proteoglycan depletion and collagen II degradation at 6 months, and severe articular cartilage destruction at 9–12 months[12,13]. The pathomechanism in $Col9a1^{-/-}$ knockout mice is characterized by the activation and enhanced expression of the collagen-binding membrane protein discoidin domain receptor 2 (DDR2), which upregulates the expression of matrix metalloproteinase-13 (MMP-13), leading to an increased production of collagen II degradation fragments[12]. To test the efficacy of IT-AFM to monitor the progression of osteoarthritis in this animal model, articular cartilage from femoral heads of $Col9a1^{-/-}$ knockout mice were analysed at various ages. Although the histology revealed no obvious changes of $Col9a1^{-/-}$ articular cartilage at 1 month, it yielded a higher

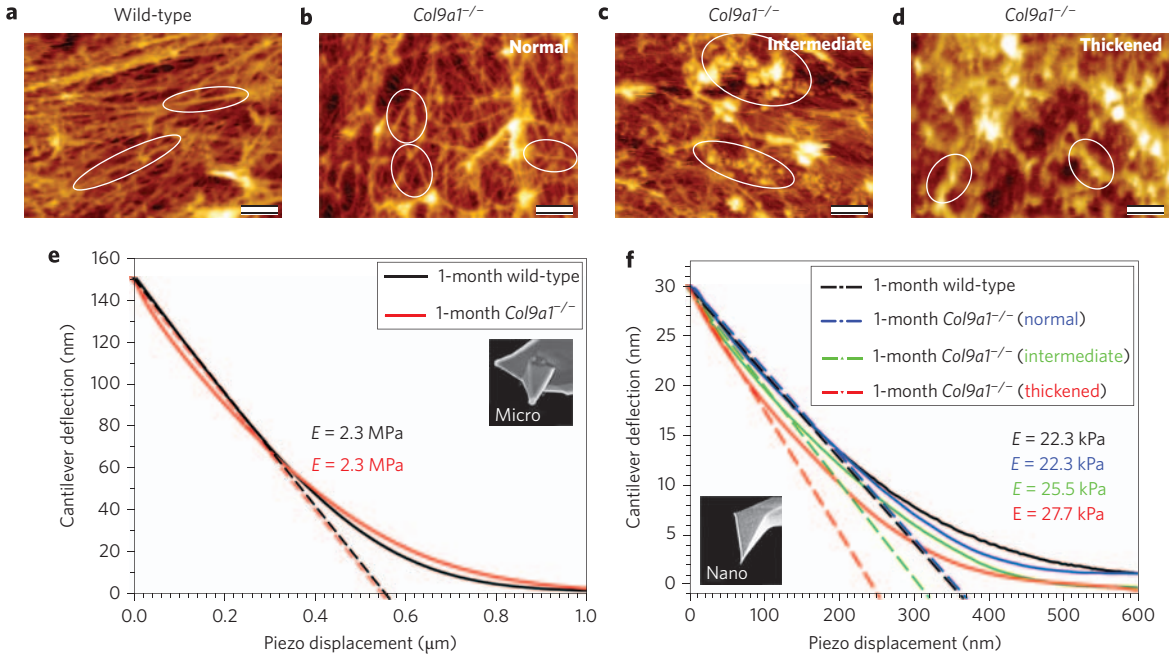

Figure 2 | Surface imaging and indentation tests for articular cartilage of wild-type control and *Col9a1*$^{-/-}$ knockout mice at 1 month of age. a–d, AFM surface topography of the articular cartilage (scale bars, 1 μm). Circles indicate individual collagen fibrils with different thicknesses. Wild-type controls (**a**) and 4 of 7 *Col9a1*$^{-/-}$ knockout mice (**b**) showed no structural differences in the collagen meshwork (normal). One *Col9a1*$^{-/-}$ articular cartilage (**c**) showed the onset of protein deposition along the fibrils (intermediate). Two *Col9a1*$^{-/-}$ knockout mice (**d**) exhibited a clear thickening of collagen fibrils (thickened). **e**, Microstiffness was indistinguishable in wild-type and *Col9a1*$^{-/-}$ knockout mice. **f**, Nanostiffness of control and *Col9a1*$^{-/-}$ knockout articular cartilages ($n = 7$). Wild-type and *Col9a1*$^{-/-}$ knockout mice with normal collagen fibril thickness showed identical nanostiffness ($E_{nano} = 22.3 \pm 1.5$ kPa). In contrast, knockout mice with intermediate and thickened collagen fibrils exhibited increased nanostiffness of $E_{nano} = 25.5 \pm 1.1$ kPa and $E_{nano} = 27.7 \pm 1.1$ kPa, respectively.

chondrocyte density at 3 months, and a roughening of the articular cartilage surface at 6 and 12 months compared to the articular cartilage of wild-type control mice (see Supplementary Information, Fig. S2a–d). SEM of proteoglycan extracted articular cartilage (see Methods) revealed an intact, regular collagen fibril meshwork in 6- and 12-month-old control and in 6-month-old knockout mice (see Supplementary Information, Fig. S2e,f). In contrast, 12-month-old *Col9a1*$^{-/-}$ articular cartilage after the same treatment for SEM inspection exhibited severe disruption of the collagen fibril meshwork together with bundling and tangling of the fibrils (see Supplementary Information, Fig. S2f). The collagen damage was accompanied by increased levels of DDR2, MMP-13 and collagen II degradation fragment staining at 12 months (see Supplementary Information, Fig. S2 g–l). These observations indicate that the femoral heads of the knockout mice develop an osteoarthritis-like phenotype by 6 months of age, with severe structural changes by 12 months.

AFM imaging of the AC surface of seven femoral heads obtained from 1-month-old *Col9a1*$^{-/-}$ knockout mice yielded four samples with a collagen fibril meshwork similar to wild-type controls (Fig. 2a,b), one with intermediate fibril thickening (Fig. 2c), and two with substantial fibril thickening (Fig. 2d). The average diameter of the fibrils varied from 'normal' ($d_{1month} = 52 \pm 8$ nm), to 'intermediate' ($d_{1month} = 73 \pm 25$ nm), to 'thickened' ($d_{1month} = 183 \pm 68$ nm) (Fig. 3a). As expected, fibril thickening correlated with an increase of the articular cartilage's nanostiffness from $E = 22.3 \pm 1.5$ kPa for wild-type and 'normal' knockout mice, to $E = 25.5 \pm 1.1$ kPa for 'intermediate', and $E = 27.7 \pm 1.1$ kPa for 'thickened' knockout mice (Figs 2f and 3c), whereas the corresponding microstiffnesses appeared unchanged (Fig. 2e). These findings suggest that early osteoarthritis-like changes in the femoral articular cartilage of knockout mice, while only detectable at the nanometre scale, may begin as early as one month of age.

In contrast to SEM imaging of the collagen meshwork (in which proteoglycans have been extracted) of aging and osteoarthritis (Fig. 4a–d; see also Supplementary Information, Fig. S2e,f), AFM imaging of native articular cartilage revealed an age-dependent increase of the average fibril thickness in both wild-type control and *Col9a1*$^{-/-}$ knockout 3-month-old mice (Fig. 3a). Accordingly, fibrils of wild-type mice exhibited an average diameter of $d_{3\,months} = 53 \pm 7$ nm, $d_{6\,months} = 61 \pm 7$ nm and $d_{12\,months} = 292 \pm 122$ nm, whereas fibrils of knockout mice had an average diameter of $d_{3\,months} = 616 \pm 190$ nm, $d_{6\,months} = 665 \pm 197$ nm and $d_{12\,months} = 989 \pm 231$ nm (Fig. 3a), indicating a pronounced and drastically accelerated fibril thickening in the *Col9a1*$^{-/-}$ mice compared to wild-type mice. As we could not detect a significant difference in the glycosaminoglycan/DNA ratio between age-matched wild-type and knockout samples (data not shown), the underlying molecular mechanism remains elusive. It is conceivable that the lack of collagen IX, which is covalently bound to the collagen II fibril surface and mediates interactions between the collagen fibrils and other components of the extracellular matrix[14], may alter the molecular architecture and thus the mechanical properties (that is, the stiffness) of the articular cartilage. Indeed, aggregated and/or fused collagen fibrils have been reported in the tectorial membrane of the inner ear of *Col9a1*$^{-/-}$ mice[15].

Next, we assessed the stiffness of articular cartilage from 3-, 6- and 12-month-old wild-type and knockout mice. At 3 months, two of five knockout mice exhibited a nanostiffness identical to that of wild-type mice ($E_{nano} = 22.3 \pm 1.5$ kPa; Fig. 3c), whereas three knockout mice revealed an increased nanostiffness of $E_{nano} = 29.5 \pm 4.4$ kPa ($n = 5$) (Fig. 3c). At 6 months, the nanostiffness increased significantly to an average value of $E_{nano} = 38.9 \pm 3.4$ kPa in knockout mice ($n = 6$) compared to $E_{nano} = 23.5 \pm 1.9$ kPa in wild-type mice (Fig. 3c). Somewhat unexpectedly, by 12 months, the average nanostiffness of the wild-type mice increased to $E_{nano} = 41.1 \pm 2.9$ kPa

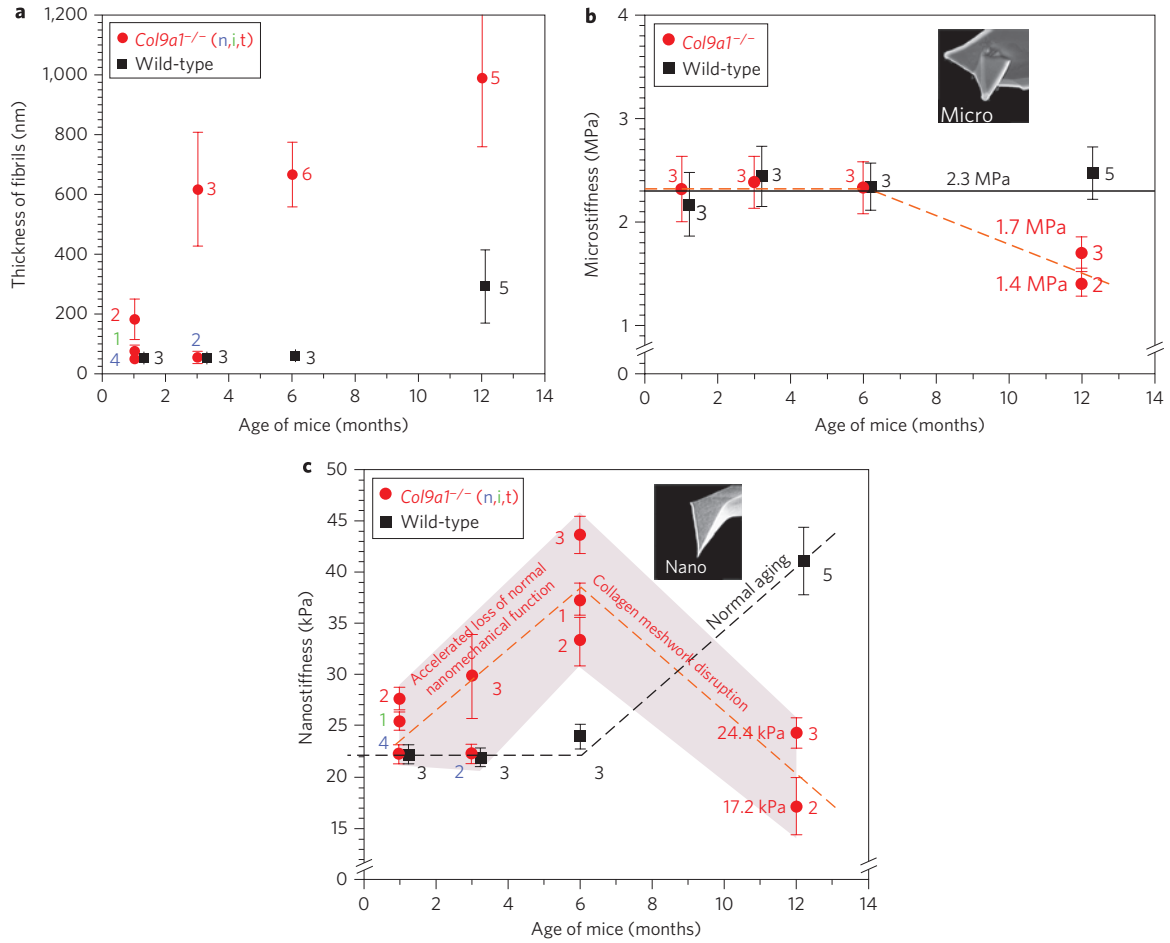

Figure 3 | Statistical analyses of articular cartilage properties assessed by AFM from wild-type control and *Col9a1*$^{-/-}$ knockout mice at various ages. **a**, Quantification of the fibril thickness. Arabic numerals denote the number of mice analysed; n, i and t refer to 'normal', 'intermediate' and 'thickened' groups as outlined in Fig. 2. At 1 month, compared to wild-type mice (52 ± 5 nm), the average fibril thickness in knockout mice were higher. Four of seven (blue number) showed a mean fibril thickness of 52 ± 8 nm, one (green number) mouse showed a thickness of 73 ± 25 nm and two (red number) knockout mice had 183 ± 68 nm. Similarly, at 3 months, knockout mice showed higher fibril thickness: two of five mice had a mean value of 56 ± 5 nm, whereas three had 616 ± 190 nm. At 6 months, the average fibril thickness increased from 61 ± 7 nm in the wild-type to 665 ± 197 nm in the knockout mice, and at 12 months, it increased from 292 ± 122 to 989 ± 231 nm. **b**, Quantifying microstiffness. In wild-type controls, microstiffness remained constant at $E_{micro} = 2.3 \pm 0.4$ MPa at all ages. In knockout mice, microstiffness was comparable to the wild-type until 6 months, and decreased at 12 months as follows: two of five mice had a mean value of $E_{micro} = 1.4 \pm 0.2$ MPa, and three had $E_{micro} = 1.7 \pm 0.4$ MPa. **c**, Quantifying nanostiffness. Average nanostiffness for the wild-type control mice remained constant up to 6 months ($E_{nano/3\ months} = 22.3 \pm 1.5$ kPa and $E_{nano/6\ months} = 23.5 \pm 1.9$ kPa) but increased to $E_{nano} = 41.1 \pm 2.9$ kPa at 12 months (normal aging). In young knockout mice, nanostiffness increased from an average of $E_{nano} = 25.2 \pm 2.3$ kPa (1 month; average calculated from four of seven mice (blue number) $E_{mean} = 22.3 \pm 1.5$ kPa, one mouse (green number) $E = 25.5 \pm 1.1$ kPa, two mice (red number) $E_{mean} = 27.7 \pm 1.1$ kPa) to $E_{nano} = 29.5 \pm 4.4$ kPa (3 months; average, two of five mice $E_{mean} = 22.3 \pm 1.5$ kPa, three mice $E_{mean} = 29.5 \pm 4.4$ kPa; compared to 22.2 ± 1.1 kPa for controls) and $E_{nano} = 38.9 \pm 3.4$ kPa (6 months; average: two of six mice $E_{mean} = 33.4 \pm 2.5$ kPa, one mouse $E = 37.3 \pm 1.7$ kPa, three mice $E_{mean} = 43.7 \pm 1.8$ kPa), suggesting the loss of normal biomechanical function of the articular cartilage. By 12 months, the average nanostiffness decreased to $E_{nano} = 20.8 \pm 3.4$ kPa due to disruption of the collagen meshwork (average: two of five mice $E_{mean} = 17.2 \pm 2.8$ kPa, three mice $E_{mean} = 24.4 \pm 2.8$ kPa).

(Fig. 3c), whereas the nanostiffness of the knockout mice ($n = 5$) decreased to an average value of $E_{nano} = 20.8 \pm 3.4$ kPa. The large differences of nanostiffness between knockout mice in each age group most likely reflect the time differences of disease onset in individual animals. In contrast to the nanostiffness, the microstiffness at 3 and 6 months did not change and remained at 2.3 ± 0.4 MPa for both the knockout and the wild-type mice (Fig. 3b). At 12 months, when the destruction of the collagen meshwork became visible by SEM (see Supplementary Information, Fig. S2f), microscale indentation also detected a softening of the knockout articular cartilage surface to an average value of $E_{micro} = 1.6 \pm 0.4$ MPa ($n = 5$) (Fig. 3b). Interestingly, the two 12-month-old knockout mice exhibiting the lowest microstiffness of $E_{micro} = 1.4 \pm 0.2$ MPa (Fig. 3b) also exhibited the lowest nanostiffness of $E_{nano} = 17.2 \pm 2.8$ kPa (Fig. 3c).

Taken together, collagen IX deficiency had no effect at the micrometre scale until 6 months of age, but at the nanometre scale significant structural (fibril thickness) and functional (nanostiffness) changes were induced upon progression from 1 to 12 months of age. Importantly, AFM imaging and nanometre-scale IT-AFM can monitor the early onset of osteoarthritis before histology, molecular markers and micrometre scale IT-AFM detect the disease.

Measuring cartilage stiffness of osteoarthritic patients

In order to establish IT-AFM for clinical practice, we examined articular cartilage biopsies obtained from seven osteoarthritis patients (Table 1; patients 1–7, age 62–96 years) undergoing total hip or knee replacement. The macroscopic changes of the samples were evaluated using the Outerbridge scale system[16,17], which

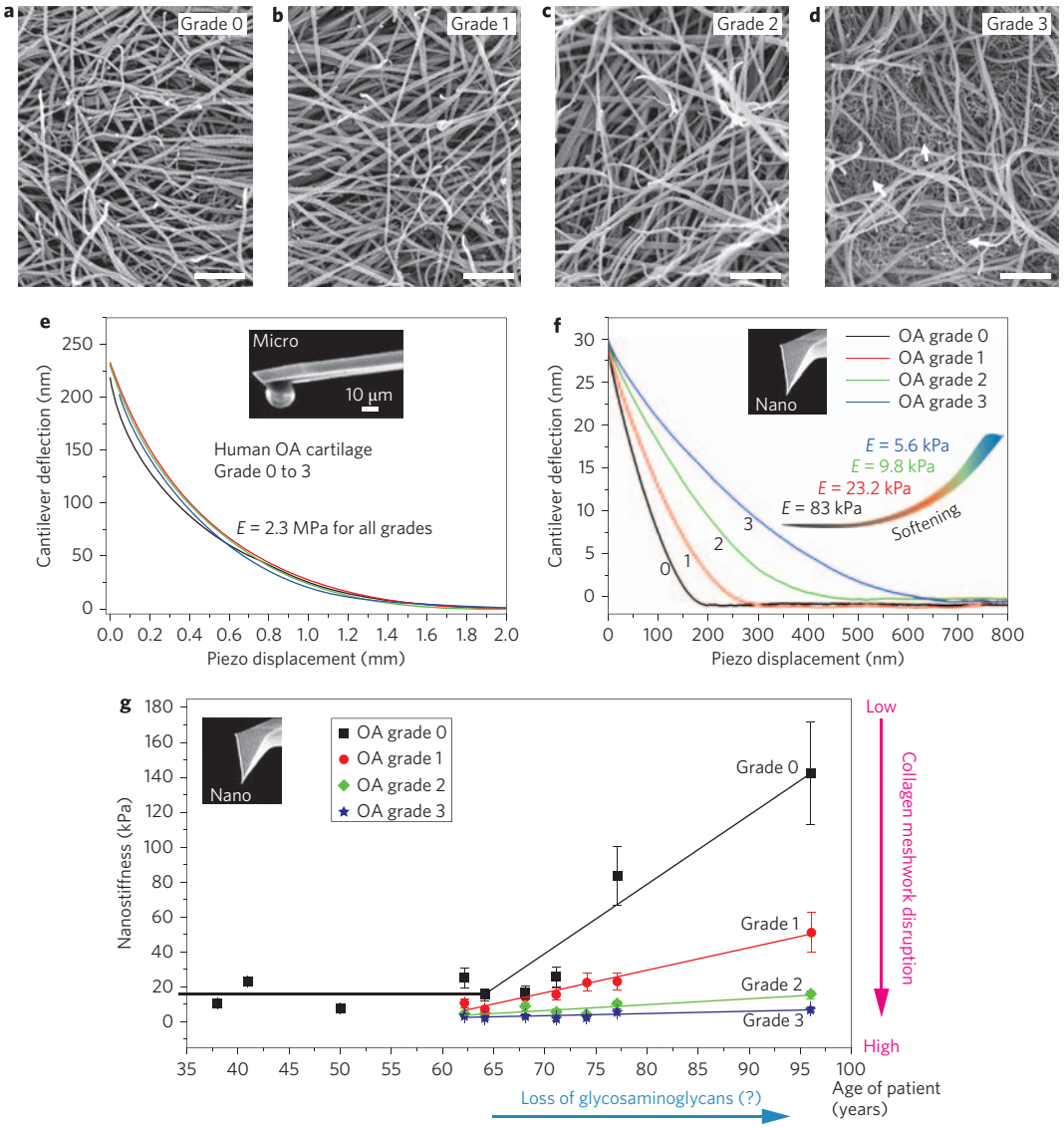

Figure 4 | Assessing osteoarthritis in human patients. a–d, SEM images of grade 0–3 articular cartilage surfaces obtained from a 77-year-old osteoarthritis (OA) patient. Grade 0 and 1 samples (**a**,**b**) exhibit no apparent changes in the collagen meshwork. Grade 2 (**c**) shows fibril tangles and disarrangement. Grade 3 (**d**) reveals disruption of the superficial collagen meshwork and extensive splitting of collagen fibrils into thinner fibrils (white arrows). Scale bars, 0.5 μm. **e**,**f**, Testing articular cartilage samples (grades 0–3) from the 77-year-old osteoarthritis patient. Microstiffness remained constant for all grades (**e**) and nanostiffness decreased with increasing grades (**f**). **g**, Nanostiffness of seven osteoarthritis patients (aged 62–96 years) and of three individuals without osteoarthritis (38, 41 and 50 years). Each of the four linear fits represents a particular Outerbridge grade. For all grades, nanostiffness increased with age and may be accompanied by reduced glycosaminoglycan content (horizontal arrow). As the slopes indicate, incremental reduction of stiffness by osteoarthritis as a function of age is greatest between grades 0 and 1 and decreases, with progression to grades 2 and 3 correlating with the increased tendency of collagen meshwork disruption (vertical arrow).

classifies articular cartilage degeneration into grades with increasing osteoarthritis severity. Grade 0 represents normal cartilage, grade 1 describes articular cartilage with softening and superficial lesions, grade 2 refers to partial-thickness defects with fissures down to $<$50% of the cartilage depth, grade 3 describes severe damage with fissuring reaching the subchondral bone, and grade 4 refers to fully exposed subchondral bone with no significant articular cartilage left. SEM imaging of articular cartilage obtained from a 77-year-old osteoarthritis patient (Table 1; patient 6) revealed a normal collagen meshwork organization in samples of grade 0 and 1 (Fig. 4a,b respectively), collagen fibril tangling in grade 2 (Fig. 4c), and extensive meshwork disintegration and fibril splitting in grade 3 samples (Fig. 4d). The micro- and nanostiffness of samples from the same 77-year-old osteoarthritis patient were then examined by IT-AFM. Microstiffness values were on the order of 2 MPa (Fig. 4e; $E_{\mathrm{micro}} = 2.3 \pm 0.3$ MPa) for all grades, in agreement with previously reported values obtained by conventional micrometre- and millimetre-size indenters[11]. In contrast, when the IT-AFM measurements of the same biopsies were performed at the nanometre scale, the corresponding nanostiffness values decreased from 83 kPa for grade 0 articular cartilage to 5.6 kPa for grade 3 osteoarthritis cartilage (Fig. 4f). In agreement with this finding, analyses of samples from other osteoarthritis patients confirmed the increasing softening of articular cartilage with progressing osteoarthritis at a given age (Table 1 and Fig. 4g). Most significantly, in all seven patients, changes occurring in grades 1 and 2 osteoarthritis cartilage could only be detected at the nanometre scale but not by micrometre indentation. We note that

Table 1 | Nanostiffness determined from cartilage biopsies from seven osteoarthritis patients with grade 0–3 cartilage (Outerbridge scale).

		E_{nano} (kPa)			
Patient	Age of patient (years)	Grade 0	Grade 1	Grade 2	Grade 3
1	62	25.0 ± 5.4	10.6 ± 2.2	4.8 ± 1.1	3.4 ± 0.7
2	64	15.3 ± 3.5	6.9 ± 1.6	4.5 ± 1.6	2.2 ± 0.5
3	68	16.8 ± 3.5	13.8 ± 3.0	9.0 ± 1.9	3.4 ± 0.7
4	71	25.8 ± 5.6	15.6 ± 3.4	5.4 ± 1.3	2.2 ± 0.5
5	74	n.a.	22.5 ± 5.0	4.0 ± 0.9	2.5 ± 0.7
6	77	83.0 ± 17.2	23.2 ± 4.9	9.8 ± 2.1	5.6 ± 1.2
7	96	142.0 ± 29.0	51.0 ± 11.0	16.1 ± 3.5	6.9 ± 1.6

n.a.—not available; knee joint exhibited only higher grades of OA cartilage

softening of grade 3 osteoarthritis cartilage was occasionally also detectable at the micrometre scale (data not shown).

The nanostiffness values of grade 0 cartilage from three individuals without osteoarthritis (age 38, 41 and 50 years) were in the same average range as those from osteoarthritis patients between 62 and 71 years of age (Fig. 4g). In contrast, we observed a pronounced, age-dependent increase in nanostiffness of 'healthy' grade 0 specimens after the age of 71 years from 15.3 ± 3.5 to 142 ± 29 kPa (Fig. 4g and Table 1). This increase in nanostiffness may be due to the gradual loss of the glycosaminoglycans with age[1,2,18–22], resulting in lower electrostatic repulsive forces between the glycosaminoglycan chains and consequently in a dehydration of the proteoglycan gel. As a consequence, the AFM probe measures the stiffness of the evidently intact collagen meshwork in an age-dependent fashion[23].

Our data also imply that morphological and biomechanical changes occurring in articular cartilage during normal aging are distinct from the pathological changes observed during osteoarthritis progression. Although the nanostiffness of normal (that is, Outerbridge scale 0) human articular cartilage increases significantly with age (Fig. 4g: osteoarthritis grade 0), the age-dependent nanostiffening is counteracted in osteoarthritis-afflicted articular cartilage (Fig. 4g: osteoarthritis grades 1, 2 and 3). The increasing cartilage softening observed in osteoarthritis is due to the progressive disintegration of the collagen meshwork (Fig. 4d) and clearly has a dominant negative effect on the age-dependent increase in the nanostiffness of normal human articular cartilage. This phenomenon is most pronounced in the two oldest patients (age 77 and 96 years, Fig. 4g and Table 1).

Conclusions

The ability to detect early changes in the structure and mechanical properties of normal aging and osteoarthritic articular cartilage in mice and patients, using AFM at the nanometre scale, has opened up the exciting prospect of using a simple nanodevice as a potential clinical tool. Towards this challenge, transgenic mice (that is, *Col9a1*$^{-/-}$ knockout mice) mimicking an osteoarthritis-like phenotype have played a crucial role, not only to scrutinize this novel diagnostics modality *ex vivo*, but also to serve as a powerful animal model for unravelling the molecular mechanism underlying osteoarthritis. The next obvious step is to move this simple, yet effective nanotool from the bench into the clinic, that is, to develop a user-friendly *in situ* IT-AFM setup that allows for direct arthroscopic inspection of, for example, a human knee joint[24,25]. Such nanotools will expand considerably the range of minimally invasive surgical interventions and allow direct inspection of articular cartilage structure and biomechanics in health and disease. In addition to its value in pre-symptomatic diagnostics of osteoarthritis, nanostiffness may also serve as a sensitive disease marker in the course of developing novel therapeutic modalities to halt progression of osteoarthritis or curing the disease. Last, but not least, IT-AFM may be used for quality control to validate *in situ* the outcome of articular cartilage repair procedures (for example, autologous chondrocyte or engineered cartilage implantation).

Methods

Preparation of mouse articular cartilage specimens. C57BL/6 and *Col9a1*$^{-/-}$ knockout mice on C57BL/6 background were used in this study. The animals had been provided with standard nutrition and physical environment in the animal facility. For the experiments, mice were killed at various ages and femoral heads were excised using a razor blade. The specimens were cleaned and stored in ice-cold phosphate-buffered saline (PBS, pH 7.0) supplemented with a protease inhibitor cocktail (Complete, Boehringer Mannheim) and 0.01% NaN_3. The mechanical testing was started within 1 h after disarticulating the hips and ended within two days. Mechanical properties of the articular cartilage remained constant during this time period.

Histology and immunohistochemistry. Femoral heads harvested from C57BL/6 and *Col9a1*$^{-/-}$ knockout mice were fixed in 4% paraformaldehyde (PFA) in PBS, decalcified in 10% EDTA–PBS and processed for paraffin embedding. Serial sections (6 μm) were taken through the entire femoral head and stained with Toluidine Blue or Safranin Orange-Fast Green to assess articular cartilage histomorphology and glycosaminoglycan content. Immunohistochemistry was conducted on hyaluronidase-treated sections using the Vectastain ABC Elite kit (Vector Laboratories) and 3,3′-diaminobenzidine (Sigma) as chromogenic substrate. Primary antibodies against the following antigens were applied: discoidin domain receptor 2, matrix metalloproteinase-13 and C1,2C collagen II fragment. For detailed histological and immunohistochemical procedures see the Supplementary Information, Methods.

Human articular cartilage specimens. Articular cartilage was obtained from seven patients undergoing total knee or hip arthroplasty. The samples were graded independently by two experienced clinicians using the Outerbridge classification system[16,17]. From each area presenting a clear Outerbridge grade from 0 to 3, three adjacent osteochondral plugs were obtained using a biopsy punch with inside diameter of 2 mm. Each punch or 'plug explant' consisted of a full-thickness articular cartilage fragment and the underlying subchondral bone. The plugs were transferred into PBS and kept on ice until the measurement. For each individual plug, force maps were taken at five different locations.

IT-AFM measurements. Samples were prepared as described previously[11]. Briefly, for the analysis of the cartilage samples by IT-AFM, mouse femoral heads or human cartilage specimens were glued onto a round Teflon disk with Histoacryl (B. Braun Surgical GmbH). The mounted specimens were kept in ice-cold PBS until use.

Stiffness (dynamic elastic modulus, E) measurements of articular cartilage samples were performed as described previously[11]. Briefly, we recorded load–displacement curves at a given sample site during both loading and unloading. An individual set of data consisted of 1,024 load–displacement curves, 512 data points each. The load–displacement curves on the mouse femoral heads were recorded at two different trigger deflections (that is, maximum applied loads) for the two types of indenter tips: at 30 nm for the sharp pyramidal tips (200-mm-long silicon nitride cantilevers, nominal cantilever spring constant $k = 0.06$ N m^{-1}; Veeco, Santa Barbara, CA) corresponding to an applied load of ~1.8 nN and a maximum indentation of ~100–600 nm, and at 150 nm for the microspheres ($k = 10$ N m^{-1}) corresponding to an applied load of ~1.5 μN and a maximum indentation of ~1 μm. Microstiffness measurements on the human articular cartilage were performed by using spherical tips exhibiting a typical diameter of $d = 15$ μm ($k = 12$ N m^{-1}). Therefore, a trigger deflection of 250 nm corresponded to an applied load of ~3 μN and resulted in an indentation of ~2 μm. Microstiffness was determined using a model for curve fitting, whereas nanostiffness was calculated using a reference curve as described earlier[11]. Both approaches include a fit of the

upper 50% of the curve as indicated in Fig. 1d,e. The stiffnesses were probed at 3 Hz, that is, close to human gait. After the indentation testing, articular cartilage topography was imaged by contact mode AFM at a scanning rate of ~0.7 lines s^{-1}.

Scanning electron microscopy. Proteoglycans were extracted from articular cartilage specimens in 100 mM Soerensen's phosphate buffer (pH 7.2) containing 1 mg ml^{-1} bovine hyaluronidase (type I, Sigma), 1 mg ml^{-1} trypsin (type I, Sigma) and 0.01% NaN_3 at 37 °C for 3 days[26]. Specimens were then fixed with 2.5% glutaraldehyde in PBS for 2.5 h at room temperature, rinsed in water and dehydrated in graded ethanol series. After critical point drying, samples were sputter-coated with 3–5 nm platinum and examined by SEM (Hitachi S-4800 FEG), operated at 1.5–5 kV accelerating voltage. Areas corresponding to the joint surface were selected for imaging, choosing flat, uniform parts.

Glycosaminoglycan quantification. Mouse femoral heads were digested with 0.5 ml proteinase K solution (1 mg ml^{-1} proteinase K, 1 mM iodoacetamide and 10 μg ml^{-1} pepstatin-A in 50 mM Tris/1 mM EDTA buffer, pH 7.4) at 56 °C for 15 h. Glycosaminoglycan content was measured spectrophotometrically after reaction with dimethylmethylene blue[27] using purified chondroitin sulphate as a reference standard. The glycosaminoglycan content was compared to the DNA content, which was measured by the CyQUANT cell proliferation assay kit (Molecular Probes), with calf thymus DNA as a standard.

Statistical analysis. Data are given as mean ± standard deviation (s.d.). The linear correlations were determined by regression analysis and correlation coefficient using SPSS 15 (SPSS) and Origin 7.5 (OriginLab), respectively. If not mentioned explicitly, statistical significance was set at $P \leq 0.05$.

Received 16 September 2008; accepted 13 December 2008; published online 1 February 2009

References

1. Mankin, H. J., Mow, V., Buckwalter, J., Iannotti, J. & Ratcliffe, A. in *Orthopaedic Basic Science* (ed. Simon, S. R.) Ch. 1, 443–488 (American Academy of Orthopaedic Surgeons, 1994).
2. Buckwalter, J. A., Mankin, H. J. & Grodzinsky, A. J. Articular cartilage and osteoarthritis. *Instr. Course Lect.* **54,** 465–480 (2005).
3. Burstein, D. & Gray, M. L. Is MRI fulfilling its promise for molecular imaging of cartilage in arthritis? *Osteoarthritis Cartilage* **14,** 1087–1090 (2006).
4. Qazi, A. A. *et al.* Separation of healthy and early osteoarthritis by automatic quantification of cartilage homogeneity. *Osteoarthritis Cartilage* **15,** 1199–1206 (2007).
5. Li, X. *et al. In vivo* T(1rho) and T(2) mapping of articular cartilage in osteoarthritis of the knee using 3 T MRI. *Osteoarthritis Cartilage* **15,** 789–797 (2007).
6. Mansfield, P. & Glover, P. M. Limits to magnetic resonance microscopy. *Rep. Prog. Phys.* **65,** 1489–1511 (2002).
7. Xia, Y. Resolution 'scaling law' in MRI of articular cartilage. *Osteoarthritis Cartilage* **15,** 363–365 (2007).
8. Poole, A. R. Biochemical/immunochemical biomarkers of osteoarthritis: utility for prediction of incident or progressive osteoarthritis. *Rheum. Dis. Clin. North Am.* **29,** 803–818 (2003).
9. Lamers, R. J. *et al.* Identification of an urinary metabolite profile associated with osteoarthritis. *Osteoarthritis Cartilage* **13,** 762–768 (2005).
10. Kleemann, R. U., Krocker, D., Cedraro, A., Tuischer, J. & Duda, G. N. Altered cartilage mechanics and histology in knee osteoarthritis: relation to clinical assessment (ICRS Grade). *Osteoarthritis Cartilage* **13,** 958–963 (2005).
11. Stolz, M. *et al.* Dynamic elastic modulus of porcine articular cartilage determined at two different levels of tissue organization by indentation-type atomic force microscopy. *Biophys. J.* **86,** 3269–3283 (2004).
12. Hu, K. *et al.* Pathogenesis of osteoarthritis-like changes in the joints of mice deficient in type IX collagen. *Arthritis Rheum.* **54,** 2891–2900 (2006).
13. Fassler, R. *et al.* Mice lacking alpha 1 (IX) collagen develop noninflammatory degenerative joint disease. *Proc. Natl Acad. Sci. USA* **91,** 5070–5074 (1994).
14. Bruckner, P. & van der Rest, M. Structure and function of cartilage collagens. *Microsc. Res. Tech.* **28,** 378–384 (1994).
15. Asamura, K. *et al.* Type IX collagen is crucial for normal hearing. *Neuroscience* **132,** 493–500 (2005).
16. Outerbridge, R. E. & Dunlop, J. A. The problem of chondromalacia patellae. *Clin. Orthop. Relat. Res.* 177–196 (1975).
17. Outerbridge, R. E. The etiology of chondromalacia patellae. *J. Bone Joint Surg. Br.* **43-B,** 752–757 (1961).
18. Buckwalter, J. A., Kuettner, K. E. & Thonar, E. J. Age-related changes in articular cartilage proteoglycans: electron microscopic studies. *J. Orthop. Res.* **3,** 251–257 (1985).
19. Poole, A. R. An introduction to the pathophysiology of osteoarthritis. *Front. Biosci.* **4,** D662–670 (1999).
20. Hollander, A. P. *et al.* Damage to type II collagen in aging and osteoarthritis starts at the articular surface, originates around chondrocytes, and extends into the cartilage with progressive degeneration. *J. Clin. Invest.* **96,** 2859–2869 (1995).
21. Bayliss, M. T., Osborne, D., Woodhouse, S. & Davidson, C. Sulfation of chondroitin sulfate in human articular cartilage. The effect of age, topographical position and zone of cartilage on tissue composition. *J. Biol. Chem.* **274,** 15892–15900 (1999).
22. Carney, S. L. & Muir, H. The structure and function of cartilage proteoglycans. *Physiol. Rev.* **68,** 858–910 (1988).
23. Yang, L. *et al.* Micromechanical bending of single collagen fibrils using atomic force microscopy. *J. Biomed. Mater. Res. A* **82,** 160–168 (2007).
24. Stolz, M., Imer, R., Staufer, U. & Aebi, U. Development of an arthroscopic atomic force microscope. *BioWorld* **4,** 2–5 (2003).
25. Imer, R. *et al.* Development of atomic force microscope for arthroscopic knee cartilage inspection. *Jpn J. Appl. Phys.* **45,** 2319–2323 (2006).
26. Segawa, K. & Takiguchi, R. Ultrastructural alteration of cartilaginous fibril arrangement in the rat mandibular condyle as revealed by high-resolution scanning electron microscopy. *Anat. Rec.* **234,** 493–499 (1992).
27. Farndale, R. W., Buttle, D. J. & Barrett, A. J. Improved quantitation and discrimination of sulphated glycosaminoglycans by use of dimethylmethylene blue. *Biochim. Biophys. Acta* **883,** 173–177 (1986).

Acknowledgements

This work was supported by an NCCR program grant on 'Nanoscale Science' awarded by the Swiss National Science Foundation, the M. E. Müller Foundation of Switzerland, the Canton Basel-Stadt, and the Max Planck Society. Part of the work has also been supported by the Hardy and Otto Frey-Zünd Foundation, ProMotio Foundation for Biomechanical Research and other private promoters supporting the efforts of the University of Basel Laboratory for Orthopedic Biomechanics. Moreover, we thank Nanoworld AG (L. Aeschimann, M. Burri) for the silicon AFM probes and for the SEM image of the microspherical tip, and Z. Farkas for technical assistance. The authors thank F. Wolf for some of the glycosaminoglycan/DNA analysis. We thank T. Staehelin for critical review of the manuscript and discussion of the data, and Z. Housley for proofreading the manuscript.

Author contributions

M.S., W.B., A.A. and U.A. conceived and designed the experiments. R.R. developed the software for analysing force maps. R.I. and U.S. developed and produced the microfabricated spherical tips. N.F. provided all issues related to clinics. M.S., R.G., S.M., A.R., M.D. and A.A. performed the experiments. M.S., I.M., A.D., A.A. and U.A. co-wrote the paper. All authors discussed the results and commented on the manuscript.

Additional information

Supplementary Information accompanies this paper at www.nature.com/naturenanotechnology. Reprints and permission information is available online at http://npg.nature.com/reprintsandpermissions/. Correspondence and requests for materials should be addressed to M.S.

Suppl. Fig. 1

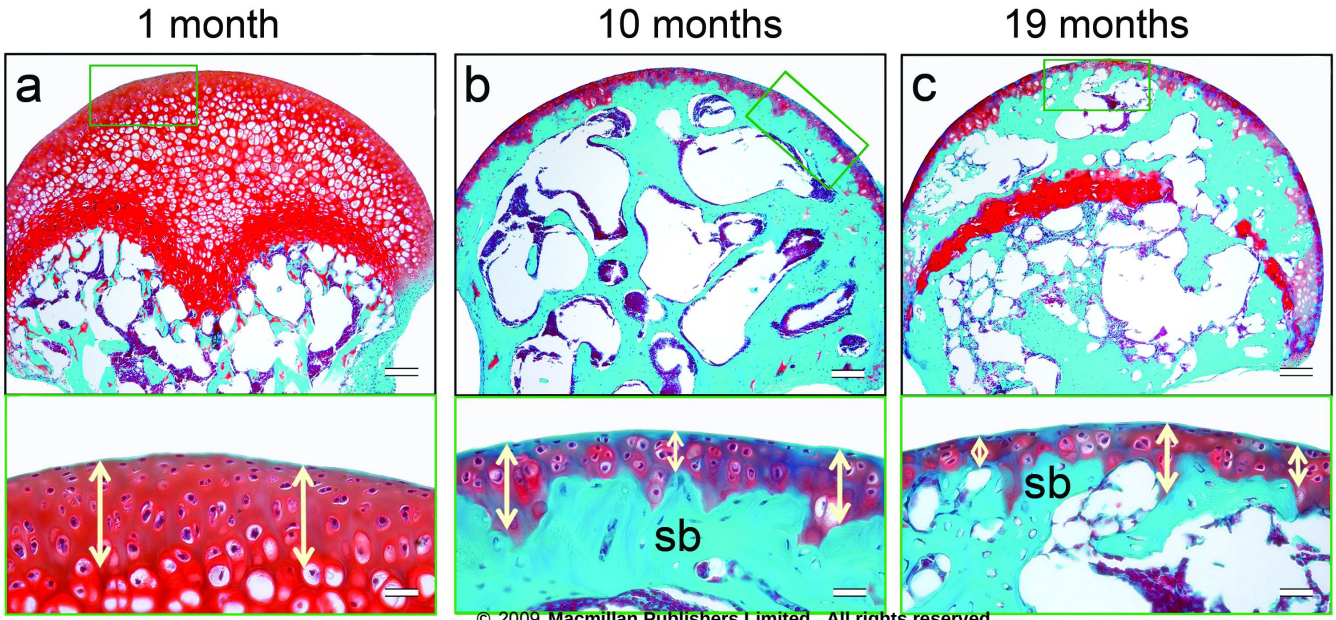

Suppl. Fig. 2

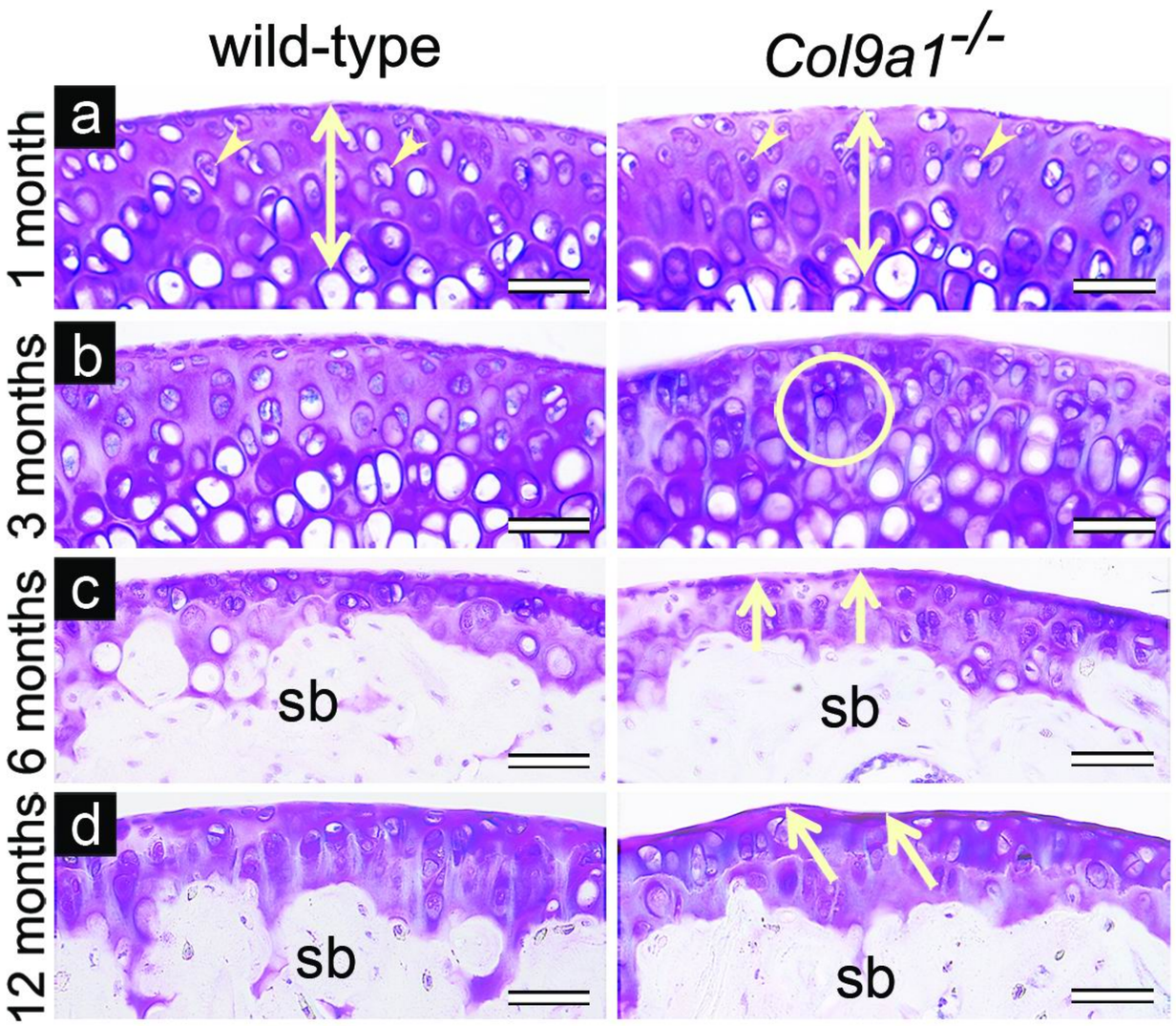

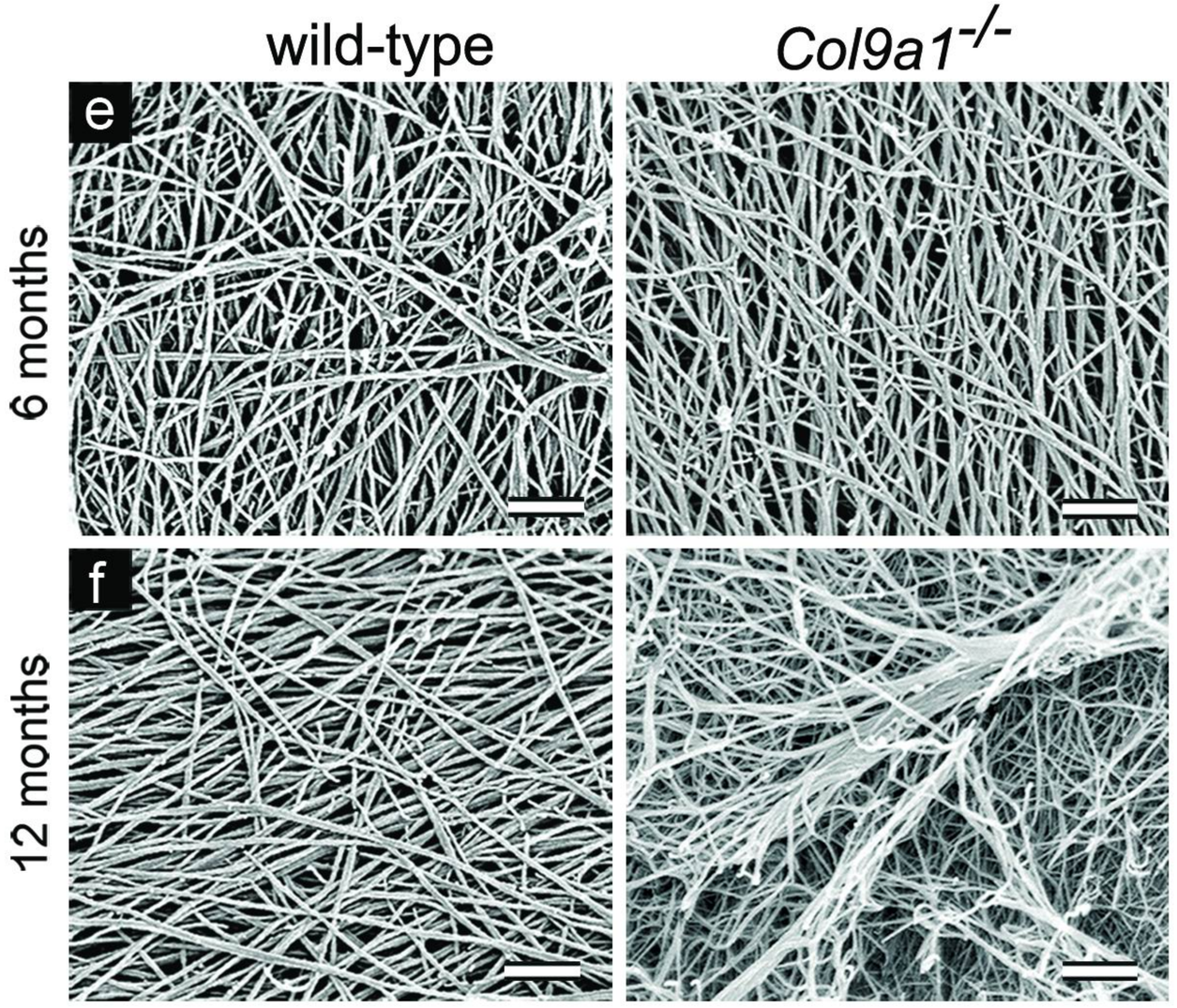

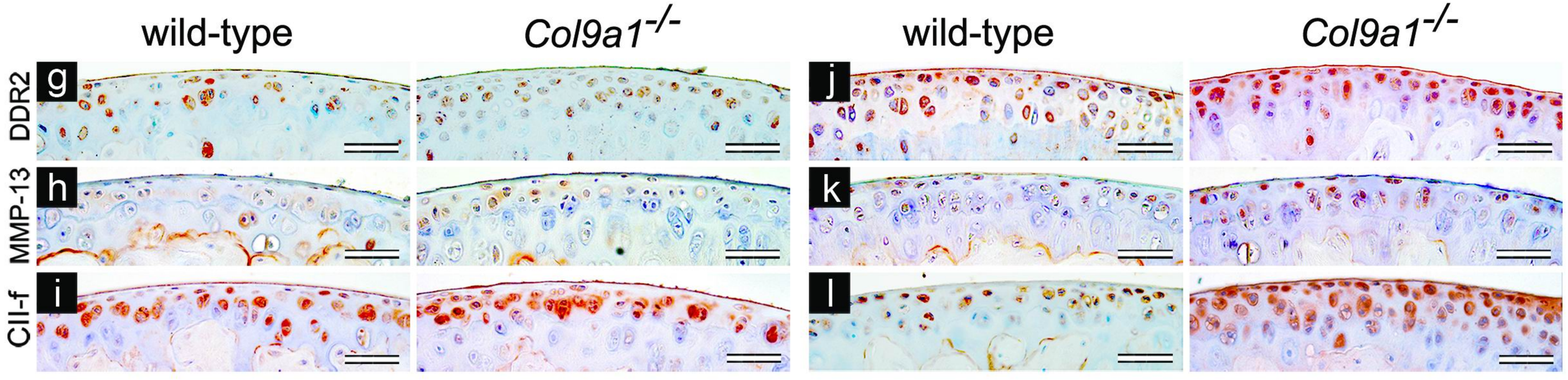

PAPER V

Cell Stem Cell
Article

Homing of Mouse Spermatogonial Stem Cells to Germline Niche Depends on β1-Integrin

Mito Kanatsu-Shinohara,[1,*] Masanori Takehashi,[1,5] Seiji Takashima,[1] Jiyoung Lee,[1] Hiroko Morimoto,[1] Shinichiro Chuma,[2] Aurelia Raducanu,[3] Norio Nakatsuji,[2] Reinhard Fässler,[3] and Takashi Shinohara[1,4]
[1]Department of Molecular Genetics, Graduate School of Medicine, Kyoto University, Kyoto 606-8501, Japan
[2]Department of Development and Differentiation, Institute for Frontier Medical Sciences, Kyoto University, Kyoto 606-8507, Japan
[3]Max Planck Institute of Biochemistry, 82152 Martinsried, Germany
[4]Japan Science and Technology Agency, CREST, Kyoto 606-8501, Japan
[5]Present address: Laboratory of Molecular Clinical Chemistry, Faculty of Pharmacy, Osaka Ohtani University, Tondabayashi, Osaka 584-8540, Japan
*Correspondence: mshinoha@virus.kyoto-u.ac.jp
DOI 10.1016/j.stem.2008.08.002

SUMMARY

Spermatogonial stem cells (SSCs) provide the foundation for spermatogenesis. In a manner comparable to hematopoietic stem cell transplantation, SSCs colonize the niche of recipient testes and reinitiate spermatogenesis following microinjection into the seminiferous tubules. However, little is known about the homing mechanism of SSCs. Here we examined the role of adhesion molecules in SSC homing. SSCs isolated from mice carrying loxP-tagged β1-integrin alleles were ablated for β1-integrin expression by in vitro adenoviral cre transduction. The β1-integrin mutant SSCs showed significantly reduced ability to recolonize recipient testes in vivo and to attach to laminin molecules in vitro. In contrast, genetic ablation of E-cadherin did not impair homing, and E-cadherin mutant SSCs completed normal spermatogenesis. In addition, the deletion of β1-integrin on Sertoli cells reduced SSC homing. These results identify β1-integrin as an essential adhesion receptor for SSC homing and its association with laminin is critical in multiple steps of SSC homing.

INTRODUCTION

One of the distinct features of stem cells is their migration and repopulation of niches, where they undergo self-renewal division (Laird et al., 2008). Of the self-renewing systems, the homing mechanisms of hematopoietic stem cells (HSCs) have been best characterized. HSCs are defined as having both the capacity for self-renewal and the ability to differentiate into all mature hematopoietic lineages after migration into niches. After damage by radiation or chemicals that destroy endogenous stem cells, transplanted HSCs can find and actively migrate into empty niches and quickly regenerate hematopoiesis, a process that can be exploited to study HSCs and repopulation. Although the molecular mechanism underlying HSC homing remained long unknown, a large number of molecules, including cell-adhesion molecules and their ligands, extracellular matrix (ECM) components, and chemokines, have been identified to be involved in the homing process (Lapidot et al., 2005).

The spermatogenic system is the only other self-renewing tissue for which a functional transplantation technique is available (Brinster and Zimmermann, 1994). When spermatogonial stem cells (SSCs) are microinjected into the seminiferous tubules of infertile testes, SSCs migrate into the niche, where they reinitiate and maintain spermatogenesis for a long period of time. While it is well known that primordial germ cells (PGCs), from which SSCs develop, migrate into genital ridges during fetal development (Molyneaux and Wylie, 2004; Raz, 2004), the microinjection of SSCs now demonstrates that postnatal SSCs retain the ability to migrate into the niche. Unlike bone marrow, which is composed of multiple cell types, the composition of the germline niche is relatively simple; the only somatic cell type that directly interacts with SSCs are the Sertoli cells (de Rooij and Russell, 2000; Meistrich and van Beek, 1993). They support spermatogenesis and also form a blood testis barrier (BTB) that is constituted by specific tight junctions between adjacent cells. Transplanted SSCs attach to Sertoli cells and, by passing through the BTB, migrate from the adluminal side of the seminiferous tubules to the niche site on the basement membrane. Approximately 10% of transplanted SSCs can accomplish this process, while the remaining cells disappear within 2 to 3 weeks (Nagano et al., 1999). SSCs are the only cell type to achieve reconstitution and long-term spermatogenesis; the rest of the cells disappear because they do not have self-renewing capabilities. Thus, SSCs exhibit strong migratory activity into their niche in a manner similar to HSCs. However, very little is known about the homing mechanisms of SSCs or whether stem cells of the two different self-renewing tissues share the common molecular machinery for homing.

In this study, we analyzed the roles of adhesion molecules in the SSC homing. SSCs express members of the integrin and cadherin family of adhesion molecules, both of which play important roles in HSC homing. We previously found that SSCs preferentially attach to laminin and express both α6- and β1-integrins that are components of the laminin receptor (Shinohara et al., 1999). Another study showed that SSCs also express E-cadherin, which is expressed in a very small population of undifferentiated spermatogonia (Tokuda et al., 2007). Using adenovirus mediated gene delivery systems, SSCs or Sertoli cells from mutant mice

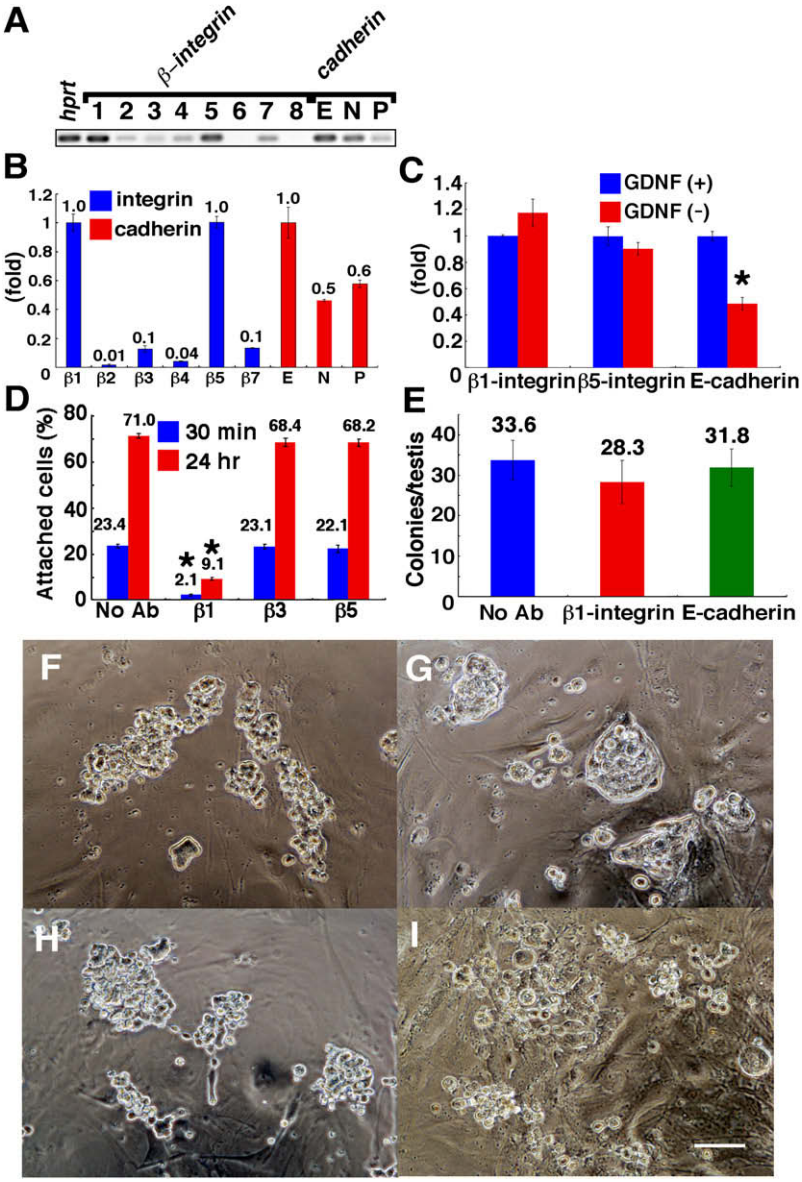

Figure 1. Expression of β-Integrin and Cadherin Family Molecules in SSCs

(A) RT-PCR analysis of *β-integrin* and *cadherin* gene expression.

(B) Real-time PCR analysis. Expression was normalized to HPRT expression.

(C) Reduced expression of E-cadherin in the absence of GDNF, as assessed by real-time PCR analysis. Expression was normalized to HPRT expression. Asterisk denotes significant difference from the control (mean ± SEM, n = 3, $p < 0.01$).

(D) Inhibition of GS cell attachment to laminin by Ha2/5. Asterisks denote significant differences from the control (mean ± SEM, n = 5, $p < 0.01$).

(E) Inhibition of GS cell colonization by neutralizing antibodies. No significant effect was observed (mean ± SEM, n = 11 to 12).

(F–I) Effects of neutralizing antibodies on colony formation. Addition of Ha2/5 (F) or ECCD1 (H) did not show significant effect on GS cells. On the other hand, while typical ES-like EG cell colonies were observed in the absence of neutralizing antibody (G), ECCD1 prevented EG cell colony development (I). Bar, 200 μm (F–I).

carrying loxP-tagged *β1-integrin* or *E-cadherin* alleles were transduced with cre to delete the loxP-tagged alleles. Germ cell transplantation technique was subsequently used to functionally assess the effect of the *β1-integrin* or *E-cadherin* genes in SSC homing.

RESULTS

Expression of β1-Integrin and E-Cadherin on SSCs

To examine the expression of integrin and cadherin family of adhesion molecules on SSCs, we used cultured spermatogonia, germline stem (GS) cells, which are highly enriched with SSCs (Kanatsu-Shinohara et al., 2003). To avoid contamination of somatic cells, GS cells on laminin-coated dishes were used for analysis. Reverse transcription polymerase chain reaction (RT-PCR) analyses indicated the expression of most β-integrin subunits (i.e., β1-, β2-, β3-, β4-, β5-, and β7-integrins) and cadherins (i.e., E-, N-, and P-cadherins) (Figure 1A). However, we were unable to detect expression of the β6- and β8-integrins. We next quantified the expression levels of these transcripts using real-time PCR (Figure 1B). Of the several integrin molecules, β1- and β5-integrins were dominantly expressed in GS cells. E-cadherin was expressed at higher levels than N- and P-cadherin.

Because adhesion molecules are dynamically regulated in HSCs by mitogenic signals (Wilson et al., 2004), we examined whether the expression of these molecules is regulated by glial cell line-derived neurotrophic factor (GDNF), a critical regulator of self-renewal division of SSCs (Meng et al., 2000). Real-time PCR analyses showed that expression of the E-cadherin is downregulated to ~50% when they are cultured in the absence of GDNF (Figure 1C). In contrast, the expression of β1- and β5-integrins did not change significantly. These results suggest that expression of integrin and cadherin adhesion molecules are regulated differentially.

To examine the function of these molecules, we initially used neutralizing antibodies. Neutralizing antibodies against β1-integrin (Ha2/5) or E-cadherin (ECCD1) inhibited colony formation of embryonic germ (EG) cells or binding of GS cells to laminin, respectively (Figures 1D and 1F–1I). However, addition of anti-β5-integrin neutralizing antibody did not have any effect, indicating that β1-integrin plays a major role in laminin binding. Both Ha2/5 and ECCD1 had no effects on GS cell colony morphology or proliferation. We also tested their effect in vivo. Because HSC homing can be blocked when bone marrow cells are preincubated with neutralizing antibodies against cell surface antigens (Lapidot et al., 2005; Laird et al., 2008), Ha2/5 or ECCD1 were preincubated with enhanced green fluorescence protein (EGFP)-expressing GS cells, and the cells were then microinjected into

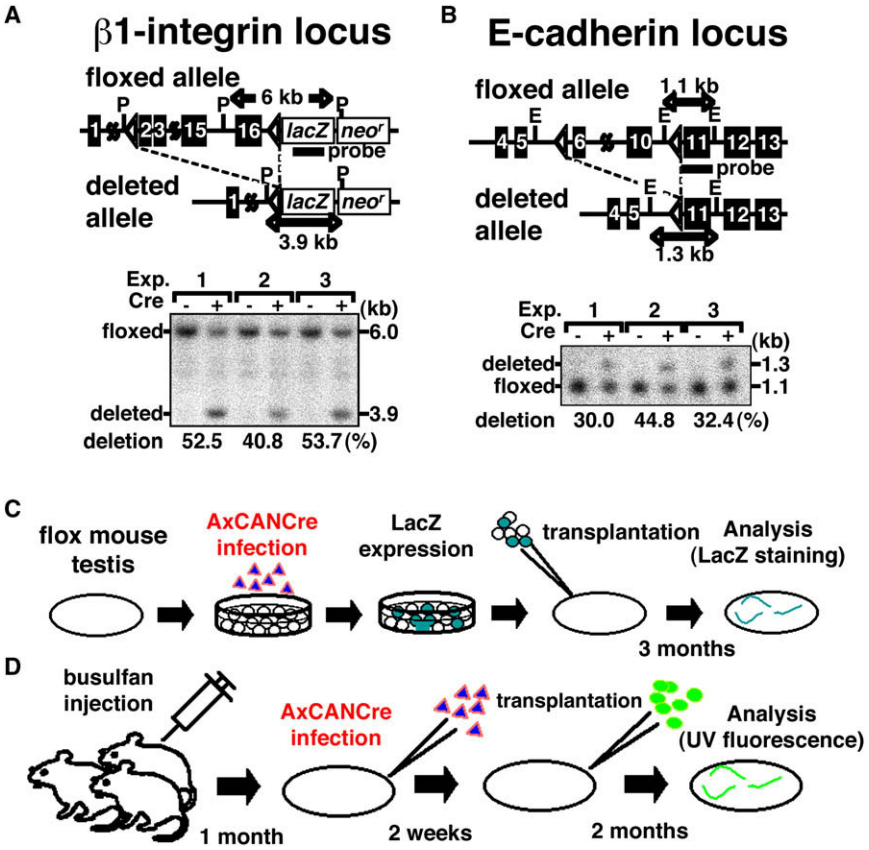

Figure 2. Functional Analysis of Homing Molecules by Adenoviral Transduction

(A and B) Conditional mutant mice used in the experiments. *LacZ* gene expression begins after cre-mediated gene deletion in β1-integrin mutant mice. Southern blots of deletion efficiency. Genomic DNA was digested with PstI (A) or *Eco*R V (B) and hybridized with a *LacZ* (A)- or *E-cadherin* (B)-specific probe, respectively. P, PstI; E, *Eco*R V.

(C) Diagram of the experimental procedure to test gene functions in SSCs. Testis cells from conditional mutant mice were dissociated and infected in vitro by AxCANCre. Cre-mediated deletion removed the target genes, and *LacZ* gene expression was initiated under the β1-integrin or ROSA26 promoters in β1-integrin or E-cadherin mutant cells, respectively. The cells were transplanted into recipient testes for assessing the SSC activity. The level of donor cell colonization was evaluated by counting LacZ-positive colony numbers or tubules with spermatogenesis.

(D) A diagram of the experimental procedure to test gene functions in Sertoli cells. The β1-integrin floxed mice were treated with busulfan to remove endogenous spermatogenesis. One month after busulfan injection, AxCANCre was microinjected into the testes. Donor cells from EGFP transgenic mice were transplanted after 2 weeks. The level of donor cell colonization was evaluated by counting the number of colonies under UV light.

the seminiferous tubules of WBB6F1-W/W^v (W) mice, which lack endogenous spermatogenesis because of mutations in the c-kit receptor (Geissler et al., 1988). Two experiments were performed, and recipients were transplanted with 2 × 10^4 GS cells. However, no evidence of impaired colonization was found (Figure 1E). The combination of these antibodies also did not show any impact on colonization.

Analysis of β1-Integrin and E-Cadherin Function in SSCs Using Conditional Knockout Mice

Although our results suggested that neither β1-integrin nor E-cadherin is involved in SSC homing, the techniques used in the HSC studies may not be applicable to SSCs because of differences in the anatomical structures of the migratory paths and the kinetics of the homing processes. We therefore took advantage of the cre/lox technology to remove both these genes individually in SSCs derived from conditional knockout animals (Figures 2A and 2B). The cre-mediated gene ablation was carried out with a recombinant, cre-expressing adenovirus (AxCANCre). We previously showed that exposure of testis cells in vitro to AxCANCre results in the deletion of the target genes in SSCs (Figure 2C) (Takehashi et al., 2007).

In the first set of experiments, we used mice carrying a *β1-integrin* gene flanked by loxP sites (β1-integrin floxed mice) (Figure 2A) (Brakebusch et al., 2002). In this mouse strain, the excision of the floxed *β1-integrin* gene can be confirmed by the activation of a reporter *LacZ* gene, which was inserted downstream of the *β1-integrin* locus. The reporter is activated after the excision of the *β1-integrin* allele by cre. Using this mouse strain, heterozygous floxed animals were bred to produce mice homozygous for the β1-integrin floxed allele. Heterozygous floxed animals were used as controls. Testis cells from both homozygous and heterozygous animals were collected from 10- to 14-day-old pups, which are enriched with SSCs because of the lack of differentiating germ cells (Shinohara et al., 2001). The cells were exposed to AxCANCre overnight and then were recovered for transplantation (Figure 2C). After trypsinization, 48%–77% of the input cells could be recovered. The adenovirus treatment resulted in the loss of the *β1-integrin* gene at an efficiency of 49.0 ± 4.1% (mean ± SEM, n = 3; Figure 2A). Three experiments were performed, and 1.5 × 10^5 testis cells were transplanted into 30 testes.

Three months after transplantation, recipient mice were sacrificed, and the testes were stained with 5-bromo-4-chloro-3-indolyl β-D-galactoside (X-gal). Recipient testes that received mutant cells had a significantly smaller number of colonies than did testes that received control cells (Figures 3A, 3B, and 3G). Because W testes do not have differentiating germ cells, all spermatogenesis in the recipient testes originated from the transplanted donor cells (Shinohara et al., 2001). We also evaluated the homing efficiency by counting the number of seminiferous tubules containing spermatogenesis by histology. Overall, whereas testes with mutant donor cells showed spermatogenesis in 13 of 757 tubules (1.7%), those that received control transplants exhibited spermatogenesis in 187 of 602 tubules (31.1%); this difference was statistically significant (Figure 3H).

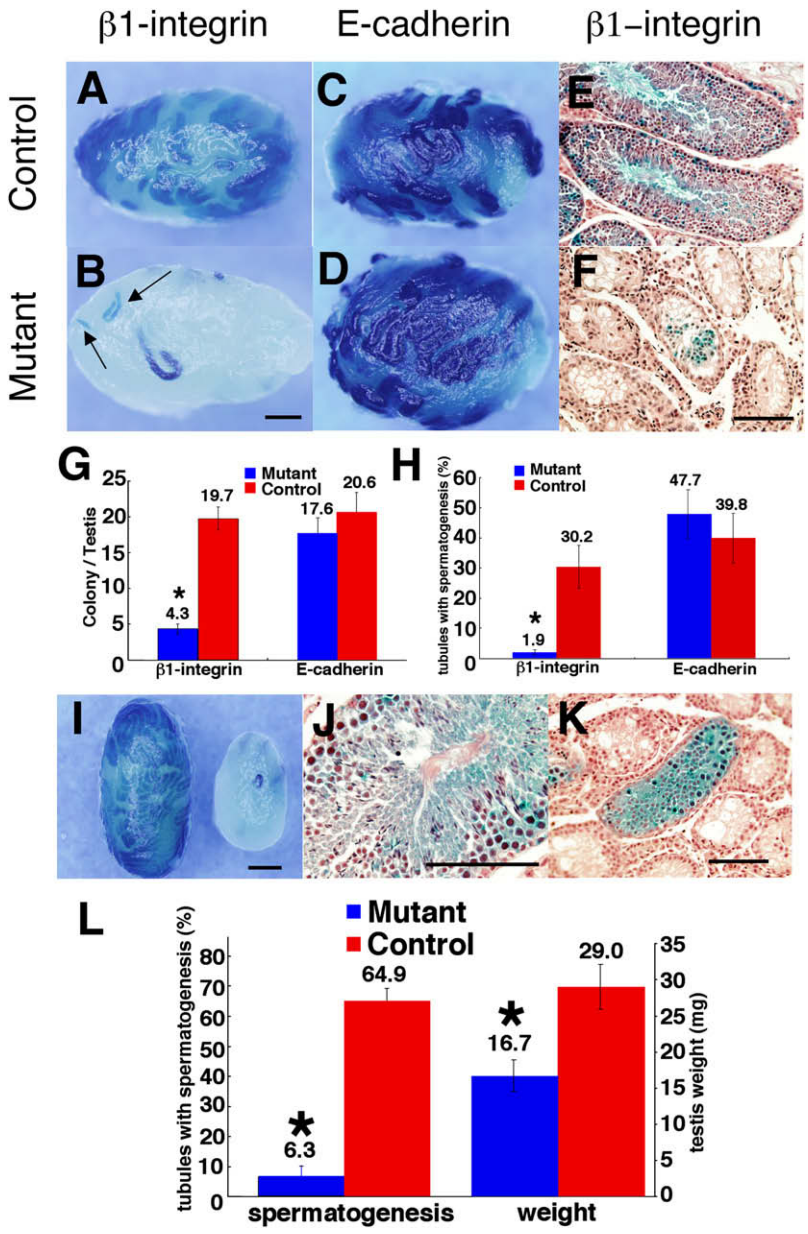

Figure 3. Reduced Colonizing Ability of β1-Integrin Mutant Cells

(A–D) Appearance of recipient testes following transplantation of AxCANCre-infected control (A and C) or β1-integrin (B) or E-cadherin (D) mutant testis cells. Blue tubules represent the colonization of donor stem cells that were infected by AxCANCre adenovirus. Weakly stained colonies were found in the recipient testis (arrows), suggesting that the cells differentiated poorly.

(E and F) Histological appearance of recipient testes that received AxCANCre-infected testis cells from control (E) or β1-integrin mutant (F) mice. Note the reduced spermatogenesis in the mutant cells.

(G) Colony count. The loss of β1-integrin induced a significant reduction. Asterisks denote significant differences from the control (mean ± SEM, n = 18 to 26, $p < 0.01$ for β1-integrin; n = 9 to 10, $p = 0.41$ for E-cadherin).

(H) Evaluation of spermatogenesis in the recipient testes. The values represent the percentage of tubules with spermatogenesis in each testis. Asterisks denote significant difference from control (mean ± SEM, n = 4 to 6, $p < 0.01$). The total number of tubules from four to eight different recipient testes was counted.

(I) Appearance of pup recipient testes that received AxCANCre-infected control (left) or β1-integrin mutant (right) testis cells. Note the larger size of the recipient testes that received control cells (left), due to enhanced colonization in the immature testis.

(J and K) Histological appearance of pup recipient testes that received AxCANCre-infected control (J) or β1-integrin mutant (K) testis cells.

(L) Weight and evaluation of spermatogenesis in the pup recipient testes. Asterisks denote significant differences from the control (mean ± SEM, n = 8 to 9, $p < 0.01$ for testis weight; n = 7–10 for histology). Bars: 1 mm, (A)–(D) and (I); 100 μm, (E), (F), (J), and (K). Stain, X-gal followed by hematoxylin and eosin (E, F, J, and K).

Blue colonies from control cells stained more darkly than did those from mutant males (Figures 3A and 3B), suggesting that β1-integrin mutant cells did not differentiate efficiently. In agreement with this result, although control cells could complete normal spermatogenesis, very few differentiated germ cells were found in the recipients that received mutant donor cells (Figures 3E and 3F).

SSC homing involves several steps: attachment to Sertoli cells, passage through the BTB, migration into the germline niche, and attachment to the basement membrane (Nagano et al., 1999). To examine which of these processes are affected, we analyzed the pattern of donor cell colonization at early time points (Figure 4A). Both control and mutant cells produced chains of spermatogonia on the basement membrane at 1 week after transplantation (Figure 4B, inset), indicating that the mutant cells were able to migrate through BTB and proliferate on basement membrane. However, when the recipient testes were analyzed at 3 weeks after transplantation, only control cells remained on the basement membrane (Figure 4B). By 6 weeks after transplantation, most of the mutant cells disappeared from the testis. In contrast, no significant effects on colonization were observed with neutralizing antibodies (Figure 4C).

To further examine the mechanism of homing defect, we next used 5- to 10-day-old immature W pups as recipients (Shinohara et al., 2001). At this stage, recipient testes lack the BTB, which forms at approximately days 12–14 after birth (de Rooij and Russell, 2000). Three experiments were performed, and a total of 12 testes were transplanted with 6×10^4 testis cells that were exposed to AxCANCre. Testis cells lacking β1-integrin showed a significantly reduced colonization (Figure 3I), while transplantation of control cells resulted in extensive colonization at 3 months after transplantation. Some haploid cells were found, but we were unable to observe complete spermatogenesis (Figures 3J and 3K). A total of 373 of 584 tubules (63.9%) showed spermatogenesis with control cells, but only 63 of 1203 (5.2%) tubules showed spermatogenesis with mutant cells. Decreased colonization was also evident by the low testicular weight of mutant cell recipients (Figure 3L).

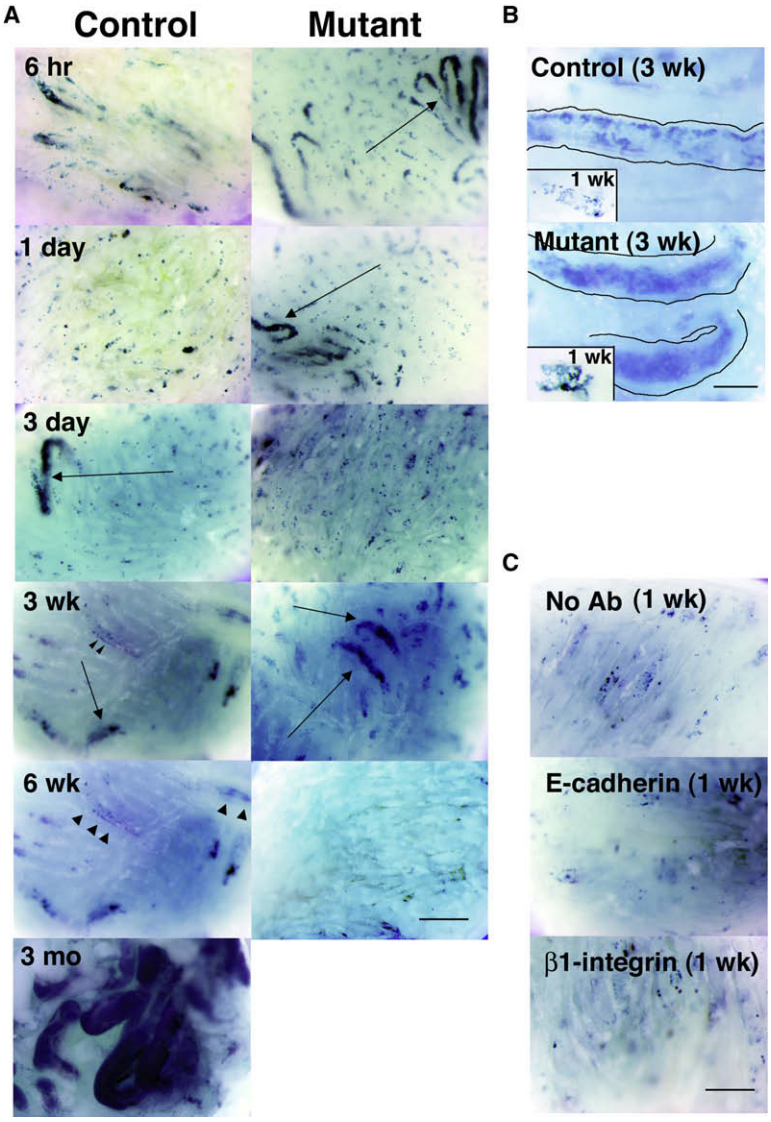

Figure 4. Colonization of Recipient Seminiferous Tubules by Donor Cells

(A) Appearance of the recipient testis that received cre-treated testis cells from homozygous and heterozygous (control) animals. Although many clusters of blue cells were initially observed (arrows), very few colonies were found in the recipient testis that received homozygous donor cells after 6 weeks. In contrast, heterozygous control cells proliferated to make germ cell colonies (arrowheads). The intense blue color in the colony at 3 months represents extensive differentiation of SSCs.

(B) Colonization of seminiferous tubules at 3 weeks after transplantation. Control cells made networks of spermaotgonia, whereas homozygous cells produced blue cell clusters. Note the greater distance between the blue cells and the outlines of the tubules in recipient with mutant cells, which suggested that they are not on the basement membrane. Inset shows chains of control and mutant spermatogonia in the tubule at 1 week after transplantation, suggesting that the cells were proliferating.

(C) Effect of neutralizing antibodies. Heterozygous donor cells were transplanted with indicated antibodies, and the recipient testes were analyzed at 1 week after transplantation. Bars: 500 μm, (A) and (C); 200 μm, (B).

To examine the role of β1-integrin in SSCs in vitro, we established GS cells from 7-day-old homozygous β1-integrin floxed mice. The established GS cells were exposed to AxCANCre to generate GS cells lacking β1-integrin. The growth rate of the mutant GS cells was comparable to that of control cells on mouse embryonic fibroblasts (MEFs). Additionally, there were no significant changes in colony morphology or size (Figure 5A). However, when the mutant cells were transferred on different kinds of ECM molecules, they showed reduced ability to bind to laminin (Figure 5B). The number of cells that attached was significantly smaller than that of control cells as early as 30 min after incubation (Figure 5C). Interestingly, the mutant cells could attach to poly L-lysine, an artificial substrate that can mediate β1-integrin independent attachment (Figure 5B).

We also analyzed the role of E-cadherin in SSC homing. Preliminary experiments using a dominant-negative E-cadherin construct did not show any effect on GS cell colony proliferation or homing (data not shown). We therefore used a conditional knockout mouse line for the *E-cadherin* gene (Figure 2B) (Boussadia et al., 2002). The E-cadherin mutant mouse strain was crossed with a ROSA26 reporter mouse strain (R26R) to visualize the mutant SSCs (Soriano, 1999). Heterozygous floxed animals were used as controls. Testis cells were collected from the homozygous mutant and control mouse and exposed to AxCANCre. After overnight incubation, 41%–75% of the input cells were recovered. Southern blots indicated that 35.7 ± 4.6% (mean ± SEM, n = 3) of the floxed allele was deleted from the *E-cadherin* gene locus (Figure 2B). Three experiments were performed, and 1.5×10^5 testis cells were transplanted into 18 recipient testes. Analysis of the recipient testes showed that both mutant and control cells could extensively colonize the seminiferous tubules (Figures 3C and 3D), and there was no significant difference in colony numbers (Figure 3G). Histological analysis also showed comparable numbers of seminiferous tubules with spermatogenesis (Figure 3H). Overall, the control and mutant cells produced spermatogenesis in 148 of 367 (40.3%) and 188 of 413 (45.5%) tubules, respectively. No apparent differentiating defects were observed. Moreover, we also did not find any differences at 1–3 weeks after transplantation (data not shown), suggesting that E-cadherin is not involved in migration in the initial phase of colonization.

Analysis of β1-Integrin and E-Cadherin Function in Sertoli Cells Using Conditional Knockout Mice

Because β1-integrin is also expressed in Sertoli cells (Yan et al., 2006), we hypothesized that β1-integrin on Sertoli cells may affect SSC homing. We examined this hypothesis by taking advantage of the in situ infection of Sertoli cells by adenovirus (Figure 2D) (Kanatsu-Shinohara et al., 2002). Wild-type (WT) or conditional β1-integrin knockout mice were injected with busulfan to deplete endogenous spermatogenesis. After 1 month,

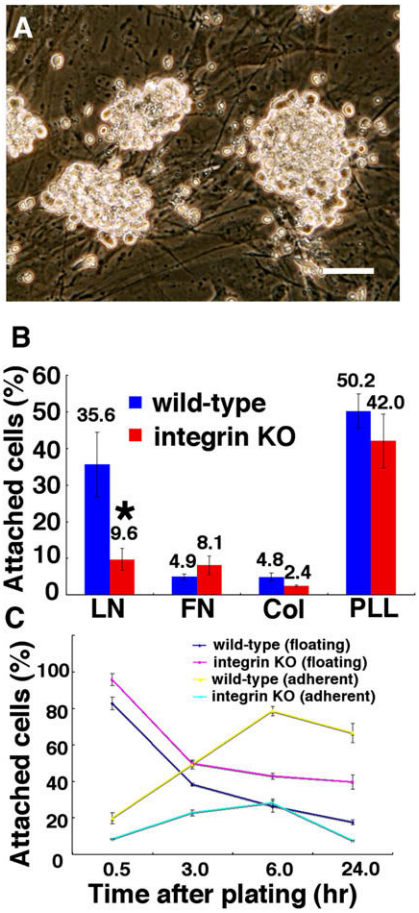

Figure 5. Reduced Laminin Binding of β1-Integrin Mutant GS Cells

(A) β1-integrin mutant GS cells. The cells retained a typical morula-like appearance.

(B) Adherence of β1-integrin mutant GS cells to ECM substrates. GS cells were plated on ECM-coated dishes for 30 min. Asterisk denotes significant difference from the control (mean ± SEM, n = 5, $p < 0.01$). LN, laminin; FN, fibronectin; Col, collagen; PLL, poly L-lysine.

(C) Reduced laminin binding of mutant GS cells. The differences between control and mutant cells were significant at all time points for both adherent and floating cells (mean ± SEM, n = 5, $p < 0.01$). Bar, 200 μm (A).

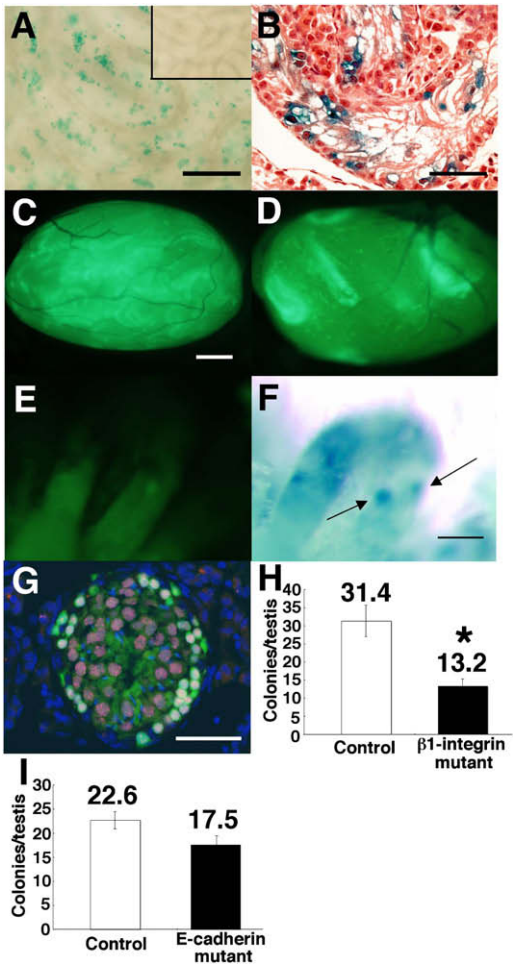

Figure 6. Evaluation of β1-Integrin Function in Sertoli Cells

(A and B) Whole mount (A) and histology (B) of recipient testes from AxCANCre-injected β1-integrin floxed mice. Injection of AxCANCre induced the loss of the β1-integrin gene, as evidenced by LacZ expression. Inset shows whole mount of cre-treated control recipient testis.

(C and D) Appearance of AxCANCre-injected control (C) and homozygous β1-integrin floxed (D) recipient testes that received EGFP-positive donor cells.

(E and F) Colonization of donor cells. EGFP-expressing cells are found among LacZ-expressing Sertoli cells (arrows).

(G) Spermatogenesis in the recipient testis. SYCP3-positive (red) meiotic cells were observed.

(H and I) Colony count. The number of colonies in β1-integrin mutants was reduced in recipient testes that received AxCANCre injection (H), whereas those in E-cadherin mutants did not decrease significantly (I). The results are from two experiments. Asterisks denote significant differences from the control (mean ± SEM, n = 14 to 17, $p < 0.01$). Bars: 200 μm, (A), (E), and (F); 1 mm, (C) and (D); 50 μm, (B) and (G).

both types of mice were injected with AxCANCre. Exposure to AxCANCre resulted in the deletion of the *β1-integrin* gene throughout the whole testis, as visualized by X-gal staining (Figure 6A). Histological analyses showed that the deletion occurred in 71.5 ± 6.4% of the seminiferous tubules (mean ± SEM, n = 6), and 19.3 ± 1.6% of Sertoli cells in each tubule expressed *LacZ* gene (mean ± SEM, n = 31) (Figure 6B).

Two weeks after AxCANCre exposure, 1×10^6 testis cells from adult EGFP transgenic mice C57BL/6 Tg14(act-EGFP)OsbY01 (designated as Green) were microinjected into the seminiferous tubules of both control and β1-integrin mutant mice. When the recipient testes were analyzed 2 months after transplantation, β1-integrin mutant recipient testes had a smaller number of EGFP-expressing colonies compared with control recipients, suggesting that the loss of β1-integrin decreased the seeding or maintenance of stem cells in recipient testis (Figures 6C, 6D, and 6H). However, some $EGFP^+$ cells overlapped in LacZ-stained areas (Figures 6E and 6F). Despite fewer colonies, those that did develop in the testes did not show any particular abnormalities, and the cells were able to differentiate at least beyond the spermatocyte stage after histological analyses, as indicated by synaptonemal complex protein 3 (SYCP3) expression (Figure 6G). In contrast, although the number of colonies decreased in E-cadherin mutants, the difference was not significant (Figure 6I).

DISCUSSION

Although the discovery of the homing activity of SSCs was surprising, the mechanism of SSC homing has been long unknown due, at least in part, to the lack of appropriate techniques for the genetic manipulation of SSCs. We took advantage of adenovirus to analyze the involvement of adhesion molecules in SSC homing. Although SSCs were thought to be refractory to adenovirus infection, adenovirus can transduce SSCs in vitro (Takehashi et al., 2007). An additional advantage of adenovirus is that it also infects Sertoli cells (Kanatsu-Shinohara et al., 2002). Because Sertoli cells are mitotically quiescent and constitute only 2% of the total testis cells in the adult (Bellvé, 1993), their role in spermatogenesis has been difficult to analyze despite the relatively simple niche structure. Our study demonstrates that adenovirus exposure to SSCs in vitro and the infection of Sertoli cells in vivo are both useful methods by which to analyze gene function in stem cells and their microenvironment.

The integrin family, which comprises various ECM receptors, plays important roles in stem cell biology. In particular, β1-integrin is involved not only in HSC homing to the fetal liver or bone marrow, but also in the proliferation of neural stem cells (Hirsch et al., 1996; Ptocnik et al., 2000; Leone et al., 2005; Campos et al., 2004). In germline cells, PGCs, precursor of SSCs, require β1-integrin to migrate into the genital ridges during fetal development (Anderson et al., 1999). Through the analysis of chimeras between β1-integrin-deficient embryos with WT embryos, it was found that β1-integrin-deficient PGCs enter the germline but fail to efficiently colonize the genital ridges. Conversely, the function of β1-integrin in postnatal germ cells remained elusive, even though its expression was demonstrated on SSCs (Shinohara et al., 1999). However, the decreased colony formation from the β1-integrin mutant SSCs now indicates that β1-integrin plays an important role in the SSC biology.

A major problem in studying SSC homing is that it is difficult to track SSCs immediately after transplantation. This is because the concentration of SSCs is very low in the testis cell suspension, and no SSC-specific markers have been identified. Stem cells could be identified retrospectively only by their ability to self-renew. During the first several weeks after transplantation, germ cell colonies cannot be defined because SSCs proliferate very slowly. In addition, numerous transplanted cells remain in the seminiferous tubules, which prevents direct identification of prospective SSC colonies. However, cells that failed to reach the niche may undergo apoptosis or are phagocytosed by Sertoli cells and disappear after 1 month. Colonies derived from SSCs can be defined at least 6 weeks after transplantation.

Although these problems make it difficult to study the homing mechanism, our results suggested strongly that β1-integrin is involved in the first several weeks of SSC colonization. First, we detected a homing defect in immature pup recipient testis, which lacks the BTB. Because SSC homing is enhanced in pup recipients, passage through the BTB is thought to be the most critical step in SSC homing (Shinohara et al., 2001). However, the homing defect of β1-integrin mutant cells was still prevalent, suggesting that β1-integrin is not involved in passage through BTB. Second, β1-integrin mutant GS cells have an impaired ability to attach to laminin in vitro. In addition, while WT GS cells attach to laminin preferentially compared with

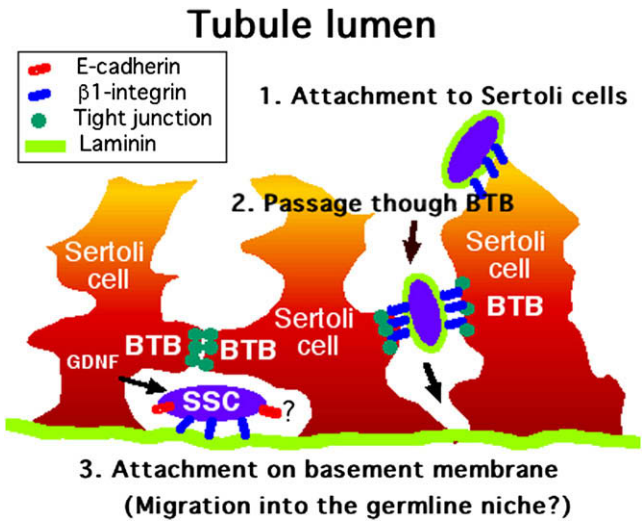

Figure 7. Potential Roles of β1-Integrin in SSC Homing

The β1-integrin is potentially involved in three distinct steps of SSC homing. Its expression on Sertoli cells may facilitate the attachment of SSCs or migration through the tight junction, whereas β1-integrin on SSCs may mediate their attachment to the basement membrane. The role of cadherin is yet to be determined.

fibronectin or collagen (Shinohara et al., 1999), anti-β1-integrin antibody specifically inhibited the attachment of WT cells in this study. Third, mutant cells retained proliferative activity both in vivo and in vitro. The mutant cells proliferated to make chains of spermatogonia at 1 week after transplantation in vivo, although it is unclear whether they originated from SSCs. Moreover, mutant GS cells could proliferate for a long term in vitro. Fourth, by 3 weeks after transplantation, most mutant cells detached from the basement membrane. These results suggest that initial phase of colony establishment is affected by β1-integrin loss. Therefore, a likely scenario is that transplanted mutant SSCs respond to a chemotactic signal and migrate from the adluminal to the basal compartment of the seminiferous tubules through the BTB, but migration to niche or retention on the basement membrane is abrogated because of a decreased ability to bind to laminin (Figure 7).

Although our results indicate the importance of β1-integrin in SSC homing, this molecule may also be involved in other aspects of spermatogenesis. In our study, we did not observe gross abnormalities in β1-integrin mutant GS cells in vitro or in the germ cell colony in vivo, suggesting that they have normal potential for spermatogenesis. Moreover, the cells were undergoing differentiation because meiotic cells were observed in the recipient testes after transplantation of mutant cells. However, we were not able to detect complete spermatogenesis from the mutant cells, which suggested that the cells are not differentiating efficiently. One possibility is the direct involvement of β1-integrin in SSC differentiation. In fact, ligand binding by β1-integrin can influence differentiation of keratinocytes (Levy et al., 2000). Alternatively, inefficient differentiation may be caused indirectly by low SSC seeding. The degree of commitment of cells to the differentiation pathway may be influenced by the stem cell and seminiferous tubule conditions (Nagano et al., 1999). Particularly, in case of low level of colonization, initiation of SSC

differentiation may be delayed due to longer period of mitotic SSC expansion. Indeed, SSCs transplanted in pup testis differentiate more quickly than in adult testis because of enhanced colonization (Shinohara et al., 2001). Considering that many abnormalities, such as missing layers of germ cells, were observed during the first several months after transplantation (Parreira et al., 1998), it remains unclear whether β1-integrin is involved in SSC differentiation. Strikingly, previous studies on HSCs showed that, although HSC homing depends on β1-integrin after transplantation, hematopoiesis proceeded normally in the absence of β1-integrin when the gene was inactivated in HSCs within the bone marrow (Brakebusch et al., 2002). Long time follow-up of the transplants is therefore necessary to determine the effect of β1-integrin loss in spermatogenic differentiation.

We also showed that SSC homing was impaired when the β1-integrin of Sertoli cells was ablated in the recipient testes. This suggests that β1-integrin on Sertoli cells plays a role in SSC homing. Although Sertoli cells may have been exposed to the virus only transiently due to the flow of seminiferous tubule fluid in vivo, the cre-mediated deletion occurred evenly in the testis, and LacZ staining showed that 72% of the seminiferous tubules were infected with the virus. However, the deletion was modest compared with SSCs, and only 19% of the Sertoli cells showed LacZ expression. Some germ cell colonies developed in areas with LacZ staining, which suggested that the cells might be heterozygous for the integrin expression in these areas. Alternatively, several Sertoli cells may cooperate to facilitate transport of SSCs to the basement membrane. More dramatic inhibition would occur in the complete absence of β1-integrin, which may be achieved using higher virus titer or injection into immature pups.

The involvement of Sertoli cells in SSC homing suggests that stem cell homing in the testis may operate in a different manner from that in the bone marrow. While active chemotaxis of stem cells alone may explain SSC homing, it was also proposed that Sertoli cells may play a major role. In this model, Sertoli cells actively sort transplanted SSCs and position them within the epithelium, using their unique cytoskeltal elements and cell configurations that enable such movements (Russell et al., 1996). Unlike normal epithelium, in which β1-integrin is usually present in the cell matrix, the β1-integrin of Sertoli cells is restricted to definite sites of intercellular contact, colocalizing with actin bundles at apical and basal ectoplasmic specialization (ES), a testis-specific, actin-based hybrid for anchoring and forming tight junctions (Yan et al., 2006). Although the ligand for β1-integrin at the ES is unknown, laminin expressed on germ cells may be a candidate (Yan et al., 2006). Because SSCs also express laminin (Kanatsu-Shinohara et al., 2006), β1-integrin on Sertoli cells may be used to capture transplanted SSCs. Alternatively, β1-integrin on Sertoli cells may be used for the transport of SSCs through the BTB. Reduced immunoreactive β1-integrin expression around the BTB in the seminiferous epithelium coincides with the migration of spermatocytes across this barrier, which suggests that Sertoli cells regulate germ cell movement during passage through the BTB (Salanova et al., 1995). Therefore, it is possible that SSCs take advantage of this distinct physiological activity of Sertoli cells to migrate into the niche. Although it remains to be determined whether SSCs exert chemotactic activity or Sertoli cells coordinate the homing process, β1-integrin on both germ cells and Sertoli cells is a key molecule in SSC homing, and accurate measurement of integrin protein levels in both SSCs and Sertoli cells will clarify how laminin- β1-integrin interactions coordinate different steps of SSC homing.

On the other hand, E-cadherin has been considered the prime candidate for stem-cell-niche interaction because it is specifically expressed to a higher extent on smaller populations of spermatogonia than is β1-integrin (Wu et al., 1993). This was also suggested by the fact that, in *Drosophila*, cadherin interaction is necessary to sustain undifferentiated stem cells (Song et al., 2002; Yamashita et al., 2003). Therefore, we had good reason to believe that cadherin also plays a similar role in mammalian spermatogenesis. In fact, E-cadherin has several important functions in mouse germline development. The addition of neutralizing antibody inhibits PGC formation from epiblasts and inhibits the migration and condensation of PGCs to the genital ridges (Bendel-Stenzel et al., 2000; Okamura et al., 2003; Di Carlo and De Felici, 2000). Based on these experiments, we expected that the loss of E-cadherin would have a detrimental effect on the homing or maintenance of SSCs. However, we found no significant effect of E-cadherin by using the neutralizing antibody, by a dominant-negative construct, or by genetic ablation. Although other family members of the cadherin genes may compensate for the loss of the E-cadherin, these results suggest that E-cadherin in the SSCs plays a lesser role than that in the PGCs. Interestingly, although *Drosophila* stem cells interact with somatic supporting cells by homophilic E-cadherin interactions, E-cadherin expression is not found in mammalian Sertoli cells (Tokuda et al., 2007). Perhaps, cadherin molecules on SSCs have a different role in the mammalian testis.

One of the important tasks in the future will be to identify the α-subunits that are involved in SSC homing. Of 18 α-subunits, several have been identified in the testes, including α1, α3, α4, α5, α6, and α9 (Yan et al., 2006). In addition, the search for other homing molecules also needs to be continued. The adenoviral gene delivery system may prove useful in such functional analyses because very few cre-expressing transgenic lines are available for analysis of the spermatogonia stage and breeding requires more time and larger numbers of animals. The biological significance of SSC migration awaits further study, but the identification of homing molecules is practically important because the low homing efficiency of SSCs has long been one of the problems in germ cell transplantation. Not all recipients become fertile despite successful germ cell transplantation. However, the manipulation of homing molecules by genetic or chemical methods may help to improve the colonization efficiency. Thus, the identification of the SSC homing machinery will not only reveal common principles of stem cell systems, but also will be important for practical SSC applications in medicine and biotechnology.

EXPERIMENTAL PROCEDURES

Animals

The generation of conditional β1-integrin or E-cadherin mutant mice was described previously (Brakebusch et al., 2002; Boussadia et al., 2002). For experiments using β1-integrin mutant mice, β1-integrin flox/flox and flox/WT littermates were used. For experiments using E-cadherin mutant mice, E-cadherin flox/flox males were crossed with homozygous R26R female mice to produce E-cadherin flox/WT offspring (both from The Jackson Laboratory,

ME), which were then crossed to produce E-cadherin flox/flox and flox/WT offspring. We also used Green mice (a gift from Dr. M. Okabe, Osaka University) and W mice (Japan SLC, Shizuoka, Japan) for transplantation. All animals were maintained in a C57BL/6 background for transplantation studies, except that β1-integrin flox/flox mouse was backcrossed to the ICR background for GS cell derivation.

Cell Culture and Adhesion Assay

Testes cells were collected from 10- to 14-day-old pups, and single-cell suspensions were obtained using a two-step enzymatic dissociation (Bellvé, 1993). The cells were cultured on mitomycin C-treated MEFs in StemPro-34 SFM (Invitrogen, Carlsbad, CA), supplemented as described (Kanatsu-Shinohara et al., 2003). For in vitro infection by the AxCANCre (RIKEN BRC, Tsukuba, Japan), 1×10^6 testis cells were plated in a 6-well plate (9.5 cm^2), whereas 3×10^5 GS cells were plated in a 12-well plate (3.8 cm^2). The cells were incubated overnight, and the virus was removed the next day. The titer of the virus was 2×10^6 plaque forming units (pfu)/ml.

GS cells were established according to a standard protocol, using newborn Green mice (backcrossed to the DBA/2 background) or 7 day-old WT or β1-integrin flox/flox mice in ICR background. GS cells were maintained on MEFs or laminin (Kanatsu-Shinohara et al., 2003, 2005). EG cells were cultured in Dulbecco's modified Eagles' medium supplemented with 15% fetal calf serum, 5×10^{-5} M 2-mercaptoethanol, and 10^3 units/ml ESGRO (Invitrogen, Carlsbad, CA). For antibody treatment, the cells were incubated with 20 μg/ml Ha2/5 (BD Biosciences, Lenexa, KS) or 200 μg/ml ECCD1 (Takara Bio Inc., Ohtsu, Japan).

Adhesion assay was performed as described previously with slight modifications (Kanatsu-Shinohara et al., 2006). In brief, cre-treated GS cells from wild-type and β1-integrin flox/flox mice were plated on ECM-coated dishes at a density of 2.5×10^5 cells per 3.8 cm^2. The dishes were coated with laminin (20 μg/ml), fibronectin (100 μg/ml), poly L-lysine (0.002%) (all from Sigma, St. Louis, MO), and collagen type I (2.4 mg/ml; Nitta gelatin, Osaka, Japan). For blocking experiments, cells were plated at a density of 3×10^5 cells per 3.8 cm^2 in the presence of 20 μg/ml anti-β1-integrin (Ha2/5), anti-β3-integrin (2C9.G2; BD Biosciences), or anti-β5-integrin (KN52; eBioscience, San Diego, CA) antibodies. Data were analyzed using Student's t test.

Transplantation

Germ cell transplantation was performed via the efferent duct, filling 75%–85% of the seminiferous tubules in each testis. Approximately 2 or 3 μl could be introduced into W mice that were 5–10 days or 4 weeks old, respectively. In experiments using neutralizing antibodies, donor cells were incubated with 200 μg/ml Ha2/5 or ECCD1 for 1 hr on ice and transplanted into the testis.

To delete genes in Sertoli cells, β1-integrin and E-cadherin mutants, or WT/WT animals, were treated with busulfan (44 mg/kg) at 4 weeks of age to destroy endogenous spermatogenesis. Four weeks after the treatment, both mutant and wild-type animals were injected with AxCANCre (2×10^6 pfu/ml). Approximately 10 μl of the donor cell suspension was injected into the seminiferous tubules of a busulfan-treated recipient, and donor cells from 8-week-old Green mice were microinjected 2 weeks after AxCANCre injection. The Institutional Animal Care and Use Committee of Kyoto University approved the animal experimentation protocols.

Analysis of Recipient Testes

The recipient testes were recovered at indicated time points after donor cell transplantation and analyzed by staining for the *LacZ* gene product, β-galactosidase, with X-gal (Wako Pure Chemical Industries, Osaka, Japan) (Nagano et al., 1999). In experiments using Green mice, colonization was evaluated by fluorescence under UV light. Germ cell clusters longer than 0.1 mm were considered as colonies.

For histological evaluation of the recipient testes, the testes were fixed with 10% neutral-buffered formalin and processed for paraffin sectioning. Two histological sections were made from each recipient testis with an interval of 12 μm. All sections were stained with hematoxylin and eosin. The number of tubule cross-sections showing spermatogenesis, defined as the presence of multiple layers of germ cells in the entire circumference of the seminiferous tubule, was recorded for one section from each testis. Deletion efficiency in Sertoli cells was evaluated by counting the number of tubules with LacZ expression. For immunohistochemistry, cryosections of the testes fixed in 4% paraformaldehyde were stained using anti-SYCP3 antibody (Chuma and Nakatsuji, 2001) and Alexa 488-conjugated anti-rabbit immunoglobulin G antibody (Molecular Probes, Eugene, USA). The slides were counterstained with Hoechst 33258 (Sigma). Statistical analysis was conducted using the Student's t test.

DNA Analysis

DNA transfer and hybridization were performed as described previously (Takehashi et al., 2007). To estimate cre-mediated deletion in β1-integrin mutant mice, full-length *LacZ* cDNA was used as a probe. For E-cadherin mutant mice, a 936-bp fragment in the exon 11-intron 11 region was amplified by PCR using the primers 5′-TGAGATGGACAGAGAAGACGC-3′ and 5′-GCCTTAATCAAGTTGGTGTGG-3′. The PCR product was digested by EcoRI to produce a 250 bp fragment, which was used as a hybridization probe. Band intensity was quantified using NIH image 1.63 software.

Analysis of Gene Expression

First-strand cDNA was synthesized using Superscript II (Invitrogen) for RT-PCR. To quantify mRNA expression using real-time PCR, comparisons were made by normalizing the expression to that of hypoxanthine phosphorybosyl transferase (HPRT) using Step One Plus Real-Time PCR System and Power-SYBR Green PCR Master mix (Roche Applied Science, Mannheim, Germany). The PCR conditions were 95°C for 10 min, followed by 40 cycles of 95°C for 15 s, 60°C for 60 s, and 72°C for 12 s.

PCR was carried out using the following primers (5′-ATCGTGCATGTTGTGGAGAC-3′and 5′-CTGCTGTGAGCTTGGTGTTG-3′ for *β1-integrin*, 5′-GGTATGACGCTGCAGACTATCC-3′ and 5′-CAGTACGACACCTACCACGG-3′ for *β2-integrin*, 5′-TGGCAAGTACTGTGAGTGCG-3′ and 5′-TCCAGTCCGAGTCACACACG-3′ for *β3-integrin*, 5′-GCCTACGAGGTCTGCTATGG-3′ and 5′-CGCCTTAACCGTGTATCGG-3′ for *β4-integrin*, 5′-GCCAAGATGGCATATCTTACC-3′ and 5′-TGCAATTGTAGGCGACTTCC-3′ for *β5-integrin*, 5′-TGGAATATCCAACTATCGGCC-3′ and 5′-ACCGCAGTTCTTCATAAGCG-3′ for *β6-integrin*, 5′-GAGGTCACACATTCTGTGCG-3′ and 5′-TCTCTCTCGAAGGCTTGAGC-3′ for *β7-integrin*, 5′-AAGGATCCACAATCAGTGC-3′ and 5′-CCAATATGACTCTCACAGACG-3′ for *β8-integrin*, 5′-ACCGATTCAAGAAGCTGGC-3′ and 5′-ACCATCCTAACACAGACAGTCC-3′ for *E-cadherin*, 5′-CATGCTGAGCCACAGTACC-3′ and 5′-CGCTACTGGAGGAGTTGAGG-3′ for *N-cadherin*, 5′-GGACCAGGACTATGACATCACC-3′ and 5′-TGTTGGCAGCCTTCAGG-3′ for *P-cadherin*, and 5′-GCTGGTGAAAAGGACCTCT-3′ and 5′-CACAGGACTAGAACACCTGC-3′ for *HPRT*).

ACKNOWLEDGMENTS

We thank Mr. H. Sakashita and Ms. Y. Ogata for technical assistance and Dr. Y. Matsui (Tohoku University) for EG cells. Financial support for this research was provided by the Ministry of Education, Culture, Sports, Science, and Technology of Japan. This work was also supported by Kanae Foundation, Program for Promotion of Fundamental Studies in Health Sciences of the National Institute of Biomedical Innovation (NIBIO), Genome Network Project, and Japan Science and Technology Agency (CREST).

Received: March 25, 2008
Revised: July 11, 2008
Accepted: August 5, 2008
Published: November 5, 2008

REFERENCES

Anderson, R., Fässler, R., Georges-Labouesse, E., Hynes, R.O., Bader, B.L., Kreidberg, J.A., Schaible, K., Heasman, J., and Wylie, C. (1999). Mouse primordial germ cells lacking β1 integrins enter the germline but fail to migrate normally to the gonads. Development *126*, 1655–1664.

Bellvé, A. (1993). Purification, culture, and fractionation of spermatogenic cells. In Guide to techniques in mouse development, P.M. Wasserman and M.L. DePamphilis, eds. (San Diego: Academic Press), pp. 84–113.

Bendel-Stenzel, M.R., Gomperts, M., Anderson, R., Heasman, J., and Wylie, C. (2000). The role of cadherins during primordial germ cell migration and early gonad formation in the mouse. Mech. Dev. *91*, 143–152.

Boussadia, O., Kutsch, S., Hierholzer, A., Delmas, V., and Kemler, R. (2002). E-cadherin is a survival factor for the lactating mouse mammary gland. Mech. Dev. *115*, 53–62.

Brakebusch, C., Fillatreau, S., Potocnik, A.J., Bungartz, G., Wilhelm, P., Svensson, M., Kearney, P., Körner, H., Gray, D., and Fässler, R. (2002). β1-integrin is not essential for hematopoiesis but is necessary for the T cell-dependent IgM antibody response. Immunity *16*, 465–477.

Brinster, R.L., and Zimmermann, J.W. (1994). Spermatogenesis following male germ-cell transplantation. Proc. Natl. Acad. Sci. USA *91*, 11298–11302.

Campos, L.S., Leone, D.P., Relvas, J.B., Brakebusch, C., Fässler, R., Suter, U., and ffrench-Constant, C. (2004). β1 integrins activate a MAPK signaling pathway in neural stem cells that contributes to their maintenance. Development *131*, 3433–3444.

Chuma, S., and Nakatsuji, N. (2001). Autonomous transition into meiosis of mouse fetal germ cells in vitro and its inhibition by gp130-mediated signaling. Dev. Biol. *229*, 468–479.

de Rooij, D.G., and Russell, L.D. (2000). All you wanted to know about spermatogonia but were afraid to ask. J. Androl. *21*, 776–798.

Di Carlo, A.D., and De Felici, M. (2000). A role for E-cadherin in mouse primordial germ cell development. Dev. Biol. *226*, 209–219.

Geissler, E.N., Ryan, M.A., and Housman, D.E. (1988). The dominant-white spotting (W) locus of the mouse encodes the *c-kit* proto-oncogene. Cell *55*, 185–192.

Hirsch, E., Iglesias, A., Potocnik, A.J., Hartmann, U., and Fässler, R. (1996). Impaired migration but not differentiation of haematopoietic stem cells in the absence of β1 integrins. Nature *380*, 171–175.

Kanatsu-Shinohara, M., Ogura, A., Ikegawa, M., Inoue, K., Ogonuki, N., Tashiro, K., Toyokuni, S., Honjo, T., and Shinohara, T. (2002). Adenovirus-mediated gene delivery and in vitro microinsemination produce offspring from infertile male mice. Proc. Natl. Acad. Sci. USA *99*, 1383–1388.

Kanatsu-Shinohara, M., Ogonuki, N., Inoue, K., Miki, H., Ogura, A., Toyokuni, S., and Shinohara, T. (2003). Long-term proliferation in culture and germline transmission of mouse male germline stem cells. Biol. Reprod. *69*, 612–616.

Kanatsu-Shinohara, M., Miki, H., Inoue, K., Ogonuki, N., Toyokuni, S., Ogura, A., and Shinohara, T. (2005). Long-term culture of mouse male germline stem cells under serum- or feeder-free conditions. Biol. Reprod. *72*, 985–991.

Kanatsu-Shinohara, M., Inoue, K., Lee, J., Miki, H., Ogonuki, N., Toyokuni, S., Ogura, A., and Shinohara, T. (2006). Anchorage-independent growth of mouse male germline stem cells in vitro. Biol. Reprod. *74*, 522–529.

Laird, D.J., von Andrian, U.H., and Wagers, A.J. (2008). Stem cell trafficking in tissue development, growth, and disease. Cell *132*, 612–630.

Lapidot, T., Dar, A., and Kollet, O. (2005). How do stem cells find their way home? Blood *106*, 1901–1910.

Leone, D.P., Relvas, J.B., Campos, L.S., Hemmi, S., Brakebusch, C., Fässler, R., ffrench-Constant, C., and Suter, U. (2005). Regulation of neural progenitor proliferation and survival by β1 integrins. J. Cell Sci. *118*, 2589–2599.

Levy, L., Broad, S., Diekmann, D., Evans, R.D., and Watt, F.M. (2000). β1-integrins regulate keratinocyte adhesion and differentiation by distinct mechanisms. Mol. Biol. Cell *11*, 453–466.

Meistrich, M.L., and van Beek, M.E.A.B. (1993). Spermatogonial stem cells. In Cell and Molecular Biololgy of the testis, C. Desjardins and L.L. Ewing, eds. (New York: Oxford University Press), pp. 266–295.

Meng, X., Lindahl, M., Hyvönen, M.E., Parvinen, M., de Rooij, D.G., Hess, M.W., Raatikainen-Ahokas, A., Sainio, K., Rauvala, H., Lakso, M., et al. (2000). Regulation of cell fate decision of undifferentiated spermatogonia by GDNF. Science *287*, 1489–1493.

Molyneaux, K., and Wylie, C. (2004). Primordial germ cell migration. Int. J. Dev. Biol. *48*, 537–544.

Nagano, M., Avarbock, M.R., and Brinster, R.L. (1999). Pattern and kinetics of mouse donor spermatogonial stem cell colonization in recipient testes. Biol. Reprod. *60*, 1429–1436.

Okamura, D., Kimura, T., Nakano, T., and Matsui, Y. (2003). Cadherin-mediated cell interaction regulates germ cell determination in mice. Development *130*, 6423–6430.

Parreira, G.G., Ogawa, T., Avarbock, M.R., França, L.R., Brinster, R.L., and Russell, L.D. (1998). Development of germ cell transplants in mice. Biol. Reprod. *59*, 1360–1370.

Ptocnik, A.J., Brakebusch, C., and Fässler, R. (2000). Fetal and adult hematopoietic stem cells require β1 integrin function for colonizing fetal liver, spleen, and bone marrow. Immunity *12*, 653–663.

Raz, E. (2004). Guidance of primordial germ cell migration. Curr. Opin. Cell Biol. *16*, 169–173.

Russell, L.D., França, L.R., and Brinster, R.L. (1996). Ultrastructural observations of spermatogenesis in mice resulting from transplantation of mouse spermatogonia. J. Androl. *17*, 603–614.

Salanova, M., Stefanini, M., de Curtis, I., and Palombi, F. (1995). Integrin receptor α6β1 is localized at specific sites of cell-to-cell contact in rat seminiferous epithelium. Biol. Reprod. *52*, 79–87.

Shinohara, T., Avarbock, M.R., and Brinster, R.L. (1999). β1- and α6-integrin are surface markers on mouse spermatogonial stem cells. Proc. Natl. Acad. Sci. USA *96*, 5504–5509.

Shinohara, T., Orwig, K.E., Avarbock, M.R., and Brinster, R.L. (2001). Remodeling of the postnatal mouse testis is accompanied by dramatic changes in stem cell number and niche accessibility. Proc. Natl. Acad. Sci. USA *98*, 6186–6191.

Song, X., Zhu, C.-H., Doan, C., and Xie, T. (2002). Germline stem cells anchored by adherens junctions in the *Drosophila* ovary niches. Science *296*, 1855–1857.

Soriano, P. (1999). Generalized *lacZ* expression with the ROSA26 Cre reporter strain. Nat. Genet. *21*, 70–71.

Takehashi, M., Kanatsu-Shinohara, M., Inoue, K., Ogonuki, N., Miki, H., Toyokuni, S., Ogura, A., and Shinohara, T. (2007). Adenovirus-mediated gene delivery into mouse spermatogonial stem cells. Proc. Natl. Acad. Sci. USA *104*, 2596–2601.

Tokuda, M., Kadokawa, Y., Kurahashi, H., and Marunouchi, T. (2007). CDH1 is a specific marker for undifferentiated spermatogonia in mouse testes. Biol. Reprod. *76*, 130–141.

Wilson, A., Murphy, M.J., Oskarsson, T., Kaloulis, K., Bettess, M.D., Oser, G.M., Pasche, A.-C., Knabenhans, C., MacDonald, H.R., and Trumpp, A. (2004). C-myc controls the balance between hematopoietic stem cell self-renewal and differentiation. Genes Dev. *18*, 2747–2763.

Wu, J.-C., Gregory, C.W., and Dephilip, R.M. (1993). Expression of E-cadherin in immature rat and mouse testis and in rat Sertoli cell cultures. Biol. Reprod. *49*, 1353–1361.

Yamashita, Y.M., Leanne Jones, D., and Fuller, M.T. (2003). Orientation of asymmetric stem cell division by the APC tumor suppressor and centrosome. Science *301*, 1547–1550.

Yan, H.H.N., Mruk, D.D., Lee, W.M., and Cheng, C.Y. (2006). Ectoplasmic specialization: a friend or a foe of spermatogenesis? Bioessays *29*, 36–48.